AN INVESTIGATION OF THE CONTRIBUTION OF LYSM PROTEINS TO THE ARBUSCULAR MYCORRHIZAL SYMBIOSIS

A Dissertation

Presented to the Faculty of the Graduate School

of Cornell University

In Partial Fulfillment of the Requirements for the Degree of

Doctor of Philosophy

by

Alexa Michel Schmitz

August 2018

AN INVESTIGATION OF THE CONTRIBUTION OF LYSM PROTEINS TO THE ARBUSCULAR MYCORRHIZAL SYMBIOSIS

Alexa Michel Schmitz, Ph. D.

Cornell University 2018

Arbuscular mycorrhiza is a mutually beneficial symbiosis between the majority of land plants and fungi from the subphylum Glomeromycotina resulting in the transfer of phosphates and other nutrients from fungi to plants in exchange for photosynthates. Throughout the interaction, arbuscular mycorrhizal (AM) fungi form several inter- and intracellular structures within plant roots, including arbuscules inside the cells of the inner root cortex, which are the site of nutrient exchange. Both plants and AM fungi release signaling molecules, reviewed in Chapter 1, that initiate signaling pathways leading to the cellular changes necessary for symbiosis. Two major types of AM fungal signaling molecules are short-chain chitooligosaccharides and lipochitooligosaccharides, which are both glucan oligomers. Additionally, AM fungal walls contain chitin and other glucan molecules that must come into close contact with plant cell membranes. Plant LysM receptors bind to chitin and other glucans at the cell membrane and trigger a ligand-specific signaling response, either for defense or symbiosis. Thus, I hypothesize that certain plant LysM proteins are important for AM symbiosis. Throughout this work, I utilized *Agrobacterium rhizogenes*-mediated root transformation of *Medicago truncatula* for RNA silencing, described in Chapter 2, and other expression and localization studies. In Chapter 3 I targeted LysM receptor-like kinases that may participate in relaying fungal signals via their intracellular kinases. In Chapter 4 I characterized small *Medicago* LysM proteins that surround arbuscules and may be important for both arbuscule development and degeneration. Finally, in Chapter 5 I characterized a

small effector-like LysM protein from the AM fungus, *Rhizophagus irregularis*, which is under positive selection and can bind to chitin and chitosan. Despite their specific expression, intriguing localization, and subtle effects on colonization as a result of mutation or over-expression, none of the *Medicago* LysM proteins proved essential for AM symbiosis, likely due to redundancy within their gene families. Deletion of multiple genes at once still does not disrupt the interaction. Such robustness is not surprising in light of 300 million years of a symbiotic relationship growing ever more stable throughout evolution.

BIOGRAPHICAL SKETCH

Originally from Lansdale, Pennsylvania, Alexa Schmitz earned a Bachelor of Arts and Bachelor of Music from Oberlin College and Conservatory, with majors in biochemistry and violin performance. After Oberlin, Alexa spent a year as an intern at the Smithsonian Tropical Research Institute on Barro Colorado Island in Panama studying ecology of arbuscular mycorrhizal fungi. She then worked in the lab of Dr. Cammie Lesser at Harvard Medical School investigating type III secretion chaperones in *Shigella flexneri*. After two years as a research technician, Alexa came to Cornell University to pursue her PhD in Plant Pathology and Plant-Microbe Biology investigating the molecular biology of arbuscular mycorrhiza. In addition to doing science, Alexa is a science writer and has written several press releases and news articles describing publications from Boyce Thompson Institute. Alongside her research endeavors, Alexa has continued to maintain her status as a professional violinist and is a member of the Cayuga Chamber Orchestra in Ithaca, NY.

To my parents, Ineke McCrea, Thomas Kramlik, Martin Ackerman, Gillian Turgeon, and many others who have inspired me to follow my dream of becoming a scientist.

ACKNOWLEDGMENTS

I would like to thank the section of Plant Pathology and Plant-Microbe Biology for giving me the opportunity to pursue my PhD at Cornell University, a mecca of plant and agricultural research. I thank my initial Dean of Graduate Studies Michael Milgroom for taking a chance on me, and also my current DGS Adam Bogdanove for his mentorship and guidance towards finishing. I would also like to thank Michael Milgroom, as well as Eric Nelson, Debra Nero, and Gillian Turgeon for mentoring me in my teaching, and Gillian Turgeon and June Nasrallah for their wisdom and support as my minor committee members. I would especially like to thank and acknowledge Maria Harrison, my advisor, for her extensive guidance and patience from start to finish. I want to thank all my friends and family who have provided emotional support and motivated me to keep going despite trials and tribulations, especially Ally MacLean for her endless encouragement and for helping me to keep sight of my true self in even the toughest moments. Finally, I want to thank Norman for taking me into his life at one of the most difficult points of my own and helping me to succeed and grow back into the person and scientist I am meant to be.

TABLE OF CONTENTS

LIST OF FIGURES

LIST OF TABLES

CHAPTER 1

SIGNALING EVENTS DURING INITIATION OF ARBUSCULAR MYCORRHIZAL SYMBIOSIS[1]

Abstract

Under nutrient-limiting conditions plants will enter into symbiosis with arbuscular mycorrhizal (AM) fungi for the enhancement of mineral nutrient acquisition from the surrounding soil. AM fungi live in close, intracellular association with plant roots where they transfer phosphate and nitrogen to the plant in exchange for carbon. They are obligate fungi, relying on their host as their only carbon source. Much has been discovered in the last decade concerning the signaling events during initiation of the AM symbiosis, including the identification of signaling molecules generated by both partners. This signaling occurs through symbiosis-specific gene products in the host plant, which are indispensable for normal AM development. At the same time, plants have adapted complex mechanisms for avoiding infection by pathogenic fungi, including an innate immune response to general microbial molecules, such as chitin present in fungal cell walls. How it is that AM fungal colonization is maintained without eliciting a defensive response from the host is still uncertain. In this review we present a summary of the molecular signals and their elicited responses during initiation of the AM symbiosis, including plant immune responses and their suppression.

[1] This chapter is published as Schmitz, AM and Harrison, MJ (2014) Signaling events during initiation of arbuscular mycorrhizal symbiosis. *J Integr Plant Biol*. 56:250-61.

Introduction

In soils depleted of mineral nutrients, plants have adapted microbial relationships for the enhancement of nutrient acquisition. In particular, phosphate and nitrogen acquisition is improved through a symbiotic association of plant roots with fungi from the phylum Glomeromycota, called the arbuscular mycorrhizal (AM) symbiosis (Smith and Read 2008). Additionally, plants from the Leguminosae family, and a few select others, have developed mechanisms for association with nitrogen-fixing rhizobia which induce the formation of a new organ, the nodule, in roots (Recently reviewed in Oldroyd et al. 2011). These mechanisms have been studied extensively, and interestingly many of the genes presumed to have been acquired to accommodate rhizobia have been shown also to be indispensable for AM symbiosis (Oldroyd 2013). The genes shared between these two symbioses make up what is referred to as the common symbiosis signaling pathway (CSSP). As a result, a better understanding of the rhizobial symbiotic mechanisms has facilitated discoveries of AM mechanisms; however, this approach may also bias hypotheses. Although plants employ similar mechanisms for the accommodation of both microbes, these symbioses have their inherent differences as well, which may be hidden by the expectation of similarities (Parniske 2000). Even while accommodating beneficial microbes, plants must be constantly prepared to deal with harmful microbial interactions, preempting them through recognition of microbe associated molecular patterns (MAMPs) leading to MAMP-triggered immunity (MTI) (Jones and Dangl 2006). In a time of nutrient stress, AM fungi and their plant hosts have developed strategies to avoid this pathogen response, without compromising innate defense against other pathogens. How exactly this happens has yet to be determined, but many clues have been found through understanding and comparing the different types of associations.

AM fungi are obligate endosymbionts, forming living structures within the cells of host roots. The fungus obtains its carbon from the host plant while providing nutrients, especially phosphate (Pi) and nitrogen, in return. This intimate interaction is obligatory for the

fungus, which can only assimilate carbon taken from a host plant (Smith and Read 2008). Despite an apparent lack of sexual reproduction, AM fungi have been around for at least 460 million years, evidenced by fossils with AM fungi in the earliest land plants, as well as fossils of AM spores and hyphae that may predate plant colonization of land (Redecker 2000; Remy et al. 1994; Simon et al. 1993). These discoveries have further led to the hypothesis that AM fungi may have assisted plants in their movement into the harsh land environment (Bonfante and Genre 2008; Pirozynski and Malloch 1975), which is further supported by phylogenetic analyses of three genes required for AM, showing that the genes were likely present in the common ancestor to all land plants (Wang et al. 2010). An estimated 80% of land plants harbor AM fungi in their roots and this includes most major crop species, making these fungi especially important for the maintenance of food security around the world. Recent discoveries of possible mycorrhiza-induced resistance add to this relevance (Jung et al. 2012; Liu et al. 2007; Pozo and Azcón-Aguilar 2007). Unfortunately *Arabidopsis thaliana*, possibly the most intensively studied model plant, does not form associations with AM fungi.

Upon sensing a host root a fungal hypha differentiates into a flattened structure, called a hyphopodium, which adheres to the root epidermis (see Figure 1-1). The underlying root cell actively prepares for penetration by reorganizing its cytoplasm into a column across the cell, called the pre-penetration apparatus (PPA), which directs the future path of the fungus (Genre et al. 2008, 2005). The fungus begins to penetrate as the plant plasma membrane invaginates and cell wall is deposited, surrounding the fungal hypha as it travels through a cell (Genre et al. 2012). This newly formed membrane is called the perifungal membrane. In the root cortex, fungal hyphae differentiate into highly branched structures called arbuscules, the predicted primary site of nutrient exchange between the two organisms (Bonfante and Genre 2010; Harrison 2012; Parniske 2008). The plant membrane surrounding an arbuscule, called the periarbuscular membrane (PAM), contains AM-specific Pi transporters that transport Pi

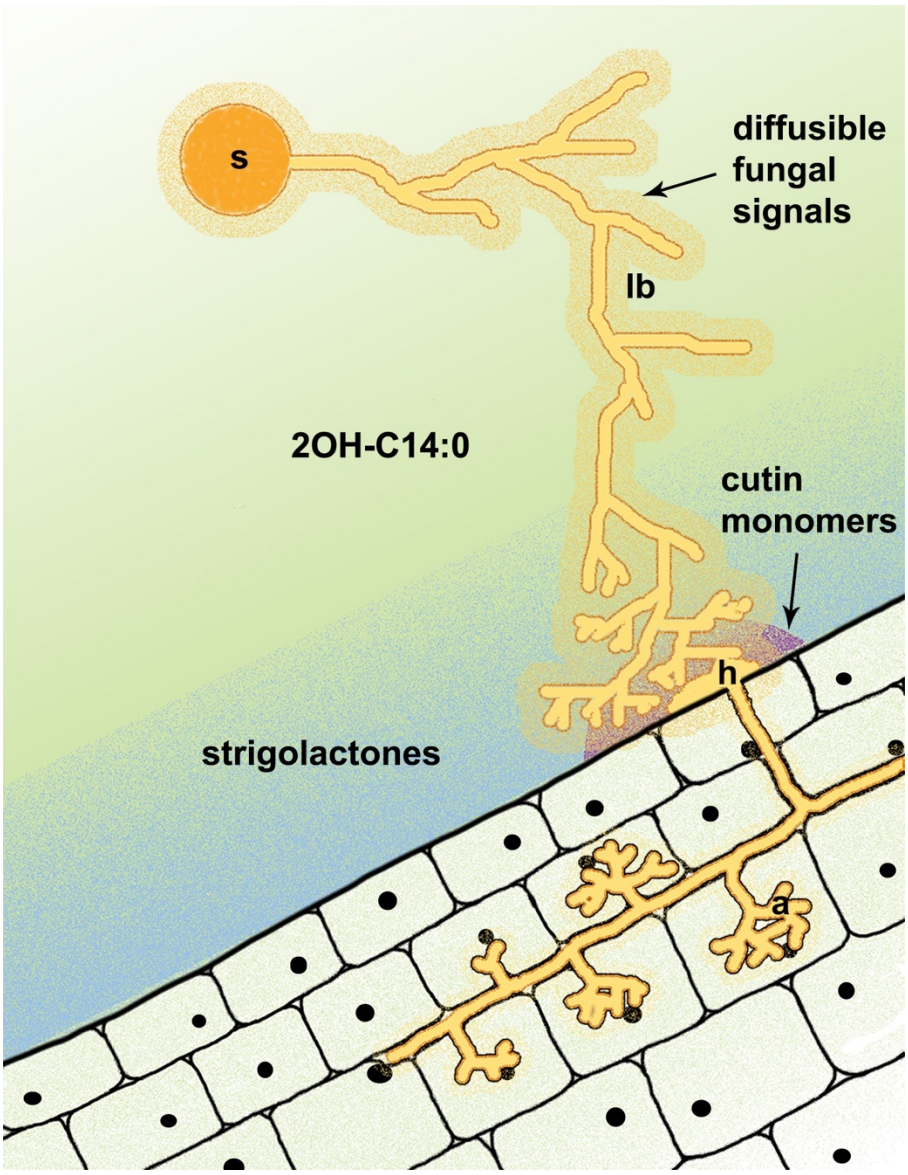

Figure 1-1: Sketch of AM fungal-plant signaling and colonization of a plant root. An AM fungal spore (s) germinates near a root, and 2OH-C14:0 fatty acids (green haze) induce elongated lateral branches (lb). Closer to the root, hyphae sense strigolactones (blue haze) and branch more complexly at higher orders. Upon sensing fungal signaling molecules (yellow haze) the plant secretes cutin monomers (purple haze), likely inducing hyphopodium (h) formation. After penetration of epidermis, the fungus travels through the cortex continuing to produce signaling molecules, penetrating individual cortical cells for the formation of highly branched arbuscules (a).

released from the fungus into the cortical cell (Javot et al. 2007a; Kobae and Hata 2010). An AM fungal hexose transporter has been detected in arbuscules, but also intercellular hyphae, indicating that uptake of carbon by the fungus may not be specifically occurring via the PAM (Helber et al. 2011). After 4-5 days the arbuscule begins to degenerate, and as the fungus disappears, the host cell returns to its pre-fungal state, eventually viable for new colonization (Bonfante-Fasolo 1984; Pumplin and Harrison 2009). As the fungal hyphae grow through the root cortex they continue to enter cortical cells and form arbuscules, creating an array of colonized cells with arbuscules at a variety of developmental stages. Outside the roots the fungus exists in a web of extraradical mycelia, which pick up nutrients from the rhizosphere and beyond the depletion zone to be transferred to its host (Govindarajulu et al. 2005; Javot et al. 2007b).

As a fungus comes into close contact with a plant cell, MAMPs and other released molecules can act as signals to the host. AM fungal germinating spore exudates (GSE) have been shown to elicit a variety of responses from potential hosts (Bonfante and Requena 2011). At the same time, AM fungal cell walls contain chitin, which is also a strong elicitor of plant innate immunity (Bonfante-Fasolo et al. 1990; Kaku et al. 2006). As a first line of defense, plants have developed an innate immune response in which receptors on the surface of a plant cell recognize MAMPs, such as chitin, released by microbes. This recognition elicits defense reactions, such as the release of chitinases, phytoalexins, reactive oxygen species (ROS), and molecules for cell-wall strengthening (Hamel and Beaudoin 2010). MAMPs are generally any molecule that is associated with a given class of microbes, such as bacteria or fungi, including non-pathogenic organisms. Some of the more broadly recognized MAMPs include bacterial lipopolysaccharides, flagellin and peptidoglycan, and fungal chitin (Boller and He 2009; Schwessinger and Ronald 2012). These microbial signatures elicit responses in the host plant through interactions with extracellular receptors, which then transduce a signal ultimately resulting in the induction of defense-gene transcription. Many microbes have developed

mechanisms for avoiding host MTI, such as decorating their structural molecules, or secreting effector proteins that directly inhibit or modify the defense signaling pathway (Schwessinger and Ronald 2012). Evidence that an initial defense response is mounted by the plant, but quickly dampened has been in the literature for decades (Harrison and Dixon 1993; Kapulnik et al. 1996; Liu et al. 2003); however, how it is that AM fungi do not continuously elicit MTI, considering the plethora of chitin in their cell walls, is still a mystery. Ultimately, AM fungi persist inside roots, where their maintenance greatly enhances the Pi status of their host.

Molecules secreted from plant roots are signals for AM fungi

Plants have evolved several mechanisms for obtaining Pi under limiting conditions. Morphological changes increase root surface area via root hair growth and lateral root development (Péret et al. 2011), while the secretion of organic acids and phosphatases free Pi from complexes in the surrounding soil (Plaxton and Tran 2011). Alternatively, plants associate with AM fungi, which in a sense increase the surface area by which plants can take up nutrients, as their extraradical mycelia extend beyond the depletion zone of the rhizosphere (Javot et al. 2007b). Pi deficiency is sensed locally and systemically, and the plant's responses involve several signaling pathways. Many plant hormones are involved in the structural responses to Pi deficiency, including strigolactones (Czarnecki et al. 2013), which are considered primary signals for initiating AM symbiosis and possibly enhance lateral root growth under low Pi conditions (Ruyter-Spira et al. 2013). Strigolactones are generated in the roots and can travel through the xylem to the shoots where they modify aboveground architecture for efficient Pi utilization, primarily through the inhibition of shoot branching and tiller formation (Brewer et al. 2013; Gomez-Roldan et al. 2008; Kohlen et al. 2011; Umehara et al. 2010, 2008). Strigolactones were first identified as the germination signal for the parasitic plants of *Striga* and *Orobanche* species, and through these studies they were determined to be terpenoid lactones derived from the carotenoid pathway (Jamil et al. 2010;

Matusova et al. 2005); however, more recent identification of strigolactone as a signal for AM fungi has revealed an important role for the hormone in AM symbiosis.

Prior to the discovery of strigolactone, its effects on AM fungi were attributed to an elusive "branching factor". Early studies showed AM fungal hypha approaching a host plant root will branch extensively as it comes into contact with the root surface, presumably due to contact with host root exudates (Bécard and Fortin 1988; Giovannetti et al. 1993), and that this branching can be inhibited by high Pi in the rhizosphere (Nagahashi et al. 1996). This branching factor was further shown to induce germination of AM fungal spores, as well as mitosis, increased mitochondrial gene expression and proliferation, and fungal respiration (Buee et al. 2000; Tamasloukht et al. 2003). Furthermore, Buee et al. (2000) showed that non-host plant root exudates were inactive. More recently the branching factor has been identified as strigolactone, which can induce many of the same changes as host root exudates (Akiyama et al. 2005; Besserer et al. 2008, 2006); however, a synthetic strigolactone GR24, commonly used for the investigation of the hormone's function, does not induce the same transcriptional responses as seen for root exudates (Besserer et al. 2008), implying that other stimulating factors may exist in the exudates and/or GR24 does not fully mimic the cocktail of strigolactones produced by a single plant species (Xie and Yoneyama 2010). Further evidence for other important factors comes from the observation of two very different hyphal branching patterns (see Figure 1-1), which have been specifically induced by different alcohol soluble fractions of carrot root exudates (Nagahashi and Douds 2007). While one of these branching patterns resembles a higher order complex branching induced by strigolactones in close proximity to a root (Akiyama et al. 2005), the other involves an increase in elongating lateral branches off the primary hyphal germ tube, and has recently been shown to be induced by 2-hydroxy tetradecanoic acid (2OH-C14:0) (Nagahashi and Douds 2011; Nagahashi et al. 2010).

Strigolactone production is induced by low Pi conditions, and its biosynthesis from carotenoids is initiated by two carotenoid cleavage dioxygenases CCD7 and CCD8 (Yoneyama et al. 2007a, 2007b). Mutant analysis has further shown the importance of strigolactone biosynthesis genes for the AM symbiosis. Root exudates from Pea *ccd8* and *ccd7* mutants were greatly reduced in their promotion of fungal hyphal branching, and the mutants themselves were much less colonized by AM fungi. Both hyphal branching and AM colonization were partially restored by GR24 application (Gomez-Roldan et al. 2008). In tomato, AM fungi were able to colonize *ccd7* at normal levels, but with a lower density of arbuscules, as well as reduction of AM-induced apocarotenoids (a class of terpenoids necessary for maintaining late-stage AM (Floss et al. 2008)), implicating an involvement of *CCD7* in arbuscule formation and maintenance (Vogel et al. 2010). Another tomato strigolactone-deficient mutant, *sl-ort1*, was shown to have reduced *SlCCD7*, but not *SlCCD8*, transcript, as well as a decrease in AM colonization rates and hyphal branching as induced by root exudates (Koltai et al. 2010). In pea, the *ccd8* mutant was poorly colonized by AM fungi, and despite low Pi or N levels, no strigolactones were detected in either *ccd8* or *ccd7* mutants (Foo et al. 2013). Recently an ATP-binding cassette (ABC) transporter, *PDR1*, from *Petunia hybrida* has been shown to be necessary for normal accommodation of AM fungi. Expression and mutant analyses indicate that PDR1 is a strigolactone exporter specific to roots, and functions in both the exudation of strigolactones from roots, especially under low Pi conditions, as well as maintaining and promoting intercellular colonization, as evidenced by retarded expansion of fungal colonization units (Kretzschmar et al. 2012). All of these reports taken together strongly connect the biosynthesis and secretion of strigolactones directly to the promotion of AM symbiosis.

Very recently, cutin monomers, ω-OH C16 fatty acids, were identified as a third class of AMF-stimulating factors. Mutants of a *Medicago* GRAS-family transcription factor, *RAM1*, as well as its identified target, *RAM2* were almost completely blocked in AM

formation, with much fewer hyphopodia and almost no intraradical hyphae as compared to wild type roots (Gobbato et al. 2012; Wang et al. 2012). RAM2, a glycerol-3-phosphate acyl transferase (GPAT) is similar to the *Arabidopsis* GPAT6, which functions in cutin deposition. Most importantly, the addition of cutin monomers could complement the *ram2* mutant (Wang et al. 2012). Interestingly, two oomycete pathogens were also blocked in their ability to form appressoria in the *ram2* mutant. While colonization by both AM fungi and the oomycetes induced expression of *RAM2*, oomycete infection was unaffected in the *ram1* mutant, implicating at least two signaling pathways for the induction of *RAM2* and cutin release (Gobbato et al. 2013; Wang et al. 2012). The ability of cutin monomers to complement *ram2* indicates that RAM2 is promoting hyphopodia formation through the production of a chemical signal rather than a physical change in the cell surface (Wang et al. 2012). This conclusion is further supported by evidence showing that plant-derived cutin monomers are able to induce filament and appressoria formation of the biotrophic pathogen, *Ustilago maydis* on maize (Mendoza-Mendoza et al. 2009), as well as appressoria formation of the hemibiotroph, *Magnaporthe grisea* on rice (Gilbert et al. 1996; Wilson and Talbot 2009).

Diffusible factors from AM fungi elicit responses in plant roots

A germinated AM fungal spore in the soil can live off its reserve of lipids for only a few days before it must find a host. In the absence of a host root, a germinated spore will pause growth, possibly due to the lack of plant signals, and retract hyphal cytoplasm for use in another germination attempt later (Logi et al. 1998; Smith and Read 2008). The first evidence that AM fungi produce diffusible signals active on plant roots came from experiments showing that hyphae separated from a plant root by a cellophane membrane were able to induce expression of the early nodulation gene, *MtENOD11*, in lateral roots, despite a lack of physical contact between the two organisms (Kosuta et al. 2003). Previous studies had shown that colonization by *Gigaspora rosea* and three *Glomus* species induced expression of

MtENOD11 in epidermal and cortical cells associated with hyphal penetration, or arbuscule formation (Chabaud et al. 2002; Journet et al. 2001). Additionally, application of rhizobial nodulation factors (NF), specific lipochito-oligosaccharide (LCO) signals secreted by rhizobia, to *Medicago* roots is able to induce expression of *MtENOD11*, which had led Kosuta et al. (2003) to hypothesize the same might be true for a diffusible AM fungal signal. They went on to show that *MtENOD11* expression induced by a diffusible AM signal was not dependent on *DMI1*, *DMI2*, or *DMI3* of the CSSP, while previous studies had shown these genes to be necessary for *MtENOD11* induction by NF from the *Medicago*-compatible, *Sinorhizobium meliloti* (Catoira et al. 2000).

MtDMI1 (*POLLUX* in *Lotus japonicus*) encodes a cation-permeable channel and *MtDMI2* (*SYMRK* in Lotus) encodes a leucine-rich repeat receptor-like kinase (LRR-RLK). Both are upstream in the CSSP from *DMI3*, a calcium- and calmodulin- dependent protein kinase (*CCaMK* in Lotus) (Oldroyd 2013). Previously the expression of *MtENOD11* during *G. rosea* hyphopodium formation was shown to be completely absent in the *dmi2* mutant (Chabaud et al. 2002), in contrast to the results from Kosuta et al. (2003), which suggests that *MtENOD11* may be induced via different signaling pathways depending on the stage of AM. Kosuta et al. (2003) further showed that two pathogenic fungi and an oomycete do not induce *MtENOD11* expression, indicating that the diffusible signal(s) is not a general fungal characteristic. In a similar experiment, transcript analysis of *Medicago* roots separated by a nitrocellulose film from germinating *Glomus mosseae* spores showed an increase in expression of several genes involved in signal transduction, transcription, and translation. In contrast to *MtENOD11*, pre-symbiotic induction of these genes was dependent *DMI3*, but *DMI1* and *DMI2* were not tested (Weidmann et al. 2004). Similarly a diffusible factor from *Glomus intraradices* hyphae was shown to induce expression of four genes from *Medicago* during hyphopodium formation, with varying dependency on *DMI2* (Kuhn et al. 2010). One of these genes, *MtMSBP1*, was further shown to be necessary for normal hyphopodium

formation. The observed differences in *DMI*-dependency of gene-induction by NF, diffusible fungal signals, and hyphopodium formation strongly supports a hypothesis for multiple signaling pathways, as well as potential for multiple diffusible signals from AM fungi.

In addition to induction of *MtENOD11* expression, a diffusible factor from germinating AM fungal spores, but not those of three pathogens, was shown to stimulate lateral root formation (LRF) in *Medicago*. This was dependent on *DMI1* and *DMI2*, but not on *DMI3* (Oláh et al. 2005). *S. meliloti* NF was also able to stimulate LRF, but required all three *DMI*. Interestingly, NF application also increased mycorrhizal colonization. Later studies further showed that germinating spore exudates (GSE) are also able to stimulate LRF in the monocots rice and maize. Rice forms two types of lateral roots, only one of which AM fungi are able to colonize, and likewise the GSE only stimulated formation of these lateral roots, but completely independently of all three *DMI* homologs (Gutjahr et al. 2009; Mukherjee and Ané 2011), indicating that lateral root formation as induced by an AM diffusible signal occurs via a separate signaling pathway in rice.

As a third line of evidence for AM diffusible signals, germinating spores are able to elicit transient changes in a plant cell's cytosolic Ca^{2+} prior to contact. Constitutively released signals from spores induced a transient spike in cytosolic Ca^{2+} of soybean cell cultures, but not in *Arabidopsis* cells (Navazio et al. 2007). A rapid cytosolic Ca^{2+} influx can also occur in response to some pathogenic fungi, likely due to MTI in response to chitin in their cell walls. Navazio et al. (2007) distinguished the AM GSE-induced Ca^{2+} spiking from a chitin-induced Ca^{2+} influx by showing a completely different Ca^{2+} signal from chitinous AM fungal spore fragments, as well as ROS production, which was not induced by the diffusible signals. In contrast to soybean cell cultures, *Medicago* roots close to highly branched AM fungal hyphae displayed an irregular oscillatory Ca^{2+} response dependent on *DMI1* and *DMI2*, but not *DMI3* (Kosuta et al. 2008). Interestingly, only highly branched hyphae induced the Ca^{2+} oscillations, implying that plant exudates responsible for the branching are necessary for these oscillations,

although they did not test GSE. A more recent study has shown Ca^{2+} oscillations in carrot and *Medicago* root organ cultures (ROC), two AM host systems that are unable to associate with rhizobia, in response to both GSE as well as hyphopodia formation. Notably, the authors demonstrated that this nuclear Ca^{2+} spiking occurs independently of the NF receptor gene in *Medicago*, *NFP*, implying that these signals are acting through a receptor other than NFP (Chabaud et al. 2011). As before, they were still dependent on both *DMI1* and *DMI2*, but not *DMI3*. These results further hint at the possibility for at least two different signaling pathways in response to fungal factors. In summary, a diffusible signal(s) from AM fungi is able to induce gene expression, as well as stimulate both LRF and irregular Ca^{2+} oscillations prior to fungal-root contact. The involvement of the CSSP in this signaling varies depending on the measured outcome, as well as the species of host plant, implying that more than one AM fungal diffusible signal exists, as well as multiple signaling pathways for these signals in the host (Summarized in Table 1).

An AM fungal signaling molecule resembles rhizobial Nod Factors

Consistent with the hypothesis for multiple diffusible signals from AM fungi, two different signals have been recently identified: LCOs, which very closely resemble NF (referred to as Myc-LCO) (Maillet et al. 2011), and short-chain chitin oligomers (COs), most active as CO4 and CO5 (Genre et al. 2013). Myc-LCOs were purified from sterile exudates of mycorrhizal carrot roots, as well as GSE of *G. intraradices*, and were identified as signals by their induction of *MtENOD11* expression in *Medicago* plants, as well as stimulation of root-hair branching in *Vicia sativa*, a bioassay typical for NF characterization (Maillet et al. 2011). The exudates were shown to contain a mixture of LCOs with a tetrameric CO backbone decorated with an N-acyl substitution of C16:0 or C18:1 fatty acid, and an O-sulfate (s) or non-sulfated (ns). Specifically, sMyc-LCOs were found in both sources, while nsMyc-LCOs were only isolated from mycorrhizal carrot roots. Due to the low yields of purified Myc-

Table 1-1: Compilation of data concerning evidence for diffusible signals from AM fungi.

Study	Plant	Fungi	Source of signal	Induced Activity	CSSP dependency				
					NFP	DMI1	DMI2	DMI3	NSP1
Journet et al. 2001	*Medicago truncatula*	*Glomus intraradices* *Glomus fasiculatum* *Glomus mosseae*	Direct inoculation/colonization	pMtENOD11-GUS expressed in arbuscules					
Chabaud et al. 2002	*M. truncatula*	*Gigaspora rosea*	Direct inoculation/colonization	pMtENOD11-GUS expressed with hyphal penetration			Y		
Kosuta et al. 2003	*M. truncatula*	*G. rosea* *Gigaspora gigantea* *Gigaspora margarita* *G. intraradices*	Branched hyphae separated from root by membrane	pMtENOD11-GUS expressed in lateral root epidermal cells close to branched hyphae		N	N	N	
Weidmann et al. 2004	*M. truncatula*	*G. mosseae*	Germ. spores separated from root by membrane	Gene induction				Y	
Kuhn et al. 2010	*M. truncatula*	*G. intraradices*	Germ. spores separated from root by membrane	Gene induction			Y/N		
Oláh et al. 2005	*M. truncatula*	*G. margarita* *G. rosea* *G. intraradices* (*Sinorhizobium meliloti* NF)[a]	Germ. spores separated from root by membrane (Direct application)	Stimulation of LRF[b] (Stimulation of LRF)	N (Y)	Y (Y)	Y (Y)	N (Y)	N (Y)
Gutjahr et al. 2009	*Oryza sativa*	*G. intraradices*	Direct inoculation/colonization	Stimulation of LRF		N		N	
Mukherjee & Ané 2011	*O. sativa* *Zea mays* *M. truncatula*	*G. intraradices*	GSE[c]	Stimulation of LRF	 N	N Y	 Y	N N	 N
Navazio et al. 2007	*Glycine max* cell culture	*G. margarita* *G. intraradices* *G. mosseae*	GSE	Elevations in cytosolic Ca^{2+}					
Kosuta et al. 2008	*M. truncatula*	*G. intraradices*	Close association with hyphae	Irregular Ca^{2+} oscillations		Y	Y	N	
Chabaud et al. 2011	*M. truncatula* ROC[d] *D. carota* ROC	*G. margarita* *G. gigantea*	GSE, hyphopodium formation	Irregular Ca^{2+} oscillations	N	Y	Y	N	

[a]Represents a bacterial signal. [b]Lateral root formation. [c]Germinating spore exudates. [d]Root organ culture.

LCOs, synthetic Myc-LCOs were engineered in bacteria for the purpose of determining their function. These synthetic Myc-LCOs stimulated both AM colonization and LRF of a legume (*Medicago*) and two non-legumes (*Tagetes patula* and *Daucus carota*). nsMyc-LCOs were somewhat better stimulators of AM colonization while sMyc-LCOs were 100 times better stimulators of LRF; however, a mixture of s/nsMyc-LCOs was best at stimulating both responses (Maillet et al. 2011). Interestingly, sMyc-LCOs are very similar to NF from *S. meliloti*, the only differences being the lack of an O-acetyl decoration and a slightly different fatty acid (Oldroyd et al. 2001). This is not surprising considering that Myc-LCOs were actively sought after based on the hypothesis that they would look like NF. Certain rhizobia have also been shown to produce a mixture of sulfated and non-sulfated NF (Pueppke and Broughton 1999), and while NF is normally a determinant of host-rhizobia specificity, mixtures of different NF may help broaden the host-range. A mixture of simple LCOs may similarly lend AM fungi their extremely broad host range; however, it is important to remember that Myc-LCOs have thus far only been purified from one AM fungus, and tested on only a few potential hosts. The transcriptional responses in *Medicago* to each s and nsMyc-LCO and to a 1:1 mixture were compared to each other as well as to those of *S. meliloti* NF (Czaja et al. 2012). All four treatments induced unique transcription profiles, notably even the s/ns mixture as compared to each Myc-LCO alone, indicating that a mixture of the two Myc-LCOs (which may be the more realistic signal) is necessary for the activation of certain AM genes. This phenomenon has been shown previously as the induction of *ENOD2* in *Glycine soja* by NF requires a combination of at least two different NF structures (D'Haeze and Holsters 2002; Minami et al. 1996). Furthermore, two structurally different NF from *Sinorhizobium meliloti nod* gene mutants elicited different physiological responses in alfalfa, hypothesized to correspond to recognition of a specific signal for entry, and a non-specific signal for the further induction of developmental plant responses. Although these differences were engineered, they demonstrate multiple roles for NF signaling throughout the symbiosis

as dependent on its molecular structure (Ardourel et al. 1994). A similar role can easily be envisioned for the different Myc-LCOs identified (Czaja et al. 2012).

In addition to the transcriptional changes, the primary morphological change induced by Myc-LCOs is LRF, which was shown to be dependent on all three DMI proteins, as well as a GRAS-family transcription factor, *NSP2* downstream from the DMI signaling in the CSSP. Additionally, the stronger sMyc-LCO-induced root branching was dependent on a second downstream GRAS transcription factor, *NSP1*, which was previously thought to be important only for rhizobial symbiosis, but recently shown to play a role in AM symbiosis as well (Delaux et al. 2013). In the absence of *NSP1*, the amount of root branching stimulated by sMyc-LCO was reduced to the level stimulated by nsMyc-LCO, which was the same with or without *NSP1* (Maillet et al. 2011), indicating the existence of two pathways leading to LRF. Both Myc-LCOs, their mixture, and NF induce expression of *NSP1* and *NSP2*, and both *NSP1* and *NSP2* are required for the production of the main strigolactones produced by rice and *Medicago* (Czaja et al. 2012; Delaux et al. 2013; Liu et al. 2011). While *mtnsp2* plants are still able to produce orobanchol, a precursor to the main strigolactone in *Medicago*, *mtnsp1* plants do not produce any strigolactones (Liu et al. 2011), implicating either a strigolactone-independent mechanism for the LRF in *mtnsp1*, or an *NSP1*-independent mechanism for strigolactone biosynthesis induced by Myc-LCOs. Although Myc-LCOs can induce LRF in the absence of *NSP1*, this weaker LRF requires *RAM1*, the transcription factor necessary for the putative cutin signaling. *RAM1* was not necessary for the stronger LRF induced by NF, but sMyc-LCOs were not tested (Gobbato et al. 2012). The involvement of *RAM1* in the weaker LRF further implies two signaling pathways for Myc-LCO-induced responses: one involving the association of *NSP2* with *NSP1*, and another involving *NSP2* and *RAM1*. Considering both *RAM1* and *RAM2* are necessary for the continuation of AM after entry, and possibly for arbuscule formation, Myc-LCO stimulation of overall AM root colonization may

also signal through the *NSP2*/*RAM1* pathway (Gobbato et al. 2013). Furthermore, *RAM1* and *RAM2* do not seem to be necessary for normal rhizobial symbiosis (Wang et al. 2012).

Analysis of Myc-LCO-induced gene transcription in the *dmi3* mutant showed that 73% of the gene expression changes depend on *DMI3*. Of these *DMI3*-dependent genes, several were still induced independently of *NSP1*, further supporting an *NSP1*-independent signaling pathway for Myc-LCOs (Czaja et al. 2012). Of the Myc-LCO-induced gene expression changes, 95% was dependent on *MtNFP*, which was consistent with a lack of any LRF in the *mtnfp* mutant (Czaja et al. 2012; Maillet et al. 2011); however, this was inconsistent with the findings from Olah et al. (2005) in which GSE do not depend on *NFP* for stimulation of LRF, implying that another diffusible AM signal may also stimulate LRF, but through a different receptor. *MtNFP*, which is necessary for NF-induced morphological changes during nodulation (Ben Amor et al. 2003), is a membrane localized LysM Receptor-Like-Kinase (LysM-RLK) with an extracellular LysM domain containing three lysin motifs, a transmembrane domain, and an intracellular inactive kinase. In *Medicago* the LysM-RLK family is greatly expanded, with two phylogenetic groups characterized by an active or inactive kinase (Arrighi et al. 2006). An additional LysM-RLK, *MtLyk3* is necessary for initiation of the rhizobial symbiosis, and predicted to act as the entry receptor (Catoira et al. 2001; Limpens et al. 2003; Smit et al. 2007); however *MtLyk3* was shown to be dispensable for Myc-LCO-induced LRF (Maillet et al. 2011). Despite the dependence of Myc-LCO-induced gene expression and LRF on *NFP*, the *mtnfp* mutant appears to have normal AM colonization morphology (Ben Amor et al. 2003), although this remains to be examined more closely. For example, two other symbiosis mutants, *mtnsp2* and *mtnsp1* were both thought to show normal AM colonization until the early stages of AM were examined more closely in the mutants, or lower amounts of spore inoculum were used (Delaux et al. 2013; Maillet et al. 2011).

Of special note is the inability of nsMyc-LCO to induce *MtENOD11* expression. *MtNFP* is required for sMyc-LCO and NF-induced expression of *MtENOD11*, but also the nsMyc-LCO-stimulated LRF (Maillet et al. 2011). NSP2 and NSP1 have been shown to directly regulate *MtENOD11* expression, while *NSP2* and *RAM1* are necessary for the nsMyc-LCO-stimulated LRF, implicating a separate signaling pathway (and possibly separate signal) for partitioning of the NFP response to s and nsMyc-LCOs through different NSP2 interactors, such as NSP1 and RAM1. Such a promiscuous role for NFP has been demonstrated by its non-specific recognition of many different NF, while Lyk3 has been shown to apply the NF stringency for entry (Bensmihen et al. 2011; Smit et al. 2007). In addition to its role in early responses to NF, NFP, and its perception of NF, has been shown to play a later role in morphological changes in the rhizobial symbiosis (Bensmihen et al. 2011; Rival et al. 2012). While transcript induction by NF reached its maximum after 24 hours, induction by Myc-LCOs as compared to NF, began to drop off after only 6 hours, (Czaja et al. 2012). While this supports a more continuous role for NF throughout the rhizobial symbiosis, this continuation may be dependent on the receptor, such that continued signaling for Myc-LCOs may require a receptor to be induced as the symbiosis progresses. Recently, the *MtNFP* paralog, *MtLyr1* has been shown to be specifically induced in cortical cells containing arbuscules (Gomez et al. 2009; Hogekamp and Küster 2013); however, thus far, no phenotypic difference in AM has been reported for an *mtlyr1* mutant. The tropical tree *Parasponia andersonii* is one of the few non-legumes able to enter into symbiosis with rhizobia, as well as AM fungi, and interestingly only contains one ortholog of *NFP* (Op den Camp et al. 2011). Remarkably, *PaNFP* RNAi roots were not only deficient in nodule formation (fewer and underdeveloped) by rhizobia, but also blocked in arbuscule formation; however, overall hyphal infection was not significantly reduced. *PaNFP* may represent a single AM signaling receptor that has become redundant in nodulating legumes through the evolutionary expansion of the NF receptor clade, but later independently co-opted by the

Parasponia-rhizobial symbiosis (Arrighi et al. 2006; Op den Camp et al. 2011; Streng et al. 2011). Additionally, the block of AM colonization prior to arbuscule formation in *PaNFP* RNAi roots further implicates a role for a receptor, and likely AM signals, throughout the symbiosis. Although the *PaNFP* RNAi roots had levels of hyphal colonization comparable to the control, number of hyphopodia were not reported, implying that closer examination may be necessary to observe initiation effects, as it was for implicating *NSP1* and *NSP2* in the AM symbiosis.

Chitin oligomers define a second AM fungal signaling molecule

The discovery of Myc-LCOs further demonstrates the parallels between the AM and rhizobial symbiosis, adding *NFP* and its homologs to the CSSP, as well as providing further evidence for the evolutionary co-option of AM signaling by rhizobia (Streng et al. 2011). However, evidence from experiments using GSE still pointed to AM fungal molecules that induce responses independently of *NFP*, as was the case for Ca^{2+} signaling from *Gigaspora margarita* GSE (Chabaud et al. 2011). Based on the inhibition of GSE-induced Ca^{2+} spiking by chitinase treatment, the diffusible AM fungal signals were predicted to be chitin oligosaccharides (Genre et al. 2013). The authors went on to test the ability of various length COs to elicit Ca^{2+} spiking in atrichoblasts of ROC. They found that CO4 and CO5 were the best elicitors, and that their Ca^{2+} spiking patterns resembled the irregular spiking induced by GSE. Furthermore, they showed that the spiking was dependent on *DMI1* and *DMI2*, but *independent* of *NFP*. Immediately this would distinguish a CO4/5 signaling pathway from the Myc-LCO signaling pathway, implying a second receptor also dependent on part of the CSSP. The addition of GR24 to germinating spores preferentially increased the levels of CO4 and CO5 in GSE, as well as the GSE-induced Ca^{2+} spiking in ROC (Genre et al. 2013). The selective boost of CO4/5 indicated that this was not simply a result of increased metabolic activity such as that induced by strigolactones (Besserer et al. 2008). Both NF and s/nsMyc-

LCOs were tested for their ability to elicit Ca^{2+} spiking in atrichoblasts of wild type and *mtnfp* mutant ROC. In either ROC genotype, NF and sMyc-LCO were only able to elicit Ca^{2+} spiking at exceedingly high concentrations, while a lower concentration of nsMyc-LCO was able to induce a low level of irregular spiking (Genre et al. 2013). Chabaud et al. 2011 had previously shown that NF are unable to induce Ca^{2+} spiking in ROC, as opposed to roots of whole plants where they elicit a regular spiking; however, NF elicits absolutely no spiking in the *mtnfp* mutant (Ben Amor et al. 2003; Genre et al. 2013). CO4/5 were confirmed to induce irregular spiking in both wild type and *mtnfp* whole plant roots; however, whether or not Myc-LCOs are able to induce Ca^{2+} spiking in the roots of whole plants, as opposed to ROC like NF, remains to be determined. The ability of CO4/5 to elicit irregular Ca^{2+} spiking had been studied previously for the purpose of analyzing requirements for NF structure (Oldroyd et al. 2001; Walker et al. 2000). Although a role for CO4/5 in symbiotic fungal signaling had not been envisioned, their elicitation of Ca^{2+} spiking was shown to be dependent on the CSSP, and in the case of Walker et al. (2000), it was further dependent on the pea *NFP* homolog, *SYM10* even at a 100-fold higher concentration than in Genre et al. (2013). This dependence on *PsSYM10*, as opposed to independence of *MtNFP*, reiterates how the degree of crosstalk among the different signaling pathways discussed above can depend greatly on the species of host plant, and possibly also on the AM fungal species. To fully understand the mechanisms underlying these pathways, they must be studied with a variety of both plant and fungal species.

How plants are able to distinguish CO's from symbionts from those of pathogens can only be speculated. GSE from the *Medicago* hemibiotrophic pathogen *Colletotrichum trifolii* were shown to contain CO4 at levels comparable to those of *G. rosea* GSE; however, *C. trifolii* GSE were not able to elicit Ca^{2+} spiking, even with co-application of exogenous CO4 (Genre et al. 2013). This last result implies that an inhibitor or competitor for the CO4-induced Ca^{2+} signaling exists in the *C. trifolii* GSE. Amounting evidence points to a role for

symbiotic signaling in suppression of plant innate immunity (Zamioudis and Pieterse 2012). Like the putative receptors for NF, the chitin receptor responsible for MTI against fungal pathogens, CERK1 in *Arabidopsis*, is also a LysM-RLK. In direct contrast to a CO4/5 receptor for symbiotic signaling, a rice plasma membrane chitin receptor has been shown to preferentially bind CO8, versus other COs, with extremely high affinity (Shibuya et al. 1996). It was recently shown that the CO8 molecule is necessary for dimerization of AtCERK1, which is further necessary for the chitin-related defense responses, including the production of reactive oxygen species (ROS) (Liu et al. 2012). One explanation for why *C. trifolii* GSE do not induce Ca^{2+} spiking is that this response is inhibited by chitin-elicited MTI; however, AM fungi have plenty of chitin in their cell walls, so they must somehow down-regulate chitin-elicited MTI. Interestingly, Liu et al. (2012) went on to show that increasing levels of CO5 mixed with CO8 attenuated its elicitation of MTI. This suggests that the enhanced levels of CO4/5 in strigolactone-treated AM fungal GSE might attenuate AM fungal-elicited MTI. In Genre et al. (2013), the addition of CO4 to the *C. trifolii* GSE did not allow Ca^{2+} spiking, indicating that a high CO4:CO8 ratio is likely not enough to allow CO-induced symbiotic signaling; however, they did not test CO5. Furthermore, Liu et al. (2012) did not test if CO4 can attenuate CO8-elicited ROS production, although evidence that this might be possible comes from a recent study in which both CO4 and CO5 were able to suppress flagellin-elicited ROS in *Arabidopsis* (Liang et al. 2013).

A group of class III chitinases has been shown to be specifically turned on during the AM symbiosis, while those typically induced during pathogen attack or nodulation were not increased in AM, implying that AM-specific chitinases may actually play a role in suppressing defense, possibly through cleaving CO elicitors (Salzer et al. 2000). This could both inhibit MTI by removing CO8, as well as enhance symbiotic signaling by producing more CO4/5. Such a strategy would likely involve a lag between fungal-plant contact and defense suppression, during which time the AM fungal chitin should inevitably briefly trigger

MTI. Evidence for such a lag comes from a slight and transient induction of defense-related transcripts during the initiation of the symbiosis, which then decreased below levels in non-AM roots (Harrison and Dixon 1993; Kapulniki et al. 1996; Liu et al. 2003). Additionally, silencing of two genes involved in the production of ROS resulted in decreased ROS production in response to germinating spores, and induced early and enhanced AM colonization, as well as infection by an oomycete root pathogen (Arthikala et al. 2013; Kiirika et al. 2012). Silencing one of these genes, an NADPH oxidase from pea, leads to greatly enlarged hyphopodia, as well as an increase in *RAM1* transcript, indicating that attenuation of initial AM fungi-elicited ROS production may be necessary for the induction of cutin signaling leading to hyphopodium formation. All of these results indicate that an initial ROS burst may help balance the level of AM colonization.

If suppression of plant defenses during AM formation involves more than a high CO4/5:CO8 ratio, and is necessary for CO4/5 signaling, then it is likely that another fungal signal is working upstream of CO4/5. Recently, several fungal effector proteins have been identified from plant pathogenic fungi that directly interfere with MTI, including LysM containing proteins that can bind CO8 for the interaction with, and deactivation of, CERK1 and other chitin receptors (de Jonge et al. 2010; Lee et al. 2013). The possibility exists for such a role in AM fungi, although through a different strategy, a recently identified effector from *G. intraradices*, SP7, is secreted from the fungus and localizes to the plant nucleus where it interacts with ERF19, a transcription factor turned on by pathogens, in order to suppress ERF19-induced defense responses (Kloppholz et al. 2011). A very similar effector protein had been previously identified from the ectomycorrhizal fungus, *Laccaria bicolor* (Plett et al. 2011). Another candidate AM signal for the suppression of defense are the Myc-LCOs; however, if they do suppress defense, this would likely occur through the DMI pathway as well as NFP, at least for *Medicago*. In support of this, transcriptome analyses of the *dmi3* mutant have identified upregulation of many genes associated with defense (Mitra et

al. 2004; Siciliano et al. 2007). Additionally, while physical stimulation of wildtype root cells has been shown to elicit nuclear repositioning, as in the first step of PPA formation, the same stimulation in the *dmi3* mutant led to programmed cell death, implying that *DMI3* is necessary for inhibiting this response (Genre et al. 2009). A number of studies have shown suppression of defense-related ROS by application of NF, and that it is dependent on *NFP*, but not *DMI1* or *DMI2* (Lohar et al. 2007; Shaw and Long 2003). Furthermore, the *nfp* mutant is also more susceptible to infection by both the root oomycete, *Aphanomyces euteiches* as well as the fungus *Colletotrichum trifolii* (Rey et al. 2013). The true mechanism behind suppression of host defense for the promotion of symbiotic signaling most likely involves a finely tuned combination of all of these possibilities.

Conclusion and Future Perspectives

For several years evidence has pointed to an initial and transient defense response triggered by close contact with AM fungi, but investigations are only just beginning to shed light on the mechanisms by which the fungus dampens these responses. Many intriguing hypotheses can be made by connecting multiple observations: such as AM fungi-induced chitinase expression and the inhibition of CO8-elicited MTI by CO5; or Myc-LCO signaling-dependency on *NFP* and NFP's potential role in defense suppression. However, most all of these hypotheses remain to be tested. The identification of an effector protein secreted by an AM fungus that acts in the nucleus is especially important, as it highlights the potential for future discoveries. Effector mining will become an easier prospect for research of AM fungi after publication of a fungal genome, although the recent publication of the *Glomus intraradices* transcriptome has already indicated high potential, revealing a group of small putatively-secreted proteins (SSP) that are highly upregulated in intraradical hyphae and arbuscules. Included in this group was the *G. intraradices* SP7 effector protein (Tisserant et al. 2012). Beyond identifying the signals, their induced responses must be examined more

closely, which was critical for identifying an AM function for *NSP1* and *NSP2* in *Medicago*. Furthermore, these signals may elicit a variety of responses depending on the stage of symbiosis, such as the case for RAM2's potential participation in both hyphopodium and arbuscule formation (Wang et al. 2012). Additionally, defense reactions should be considered throughout the symbiosis. While ROS may be released initially as a transient defense signal, it has also been observed to accumulate around developing fungal structures later in the symbiosis, where it may continue to play an important role in optimizing the interaction (Puppo et al. 2013). Integration of all of these signaling events and mechanisms will lead to a broader understanding of how plants balance beneficial and pathogenic interactions, and how this balancing is important for both ecological and agricultural systems.

REFERENCES

Akiyama K, Matsuzaki K, Hayashi H (2005) Plant sesquiterpenes induce hyphal branching in arbuscular mycorrhizal fungi. **Nature** 435: 824–827.

Ardourel M, Demont N, Debellé F, Maillet F, de Billy F, Promé JC, Dénarié J, Truchet G (1994) *Rhizobium meliloti* lipooligosaccharide nodulation factors: different structural requirements for bacterial entry into target root hair cells and induction of plant symbiotic developmental responses. **Plant Cell** 6: 1357–1374.

Arrighi J-F, Barre A, Ben Amor B, Bersoult A, Soriano LC, Mirabella R, de Carvalho-Niebel F, Journet E-P, Ghérardi M, Huguet T, Geurts R, Dénarié J, Rougé P, Gough C (2006) The *Medicago truncatula* Lysin Motif-receptor-like kinase gene family includes NFP and new nodule-expressed genes. **Plant Physiol.** 142: 265–279.

Arthikala M-K, Montiel J, Nava N, Santana O, Sánchez-López R, Cárdenas L, Quinto C (2013) PvRbohB negatively regulates *Rhizophagus irregularis* colonization in *Phaseolus vulgaris*. **Plant Cell Physiol.** 54: 1391–1402.

Bécard G, Fortin J (1988) Early events of vesicular-arbuscular mycorrhiza formation on Ri T-DNA transformed roots. **New Phytol.** 108: 211–218.

Ben Amor B, Shaw SL, Oldroyd GED, Maillet F, Penmetsa RV, Cook D, Long SR, Dénarié J, Gough C (2003) The NFP locus of *Medicago truncatula* controls an early step of Nod factor signal transduction upstream of a rapid calcium flux and root hair deformation. **Plant J.** 34: 495–506.

Bensmihen S, de Billy F, Gough C (2011) Contribution of NFP LysM domains to the recognition of Nod factors during the *Medicago truncatula*/*Sinorhizobium meliloti* symbiosis. **PLoS One** 6: e26114.

Besserer A, Bécard G, Jauneau A, Roux C, Séjalon-Delmas N (2008) GR24, a synthetic analog of strigolactones, stimulates the mitosis and growth of the arbuscular mycorrhizal fungus *Gigaspora rosea* by boosting its energy metabolism. **Plant Physiol.** 148: 402–413.

Besserer A, Puech-Pagès V, Kiefer P, Gomez-Roldan V, Jauneau A, Roy S, Portais J-C, Roux C, Bécard G, Séjalon-Delmas N (2006) Strigolactones stimulate arbuscular mycorrhizal fungi by activating mitochondria. **PLoS Biol.** 4: e226.

Boller T, He SY (2009) Innate immunity in plants: an arms race between pattern recognition receptors in plants and effectors in microbial pathogens. **Science** 324: 742–744.

Bonfante P, Genre A (2008) Plants and arbuscular mycorrhizal fungi: an evolutionary-developmental perspective. **Trends Plant Sci.** 13: 492–498.

Bonfante P, Genre A (2010) Mechanisms underlying beneficial plant-fungus interactions in mycorrhizal symbiosis. **Nat. Commun.** 1: 48.

Bonfante P, Requena N (2011) Dating in the dark: how roots respond to fungal signals to establish arbuscular mycorrhizal symbiosis. **Curr. Opin. Plant Biol.** 14: 451–457.

Bonfante-Fasolo P (1984) Anatomy and morphology of VA mycorrhizae, in: Powell C, Bagyaraj D eds., *VA Mycorrhizae*. CRC Press, Boca Raton, FL, pp. 5–33.

Bonfante-Fasolo P, Faccio A, Perotto S, Schubert A (1990) Correlation between chitin distribution and cell wall morphology in the mycorrhizal fungus *Glomus versiforme*. **Mycol. Res.** 94: 157–165.

Brewer PB, Koltai H, Beveridge CA (2013) Diverse roles of strigolactones in plant development. **Mol. Plant** 6: 18–28.

Buee M, Rossignol M, Jauneau A, Ranjeva R, Bécard G (2000) The pre-symbiotic growth of arbuscular mycorrhizal fungi is induced by a branching factor partially purified from plant root exudates. **Mol. Plant. Microbe. Interact.** 13: 693–698.

Catoira R, Galera C, de Billy F, Penmetsa R, Journet E, Maillet F, Rosenberg C, Cook D, Gough C, Dénarié J (2000) Four genes of *Medicago truncatula* controlling components of a nod factor transduction pathway. **Plant Cell** 12: 1647–1666.

Catoira R, Timmers A, Maillet F, Galera C, Penmetsa R, Cook D, Dénarié J, Gough C (2001) The *HCL* gene of *Medicago truncatula* controls *Rhizobium*-induced root hair curling. **Development** 128: 1507–1518.

Chabaud M, Genre A, Sieberer BJ, Faccio A, Fournier J, Novero M, Barker DG, Bonfante P (2011) Arbuscular mycorrhizal hyphopodia and germinated spore exudates trigger Ca^{2+} spiking in the legume and nonlegume root epidermis. **New Phytol.** 189: 347–355.

Chabaud M, Venard C, Defaux-Petras A, Becard G, Barker DG (2002) Targeted inoculation of *Medicago truncatula* in vitro root cultures reveals *MtENOD11* expression during early stages of infection by arbuscular mycorrhizal fungi. **New Phytol.** 156: 265–273.

Czaja LF, Hogekamp C, Lamm P, Maillet F, Martinez EA, Samain E, Dénarié J, Küster H, Hohnjec N (2012) Transcriptional responses toward diffusible signals from symbiotic microbes reveal *MtNFP*- and *MtDMI3*-dependent reprogramming of host gene expression by arbuscular mycorrhizal fungal lipochitooligosaccharides. **Plant Physiol.** 159: 1671–1685.

Czarnecki O, Yang J, Weston DJ, Tuskan GA, Chen J-G (2013) A dual role of strigolactones in phosphate acquisition and utilization in plants. **Int. J. Mol. Sci.** 14: 7681–7701.

D'Haeze W, Holsters M (2002) Nod factor structures, responses, and perception during initiation of nodule development. **Glycobiology** 12: 79R–105R.

De Jonge R, Peter van Esse H, Kombrink A, Shinya T, Desaki Y, Bours R, van der Krol S, Shibuya N, Joosten MHAJ, Thomma BPHJ (2010) Conserved Fungal LysM Effector Ecp6 Prevents Chitin-Triggered Immunity in Plants. **Science** 329: 953–955.

Delaux P, Bécard G, Combier J (2013) NSP1 is a component of the Myc signaling pathway. **New Phytol.** 11: 59–65.

Floss DS, Hause B, Lange PR, Küster H, Strack D, Walter MH (2008) Knock-down of the MEP pathway isogene 1-deoxy-D-xylulose 5-phosphate synthase 2 inhibits formation of arbuscular mycorrhiza-induced apocarotenoids, and abolishes normal expression of mycorrhiza-specific plant marker genes. **Plant J.** 56: 86–100.

Foo E, Yoneyama K, Hugill CJ, Quittenden LJ, Reid JB (2013) Strigolactones and the regulation of pea symbioses in response to nitrate and phosphate deficiency. **Mol. Plant** 6: 76–87.

Genre A, Ivanov S, Fendrych M, Faccio A, Zársky V, Bisseling T, Bonfante P (2012) Multiple exocytotic markers accumulate at the sites of perifungal membrane biogenesis in arbuscular mycorrhizas. **Plant Cell Physiol.** 53: 244–255.

Genre A, Chabaud M, Balzergue C, Puech-Pagès V, Novero M, Rey T, Fournier J, Rochange S, Bécard G, Bonfante P, Barker DG (2013) Short-chain chitin oligomers from arbuscular mycorrhizal fungi trigger nuclear Ca^{2+} spiking in *Medicago truncatula* roots and their production is enhanced by strigolactone. **New Phytol.** 198: 190–202.

Genre A, Chabaud M, Faccio A, Barker DG, Bonfante P (2008) Prepenetration apparatus assembly precedes and predicts the colonization patterns of arbuscular mycorrhizal fungi within the root cortex of both *Medicago truncatula* and *Daucus carota*. **Plant Cell** 20: 1407–20.

Genre A, Chabaud M, Timmers T, Bonfante P, Barker DG (2005) Arbuscular mycorrhizal fungi elicit a novel intracellular apparatus in *Medicago truncatula* root epidermal cells before infection. **Plant Cell** 17: 3489–3499.

Genre A, Ortu G, Bertoldo C, Martino E, Bonfante P (2009) Biotic and Abiotic Stimulation of Root Epidermal Cells Reveals Common and Specific Responses to Arbuscular Mycorrhizal Fungi. **Plant Physiol.** 149: 1424–1434.

Gilbert R, Johnson A, Dean R (1996) Chemical signals responsible for appressorium formation in the rice blast fungus *Magnaporthe grisea*. **Physiol. Mol. Plant Pathol.** 48: 335–346.

Giovannetti M, Sbrana C, Avio L, Citernesi A, Logi C (1993) Differential hyphal morphogenesis in arbuscular mycorrhizal fungi during pre-infection stages. **New Phytol.** 125: 587–593.

Gobbato E, Marsh JF, Vernié T, Wang E, Maillet F, Kim J, Miller JB, Sun J, Bano SA, Ratet P, Mysore KS, Dénarié J, Schultze M, Oldroyd GED (2012) A GRAS-type transcription factor with a specific function in mycorrhizal signaling. **Curr. Biol.** 22: 1–6.

Gobbato E, Wang E, Higgins G, Bano S, Henry C, Schultze M, Oldroyd G (2013) *RAM1* and *RAM2* function and expression during Arbuscular Mycorrhizal Symbiosis and *Aphanomyces euteiches* colonization. **Plant Signal. Behav.** 8: e26049.

Gomez SK, Javot H, Deewatthanawong P, Torres-jerez I, Tang YH, Blancaflor EB, Udvardi MK, Harrison MJ (2009) *Medicago truncatula* and *Glomus intraradices* gene expression in cortical cells harboring arbuscules in the arbuscular mycorrhizal symbiosis. **BMC Plant Biol.** 9: 10–29.

Gomez-Roldan V, Fermas S, Brewer PB, Puech-Pagès V, Dun EA, Pillot J-P, Letisse F, Matusova R, Danoun S, Portais J-C, Bouwmeester H, Bécard G, Beveridge CA, Rameau C, Rochange SF (2008) Strigolactone inhibition of shoot branching. **Nature** 455: 189–194.

Govindarajulu M, Pfeffer PE, Jin H, Abubaker J, Douds DD, Allen JW, Bücking H, Lammers PJ, Shachar-Hill Y (2005) Nitrogen transfer in the arbuscular mycorrhizal symbiosis. **Nature** 435: 819–823.

Gutjahr C, Casieri L, Paszkowski U (2009) *Glomus intraradices* induces changes in root system architecture of rice independently of common symbiosis signaling. **New Phytol.** 182: 829–837.

Hamel L-P, Beaudoin N (2010) Chitooligosaccharide sensing and downstream signaling: contrasted outcomes in pathogenic and beneficial plant-microbe interactions. **Planta** 232: 787–806.

Harrison M, Dixon R (1993) Isoflavonoid accumulation and expression of defense gene transcripts during the establishment of vesicular-arbuscular mycorrhizal associations in roots of *Medicago truncatula*. **Mol. Plant Microbe Interact.** 6: 643–654.

Harrison MJ (2012) Cellular programs for arbuscular mycorrhizal symbiosis. **Curr. Opin. Plant Biol.** 15: 691–698.

Helber N, Wippel K, Sauer N, Schaarschmidt S, Hause B, Requena N (2011) A versatile monosaccharide transporter that operates in the arbuscular mycorrhizal fungus *Glomus* sp is crucial for the symbiotic relationship with plants. **Plant Cell** 23: 3812–3823.

Hogekamp C, Küster H (2013) A roadmap of cell-type specific gene expression during sequential stages of the arbuscular mycorrhiza symbiosis. **BMC Genomics** 14: 306.

Jamil M, Charnikhova T, Verstappen F, Bouwmeester H (2010) Carotenoid inhibitors reduce strigolactone production and *Striga hermonthica* infection in rice. **Arch. Biochem. Biophys.** 504: 123–131.

Javot H, Penmetsa RV, Terzaghi N, Cook DR, Harrison MJ (2007a) A *Medicago truncatula* phosphate transporter indispensable for the arbuscular mycorrhizal symbiosis. **Proc. Natl. Acad. Sci.** 104: 1720–1725.

Javot H, Pumplin N, Harrison MJ (2007b) Phosphate in the arbuscular mycorrhizal symbiosis: transport properties and regulatory roles. **Plant. Cell Environ.** 30: 310–322.

Jones JDG, Dangl JL (2006) The plant immune system. **Nature** 444: 323–329.

Journet E, El-Gachtouli N, Vernoud V, de Billy F, Pichon M, Dedieu A, Arnould C, Morandi D, Barker D, Gianinazzi-Pearson V (2001) *Medicago truncatula ENOD11*: a novel RPRP-encoding early nodulin gene expressed during mycorrhization in arbuscule-containing cells. **Mol. Plant. Microbe. Interact.** 14: 737–748.

Jung SC, Martinez-Medina A, Lopez-Raez JA, Pozo MJ (2012) Mycorrhiza-induced resistance and priming of plant defenses. **J. Chem. Ecol.** 38: 651–664.

Kaku H, Nishizawa Y, Ishii-Minami N, Akimoto-Tomiyama C, Dohmae N, Takio K, Minami E, Shibuya N (2006) Plant cells recognize chitin fragments for defense signaling through a plasma membrane receptor. **Proc. Natl. Acad. Sci.** 103: 11086–11091.

Kapulnik BYY, Volpin H, Itzhakp H, Ganon D, Galilp S, Orna RD, Yigal S, Ilan E, Okon Y (1996) Suppression of defence responses in mycorrhizal alfalfa and tobacco roots. **New Phytol.** 133: 59–64.

Kiirika LM, Bergmann HF, Schikowsky C, Wimmer D, Korte J, Schmitz U, Niehaus K, Colditz F (2012) Silencing of the Rac1 GTPase *MtROP9* in *Medicago truncatula* stimulates early mycorrhizal and oomycete root colonizations but negatively affects rhizobial infection. **Plant Physiol.** 159: 501–516.

Kloppholz S, Kuhn H, Requena N (2011) A secreted fungal effector of *Glomus intraradices* promotes symbiotic biotrophy. **Curr. Biol.** 21: 1204–1209.

Kobae Y, Hata S (2010) Dynamics of periarbuscular membranes visualized with a fluorescent phosphate transporter in arbuscular mycorrhizal roots of rice. **Plant Cell Physiol.** 51: 341–353.

Kohlen W, Charnikhova T, Liu Q, Bours R, Domagalska MA, Beguerie S, Verstappen F, Leyser O, Bouwmeester H, Ruyter-Spira C (2011) Strigolactones are transported through the xylem and play a key role in shoot architectural response to phosphate deficiency in nonarbuscular mycorrhizal host Arabidopsis. **Plant Physiol.** 155: 974–987.

Koltai H, LekKala SP, Bhattacharya C, Mayzlish-Gati E, Resnick N, Wininger S, Dor E, Yoneyama Kaori, Yoneyama Koichi, Hershenhorn J, Joel DM, Kapulnik Y (2010) A tomato strigolactone-impaired mutant displays aberrant shoot morphology and plant interactions. **J. Exp. Bot.** 61: 1739–1749.

Kosuta S, Chabaud M, Gough C, De J, Barker DG, Bécard G (2003) A Diffusible Factor from Arbuscular Mycorrhizal Fungi Induces Symbiosis-Specific *MtENOD11* Expression in Roots of *Medicago truncatula*. **Plant Physiol.** 131: 952–962.

Kosuta S, Hazledine S, Sun J, Miwa H, Morris RJ, Downie JA, Oldroyd GED (2008) Differential and chaotic calcium signatures in the symbiosis signaling pathway of legumes. **Proc. Natl. Acad. Sci.** 105: 9823–9828.

Kretzschmar T, Kohlen W, Sasse J, Borghi L, Schlegel M, Bachelier JB, Reinhardt D, Bours R, Bouwmeester HJ, Martinoia E (2012) A petunia ABC protein controls strigolactone-dependent symbiotic signalling and branching. **Nature** 483: 341–344.

Kuhn H, Küster H, Requena N (2010) Membrane steroid-binding protein 1 induced by a diffusible fungal signal is critical for mycorrhization in *Medicago truncatula*. **New Phytol.** 185: 716–733.

Lee W, Rudd J, Hammon-Kosack K, Kanyuka K (2013) *Mycosphaerella graminicola* LysM effector-mediated stealth pathogenesis subverts recognition through both CERK1 and CEBiP homologues in wheat. **Mol. Plant-Microbe Interact.** Accepted for publication.

Liang Y, Cao Y, Tanaka K, Thibivilliers S, Wan J, Choi J, Kang CH, Qiu J, Stacey G (2013) Nonlegumes Respond to Rhizobial Nod Factors by Suppressing the Innate Immune Response. **Science** 341: 1384–1387.

Limpens E, Franken C, Smit P, Willemse J, Bisseling T, Geurts R (2003) LysM domain receptor kinases regulating rhizobial Nod factor-induced infection. **Science** 302: 630–633.

Liu J, Blaylock L, Endre G, Cho J, Town CD, Vandenbosch KA, Harrison MJ (2003) Transcript profiling coupled with spatial expression analyses reveals genes involved in disinct developmental stages of an arbuscular mycorrhizal symbiosis. **Plant Cell** 15: 2106–2123.

Liu J, Maldonado-Mendoza I, Lopez-Meyer M, Cheung F, Town CD, Harrison MJ (2007) Arbuscular mycorrhizal symbiosis is accompanied by local and systemic alterations in gene expression and an increase in disease resistance in the shoots. **Plant J.** 50: 529–544.

Liu T, Liu Z, Song C, Hu Y, Han Z, She J, Fan F, Wang J, Jin C, Chang J, Zhou J-M, Chai J (2012) Chitin-induced dimerization activates a plant immune receptor. **Science** 336: 1160–1164.

Liu W, Kohlen W, Lillo A, Op den Camp R, Ivanov S, Hartog M, Limpens E, Jamil M, Smaczniak C, Kaufmann K, Yang W-C, Hooiveld GJEJ, Charnikhova T, Bouwmeester HJ, Bisseling T, Geurts R (2011) Strigolactone biosynthesis in *Medicago truncatula* and rice requires the symbiotic GRAS-type transcription factors NSP1 and NSP2. **Plant Cell** 23: 3853–3865.

Logi C, Sbrana C, Giovannetti M (1998) Cellular events involved in survival of individual arbuscular mycorrhizal symbionts growing in the absence of the host. **Appl. Environ. Microbiol.** 64: 3473–3479.

Lohar DP, Haridas S, Gantt JS, VandenBosch KA (2007) A transient decrease in reactive oxygen species in roots leads to root hair deformation in the legume-rhizobia symbiosis. **New Phytol.** 173: 39–49.

Maillet F, Poinsot V, André O, Puech-Pagès V, Haouy A, Gueunier M, Cromer L, Giraudet D, Formey D, Niebel A, Martinez EA, Driguez H, Bécard G, Dénarié J (2011) Fungal lipochitooligosaccharide symbiotic signals in arbuscular mycorrhiza. **Nature** 469: 58–63.

Matusova R, Rani K, Verstappen W, Franssen M, Beale M, Bouwmeester H (2005) The strigolactone germination stimulants of the plant-parasitic *Striga* and *Orobanche* spp. are derived from the carotenoid pathway. **Plant Physiol.** 139: 920–934.

Mendoza-Mendoza A, Berndt P, Djamei A, Weise C, Linne U, Marahiel M, Vranes M, Kämper J, Kahmann R (2009) Physical-chemical plant-derived signals induce differentiation in *Ustilago maydis*. **Mol. Microbiol.** 71: 895–911.

Minami E, Kouchi H, Carlson R, Cohn J, Kolli V, Day R, Ogawa T, Stacey G (1996) Cooperative action of lipo-chitin nodulation signals on the inductions of the early nodulin, ENOD2, in soybean roots. **Mol. Plant Microbe Interact.** 9: 574–583.

Mitra RM, Shaw SL, Long SR (2004) Six nonnodulating plant mutants defective for Nod factor-induced transcriptional changes associated with the legume-rhizobia symbiosis. **Proc. Natl. Acad. Sci.** 101: 10217–10222.

Mukherjee A, Ané J-M (2011) Germinating spore exudates from arbuscular mycorrhizal fungi: molecular and developmental responses in plants and their regulation by ethylene. **Mol. plant-microbe Interact.** 24: 260–270.

Nagahashi G, Douds D (2007) Separated components of root exudate and cytosol stimulate different morphologically identifiable types of branching responses by arbuscular mycorrhizal fungi. **Mycol. Res.** 111: 487–492.

Nagahashi G, Douds DD (2011) The effects of hydroxy fatty acids on the hyphal branching of germinated spores of AM fungi. **Fungal Biol.** 115: 351–358.

Nagahashi G, Douds DD, Ferhatoglu Y (2010) Functional categories of root exudate compounds and their relevance to AM fungal growth, in: Koltai H, Kapulnik Y eds., *Arbuscular Mycorrhizas: Physiology and Function*. Springer Netherlands, Dordrecht, pp. 33–56.

Nagahashi G, Douds Jr DD, Abney GD (1996) Phosphorus amendment inhibits hyphal branching of the VAM fungus *Gigaspora margarita* directly and indirectly through its effect on root exudation. **Mycorrhiza** 6: 403–408.

Navazio L, Moscatiello R, Genre A, Novero M, Baldan B, Bonfante P, Mariani P (2007) A diffusible signal from arbuscular mycorrhizal fungi elicits a transient cytosolic calcium elevation in host plant cells. **Plant Physiol.** 144: 673–681.

Oláh B, Brière C, Bécard G, Dénarié J, Gough C (2005) Nod factors and a diffusible factor from arbuscular mycorrhizal fungi stimulate lateral root formation in *Medicago truncatula* via the DMI1/DMI2 signalling pathway. **Plant J.** 44: 195–207.

Oldroyd GE, Mitra RM, Wais RJ, Long SR (2001) Evidence for structurally specific negative feedback in the Nod factor signal transduction pathway. **Plant J.** 28: 191–199.

Oldroyd GED (2013) Speak, friend, and enter: signalling systems that promote beneficial symbiotic associations in plants. **Nat. Rev. Microbiol.** 11: 252–263.

Oldroyd GED, Murray JD, Poole PS, Downie JA (2011) The rules of engagement in the legume-rhizobial symbiosis. **Annu. Rev. Genet.** 45: 119–144.

Op den Camp R, Streng A, De Mita S, Cao Q, Polone E, Liu W, Ammiraju JSS, Kudrna D, Wing R, Untergasser A, Bisseling T, Geurts R (2011) LysM-type mycorrhizal receptor recruited for rhizobium symbiosis in nonlegume *Parasponia*. **Science** 331: 909–912.

Parniske M (2000) Intracellular accommodation of microbes by plants: a common developmental program for symbiosis and disease? **Curr. Opin. Plant Biol.** 3: 320–328.

Parniske M (2008) Arbuscular mycorrhiza: the mother of plant root endosymbioses. **Nat. Rev. Microbiol.** 6: 763–775.

Péret B, Clément M, Nussaume L, Desnos T (2011) Root developmental adaptation to phosphate starvation: better safe than sorry. **Trends Plant Sci.** 16: 442–450.

Pirozynski K, Malloch D (1975) The origin of land plants: A matter of mycotrophism. **Biosystems** 6: 153–164.

Plaxton WC, Tran HT (2011) Metabolic adaptations of phosphate-starved plants. **Plant Physiol.** 156: 1006–1015.

Plett JM, Kemppainen M, Kale SD, Kohler A, Legué V, Brun A, Tyler BM, Pardo AG, Martin F (2011) A secreted effector protein of *Laccaria bicolor* is required for symbiosis development. **Curr. Biol.** 21: 1197–1203.

Pozo MJ, Azcón-Aguilar C (2007) Unraveling mycorrhiza-induced resistance. **Curr. Opin. Plant Biol.** 10: 393–398.

Pueppke SG, Broughton WJ (1999) *Rhizobium* sp. strain NGR234 and *R. fredii* USDA257 share exceptionally broad, nested host ranges. **Mol. Plant. Microbe. Interact.** 12: 293–318.

Pumplin N, Harrison MJ (2009) Live-cell imaging reveals periarbuscular membrane domains and organelle location in *Medicago truncatula* roots during arbuscular mycorrhizal symbiosis. **Plant Physiol.** 151: 809–819.

Puppo A, Pauly N, Boscari A, Mandon K, Brouquisse R (2013) Hydrogen peroxide and nitric oxide: key regulators of the Legume-*Rhizobium* and mycorrhizal symbioses. **Antioxid. Redox Signal.** 18: 2202–19.

Redecker D (2000) Glomalean Fungi from the Ordovician. **Science** 289: 1920–1921.

Remy W, Taylor T, Hass H, Kerp H (1994) Four hundred-million-year-old vesicular arbuscular mycorrhizae. **Proc. Natl. Acad. Sci.** 91: 11841–11843.

Rey T, Nars A, Bonhomme M, Bottin A, Huguet S, Balzergue S, Jardinaud M-F, Bono J-J, Cullimore J, Dumas B, Gough C, Jacquet C (2013) NFP, a LysM protein controlling Nod factor perception, also intervenes in *Medicago truncatula* resistance to pathogens. **New Phytol.** 198: 875–886.

Rival P, de Billy F, Bono J-J, Gough C, Rosenberg C, Bensmihen S (2012) Epidermal and cortical roles of *NFP* and *DMI3* in coordinating early steps of nodulation in *Medicago truncatula*. **Development** 139: 3383–3391.

Ruyter-Spira C, Al-Babili S, van der Krol S, Bouwmeester H (2013) The biology of strigolactones. **Trends Plant Sci.** 18: 72–83.

Salzer P, Bonanomi A, Beyer K, Vögeli-Lange R, Aeschbacher R, Lange J, Wiemken A, Kim D, Cook DR, Boller T (2000) Differential expression of eight chitinase genes in *Medicago truncatula* roots during mycorrhiza formation, nodulation, and pathogen infection. **Mol. Plant. Microbe. Interact.** 13: 763–777.

Schwessinger B, Ronald PC (2012) Plant innate immunity: perception of conserved microbial signatures. **Annu. Rev. Plant Biol.** 63: 451–482.

Shaw S, Long S (2003) Nod factor inhibition of reactive oxygen efflux in a host legume. **Plant Physiol.** 132: 2196–2204.

Shibuya N, Ebisu N, Kamada Y, Kaku H, Conn J, Ito Y (1996) Localization and binding characteristics of a high-affinity binding site for N-acetylchitooligosaccharide elicitor in the plasma membrane from suspension-cultured rice cells suggest a role as a receptor for the elicitor signal at the cell surface. **Plant Cell Physiol.** 37: 894–898.

Siciliano V, Genre A, Balestrini R, Cappellazzo G, DeWit PJGM, Bonfante P (2007) Transcriptome analysis of arbuscular mycorrhizal roots during development of the prepenetration apparatus. **Plant Physiol.** 144: 1455–1466.

Simon L, Bousquet J, Lévesque R, Lalonde M (1993) Origin and diversification of endomycorrhizal fungi and coincidence with vascular land plants. **Nature** 363: 67–69.

Smit P, Limpens E, Geurts R, Fedorova E, Dolgikh E, Gough C, Bisseling T (2007) Medicago LYK3, an entry receptor in rhizobial nodulation factor signaling. **Plant Physiol.** 145: 183–191.

Smith S, Read D (2008) *Mycorrhizal Symbiosis*, 3rd ed. Academic Press, London, UK.

Streng A, op den Camp R, Bisseling T, Geurts R (2011) Evolutionary origin of rhizobium Nod factor signaling. **Plant Signal. Behav.** 6: 1510–1504.

Tamasloukht M, Séjalon-Delmas N, Kluever A, Jauneau A, Roux C, Bécard G, Franken P (2003) Root factors induce mitochondrial-related gene expression and fungal respiration during the dvelopment switch from asymbiosis to presymbiosis in the arbuscular mycorrhizal fungus *Gigaspora rosea*. **Plant Physiol.** 131: 1468–1478.

Tisserant E, Kohler A, Dozolme-Seddas P, Balestrini R, Benabdellah K, Colard A, Croll D, Da Silva C, Gomez SK, Koul R, Ferrol N, Fiorilli V, Formey D, Franken P, Helber N, Hijri M, Lanfranco L, Lindquist E, Liu Y, Malbreil M, Morin E, Poulain J, Shapiro H, van Tuinen D, Waschke A, Azcón-Aguilar C, Bécard G, Bonfante P, Harrison MJ, Küster H, Lammers P, Paszkowski U, Requena N, Rensing S, Roux C, Sanders IR, Shachar-Hill Y, Tuskan G, Young JPW, Gianinazzi-Pearson V, Martin F (2012) The transcriptome of the arbuscular mycorrhizal fungus *Glomus intraradices* (DAOM 197198) reveals functional tradeoffs in an obligate symbiont. **New Phytol.** 193: 755–769.

Umehara M, Hanada A, Magome H, Takeda-Kamiya N, Yamaguchi S (2010) Contribution of strigolactones to the inhibition of tiller bud outgrowth under phosphate deficiency in rice. **Plant Cell Physiol.** 51: 1118–1126.

Umehara M, Hanada A, Yoshida S, Akiyama K, Arite T, Takeda-Kamiya N, Magome H, Kamiya Y, Shirasu K, Yoneyama K, Kyozuka J, Yamaguchi S (2008) Inhibition of shoot branching by new terpenoid plant hormones. **Nature** 455: 195–200.

Vogel JT, Walter MH, Giavalisco P, Lytovchenko A, Kohlen W, Charnikhova T, Simkin AJ, Goulet C, Strack D, Bouwmeester HJ, Fernie AR, Klee HJ (2010) SlCCD7 controls strigolactone biosynthesis, shoot branching and mycorrhiza-induced apocarotenoid formation in tomato. **Plant J.** 61: 300–311.

Walker S, Viprey V, Downie J (2000) Dissection of nodulation signaling using pea mutants defective for calcium spiking induced by nod factors and chitin oligomers. **Proc. Natl. Acad. Sci. U. S. A.** 97: 13413–13418.

Wang B, Yeun LH, Xue J-Y, Liu Y, Ané J-M, Qiu Y-L (2010) Presence of three mycorrhizal genes in the common ancestor of land plants suggests a key role of mycorrhizas in the colonization of land by plants. **New Phytol.** 186: 514–525.

Wang E, Schornack S, Marsh JF, Gobbato E, Schwessinger B, Eastmond P, Schultze M, Kamoun S, Oldroyd GED (2012) A common signaling process that promotes mycorrhizal and oomycete colonization of plants. **Curr. Biol.** 22: 2242–2246.

Weidmann S, Sanchez L, Descombin J, Chatagnier O, Gianinazzi S, Gianinazzi-Pearson V (2004) Fungal elicitation of signal transduction-related plant genes precedes mycorrhiza establishment and requires the *dmi3* gene in *Medicago truncatula*. **Mol. Plant. Microbe. Interact.** 17: 1385–1393.

Wilson RA, Talbot NJ (2009) Under pressure: investigating the biology of plant infection by *Magnaporthe oryzae*. **Nat. Rev. Microbiol.** 7: 185–195.

Xie X, Yoneyama K (2010) The strigolactone story. **Annu. Rev. Phytopathol.** 48: 93–117.

Yoneyama Kaori, Xie X, Kusumoto D, Sekimoto H, Sugimoto Y, Takeuchi Y, Yoneyama Koichi (2007a) Nitrogen deficiency as well as phosphorus deficiency in sorghum promotes the production and exudation of 5-deoxystrigol, the host recognition signal for arbuscular mycorrhizal fungi and root parasites. **Planta** 227: 125–132.

Yoneyama Kaori, Yoneyama Koichi, Takeuchi Y, Sekimoto H (2007b) Phosphorus deficiency in red clover promotes exudation of orobanchol, the signal for mycorrhizal symbionts and germination stimulant for root parasites. **Planta** 225: 1031–1038.

Zamioudis C, Pieterse CMJ (2012) Modulation of host immunity by beneficial microbes. **Mol. Plant. Microbe. Interact.** 25: 139–150.

CHAPTER 2

GENE SILENCING IN *MEDICAGO TRUNCATULA* ROOTS USING RNAi[2]

Abstract[3]

Medicago truncatula is used widely as a model system for studies of root symbioses, interactions with parasitic nematodes and fungal pathogens, as well as studies of development and secondary metabolism. In *Medicago truncatula* as well as other legumes, RNA interference (RNAi) coupled with *Agrobacterium rhizogenes*-mediated root transformation, has been used very successfully for analyses of gene function in roots. One of the major advantages of this approach is the ease and relative speed with which transgenic roots can be generated. There are several methods, both for the generation of the RNAi constructs and the root transformation. Here we provide details of an RNAi and root transformation protocol that has been used successfully in *M. truncatula* and which can be scaled up to enable the analysis of several hundred constructs.

---

[2] This chapter is published as Floss D.S., Schmitz A.M., Starker C.G., Gantt J.S., Harrison M.J. (2013) Gene Silencing in *Medicago truncatula* Roots Using RNAi. In: Rose R. (eds) Legume Genomics. Methods in Molecular Biology (Methods and Protocols), vol 1069. Humana Press, Totowa, NJ

[3] Section was contributed by other author on paper.

Introduction[4]

Double-stranded RNAs, which have the capacity to 'silence' gene expression, have been widely used for studies of gene function in plant animal and invertebrate systems (Helliwell et al. 2002; Pasquinelli and Ruvkun 2002; Hannon 2002). There is a variety of different approaches (Ossowski, Schwab, and Weigel 2008), but RNA interference (RNAi) by inverted repeat or so-called hairpin constructs has proved to be particularly effective in range of plant species, including legumes (Wesley et al. 2001; Gubler et al. 2008; Limpens et al 2003; Javot et al. 2007; Subramanian et al 2005). Expression of an inverted repeat construct, homologous to the gene of interest, results in the creation of a hairpin (hp) RNA which is recognized and cleaved by an RNAse-III endoribonuclease, Dicer, into 21-22 nucleotides. Generally one strand of these short RNA oligonucleotides is then incorporated into the RNA-induced Silencing Complex (RISC) and this complex facilitates recognition of the homologous mRNA, and subsequently cleavage and degradation, or in some cases inhibition of translation (Dunoyer et al. 2007). In plants, RNAi constructs are generally delivered to plant cells in binary vectors. Efficient cloning of the inverted repeats constructs in binary vectors has been facilitated by the generation of Gateway©(GW) compatible binary vectors such as the pHellsgate vector series (Helliwell et al. 2002; Helliwell and Waterhouse 2003; Helliwell and Waterhouse 2005), which permit the use of the Gateway site-specific recombination cloning technology for simultaneous, directional insertion of inverted repeats (Hartley, Temple and Brasch 2000) (Invitrogen). pHellsgate8, a vector used successfully in many plant species, also contains a spacer that encodes an intron, which has been shown to increase silencing efficiency (Wesley et al. 2001).

The binary vectors containing the RNAi hairpin constructs are readily introduced into plant cells through *Agrobacterium tumefaciens*- or *Agrobacterium rhizogenes*-mediated transformation. In recent years, *A. rhizogenes*-mediated transformation has been used to

[4] Section was contributed by other author on paper.

generate 'composite plants', which have genetically transformed roots but wild-type shoots (Boisson-Dernier et al. 2001; Collier et al. 2005). This approach is particularly useful for studies of many aspects of gene function in roots because of the speed with which composite plants can be generated. This approach has accelerated the pace of root biology research and has been used widely, particularly in legumes (Floss et al. 2008; Pumplin et al. 2010), where the generation of stable transformants via *A. tumefaciens*-mediated transformation is a lengthy process. Several protocols for efficient *A. rhizogenes*-mediated transformation of *M. truncatula* have been published (Boisson-Dernier et al. 2001; Vieweg et al. 2004).

Here, we describe a cloning procedure based on Gateway technology to generate RNAi constructs, and a procedure for their introduction into *M. truncatula* roots via *A. rhizogenes*-mediated transformation. The latter is modified from Boisson-Dernier et al. 2001. The resulting composite plants are suitable for studies of gene function in roots, nodules and during AM symbiosis (Ivashuta et al. 2005).

Materials[5]

General

1. PCR reagents: sterile deionized distilled H_2O (H_2O_{dd}), primers (see Methods), template (*M. truncatula* cDNA or PCR product from step 1 in Methods), dNTPs, clear Taq polymerase buffer, Taq polymerase
2. Plasmids: donor vector with *att*P sites; binary destination vector appropriate for RNAi with *att*R sites. For the purpose of this chapter we will present methods concerning the use of pDONR207 (gentamicin selection) and pHellsgate8 (Helliwell et al. 2002) (spectinomycin selection) as donor and destination vectors, respectively. The plasmid concentrations should be approximately 150 ng/µL (Note 1).

[5] Section was jointly contributed by all authors.

3. Gateway® reagents: BP Clonase™ II Enzyme mix, LR Clonase™ II mix, Proteinase K (Invitrogen)
4. Antibiotics: gentamicin (50 mg/mL stock solution), spectinomycin (50 mg/mL stock solution), streptomycin (100 mg/mL stock solution), and kanamycin (50 mg/mL stock solution)
5. Heat-shock competent DH5α *E. coli*
6. Heat-shock competent *A. rhizogenes* ARqua1
7. 50% glycerol in H_2O_{dd}
8. *M. truncatula* seeds
9. Concentrated sulphuric acid (H_2SO_4)
10. Bleach solution containing 6% sodium hypochlorite
11. 0.1% Tween 20 in H_2O_{dd}
12. Petri plates for germinating the seeds (we use glass petri plates as they can be re-used).

Media

1. LB medium: Dissolve 10 g tryptone, 10 g NaCl, and 5 g yeast extract in just under 1 L H_2O_{dd}. Adjust pH to 7.0 with NaOH. Bring volume to exactly 1 L with H_2O_{dd} in a graduated cylinder. Pour solution into a 2-L Erlenmeyer flask. For solid media, add 15 g agar. Autoclave 30 minutes on a liquid cycle. For solid media, allow solution to cool to 50ºC then add 50 mg/L gentamicin for selection of pDONR207 in DH5α, or 100 mg/L spectinomycin for selection of pHellsgate8 in DH5α and pour plates immediately.
2. YEP media: Dissolve 10 g bacto peptone, 5 g NaCl, and 10 g yeast extract in just under 1L H_2O_{dd}. Adjust pH to 7.0 with NaOH. Bring volume to exactly 1 L with H_2O_{dd} in a graduated cylinder. Pour solution into a 2-L Erlenmeyer flask. For solid media, add 15 g agar. Autoclave 30 minutes on a liquid cycle. For solid media, allow

solution to cool to 50ºC then add 150 mg/L spectinomycin for selection of pHellsgate8 in *A. rhizogenes* ARqua1 and 100 mg/L streptomycin for selection of ARqua1's tumor-inducing plasmid, and pour plates immediately.

3. TY medium for *A. rhizogenes* ARqua1: Dissolve 5 g tryptone, 880 mg $CaCl_2$, and 3 g yeast extract in just under 1 L H_2O_{dd}. Adjust pH to 7.0 with NaOH. Bring volume to exactly 1 L with H_2O_{dd} in a graduated cylinder. Pour solution into a 2-L Erlynmeyer flask. Add 15 g agar. Autoclave 30 minutes on a liquid cycle. Allow solution to cool to 50ºC then add 150 mg/L spectinomycin for selection of pHellsgate8 in *A. rhizogenes* ARqua1 and 100 mg/L streptomycin for selection of ARqua1's tumor-inducing plasmid, and pour plates immediately.
4. Modified Fähraeus medium for *M. truncatula*: 0.9 mM $CaCl_2$, 0.5 mM $MgSO_4$, 20 µM KH_2PO_4, 10 µM Na_2PO_4, 20 µM ferric citrate, 1.0 mM NH_4NO_3, 33 µg/L $MnCl_2$, 33 µg/L $CuSO_4$, 7 µg/L $ZnSO_4*7H_2O$, 100 µg/L H_3BO_3, 33 µg/L Na_2MoO_4, 218 mg/L MES free acid monohydrate, and 2.5 g/L Gelzan™ CM (Sigma-Aldrich®) (Liu et al. 2003). This version of Fähraeus was modified from the version described by Boisson-Dernier et al. 2001.

   Prepare individual stock solutions for the first 11 ingredients. We typically make stocks with the following concentrations: 0.9 M $CaCl_2$, 0.5 M $MgSO_4$, 0.35 M KH_2PO_4, 0.2 M Na_2HPO_4, 20 mM ferric citrate, 0.5 M NH_4NO_3, 1 mg/ml H_3BO_3 and 1 mg/ml Na_2MoO_4. The $MnCL_2$, $CuSO_4$ and $ZnSO_4*7H_2O$ can be combined in a micro-nutrient stock solution of 1 mg/ml $MnCL_2$, 1 mg/ml $CuSO_4$ and 0.42 mg/ml $ZnSO_4*7H_2O$.

   For 1L of Fähraeus media add the appropriate amount of each stock solution and 218 mg MES free acid monohydrate to 500 mL H_2O_{dd}. Bring volume very close to 1 L and adjust pH to 7.4 with 1 M NaOH. Carefully add 2.5 g Gelzan™ (see Note 2). Autoclave for 35 min and allow solution to cool to 50˚C. Add 25mg/L kanamycin to

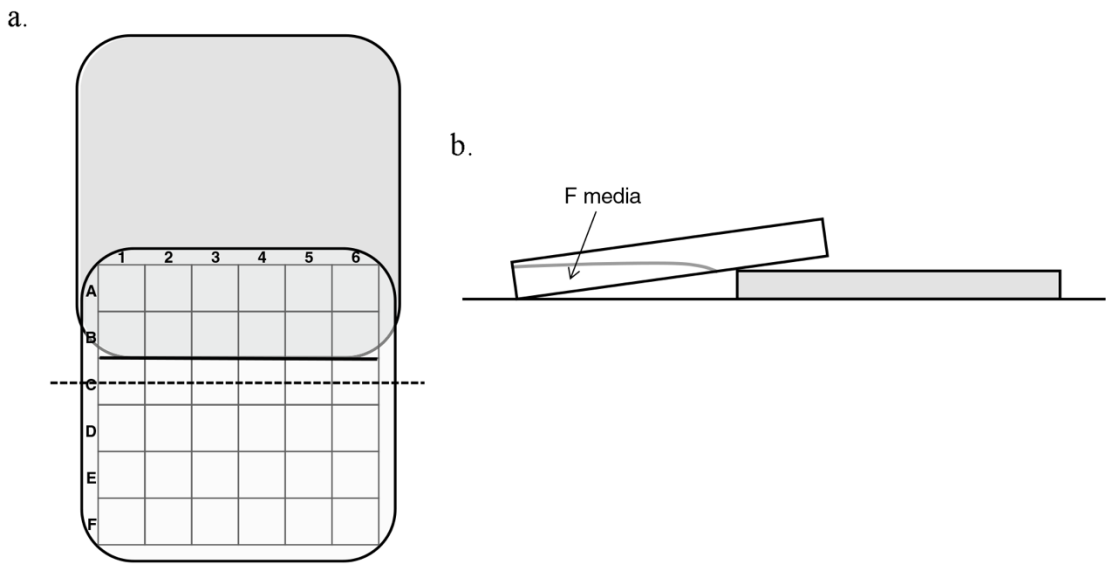

Figure 2-1: Preparation of plates containing a slant of F media. a) Plan view. **b)** Lateral view. The square petri plates have a grid printed on the bottom. This is a convenient marker. To create the appropriate angle, tilt the bottom of the plate and rest it on the lid. The point of contact between the bottom and the lid (grey) should be the line at the lower edge of row B on the grid (see thick black line). Add media to the bottom plate until it reaches half-way through row C (dotted line)

the media (see Note 3). Under sterile conditions, pour the media into square plates (100 x 100 x 15 mm, Laboratory Products Sales) on a slant as shown in Figure 2-1. 1 liter of media is sufficient for the preparation of 25 plates. Allow the plates to dry for 2 hours before storage at 4˚C. The plates are normally prepared one or two days before use.

Methods

Generation of RNAi constructs in pHellsgate8

The Gateway® cloning technology enables easy insertion of a DNA fragment into a destination vector via lambda phage-based site-specific recombination (Hartley et al. 2000) (Invitrogen). This system, which eliminates many of the difficulties involved in restriction enzyme cloning, requires three steps: (1) amplification of a target DNA fragment flanked by *att*B sites via PCR (2) recombination of the DNA fragment with *att*B sites into a donor vector (for example, pDONR207) containing *att*P sites in a BP reaction producing an entry clone with *attL* sites (comprised of parts of the *att*B and *att*P sites) and (3) an LR reaction in which the entry vector containing *attL* sites surrounding the insert recombines with a destination vector (for example, pHellsgate8) containing *attR* sites flanking the ccdB toxin gene to produce an expression plasmid containing the new insert (Gateway Technology Manual, Invitrogen). Transformants containing the empty donor or destination vectors are selected against due to the toxicity of the ccdB gene product (Note 4). The destination vector, pHellsgate8, contains two ccdB genes that must each be replaced by the target fragment from pDONR207 for the survival of the bacteria maintaining this plasmid. The site-specific recombination of the Gateway® technology provides the directional insertion of the fragment from pDONR207, creating the inverted repeats necessary for RNAi (Wesley et al. 2001). Alternate approaches for the initial stages of the procedure are indicated in Note 5.

*Amplification of att*B *flanked target fragment.*

The target fragment should contain 300-600 base pairs homologous to a region of the targeted mRNA. To avoid cross-silencing the target should have no region of identity longer than 20 nucleotides with any other gene in M. truncatula (Note 6). Do not choose a region that includes any conserved motifs, and in the case of a highly conserved gene, either the 3' or 5' UTR can be used with equal silencing efficiency (Helliwell and Waterhouse 2003).

1. Design two sets of primers to amplify your target region by PCR. The first set should be complementary to 20-25 nucleotides at the 5' and 3' ends of the target region to enable amplification of the region from cDNA. The second set should include 20 nucleotides complementary to the target with the addition of the following *att*B1 and *att*B2 sites to the 5' end of the forward and reverse primers, respectively (Helliwell and Waterhouse 2003) (Note 7):

   *att*B1: 5' GGGGACAAGTTTGTACAAAAAAGCAGGCT 3'
   *att*B2: 5' GGGGACCACTTTGTACAAGAAAGCTGGGT 3'

2. With the first set of primers complementary to the target region, PCR amplify the target region from *M. truncatula* cDNA. Purify this product with a method of your choice, and use as template for a second round of PCR with the second pair of primers. For the second round, program three cycles with a Tm appropriate for the target-homologous sequence, and then all additional cycles with a Tm appropriate for the full primer. This round adds the *att*B-flanked sequence to the target region. Gel-purify the PCR product to remove primers, which can interfere with the following clonase reaction (Invitrogen).

Generation of entry vector with target region

A BP reaction is carried out with the *att*B-flanked PCR product and a donor vector with *att*P recombination sites (pDONR207) to create an entry vector with the target region flanked by *att*L sites, according to Invitrogen's protocol (Invitrogen) modified as shown below (Note 8):

1. Add the following components to a 1.5 ml tube at room temperature and mix: *att*B-flanked PCR product (=10 ng/µl; final amount ~15-150 ng) 1-7 µl pDONR207 empty vector (150 ng/µl) 1 µl TE buffer, pH 8.0 to 8 µl
2. To each sample, add 2 µl of BP Clonase™ II enzyme mix to the reaction resulting in a total volume of 10 µl, and mix well by vortexing briefly. Centrifuge briefly.
3. Incubate reactions at 25°C for 1-16 hours.
4. Add 1 µl of the Proteinase K solution to each sample to terminate the reaction. Vortex briefly. Incubate samples at 37°C for 10 minutes.
5. Transform 1-3 µl of reaction mix into heat-shock competent *E. coli* DH5α cells using a standard method. Plate on LB media with 50 mg/mL gentamicin to select bacteria with the recombined vector.
6. Select a colony from transformation and inoculate 3 mL LB media containing 50 mg/mL gentamicin for plasmid maintenance. Incubate at 37°C, with shaking, overnight.
7. Extract pDONR207 containing the target fragment from the culture using a miniprep of your choice. Sequence the vector for insertion verification in the forward and reverse directions with the following primers (Invitrogen):

   SeqL-A: 5' TCGCGTTAACGCTAGCATGGATCTC 3'

   SeqL-B: 5' GTAACATCAGAGATTTTGAGACAC 3'

As indicated earlier, an alternative approach for this initial phase of the cloning is possible (Note 5).

Generation of binary vector with target region as inverted repeats

A LR reaction is carried out with the entry clone (pDONR207 containing the target fragment) and a binary destination vector containing *att*R recombination sites (pHellsgate8) to create the final binary vector containing inverted repeats of the target region. The protocol shown below is as described by Invitrogen with minor modifications:

1. Add the following components to a 1.5 ml tube at room temperature and mix: pDONR207 containing target fragment (50-150 ng) 1-7 µl pHellsgate8 (150 ng/µl) 1 µl TE buffer, pH 8.0 to 8 µl
2. To each sample, add 2 µl of LR Clonase ™II enzyme mix to the reaction for a total volume of 10 µl, and mix well by flicking the tube. Centrifuge briefly.
3. Incubate reactions at 25°C 1-16hrs (For large inserts, longer incubation times are better).
4. Add 1 µl of the Proteinase K solution to each sample to terminate the reaction. Vortex briefly. Incubate samples at 37°C for 10 minutes.
5. Transform 1-3 µl of reaction mix into heat-shock competent *E. coli* DH5α cells using a standard method. Plate on LB media with 100 mg/L spectinomycin to select bacteria with the recombined vector.
6. Select a colony from the transformation and inoculate 3 mL LB media containing 100 mg/L spectinomycin. Incubate on a 37°C shaker overnight.
7. Extract pHellsgate8 containing your target inverted repeats from the culture using a miniprep of your choice.

8. Check for proper insertion of inverted repeats into pHellsgate8 with PCR using the reverse primer complimentary to the target region with a primer complimentary to either the promoter region (CaMV35S promoter) or terminator (OCS3'). The following primers are an option (Helliwell and Waterhouse 2003):

   P27-5: 5' GGGATGACGCACAATCC 3'
   P27-3: 5' GAGCTACACATGCTCAGG 3'

9. Verify the correct direction of the intron via restriction digest (Note 9). Sequences and vector maps can be found online at www.pi.csiro.au/tech_licensing_biol/MapsProtocol.htm.

A. rhizogenes transformation with binary vector

For transformation of *M. truncatula*, we routinely use *A. rhizogenes* strain ARqua1 (Quandt, Puhler and Broer 1993) (Note 10). Prior to plant transformation, pHellsgate8 containing the target inverted repeats must be transformed into *A. rhizogenes* ARqua1.

1. Add 2 µl (~500ng) of pHellsgate8 containing target inverted repeats of heat-shock competent *A. rhizogenes* ARqua1 cells.
2. Incubate cells on ice for 30 minutes
3. Heat-shock at 37°C for two minutes
4. Leave cells on ice for 5 more minutes.
5. Add 500 µl liquid YEP media and shake at 200rpm for 1-2 hours at 30°C.
6. Plate transformation on YEP plates with 100 mg/L streptomycin and 150 mg/L spectinomycin for selection of pHellsgate8 and the Arqua1 helper plasmid (Note 11).
7. Allow colonies to grow for two days at 30°C.

8. Screen *A. rhizogenes* colonies for pHellsgate8 containing inverted repeats by colony PCR.
9. Grow a positive colony overnight in YEP media containing 100 mg/L streptomycin and 150 mg/L spectinomycin at 30°C.
10. Create a glycerol stock using 0.4 mL of 50% glycerol and 0.6 mL of overnight ARqua1 culture with pHellsgate8 containing inverted repeats. Freeze and store at -80°C (Note 12).

Generation of M. truncatula transgenic roots expressing the RNAi construct via A. rhizogenes-mediated transformation[6]

A. rhizogenes cultivation

To enable the investigation of the phenotype in 10-15 independent root systems expressing the RNAi construct, 24 seedlings should be transformed per construct. Start cultivation of ARqua1 four days prior to the day on which seedlings will be inoculated. Streak bacteria carrying the pHellsgate 8 construct from glycerol stocks on TY agar plates containing appropriate antibiotics. For ARqua1 carrying pHellsgate 8 include spectinomycin (150mg/L) and streptomycin (100 mg/L). Grow the bacteria for 48 hours at 28˚C. Re-streak bacteria on TY agar plates with the appropriate antibiotics. At this time, it is important to spread bacteria over the whole agar plate so that a thick lawn of *A. rhizogenes* will grow on the plate. This can be done by using a sterile, bent pipet tip or a sterile, flat toothpick. Incubate the plate at 28˚C for 48 hours. To calculate the amounts of TY agar plates of *A. rhizogenes* that you will need for one RNAi construct of interest, take in consideration that one TY agar plate is sufficient to inoculate 24 *M. truncatula* seedlings.

[6] Section contributed by DSF.

Seed sterilization and germination

Start seed sterilization procedure 2 days prior to the day on which seedlings will be inoculated. The method described below is suitable for *M. truncatula* ecotypes Jemalong A17 and R108. In our hands, freshly shelled seeds of these genotypes give germination rates ~80%. The germination rate should be considered for the calculation of the amount of seeds needed for the experiment.

1. Collect unbroken *M. truncatula* seeds and place them into a 50 ml tube. Add a few milliliters of concentrated sulphuric acid (H_2SO_4), just sufficient to cover the seeds (Perform this operation in the fume hood and wear gloves, lab coat and safety glasses). Soak the seeds for 10 min to scarify the seed coat. This is required for the subsequent germination steps (Note 13).
2. Carefully remove as much H_2SO_4 as possible with a pipette. Quickly add 50 ml of H_2O_{dd} to dilute the H_2SO_4 (Note 14). Decant the water and rinse the seeds a further 6 times with H_2O_{dd}.
3. To surface sterilize the seeds soak them in 10 ml bleach solution (10% bleach [bleach solution containing 6% sodium hypochlorite], 0.1% Tween 20) for 10 min with gentle agitation in a laminar flow hood.
4. Remove the bleach solution by decanting. Rinse the seeds at least 6 times using sterile H_2O_{dd}.
5. Place the seeds in sterile H_2O_{dd} and cover the 50 ml tube with aluminum foil. Leave the tube on a shaker at approximately 60 RPM for 3 hours at room temperature. The seeds will imbibe.
6. Decant the water and rinse the seeds once with sterile H_2O_{dd}. Place the seeds in fresh sterile H_2O_{dd} and incubate the seeds at 4˚C for 26 hours in the dark. This breaks seed dormancy and allows synchronized germination.

7. Decant the water and transfer the seeds in sterile petri plates of 10 cm diameter (we use glass petri plates that can be washed, sterilized and re-used). Since crowding lowers the germination rate, distribute ~60 seeds uniformly across the plate using sterile forceps or tips. Add some drops of sterile H_2O_{dd} between the seeds. To allow the development of straight radicles, invert the plates. The seeds will stick to the bottom because of surface tension. Add a thin layer of sterile H_2O_{dd} in the lid of the petri plates, which is now on the bottom (Figure 2-2). This will help maintain higher humidity. Wrap the inverted plates in aluminum foil and incubate at 28˚C for 18 hours. During this 18 hour period, the seeds will germinate and the radical will grow straight down. (Note 15).

Induction of transgenic roots

The following steps should be performed in the laminar flow hood to ensure sterile conditions:

1. After 18 hours, remove aluminum foil from the plates. The seeds will have germinated and the roots will be approximately 1 cm in length and will have grown straight down. This is helpful for inoculation with *A. rhizogenes*. Add a shallow layer of sterile H_2O_{dd} to the petri dish containing the seedlings to avoid desiccation of their radicles.
2. Select 12 seedlings with straight radicles of 1 cm length and remove their seed coat with a sterile forceps or scalpel while gently holding the hypocotyl with a sterile, flat forceps (Note 16). Transfer the seedlings to a sterile petri plate containing a shallow layer of sterile H_2O_{dd}.
3. Using a sharp, sterile scalpel, cut the radicle approximately 3 mm from the root tip (the 3mm excised root tips are discarded).

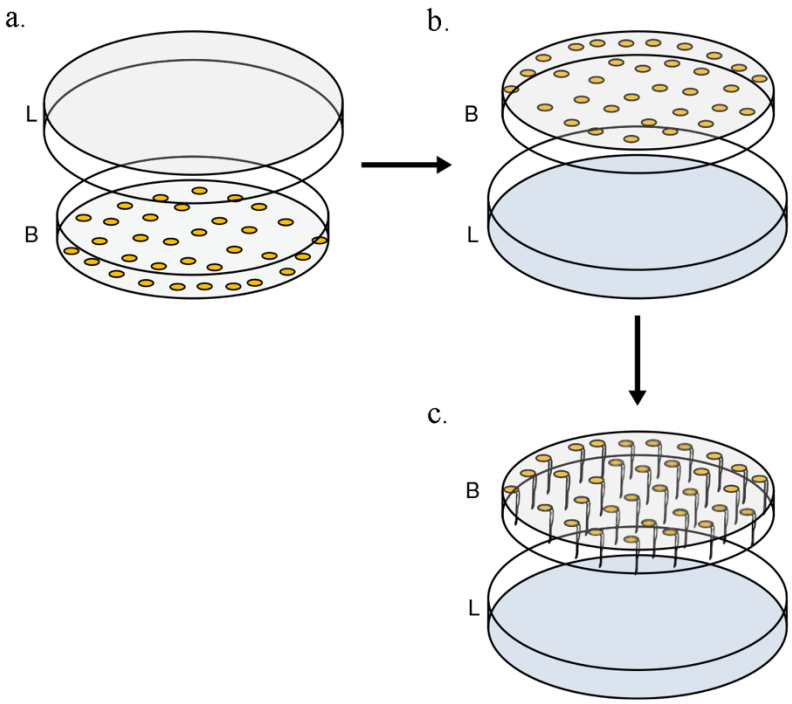

Figure 2-2: Plate setup for seed germination. B: Bottom of petri plate. L: lid of petri plate. **a)** Seeds are spread uniformly in the bottom of a petri plate. **b)** Invert the plates. Add a thin layer of sterile H_2O_{dd} in the lid. Wrap the inverted plates with aluminum foil. 3 Seedlings after 18 h at 28 °C. The seeds have germinated, and their roots have grown straight down

4. Using sterile, flat forceps, hold the seedling by the cotyledons and coat the cut end of the radicle with *A. rhizogenes* by lightly scraping the cut end of the radicle on the surface of the TY agar plate with *A. rhizogenes* containing the appropriate construct. This will result in the accumulation of bacteria on the cut end of the radicle.
5. Place the seedlings on a Fähraeus agar plate with the appropriate antibiotics. To keep the radicles in place, shallow grooves can be made with the forceps on the agar. All 12 seedlings can be placed side by side on a single Fähraeus agar plate (Note 17).
6. Carefully seal the plate with parafilm. On the top of the plate, make several incisions in the parafilm with a scalpel to allow gas exchange.
7. Place the plates in a slanting position (angle of approx. 45°) in an 18˚C incubator (16 hours light/8 hours dark) with a light intensity of 6.5 µmol/m^2s. To create an appropriate slant rest one edge of on plate on top of the lid of a petri dish (Note 18).
8. 5 days after inoculation transfer the plates to a growth chamber with a 16 hour light (25˚C)/8 hour dark (22˚C) regime with a light intensity of 50 µmol/m^2s. Keep the plates in a slanting position. Within 7-10 days transgenic roots emerge from the inoculated radical. By using the protocol described above 50-75% of the plants develop transgenic roots (Note 19).
9. 2-3 weeks after inoculation with *A. rhizogenes* the roots are well developed, and if required, the plants can be transplanted in 11cm pots filled with growth medium such as turface or soil (10 plants/pot). Since the plants have been growing on plates in an environment with a high humidity, they have to be adapted to a lower humidity. To do this, open the lids of the petri plates, add enough H_2O_{dd} to cover the roots, and leave the lids partially offset for one day (the lid covers 1/3 of the plate). The plants should be transplanted the next day (Note 14). Cover the pots with domes to keep high humidity conditions for a few more days (Note 20).

Notes

1. pDONR207 and pHellsgate8 have origins of replication with low and high copy numbers, respectively. A standard Qiagen© miniprep (Qiagen) from overnight culture will yield about 50-100 ng/µL of pDONR207 and 200-250 ng/µL of pHellsgate8 if the final elution is 50µL. This concentration of pDONR207 will suffice, provided the molar concentration of *att*B-flanked PCR product is less than that of the donor vector. To increase the yield from the miniprep, Qiagen© recommends including the PB washing step or eluting in only 30 µL EB buffer (Qiagen protocol). Additionally, one can increase the concentration by repeating the culture spin, doubling the amount of starting material.
2. Gelzan^{TM} tends to agglomerate, and the clumps won't dissolve during the sterilization process. Therefore, slowly add the appropriate amount of Gelzan^{TM} while shaking the flask. Alternatively, Plant Cell Culture certified agar may be used as a gelling agent.
3. In order to increase the percentage of roots cotransformed with the binary T-DNA the use of antibiotic counter selection is recommended. The RNAi constructs carry the neomycin phosphotransferase II gene, which inactivates, by phosphorylation, a range of aminoglycoside antibiotics such as kanamycin. We typically use kanamycin at 25mg/mL but it may be necessary to determine the best selective concentration experimentally.
4. Due to the toxicity of the ccdB gene product, Gateway®-compatible empty vectors must be maintained in *E. coli* resistant to this toxin, such as DB3.1 (Invitrogen).
5. Alternatively, portions of the cDNA to be targeted can be amplified and cloned into the Gateway-compatible pENTR/D-TOPO or similar vector without the need to add *att*B sites onto PCR products since *attL* sites are already present in this vector. This allows the user to avoid the expense of primers that contain the *attB* sites and BP

clonase as well as the associated effort. After this, go to the section 3.1.3 and continue with the protocol as described to recombine to pHellsgate8 through an LR reaction. The approach using pENTR/D-TOPO vectors was used for the generation of approximately1500 RNAi constructs by C. Starker and J.S. Gantt.

6. In some instances, silencing multiple genes may be desirable. Up to three transcribed genes can be targeted at the same time by amplifying regions from each and fusing the fragments together via PCR before adding the *att*B sites to the ends of the fused product. Each gene should be represented by at least 200 nucleotides complimentary to its mRNA, and the total fragment should not be much greater 600 nucleotides.
7. Alternatively, one can use only the second set of primers directly, especially when amplifying from a more concentrated source of the targeted gene, such as a cloned vector. The success of this method depends on the target and quality of template.
8. A half reaction (5 µL final volume) is sufficient for both Gateway reactions. For larger inserts, allow reactions to sit overnight before stopping with Proteinase K. Addition of Proteinase K is essential.
9. In some cases the direction of the intron reverses during the LR reaction, presumably due to the intron's *att*P2 sites on both sides, allowing either side to recombine with either insert's *att*B2. Frequency of intron inversion depends on the insert sequence, but no correlation has been determined (Helliwell and Waterhouse 2003). After sequencing >200 pHellsgate8-derived plasmids that were first confirmed by colony PCR for correct recombination of the 5' portion of the RNAi construct, sequence data confirmed that all clones had the undergone recombination of the 3' portion of the RNAi construct as well.
10. To generate transgenic roots with growth and morphology comparable to normal roots, low virulence *A. rhizogenes* strains such as ARqua1 are used. These strains elicit a limited number of genetically transformed roots. Whereas roots generated by

using high virulence strains might show abnormal root structure and growth, which could negatively impact phenotypic characterization.

11. Up to Spectinomycin 300mg/L may be used for selection of pHellsgate-derived plasmids. This concentration will help reduce background, but will also cause Arqua1 to grow slower than normal. Spectinomycin 150mg/L is sufficient for maintenance of the plasmid.
12. For larger scale, it is recommended to transform 100-110 pHellsgate-derived plasmids (separately) into Arqua1 in a single day. This allows more convenient, full 96-well screening of Arqua1 clones, and the eventual preparation of glycerol stocks in 96 well plates. More than 96 transformations are recommended as a few will fail on the first transformation attempt.
13. The duration of the H_2SO_4 treatment is critical and may vary between seed batches. Therefore, it is necessary to monitor the progress of scarification. If small black dots appear on the seed surface (usually after 5-12 min), immediately remove H_2SO_4 and rinse the seeds with water.
14. Addition of water to sulfuric acid-coated seeds causes an exothermic reaction, with the result that the excessive heat may kill some or all seeds. To mitigate the local heating of seeds, which may damage them, it is extremely important to use a large amount of cold water.
15. Alternatively, a very thin layer of 1% water-agar can be made and poured into the bottom of 2cm deep sterile plastic petri plates. The seeds will stick to the agar and it will help maintain appropriate humidity.
16. The removal of the seed coat helps the cotyledons to open.
17. If antibiotic counter selection is used, include seedlings without *A. rhizogenes* inoculation as a control. This will confirm that growth of non-transformed roots is inhibited in presence of the antibiotic.

18. An experienced researcher can transform 250-450 plants in a single day. However, since planting and analyzing transgenic plants is far more time consuming than transforming them, care should be taken to avoid producing more plants than can be examined.
19. Since non-transformed roots may occasionally escape antibiotic selection, we recommend using a construct which includes a fluorescent marker protein such as DsRED (Limpens et al 2004), which further enables identification of transgenic roots.
20. These composite plants should express the RNAi hairpin construct and as each independent root arises from an independent transgenic event, the level of gene expression can be expected to vary between independent roots. Silencing of gene expression should be confirmed by RT-PCR. If possible, phenotypic analysis and analysis of transcript levels should be performed on the same roots.

REFERENCES

Boisson-Dernier, A., Chabaud, M., Garcia, F., Becard, G., Rosenberg, C., and Barker, D.G. (2001) *Agrobacterium* rhizogenes-transformed roots of *Medicago truncatula* for the study of nitrogen-fixing and endomycorrhizal symbiotic associations. *Molecular Plant-Microbe Interactions* 14, 695-700.

Collier, R., Fuchs, B., Walter, N., Kevin Lutke, W., and Taylor, C.G. (2005) Ex vitro composite plants: an inexpensive, rapid method for root biology. *Plant Journal* 43, 449-457.

Dunoyer, P., Himber, C., Ruiz-Ferrer, V., Alioua, A., and Voinnet, O. (2007) Intra- and intercellular RNA interference in Arabidopsis thaliana requires components of the microRNA and heterochromatic silencing pathways. . *Nature Genetics* 39, 848-56.

Floss, D.S., Hause, B., Lange, P.R., Kuster, H., Strack, D., and Walter, M.H. (2008) Knock-down of the MEP pathway isogene 1-deoxy-D-xylulose 5-phosphate synthase 2 inhibits formation of arbuscular mycorrhiza-induced apocarotenoids, and abolishes normal expression of mycorrhiza-specific plant marker genes. *Plant Journal* 56, 86-100.

Gubler, F., Hughes, T., Waterhouse, P., and Jacobsen, J. (2008) Regulation of dormancy in barley by blue light and after-ripening: Effects on abscisic acid and gibberellin metabolism. *Plant Physiology* 147, 886-896.

Hannon, G.J. (2002) RNA interference. *Nature* 418, 244-251.

Hartley, J., Temple, G., and Brasch, M. (2000) DNA Cloning Using In Vitro Site-Specific Recombination. *Genome Research* 10, 1788-1795.

Helliwell, C. and Waterhouse, P. (2003) Constructs and methods for high-throughput gene silencing in plants. *Methods* 30, 289-295.

Helliwell, C.A. and Waterhouse, P.M. (2005) *Constructs and Methods for Hairpin RNA-Mediated Gene Silencing in Plants*. In: Engelke, D. and Rossi, J., Ed. *Methods in Enzymology*. Academic Press, San Diego. p. 24-35.

Helliwell, C.A., Wesley, S.V., Wielopolska, A.J., and Waterhouse, P.M. (2002) High-throughput vectors for efficient gene silencing in plants. *Functional Plant Biology* 29, 1217-1225.

Ivashuta, S., Liu, J., Liu, J., Lohar, D.P., Haridas, S., Bucciarelli, B., VandenBosch, K.A., Vance, C.P., Harrison, M.J., and Gantt, J.S. (2005) RNA interference identifies a calcium-dependent protein kinase involved in *Medicago truncatula* root development. *Plant Cell* 17, 2911-2921.

Javot, H., Penmetsa, R.V., Terzaghi, N., Cook, D.R., and Harrison, M.J. (2007) A *Medicago truncatula* phosphate transporter indispensable for the arbuscular mycorrhizal symbiosis. *Proceedings of the National Academy of Sciences, USA* 104, 1720-1725.

Limpens, E., Franken, C., Smit, P., Willemse, J., Bisseling, T., and Geurts, R. (2003) LysM domain receptor kinases regulating rhizobial Nod factor-induced infection. *Science* 302, 630-633.

Limpens, E., Ramos, J., Franken, C., Raz, V., Compaan, B., Franssen, H., Bisseling, T., and Geurts, R. (2004) RNA interference in Agrobacterium rhizogenes-transformed roots of Arabidopsis and Medicago truncatula. *J. Exp. Bot.* 55, 983-992.

Liu, J., Blaylock, L., Endre, G., Cho, J., Town, C.D., VandenBosch, K., and Harrison, M.J. (2003) Transcript profiling coupled with spatial expression analyses reveals genes involved in distinct developmental stages of the arbuscular mycorrhizal symbiosis. *Plant Cell* 15, 2106-2123.

Ossowski, S., Schwab, R., and Weigel, D. (2008) Gene silencing in plants using artificial microRNAs and other small RNAs. *Plant Journal* 53, 674-690.

Pasquinelli, A.E. and Ruvkun, G. (2002) Control of developmental timing by microRNAs and their targets. *Annual Review of Cell and Developmental Biology* 18, 495-513.

Pumplin, N., Mondo, S.J., Topp, S., Starker, C.G., Gantt, J.S., and Harrison, M.J. (2010) Medicago truncatula Vapyrin is a novel protein required for arbuscular mycorrhizal symbiosis. *Plant Journal* 61, 482-494.

Quandt, H.J., Puhler, A., and Broer, I. (1993) Transgenic root nodules of Vicia hirsuta: a fast and efficient system for the study of gene expression in indeterminate-type nodules. *MPMI* 6, 699-706.

Subramanian, S., Graham, M.Y., Yu, O., and Graham, T.L. (2005) RNA interference of soybean isoflavone synthase genes leads to silencing in tissues distal to the transformation site and to enhanced susceptibility to Phytophthora sojae. *Plant Physiology* 137, 1345-1353.

Vieweg, M.F., Fruhling, M., Quandt, H.J., Heim, U., Baumlein, H., Puhler, A., Kuster, H., and Perlick, A.M. (2004) The promoter of the Vicia faba L. leghemoglobin gene VfLb29 is specifically activated in the infected cells of root nodules and in the arbuscule-containing cells of mycorrhizal roots from different legume and nonlegume plants. *Molecular Plant-Microbe Interactions* 17, 62-69.

Wesley, S.V., Helliwell, C.A., Smith, N.A., Wang, M.B., Rouse, D.T., Liu, Q., Gooding, P.S., Singh, S.P., Abbott, D., Stoutjesdijk, P.A., Robinson, S.P., Gleave, A.P., Green, A.G., and Waterhouse, P.M. (2001) Construct design for efficient, effective and high-throughput gene silencing in plants. *Plant Journal* 27, 581-590.

CHAPTER 3

LYSM RECEPTOR-LIKE KINASES, NFP, LYR1, AND LYK10 ARE DISPENSABLE FOR ARBUSCULAR MYCORRIZAL SYMBIOSIS IN *MEDICAGO TRUNCATULA*

Abstract

Plant receptor-like-kinases (RLKs) perceive microbe-associated molecules at the cell surface and initiate signaling cascades that can result in defense-related responses or intracellular accommodation of a symbiotic microbe. LysM-RLKs bind to and distinguish between many different complex carbohydrates. The LysM-RLK gene family is greatly expanded, and deletion of individual LysM-RLKs often only partly reduces the signaling response due to functional redundancy. Rhizobial Nod factors are sensed by NFP and Lyk3 in *Medicago truncatula*, and deletion of either gene blocks the formation of root nodules. One of the two major signaling molecules from arbuscular mycorrhizal (AM) fungi are very similar to Nod factors and hypothesized to signal via the closest homolog of NFP, Lyr1. Here we show that *Lyr1* and *NFP* are both dispensable for AM symbiosis, although *nfp* mutants may allow for greater colonization than wild type. We further show that the double mutant, *lyr1nfp* can still establish AM symbiosis. We identified five new LysM-RLK genes, and a phylogenetic reconstruction of the *M. truncatula* LysM-RLK family revealed an AM symbiosis-conserved LysM-RLK, Lyk10. *lyk10* mutants are also able to establish AM symbiosis, although *lyk10* plants are less colonized than wild type. Our results emphasize the importance of maintaining a low level of AM fungal colonization when assessing partial contributions of redundant genes to mechanisms of interest. Furthermore, we propose considering the effect of other microorganisms or microbial signals when investigating the importance of receptor-kinases for AM symbiosis.

Introduction

As multicellular organisms in an ever-changing environment, plants have adapted to sense signals at the cell surface that initiate the metabolic and developmental changes necessary to respond to external stimuli. Receptor-like kinases (RLKs) interact with signaling molecules and transduce the signal intracellularly via their kinase domains. Many RLKs sense conserved molecular patterns of microbes that may launch an attack if not otherwise suppressed by the plant's innate immune response (Jones and Dangl 2006). Alternatively, they may sense symbiotic signals and instead initiate a signaling cascade leading to the accommodation of a mutualistic microbe. In some cases, a single RLK can recognize and differentiate between a variety of signals, and even facilitate either defense or symbiosis (Zipfel and Oldroyd 2017). Plant genomes encode hundreds of RLKs, all of which contain a cytoplasmic kinase, transmembrane domain, and one of several types of extracellular receptor domains. Several RLKs have been shown to bind ligands directly, while others act as co-receptors, interacting with receptors in a ligand-dependent manner (Hohman, Lau, and Hothorn 2017). Receptors and co-receptors share molecularly similar extracellular domains that recognize a specific type of molecule, such as short peptides or hormones, in the case of leucine-rich-repeat RLKs, or carbohydrate molecules, in the case of lectin and lysin motif (LysM)-RLKs (Desaki et al. 2017).

In the past decade several publications have reported the involvement of LysM-RLKs in both symbiosis signaling and immunity (Desaki et al. 2017; Zipfel and Oldroyd 2017). LysM domains of receptors can interact with a variety of molecules from bacteria and fungi, including rhizobial Nod factors (NF), myc-LCOs, peptidoglycan, exopolysaccharides, and many forms of chitin (Desaki et al. 2017). A recent report suggests LysM domains may interact with β-1,3 glucans, which are also present in the walls of many fungi (Mélida et al. 2018). The extracellular domain of LysM-RLKs typically contain three LysMs, which are defined by their $\beta\alpha\alpha\beta$ secondary structure that fold to form an anti-parallel β-sheet. In the

LysM-RLKs the LysM domain is linked, via a single-pass transmembrane domain, to an intracellular kinase that may be active or inactive depending on the presence of an activation loop and a phosphorylation (P) loop (Zhang et al. 2009).

The LysM domain has been identified in proteins from all kingdoms except Archaea and can be found in proteins containing a diversity of other domains (Bateman and Bycroft 2000), but LysM-RLKs have thus far been identified only in plants (Buist et al. 2008). The first LysM-RLKs were characterized for their role in root-nodule (RN) symbiosis where they regulate entry and determine the host range of rhizobia through recognition of specific NFs (Limpens et al. 2003; Ben Amor et al. 2003; Madsen et al. 2003; Radutoiu et al. 2003; Radutoiu et al. 2007). These ground-breaking studies were done in *Medicago truncatula* and *Lotus japonicus*, in which deletion mutants of the nod-factor receptors MtNFP/LjNFR5 or MtLyk3/LjNFR1 are unable to establish RN symbiosis. Their orthologs have since been identified and characterized in pea and soybean (Zhukov et al. 2008; Indrasumunar et al. 2010a,b).

Recently, an additional LysM-RLK was identified in *L. japonicus* as the receptor for rhizobial exopolysaccharides (EPS) (Kawaharada et al. 2015). The receptor EPR3 binds directly to EPS and can distinguish different EPS variants from compatible and incompatible rhizobia. While rhizobia engineered to produce a truncated EPS are able to induce root-hair curling and infection thread formation, which depend on the correct NF, they cannot pass through the root's epidermal layer; however, this restriction is absent in the *epr3* mutant, which allows for some formation of functional nodules (Kawaharada et al. 2015). *Epr3* expression is induced by NF and dependent on NF receptors, indicating that infection by rhizobia is controlled by a two-step process first involving perception of compatible Nod factors, which then induce an EPS receptor that further confirms the compatibility of rhizobia (Kawaharada et al. 2015). While rhizobia EPS contribute to determination of host range (Skorupska et al. 2006), they are also hypothesized to play a role in suppressing host defense

responses (Pinto et al. 2003; Aslam et al. 2008; Jones and Walker 2008; Zamioudis et al. 2012). The closest paralog to EPR3 in *Arabidopsis thaliana*, Lyk3, is necessary for NF and short-chain chitooligosaccharide inhibition of both peptidoglycan and chitin-elicited defense responses (Liang et al. 2013), which supports a role for this LysM-RLK clade in signaling defense suppression.

In *A. thaliana*, the LysM-RLK, CERK1 is required for responses to both peptidoglycan and chitin, but these separate responses are facilitated by different receptors for which CERK1 is a co-receptor (Desaki et al. 2017). Another *A. thaliana* LysM-RLK, Lyk5 is the receptor and major-binding protein for chitin but requires CERK1 for chitin-elicited responses (Cao et al. 2014). The receptors for peptidoglycan are GPI-anchored extracellular LysM domain proteins that bind directly to peptidoglycan but rely on CERK1 to transduce the signal via its kinase domain (Willmann et al. 2011). In rice, the ortholog OsCERK1 is also a co-receptor for chitin and peptidoglycan defense signaling, however both mechanisms depend on the GPI-anchored LysM domain proteins, CEBiP and LYP4/6 (Shimizu et al. 2010; Liu (B) et al. 2012a). While AtCERK1 can bind weakly to chitin, OsCERK1 cannot (Liu et al. 2012a; Liu (T) et al. 2012b). CEBiP is only involved in chitin signaling, whereas LYP4 and LYP6 are involved in both chitin and peptidoglycan signaling, and all three receptors can bind directly to chitin and interact with CERK1 (Shimizu et al. 2010; Liu et al. 2012a).

Recent reports have added a third role for OsCERK1 as a co-receptor of symbiotic signals during AM symbiosis (Miyata et al. 2014; Zhang et al. 2015). AM fungal signals include both short-chain chitooligosaccharides (CO4/5) that are similar to the longer chain (CO7/8) chitin defense elicitors and lipo-chitooligosacchardes (LCOs) that resemble NF (Genre et al. 2013; Maillet et al. 2011). OsCERK1, but not OsCEBiP, is essential for AM symbiosis and induction of symbiotic calcium signals by CO4 and germinating spore exudates (Miyata et al. 2014; Carotenuto et al. 2017). In pea, PsLyk9 is necessary for chitin-elicited defense responses, as well as CO5-elicited symbiotic responses, indicating it may also play a

role in both defense and symbiosis (Leppyanen et al. 2018). Conversely, while its orthologs in *M. truncatula* and *L. japonicus*, MtLyk9 and LjLys6, are involved in chitin-elicited defense responses, *ljlys6* mutants are able to establish normal AM symbiosis (Bozsoki et al. 2017). The lack of a dual role for Lys6 may be explained by the expansion of the CERK1 orthologous clade in legumes. Whereas rice only has one gene in this clade (OsCERK1), the legumes have several, yielding high potential for redundancy (Bozsoki et al. 2017).

Dual functions of LysM-RLKs in immunity and symbiosis are not surprising considering the similarities in signaling molecules. Likewise, since the discovery of LCOs as AM fungal signals (myc-LCOs), and, considering how RN and AM symbioses utilize many of the same genes for establishment, several reports have hypothesized dual roles for NF receptors in both rhizobial and AM symbiosis. A recent report demonstrated that Nod factor receptors MtLyk3/LjNFR1, which are closely-related to CERK1, contribute to myc-LCO signaling, and their deletion results in a reduction of mycorrhizal colonization (Zhang et al. 2015). Conversely, MtNFP/LjNFR5 are both dispensable for AM symbiosis, although NFP contributes to myc-LCO signaling and stimulation of lateral root formation (Maillet et al. 2011; Czaja et al. 2012; Sun et al. 2015; Zhang et al. 2015).

The lack of a role for NFP/NFR5 in legumes may be due to a relatively recent duplication event and possible specialization for rhizobial or AM symbiosis (Streng et al. 2011). In non-legume plants, mutants in *nfp/nfr5* orthologs are impaired in AM formation or AM signaling (Op den Camp et al. 2011; Buendia et al. 2016; Miyata et al. 2016). In *Parasponia andersonii*, a non-legume capable of establishing RN symbiosis, the *NFP* ortholog has not been duplicated, and its deletion impairs AM fungal colonization and formation of arbuscules (Op den Camp et al. 2011). Furthermore, the ortholog in tomato, SlLyk10 is essential for AM formation (Buendia et al. 2016).

The NFR5 paralog in *Lotus*, *LjLYS11* is specifically expressed in root cortical cells containing arbuscules and can act as a receptor for LCOs, as determined through

complementation of *nfr5* during rhizobial symbiosis; however, *ljlys11* and *nfr1nfr5lys11* triple mutant were unimpaired in their ability to form AM symbiosis (Rasmussen et al. 2016). Interestingly, the lack of an effect of the triple mutation on AM formation contradicts the earlier report that *nfr1* mutants experience reduced colonization (Zhang et al. 2015). In *Medicago*, NFP has a similar paralog, referred to as *Lyr1* (Arrighi et al. 2006). Microarray analysis of laser-capture microdissected cells containing arbuscules and cells in non-mycorrhizal cortex revealed that *Lyr1* is upregulated in roots colonized by AM fungi (Gomez et al. 2009). The work in this chapter was initiated several years before the LjLYS11 experiments were published, and the initial hypothesis to be tested was the specialized role of MtLyr1 in AM symbiosis. Additionally, we evaluated potential functional redundancy through generation of a *lyr1nfp* double mutant. Using the recently published *M. truncatula* genome, version 4.0 (Tang et al. 2014), we identified additional LysM-RLKs, and phylogenetic analyses revealed an AM-conserved LysM-RLK, which we have tested for its role in AM symbiosis.

Results

The Medicago truncatula genome contains 21 predicted LysM-RLK genes

A previous survey identified 17 LysM-RLK genes in the *M. truncatula* genome (Arrighi et al. 2006). To ensure that all potential LysM-RLKs would be considered for involvement in AM symbiosis, we searched the *M. truncatula* genome, version 4.0 (Tang et al. 2014) for previously unidentified LysM-RLKs. To do so, we used pBLAST with the extracellular region of each *M. truncatula* LysM-RLK as a query since the kinase domains are more conserved, and the full-length sequence retrieved many protein kinases. The search identified five additional LysM-RLKs that were not previously reported, none of which are located near any other LysM-RLKs in the genome (Table 3-1). LysM-RLKs in *M. truncatula* group into two major clades: Lyk and Lyk-related (Lyr) (Arrighi et al. 2006). A phylogenetic reconstruction of the 21 *M. truncatula* LysM-RLKs indicated that one newly-identified gene is part of the Lyk clade, and thus we named it Lyk11 (Figure 3-1, Table 3-1). The four others are part of the Lyr clade, and so we named them Lyr7-Lyr10.

We also identified several short genes with high similarity to LysM-RLKs, which mostly encode only portions of extracellular domains (Table 3-2). The lengths of these genes vary, from 56 to 311 amino acids. The largest was previously reported as the LysM-RLK, Lyk2 (Arrighi et al. 2006), which only contains two of three LysM domains, and just the beginning of the kinase domain, truncated after the P-loop. Due to its lack of a LysM domain and full kinase, Lyk2 is not considered a true LysM-RLK. Only three of the short genes contain signal peptides, and among those only one, which is most similar to Lyr8, contains a full LysM domain.

All 21 *M. truncatula* LysM-RLKs have conserved cysteines at the N terminus of the mature protein, followed by CXC motifs between LysM1-LysM2 and LysM2-LysM3 (Lefebvre et al. 2012). In the Ser-Thr kinase domain, all Lyr proteins except Lyr5 and Lyr6

Table 3-1: List of all LysM-RLK genes in the *M. truncatula* genome. Probe ID refers to the associated transcript probe on the *Medicago* Affymetrix Gene Chip. Expression describes the *Medicago* Gene Atlas profile for those that have Probe IDs, or the results from RT-PCR with mock and *G. versiforme* -inoculated roots. Bold text are newly-identified LysM-RLKs.

Name	Gene	Probe ID/primers	Expression
MtLyk1	Medtr5g086540	Mtr.3201.1.S1_at	none in roots
MtLyk3	Medtr5g086130	Mtr.142.1.S1_s_at	only in roots, not AM regulated
MtLyk4	Medtr5g086120	Mtr.25025.1.S1_s_at	low in roots, not AM regulated
MtLyk5	Medtr5g086090	Mtr.51452.1.S1_x_at	only in roots, not AM regulated
MtLyk6	Medtr5g086040	Mtr.15753.1.S1_s_at	higher in roots, not AM regulated
MtLyk7	Medtr5g086030	Mtr.26293.1.S1_s_at	constitutive in most tissue
MtLyk8	Medtr2g024290	Mtr.45170.1.S1_at	only in roots, not AM regulated
MtLyk9	Medtr3g080050	Mtr.14019.1.S1_at	constitutive in most tissue
MtLyk10	Medtr5g033490	Mtr.25148.1.S1_at	mostly roots, not AM regulated
MtLyk11	**Medtr8g014500**	**Mtr.45512.1.S1_at**	**constitutive in most tissues**
MtNFP	Medtr5g019040	Mtr.15789.1.S1_at	only in roots, not AM regulated
MtLyr1	Medtr8g078300	Mtr.19870.1.S1_at	only in roots, AM regulated
MtLyr2	Medtr5g042440	B3080/3081	high in roots, not AM regulated
MtLyr3	Medtr5g019050	Mtr.15787.1.S1_at	mostly roots, not AM regulated
MtLyr4	Medtr5g085790	Mtr.31312.1.S1_at	constitutive in most tissue
MtLyr5	Medtr7g079350	Mtr.6154.1.S1_s_at	hypocotyl, roots, not AM regulated
MtLyr6	Medtr7g079320	Mtr.20804.1.S1_at	leaves, hypocotyl, roots slightly AM-induced
MtLyr7	**Medtr3g080170**	**B2676/2677**	**low in roots**
MtLyr8	**Medtr4g058570**	**B2678/2679**	**AM-suppressed**
MtLyr9	**Medtr7g029650**		**not tested**
MtLyr10	**Medtr1g021845**	**Mtr.27990.1.S1_at**	**low in roots, not AM regulated**

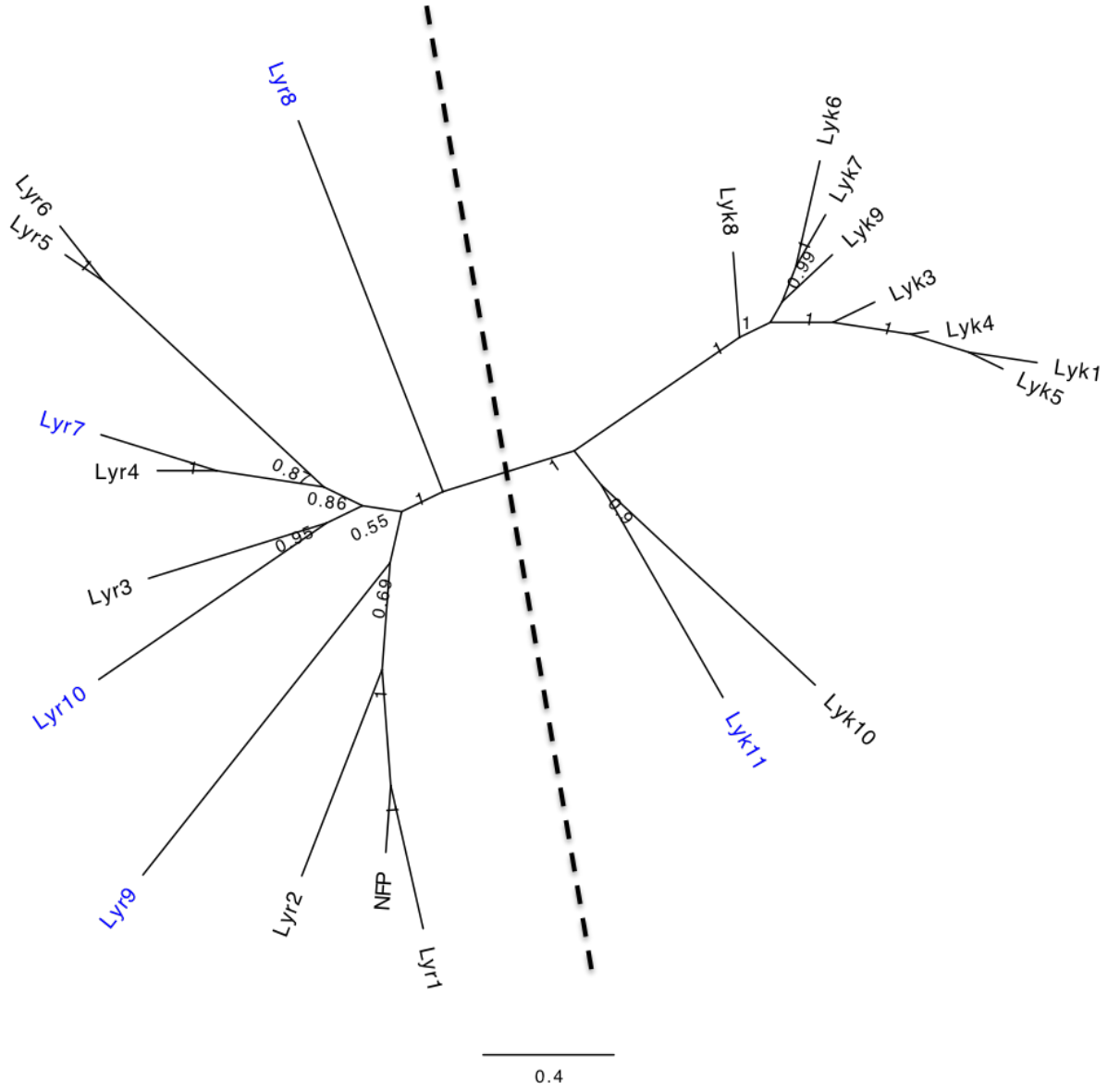

Figure 3-1: Phylogenetic reconstruction of the LysM-RLK family in *Medicago truncatula*. The phylogeny divides into two clades, Lyks and Lyrs, demonstrated by the dashed line. Newly-identified genes are in blue. Nodes are labeled with posterior probabilities. Bar represents amino acid substitutions per branch-length.

Table 3-2: List of LysM-RLK duplications in the *M. truncatula* genome. Best hit refers to first LysM-RLK gene retrieved with pBLAST. SP = signal peptide

Gene ID	best hit	Predicted motifs	SP?	Protein length
Medtr5g086110	MtLyk5	none	Y	311
Medtr5g086050	MtLyk6	none	Y	150
Medtr0219s0050	MtLyr8	LysM1	Y	145
Medtr5g086660	MtLyk1	none	N	163
Medtr5g086310 (Lyk2)	MtLyk3	LysM2, LysM3, TM, P-loop	N	340
Medtr5g078600	MtLyk3	chimera	N	324
Medtr5g086080	MtLyk5	kinase portion	N	447
Medtr8g078320	MtLyr1	1 LysM	N	85
Medtr8g078340	MtLyr1	none	N	56
Medtr8g078360	MtLyr1	1 LysM	N	166

are missing the GXGXF/YG P-loop (Figure 3-2a). Only NFP, Lyr1, and Lyr8 are missing the activation segment, however all Lyr proteins except Lyr 5/6 are missing the magnesium-binding DFG motif, and all except Lyr5/6 and Lyr10 are missing a Ser/Thr in the activation loop (Figure 3-2b) (Nolen et al. 2004; Arrighi et al. 2006). The Affymetrix Medicago Gene Chip® has yielded a vast array of normalized expression data accessible through the *Medicago truncatula* Gene Expression Atlas (Benedito et al. 2008; He et al. 2009). All but four of the LysM-RLKs are represented on the gene chip, and their gene expression profiles are briefly summarized in Table 3-1. We checked expression of three of the non-represented LysM-RLKs using RT-PCR in mock and AM fungal-inoculated roots and found expression of *Lyr8* is down-regulated by both *Glomus versiforme* and *Gigaspora gigantea* (Figure 3-3).

To identify which *M. truncatula* LysM-RLKs are orthologs of characterized proteins from other species, we reconstructed the protein phylogeny using all LysM-RLK sequences from plants with characterized LysM-RLKs and an available genome sequence. In addition, we included several monocots, two basal land plants (*Selaginella moellendorffii* and *Azolla filiculoides*), and *Lupinus angustifolius*, which can form RN, but not AM symbiosis. The latter can help us identify those genes important for AM that are likely not important for RN symbiosis (Bravo et al. 2016). The resulting tree (Figure 3-4) confirms previous cladal predictions (Streng et al. 2011; De Mita et al. 2014), including a "CERK1" clade that includes both AtCERK1 and OsCERK1, as well as MtLyk3/LjNFR1, and a "symbiosis" clade including NFP/NFR5 and Lyr1/Lys11, and AM-essential LysM-RLKs, PaNFP and SlLyk10. The newly-identified Lyr7-Lyr10 all resolved with previously identified genes in the *L. japonicus* LysM-RLK family (Lohmann et al. 2010). The newly-identified Lyk11 was placed with AtLyk3, the LysM-RLK necessary for LCO and CO4 inhibition of chitin-elicited defense responses (Liang et al. 2013). Interestingly, while the EPR3 clade does not contain any *Arabidopsis* genes, it does contain orthologs in the non-legumes that can form AM symbiosis, including both dicots and monocots, but no ortholog from *L. angustifolius* (Figure 3-3, blue

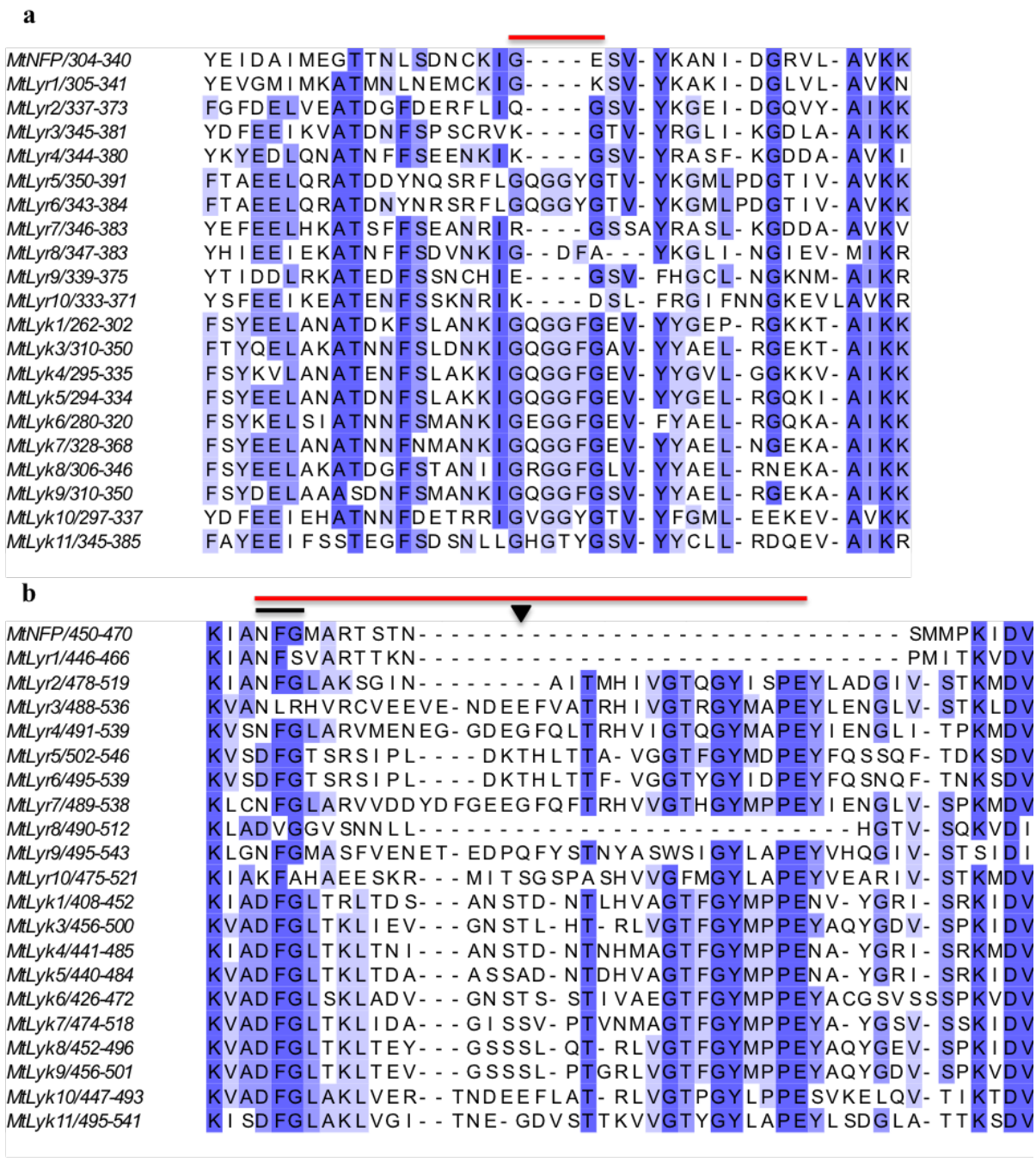

Figure 3-2: Alignment of non-conserved elements of the LysM-RLK kinase domains. (a) The P-loop (GXGXF/YG, red line) is missing in most Lyrs. **(b)** The activation segment (red line) begins with the Mg-binding DFG motif (black line) and includes a conserved Ser or Thr residue (black arrowhead). Most of the activation segment is missing in NFP, Lyr1, and Lyr8, and most Lyrs are missing the Mg-binding motif.

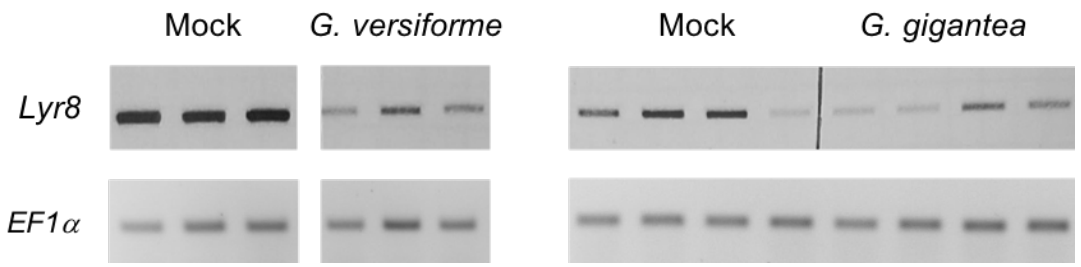

Figure 3-3: *Lyr8* is down-regulated by AM colonization. RT-PCR of *Lyk8* transcript in biological replicates of cDNA from mock and AM fungal-inoculated roots at a single timepoint. RNA from *G. versiforme* and *G. gigantea* was provided by Xinchun Zhang and Kishor Bhattarai, respectively. Time of harvest is unknown, but likely between 3-5 wpi.

highlight). This result is in line with the previous phylogenetic analysis that identified *Lyk10* as a mycorrhiza-conserved gene (Bravo et al. 2016).

Lyr1 is induced in mycorrhizal roots

Considering previous expression data that demonstrated an induction of *Lyr1* in cells containing arbuscules, and the conservation of *Lyk10* in plants capable of establishing AM (Gomez et al. 2009; Bravo et al. 2016), we predicted these two genes are important for AM symbiosis. We measured expression of *Lyr1*, *Lyk10*, and *NFP* in roots with and without AM fungi, *G. versiforme* and *Rhizophagus irregularis*, using qRT-PCR (Figure 3-5). All three genes were expressed in non-colonized roots of *Medicago*, however *Lyr1* expression was very low. Expression of *NFP* was not significantly affected by colonization of either AM fungus. Expression of *Lyk10* was induced slightly, but significantly only in roots with *G. versiforme*. Conversely, *Lyr1* expression was much higher in roots colonized by either AM fungus than in mock-inoculated roots.

At the time this work was initiated, the only sample in the *M. truncatula* Gene Atlas demonstrating *Lyr1* induction was the only mycorrhizal sample, representing results from Gomez et al. 2009. This led us to believe that *Lyr1* is specifically induced during AM symbiosis. Since then, a new version of the Gene Expression Atlas was released with many more samples representing expression in both AM and nodulated roots, revealing that *Lyr1*'s expression is not specific to AM symbiosis. In the new version of the atlas, *Lyr1* is also induced by rhizobial inoculation and nitrogen starvation. Both *NFP* and *Lyk10* are constitutively expressed throughout root samples with and without AM fungi or rhizobia.

To investigate when during AM symbiosis *Lyr1* is expressed, we used RT-PCR to analyze *Lyr1* expression in *mtpt4* and *vapyrin* mutant roots colonized by *G. gigantea*. MtPt4 is an AM-specific phosphate transporter that localizes to the periarbuscular membrane, and roots of *mtpt4* are enriched in degenerating arbuscules and have almost no mature arbuscules (Javot

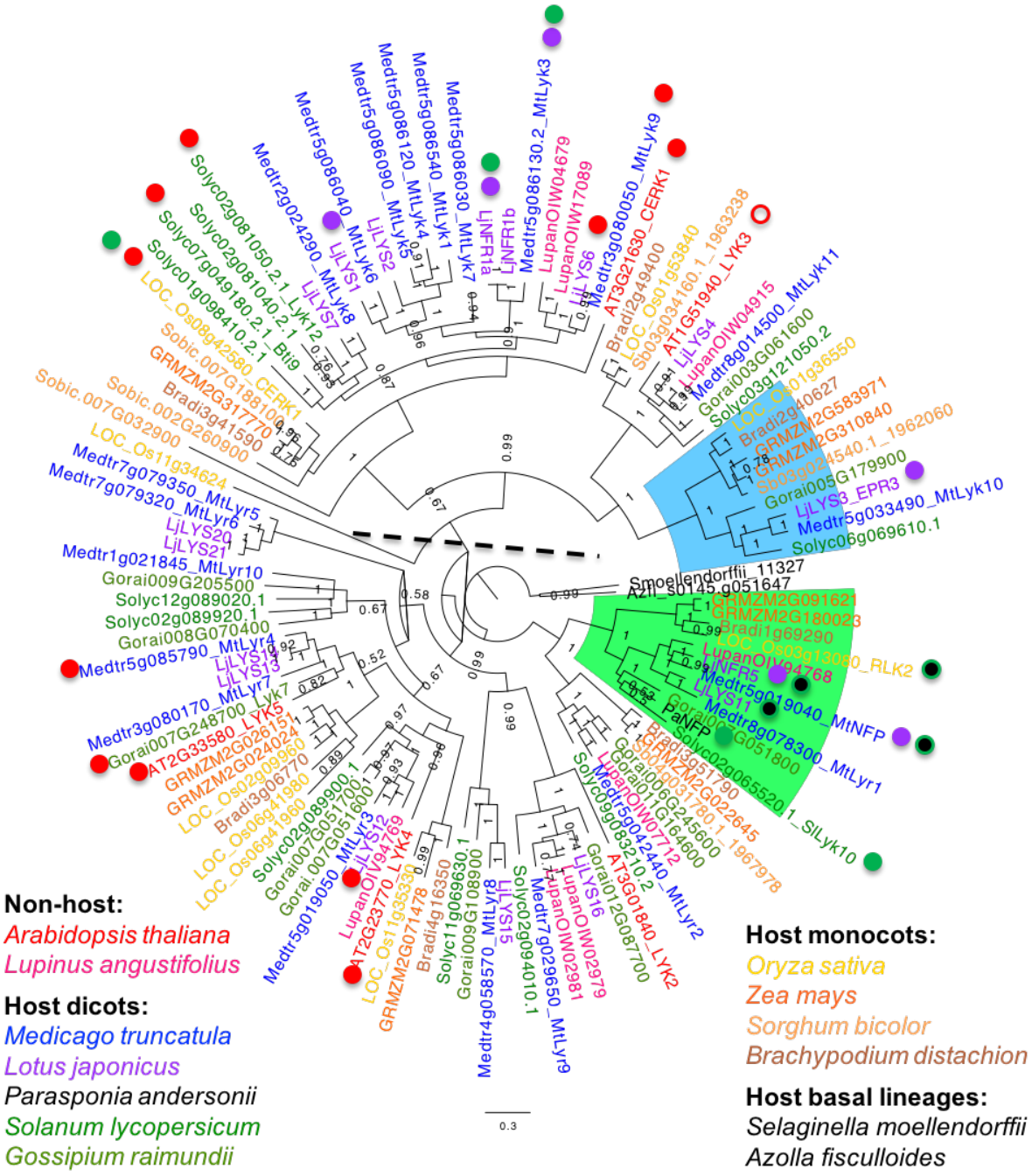

Figure 3-4: Phylogenetic reconstruction of LysM-RLK family. The phylogeny divides into two major clades (dashed line). Blue highlight is the rhizobia/symbiosis-specific clade. Green highlight is the EPR3 clade. Filled circles represent confirmed association with defense (red), root-nodule symbiosis (purple), or AM symbiosis (green). Black fill indicates confirmed lack of association. Open circle represents supported, but unconfirmed association. Nodes are labeled with posterior probabilities. Bar represents amino acid substitutions per branch-length

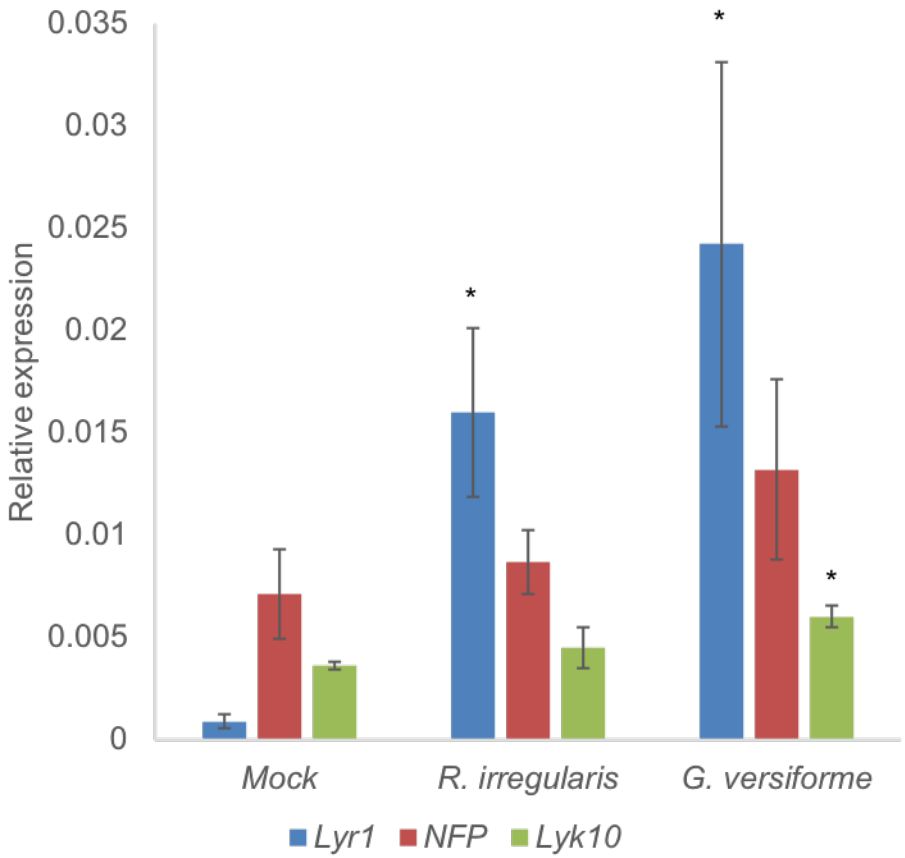

Figure 3-5: *MtLyr1* is upregulated in roots colonized by AM fungi. Expression, relative to *M. truncatula elongation factor*, of *NFP, MtLyr1*, and *MtLyk10* in mock-inoculated roots, and roots colonized by *Rhizophagus irregularis* or *Glomus versiforme.* Bars are standard error, n = 4. Stars denote significant difference between colonized and mock, Student's t test, $p < 0.05$.

et al. 2007). Vapyrin is a protein of unknown function predicted to play a role in cellular accommodation of intracellular fungal structures, and roots of *vapyrin* do not contain arbuscules (Pumplin et al. 2009). *Lyr1* transcript was detected at similar levels in wild type and *mtpt4*, however it was barely detectable in roots of *vapyrin* (Figure 3-6). As expected, *Lyr1* was not detected in mock-inoculated roots (Figure 3-6a), consistent with Gomez et al. 2009.

lyr1 roots form normal mycorrhiza, but nfp and lyr1nfp are more colonized than wild type

Considering the induction of *Lyr1* during AM symbiosis, and an apparently specific expression, we hypothesized that the gene is essential for normal symbiosis. A preliminary RNAi experiment targeting *Lyr1* demonstrated fewer and slightly shriveled arbuscules in the mutant roots (Karen Gomez, unpublished data). We then obtained a *lyr1* ethyl methanesulfonate mutant, courtesy of Dr. Clare Gough, INRA, Toulouse France, that contains a stop codon at the twentieth codon of the gene; however, analysis of this mutant did not reproduce the RNAi results, and *G. versiforme* was able to colonize the *lyr1* roots as well as wild type roots (data not shown). Considering the possibility that the RNAi could have silenced an off-target gene, such as the similar *NFP* that may function redundantly with *Lyr1*, we crossed *lyr1* with the *nfp-1* mutant, which has a stop codon in place of its start codon (Arrighi et al. 2006), to see if a loss of both genes would lead to a defect in AM formation.

We inoculated roots of single mutants *lyr1* and *nfp*, two double mutants, and a wild type segregant from the *lyr1nfp* F2 population with *G. versiforme*. At 4 weeks post inoculation (wpi) we found that *lyr1* roots were again colonized at the same level as wild type (Figure 3-7), and we observed no obvious differences in arbuscule number or size. Opposite to our hypothesis, roots containing the *nfp* mutation, including the single and double mutants, were more colonized than those of wild type and *lyr1*. At first glance, colonization units (the length of root containing hyphae from a single penetration event) in roots of *nfp* and *lyr1nfp* were much longer than those of wild type and *lyr1* (Figure 3-7a). To quantify this, we

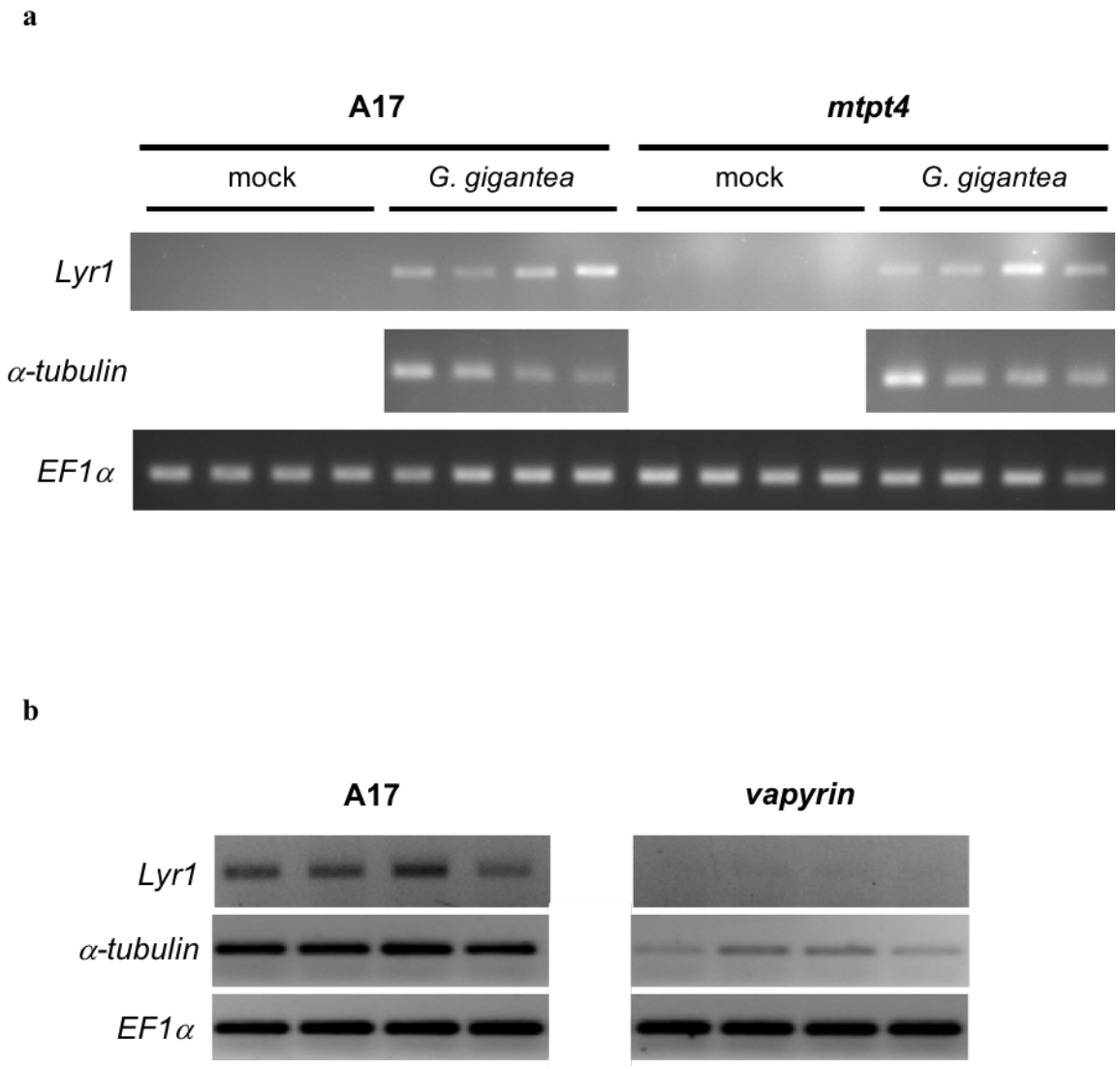

Figure 3-6: *Lyr1* is expressed in roots of *mtpt4*, but very little in *vapyrin*.
RT-PCR demonstrating *Lyr1* expression in roots of *M. truncatula* wild type (A17) and *mtpt4* mutants **(a)** and *vapyrin* mutants **(b)** colonized with *Gigaspora gigantea*.

randomly selected and measured ten colonization units from each root system and found the increase in expansion to be strongly significant in the single and double mutants (Figure 3-7b). To demonstrate an overall increase in colonization, we counted total number of colonization units in *nfp* and wild type roots and found a strongly significant increase in total colonization events in *nfp* roots (Figure 3-7c).

To confirm the effect of *nfp* deletion on *G. versiforme* colonization, we repeated the experiment with the same segregating single and double mutants. We again found longer colonization units in *nfp* roots, but with less significance (Figure 3-8a). We used qPCR to measure levels of symbiosis-related transcripts in the roots, including the AM-specific phosphate transporter, *MtPt4*, and an arbuscule marker, *MtLec5*. While transcripts of *MtPt4* and *MtLec5* appeared to be higher in *nfp* mutants, the only significant increase was *MtLec5* in the single *nfp* mutant (Figure 3-8b). In both experiments, root colonization was greatly variable between samples of each genotype. To better control for this variability, and to test the mutants with a different fungus, we repeated the experiment with *G. gigantea*, whose large spores allow for application of an exact number of spores. Preliminary analysis of fungal colonization levels revealed no obvious difference between *nfp* mutants and wild type. We used qRT-PCR to check expression of fungal tubulin and symbiosis markers. Interestingly, *G. gigantea* may colonize *nfp* roots less efficiently than wild type, as *MtPt4* and *MtLec5* were significantly lower in *nfp* and *lyr1nfp*; however overall colonization seemed unaffected, as demonstrated by levels of *G. gigantea α-tubulin* (Figure 3-9).

To confirm the results observed in both experiments using *G. versiforme*, we tested if the increase in colonization is truly due to the loss *NFP* or the result of a separate mutation that may be segregating with the *nfp* allele. To do so, we measured *G. versiforme* colonization unit length in two segregating *nfp* mutants, the parent *nfp* mutant, and a segregating wild type. Plants in this experiment were accidentally given twice as much fertilizer and grew much more quickly than previous experiments. A test harvest at 2 wpi led us to harvest the entire

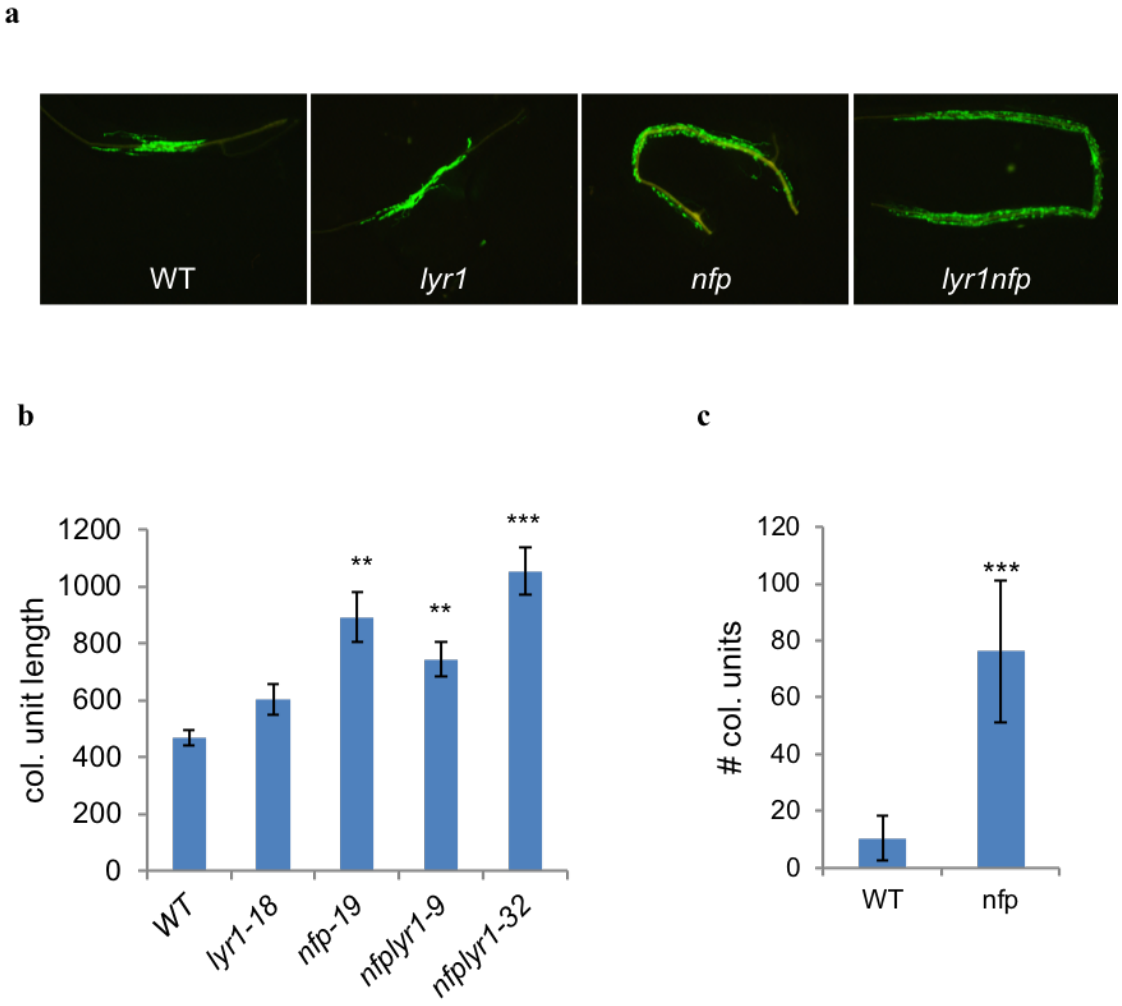

Figure 3-7: *nfp* is more greatly colonized by *G. versiforme* than *lyr1* and wild type. **(a)** Examples of colonization units from each segregating genotype. **(b)** Average length of colonization units formed on each segregant for the first experiment with *G. versiforme,* n ≥ 50 **(c)** Number of individual infection units from all samples in second experiment, n = 6 **(d)** Average levels of free phosphate in shoots, n = 3 **(b-d)** Bars are standard error. Stars denote significance in comparison to WT, Student's t-test, *p < 0.05; **p < 0.01; ***p < 0.001.

a

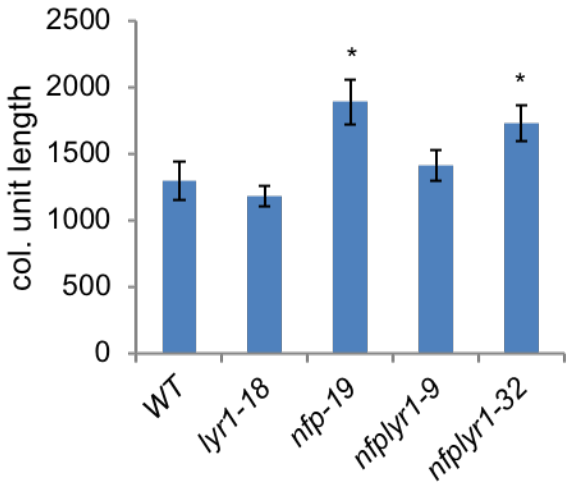

b

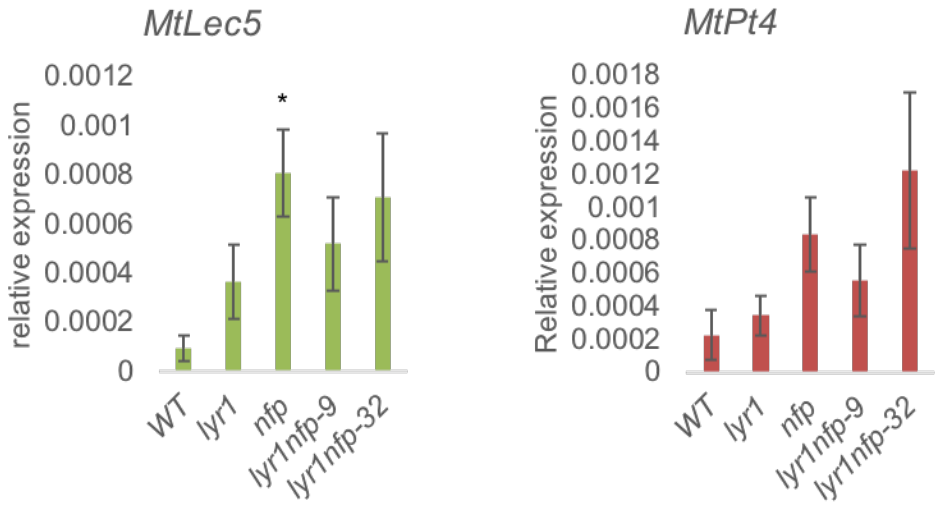

Figure 3-8: In a second, independent experiment, colonization of *nfp* is greater than *lyr1* and wild type in the repeated experiment. (a) Average length of colonization units from a second experiment with *G. versiforme*. n ≥ 43, bars are standard error. **(b)** Expression of *MtLec5* and *MtPt4* in roots of segregating mutants from second experiment with *G. versiforme*. Stars denote significance in comparison to WT, Student's t-test, *p < 0.05

experiment at 2wpi (the next day) because colonization had already progressed further than in previous experiments. Although colonization units appeared to be slightly longer in all *nfp* mutants than in wild type, the result was not significant for any of the samples (Figure 3-10). Overall, colonization progressed further in this experiment than it had in the previous two, as demonstrated by the longer colonization unit lengths overall in Figure 3-10 (measured in pixels), as compared with Figure 3-7b and 3-8a.

Three short LysM-RLK-like genes have high similarity to Lyr1 and are induced by AM fungi

Among the several short LysM-RLK-like genes identified in our genomic search (Table 3-2), three are located in tandem with *Lyr1* on chromosome 8 (Figure 3-11a), which we refer to as LysM320, LysM340, and LysM360 based on the last three numbers of their gene IDs. All three are directly upstream from and on the same strand as *Lyr1*, but between each pair is an unrelated gene on the opposite strand (Figure 3-11a). All three short genes share high identity with portions of the extracellular domain of *Lyr1*; 83%, 85% and 90% for LysM320, LysM340, and LysM360, respectively. The smallest, LysM340 does not contain a full LysM, while LysM320 contains one LysM similar to the third LysM of Lyr1, and LysM360 contains two LysMs similar to the first and third LysMs of Lyr1. Their alignment with the extracellular domain of Lyr1 is shown in Figure 3-11b.

Considering these short LysM genes may have been off-target hits of the *Lyr1* RNAi hairpin, we were interested to know if they are expressed in *M. truncatula* roots. *LysM340* and *LysM360* contain an upstream promoter region similar to that of *Lyr1*. Using RT-PCR, we were able to detect transcripts for LysM320 and LysM360, but only in colonized roots, indicating these two genes are induced by AM fungi (Figure 3-12a). This expression pattern reflects data from the *M. truncatula* Gene Atlas for LysM360. LysM320 and LysM340 are not represented in the Gene Atlas. According to the available data for LysM360, this gene is only

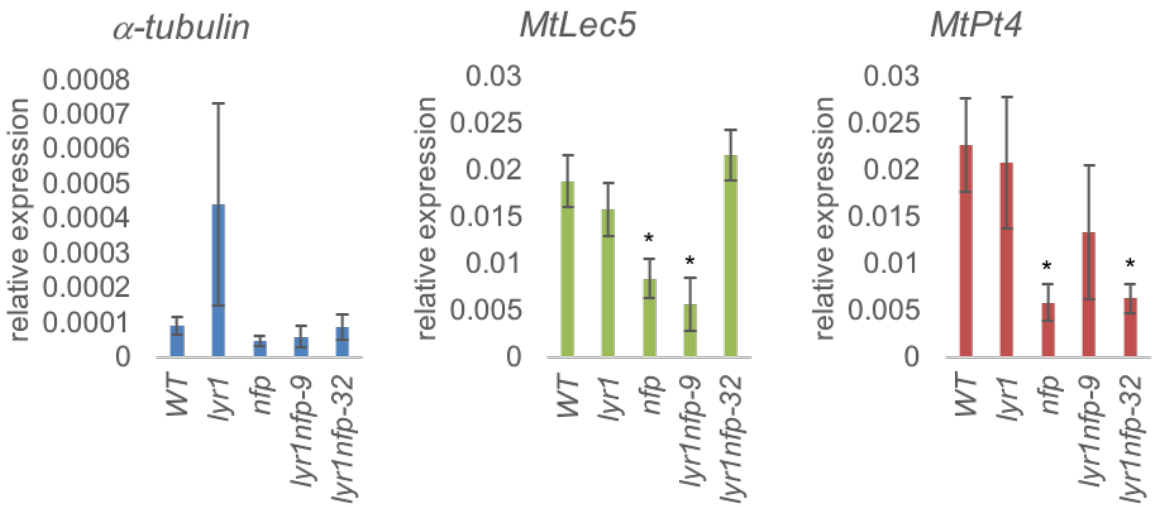

Figure 3-9: *Gigaspora gigantea* does not colonize *nfp* mutants differently than wild type. Expression of *α-tubulin*, *MtLec5*, and *MtPt4* in roots of segregating mutants from experiment with *G. gigantea*. All expression is relative to *M. truncatula elongation factor*. Bars are standard error, n = 3. Stars denote significance in comparison to WT, Student's t-test, *p < 0.05.

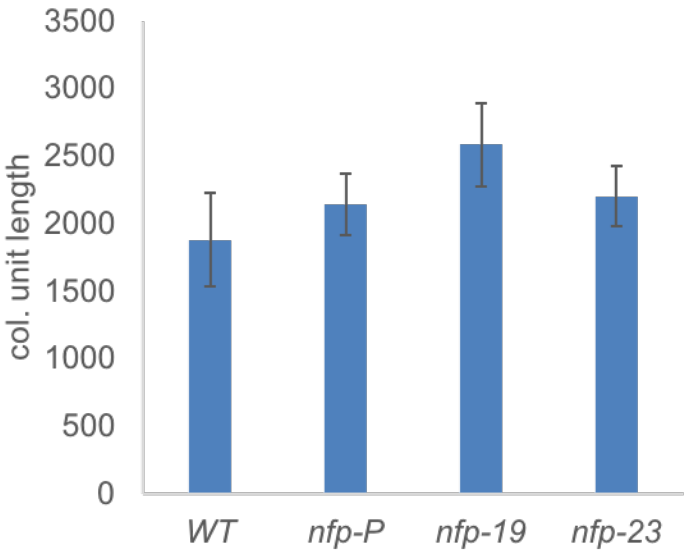

Figure 3-10: AM colonization of segregating *nfp* mutants is not significantly different from that of the segregating wild type. Length of colonization units in *nfp* mutants. WT is a segregating wild type from *lyr1* x *nfp*, *nfp-P* is the parent, and *nfp-19* and *nfp-23* are segregating mutants. Bars are standard error, n = 30. No significance, Student's t-test, $p < 0.05$.

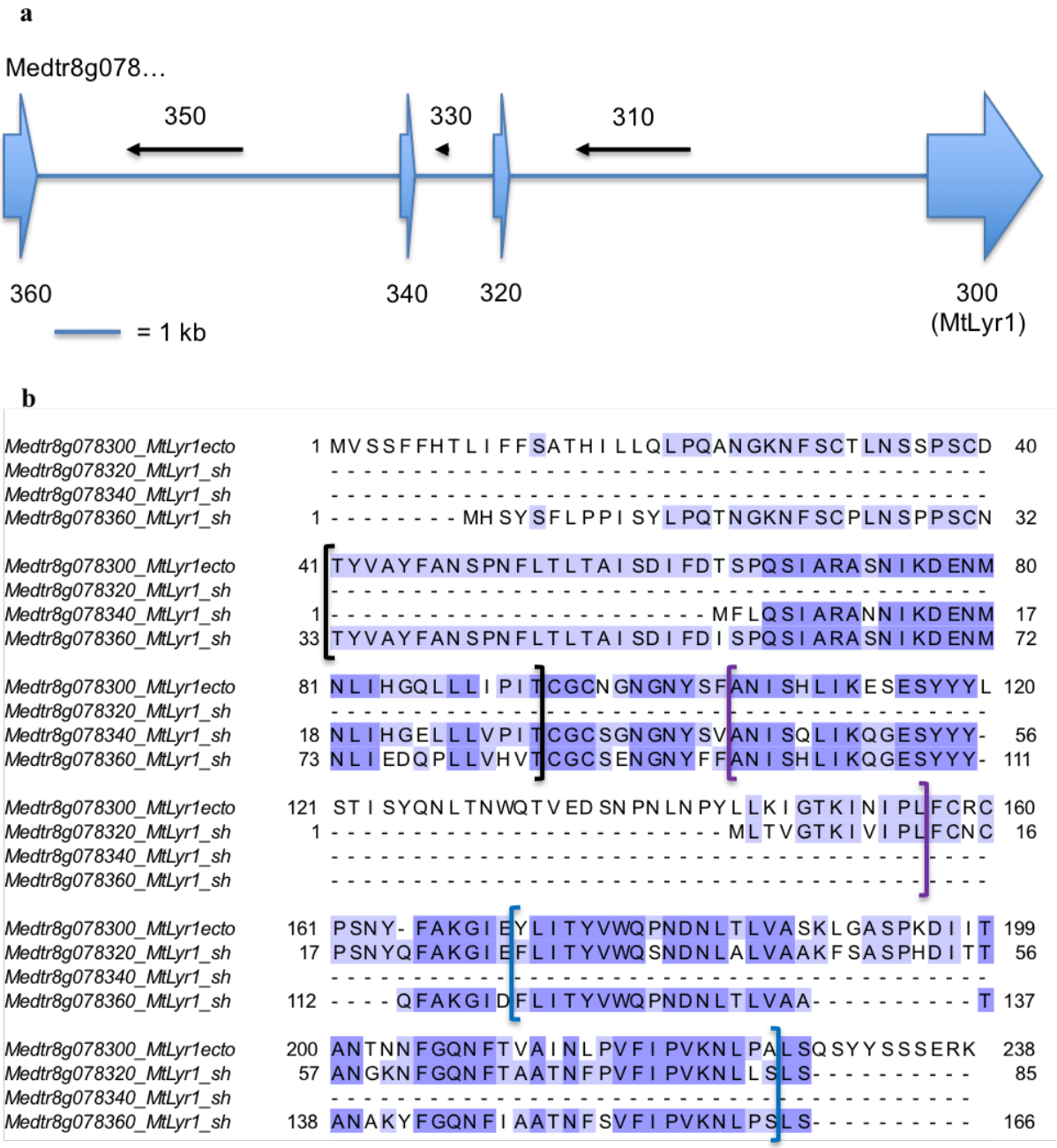

Figure 3-11: LysM domains of *MtLyr1* have been duplicated. (a) Three duplications of the *MtLyr1* gene exist in tandem with *MtLyr1* on chromosome 8. Large blue arrows represent *MtLyr1* and duplications. Black arrows represent other genes on the chromosome. **(b)** Protein alignment of MtLyr1 ectodomain and all three duplications. LysM domains of Lyr1 are indicated by brackets: LysM1, black; LysM2, purple; LysM3, blue.

expressed in samples with AM fungi, and even much more highly than *Lyr1* in LCM samples (Figure 3-12b).

Mutants in lyk10 experience a delay in AM fungal colonization

Of the 21 LysM-RLKs in *M. truncatula*, Lyk10 is the only gene that is conserved in AM hosts and absent in plants unable to establish AM symbiosis (Bravo et al. 2016). To test if it has a role in AM symbiosis, we ordered two *Tnt1* insertion lines with insertions in the first exon of *Lyk10*. Both came as segregating seed, and with one planting we identified a wild type and homozygous mutant in each. Using seed from that first planting, we tested colonization with *G. versiforme*, but observed no difference between mutant and wild type. Colonization was very high in this experiment, which may have masked any subtle phenotype. Such subtle differences would also be difficult to quantify in the *Tnt1* insertion lines, which have other segregating insertions that may influence colonization.

To address this, we back-crossed each *lyk10* mutant to the parent ecotype, R108, and tested one of them for colonization by *G. versiforme*, this time with 1/5 as many spores, and 10X higher P_i concentration to slightly limit colonization (Breuillin et al. 2010; Bravo et al. 2016). Plants were harvested at three timepoints and analyzed for percent root colonization at each[7]. At 3 and 5 wpp, no significant difference was observed between mutant and segregating wild type, but at 7wpp, colonization was significantly lower in the *lyk10* roots than in the wild type roots (Figure 3-13). The experiment was later repeated with both *lyk10 Tnt1* insertion mutants. As observed previously, the first mutant showed reduced colonization; however, the second *lyk10* mutant and its segregating wild type both had reduced colonization relative to the first wild type, and were not significantly different from each other, making our results inconclusive (Armando Bravo, personal communication).

[7] This experiment was done by Armando Bravo.

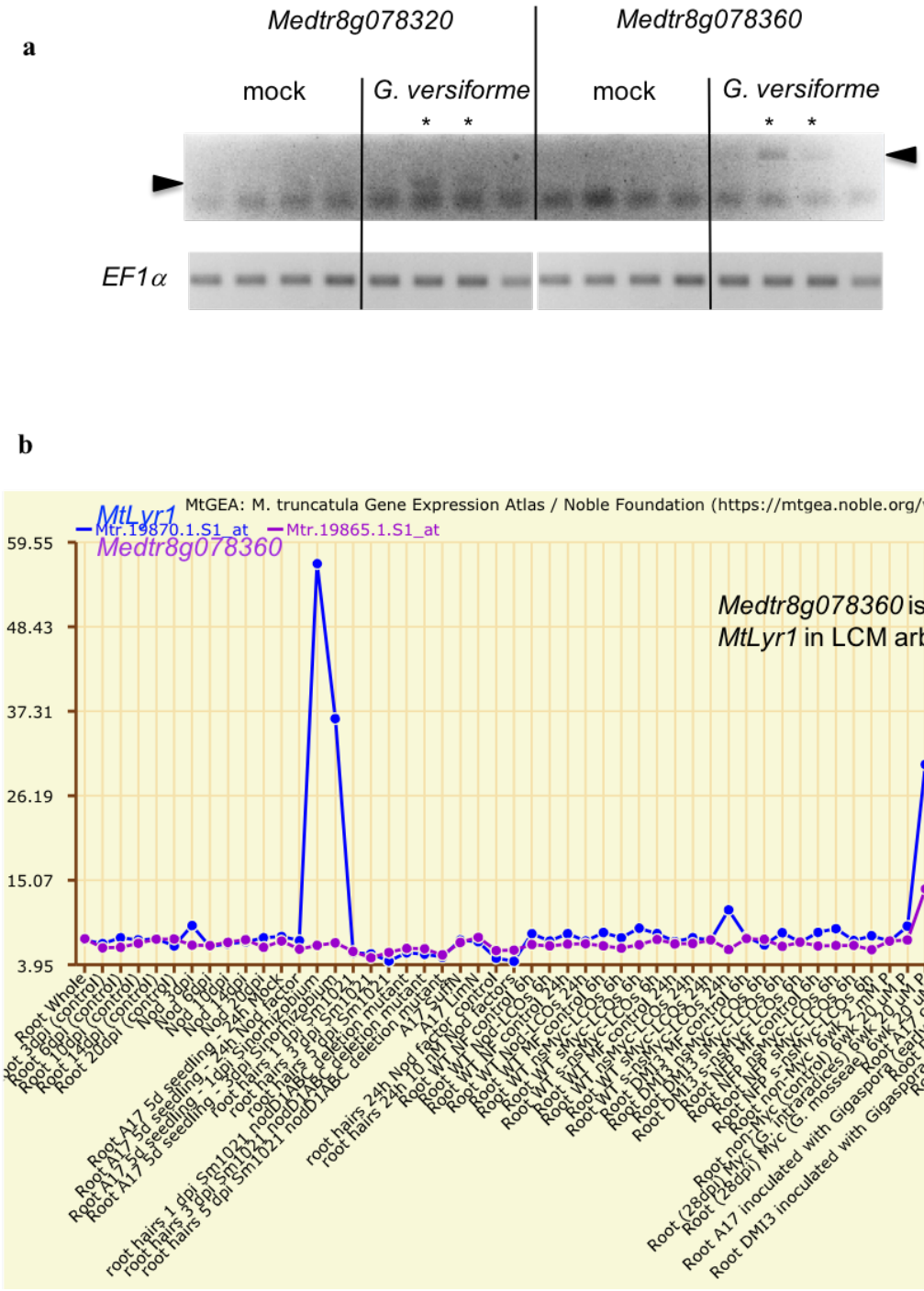

Figure 3-12: *Medtr8g078360* is induced in roots with AM (a) RT-PCR demonstrating induction of both *Medtr8g078320* and *Medtr8g078360* in mock and *G. versiforme*-inoculated roots. Stars mark samples in which transcript was detected. **(b)** *M. truncatula* Gene Atlas normalized levels of *MtLyr1* and *Medtr8g078360* transcripts in root samples.

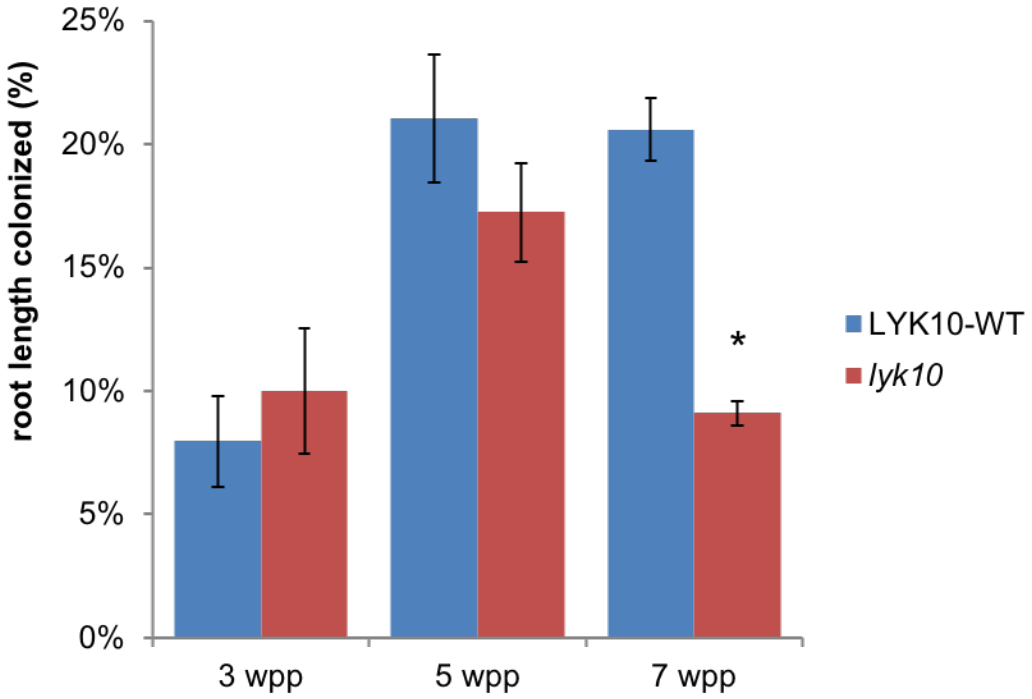

Figure 3-13: Roots of *mtlyk10* are less colonized at 7 wpp than those of the segregating wild type. Graph shows percent colonization by gridline-intersect quantification. Bars represent standard error, n = 4. Star denotes significance relative to wild type roots for each time point, Student's t-test, $p < 0.05$.

Discussion

The LysM-RLK family in plants includes receptors and co-receptors for signaling molecules involved in a spectrum of interactions, from defense to symbiosis (Zipfel and Oldroyd 2017). The family is greatly expanded, especially in legumes, offering potential for functional redundancy, but also functional diversity. We have identified five LysM-RLKs in *M. truncatula* that had not been previously reported, bringing the total number for this plant to 21 LysM-RLKs. Lyr7 is an ortholog of the major chitin receptor protein in *A. thaliana*, AtLyk5 (Cao et al. 2014), and highly similar to Lyr4, which is required for resistance to the necrotrophic fungal pathogen, *Botrytis cinerea* (Bozsoki et al. 2017). While Lyr8, Lyr9, and Lyr10 did not group with any characterized LysM-RLKs in our phylogenetic reconstruction, Lyr8 is intriguing for multiple reasons. Its kinase is missing both the P-loop and the activation segment, which is otherwise only the case for NFP and Lyr1 (Arrighi et al. 2006). Furthermore, like Lyr1, the LysM domain of Lyr8 has been duplicated in the genome. Interestingly, contrary to Lyr1, Lyr8 appears to be down-regulated by AM symbiosis, suggesting it could be involved in negative regulation. The newly identified Lyk11 is an ortholog of AtLyk3, which is necessary for NF attenuation of defense responses to flagellin (Liang et al. 2013). Without Lyk11, Lyk10 would be considered the ortholog of AtLyk3, and would not be considered AM-conserved. The duplication of the AtLyk3 clade is conserved among plant species capable of establishing AM symbiosis and absent in those that have lost this capability, indicating this clade may be important for AM symbiosis (Bravo et al. 2016; this study).

Of the 21 LysM-RLKs in *M. truncatula*, only *Lyr1* is consistently induced by AM symbiosis (although *Lyr9* remains to be tested). By RT-PCR, we only ever detected *Lyr1* transcript in inoculated roots, and expression in the mock-inoculated roots was very low when quantified by qRT-PCR. Based on this expression data, and the preliminary results with RNAi, we were surprised by the lack of any effect of the *lyr1* mutant on AM fungal

colonization. We hypothesized that Lyr1 and NFP could act redundantly in AM symbiosis, and although the *lyr1nfp* double mutants were colonized differently than wild type, there was no difference between the single *nfp* mutant and *lyr1nfp*, indicating that loss of *Lyr1* did not contribute to the effect. One possible reason we might miss an effect of the *lyr1* deletion would be if the gene is important for later stages in symbiosis, including arbuscule degeneration. The near lack of *Lyr1* transcript in colonized roots of *vapyrin* suggests the gene is predominantly expressed in cells containing arbuscules, consistent with earlier data demonstrating expression of *Lyr1* in cells containing arbuscules (Gomez et al. 2009). *Lyr1* is not upregulated in *mtpt4* roots, and thus not upregulated for arbuscule degeneration (Floss et al. 2017).

Rasmussen et al. 2016 reported a similar lack of contribution to AM symbiosis for LjLys11, the paralog of NFR5 corresponding to Lyr1, but in *L. japonicus*. They also tested for colonization by two different fungi, *R. irregularis* and *Gigaspora margarita*, and neither was affected by the *ljlys11* deletion. Like us, they then tried a combination of mutants, hypothesizing that the similar LysM-RLKs could be acting redundantly. They went a step further and tested the triple mutant, *lys11nfr5nfr1*, which eliminates both Nod factor receptors and *Lys11*. The equivalent in *Medicago* would be *lyr1nfplyk3*. This triple deletion had no effect on AM formation in their experimental systems (Rasmussen et al. 2016). The result of the triple mutant is surprising considering that *nfr1* was previously shown to be less efficiently colonized by *R. irregularis* (Zhang et al. 2015). In the previous experiments, the authors observed the effect of *nfr1* only when they used a low spore density, with about one-fifth as many spores as our experiments. This degree of stringency for mycorrhiza formation should be tested with the *lyr1* mutant before any final conclusion is drawn as to its contribution to AM symbiosis.

While lower AM fungal colonization may be necessary to demonstrate subtle contributions of redundant genes, such as *Lyr1*, to AM symbiosis, it does not explain why

Lyr1 RNAi roots had fewer and slightly shriveled arbuscules in comparison to the control. If the result of silencing *Lyr1* were due to loss of its transcript alone, we would expect the effect to be amplified in a deletion mutant. Loss of the effect suggests that the RNAi phenotype was not a result of *Lyr1* silencing but may have resulted from off-target silencing. In our search of the *M. truncatula* genome for additional LysM-RLKs, we identified three genes with high similarity to the *Lyr1* LysM domain, two of which are expressed and induced in mycorrhizal roots and may even be more highly-expressed than *Lyr1* in cells containing arbuscules, according to the *M. truncatula* Gene Atlas. Short paralogs of LysM-RLKs have been previously reported as pseudogenes, as they resemble the longer versions with early stop codons, and thus have not been investigated (Arrighi et al. 2006; De Mita et al. 2014). Recently, a novel mutant of AtCERK1 led to the discovery that this protein sheds its ectodomain, which acts as a deregulator of cell death in response to biotrophic pathogens (Petutschnig et al. 2014). If ectodomain shedding is necessary for Lyr1's contribution to AM formation, then LysM360 or LysM320 may act redundantly with Lyr1. These short *Lyr1* paralogs should be carefully targeted by RNAi in the *lyr1* mutant background to test this hypothesis.

Although our deletion mutant analyses demonstrated a lack of effect of the *lyr1* mutant on AM symbiosis, we were surprised to find that the *nfp* mutant had more expansive colonization. This result suggests that NFP may be a negative regulator of symbiosis, which is further supported by reports that *nfp* mutants are more susceptible to biotrophic fungal pathogens (Ben et al. 2012; Rey et al. 2013). In the end, our results regarding the effect of *nfp* deletion on AM symbiosis are inconclusive, as we were not able to show a significant difference between the segregating *nfp* mutants and wild type roots. However, the lack of a difference is likely due to an environmental factor, since one of the *nfp* mutants had been included in earlier experiments and had an increase in colonization in both.

One major difference between the segregating *nfp* experiment and the previous two was that the plants were accidentally fertilized twice as much. With more nutrients, both the plants and fungi grew more quickly, and the colonization units were overall much longer than the original experiments with *lyr1nfp*. Longer colonization units increase the risk that two overlapping units will be measured as one, which would increase variability within each root system and any subtle effects would be lost. Zhang et al. 2015 tested AM fungal colonization of *nfp* roots using their stringent inoculation protocol, but saw no difference from wild type; however, they only measured percent colonization at a timepoint when 50% of the root system was colonized. At that level of colonization, measuring individual colonization units would be nearly impossible due to overlap. An overexpression experiment may more easily reveal if NFP is a regulator of symbiosis – we would expect higher levels of NFP to limit growth of the AM fungus, and possibly also limit (hemi)biotrophic pathogens.

By the time we tested the backcrossed *lyk10* mutants, Zhang et al. 2015 had reported their success in using stringent inoculation to reveal subtle phenotypes. Using a similar stringency with *lyk10*, we were able to detect a defect in AM fungal colonization, but only well after the symbiosis was established. A simple explanation for only a slight decrease in colonization of the mutants would be if its contribution is redundant with its paralog, *Lyk11*, which is orthologous to *AtLyk3*, the LysM-RLK required for CO5 and LCO inhibition of flg22 and chitin-elicited defenses (Liang et al. 2013). Several studies have reported an early induction of defense genes in response to AM fungi that is later suppressed (Spanu and Bonfante-Fasolo, 1988; Spanu et al., 1989; Lambais and Mehdy, 1995; Harrison and Dixon, 1993; Liu et al., 2003). Additionally, silencing of genes involved in production of ROS enhances early colonization (Kiirika et al., 2012; Arthikala et al., 2013). AM fungi produce LCOs and CO4/5 that may signal through both Lyk10 and Lyk11 to suppress immune responses triggered by chitin and other elicitors in their cell walls. If this is true, we would

predict the double *lyk10lyk11* mutant would have even lower levels of fungal colonization than the *lyk10* mutant and induction of defense-related genes.

As the putative receptor for EPS during RN symbiosis, an alternative role for Lyk10 may be to facilitate bacterial enhancement of AM symbiosis through EPS-mediated suppression of plant defenses. Such a role would be missed in our experimental system since we begin our experiments with completely sterile growth media and spores; however, our growth system is not axenic, and bacteria and other fungi have been known to make their way into the root systems of some experiments, well before 7 wpp. Concurrent colonization by rhizobia and AM fungi can have synergistic effects on plant growth and nutrient status (van der Heijden et al. 2015), Considering both NF and myc-LCOs induce expression of *Lyk10*/*EPR3* (*M. truncatula* Gene Atlas, Kawaharada et al. 2015) we can speculate that in dually-inoculated legumes, rhizobial NF and myc-LCOs would induce expression of *Lyk10*, through which rhizobial EPS would suppress plant immune responses and enhance colonization by both symbionts.

Although a clear role has been demonstrated for EPR3 in rhizobial symbiosis (Kawaharada et al. 2015), the Lyk10/EPR3 clade contains orthologs from non-legumes incapable of establishing RN symbiosis. Likewise, bacterial endophytes of non-legumes also produce EPS (Meneses et al. 2011), and may signal through Lyk10/EPR3, although the importance for AM symbiosis is suggested by the lack of an ortholog in species that do not host AM fungi (Bravo et al. 2016). Further hinting at the importance for EPS in AM symbiosis, *Sinorhizobium meliloti*, a rhizobium compatible with *M. truncatula*, produces two distinct EPS molecules, succinoglycan and galactoglucan, the former of which facilitates bacterial entry, while production of the other is induced under phosphate-limiting conditions (Zhan et al. 1991; Skorupska et al. 2006) – conditions known to promote AM symbiosis.

Conclusion

Our results from this chapter of work supplement the growing body of literature demonstrating the complex mechanisms involving LysM-RLKs in plants (Desaki et al 2017). The discovery of five more LysM-RLK family members in *M. truncatula* adds to the potential for functional redundancy and increases the number of possible combinations of receptors and co-receptors that may be involved in only slightly diverging functions. We approached this work hopeful, almost expecting, to discover a near loss-of-function symbiosis mutant, but found instead subtleties that may or may not be resolved through careful tweaking of experimental variables, such as stringent spore load, pyramid gene deletion, or the addition of other microbes or microbial signals. What we can conclude is that *Lyr1*, *NFP*, and *Lyk10* are dispensable for AM symbiosis in the experimental conditions we have tested. These genes may still have been selected and maintained for their roles in symbiosis, as evolution favors even subtle advantages. AM fungi are able to colonize host roots and confer an advantage in many different types of environments; however, the one thing they have in common that differs from the lab is a plethora of other microorganisms often competing for the same source of carbon from the plant. While other microorganisms are often left out of experiments in order to simplify the analysis, for the LysM-RLKs which initiate signaling for a diversity of microbes, considering multi-partite interactions may be necessary for finally resolving some of the bigger pictures.

Materials and Methods

Plant material

Both *lyr1* and *nfp-1* are tilling mutants in *M. truncatula* var. Jemalong A17 and were identified prior to this work. *lyr1* was provided by Clare Gough and has not been published. The *Tnt1* insertions in *lyk10* are in *M. truncatula* var. R108 background and were ordered from the Noble Research Institute's database of *M. truncatula* mutants (Tadege et al. 2008). Two insertion lines, NF11530 and NF9690, were identified, each with the *Tnt1* transposon inserted at the end of the first exon. Both insertion lines were back-crossed to R108 and selfed for the production of homozygous mutant and wild type. Results reported in this chapter were from experiments done with segregants from the back-crossed NF11530.

Plant growth and fungal inoculum

Unless otherwise stated, plants were grown in a growth chamber with 16 h light at 25°C / 8 h dark at 22°C, at 40% relative humidity. Spores of *G. versiforme* and *G. gigantea* were cultured on leek and bahia grass, respectively, harvested, and surface sterilized as previously described (Liu et al. 2007). Experiments with *G. versiforme* were done in 11 cm pots with turface and a 1 cm layer of sand on which roots of 1 wk old seedlings, previously grown in turface, were each directly inoculated with 500 spores then covered with more turface. Each pot contained 3-4 seedlings, and 3 pots were used per treatment. Each plant was considered a biological replicate. Experiments with *G. gigantea* were done in 22.5 cm cone-tainers with turface and a 1 cm sand layer 7 cm below the surface, on which 10 spores were pipetted and covered with turface. Two 2-day old seedlings were then planted into the top layer of turface and inoculated by growing through the sand layer with spores. Each cone was considered a biological replicate. Inoculated plants were only misted for the first 5 days to avoid disturbing the spores. They were then watered daily and fertilized every third day with a

modified half-strength Hoagland's solution containing 20 μM potassium phosphate (Arnon and Hoagland 1940). Expect in the case of the segregating *nfp* mutants where they were given double, pots were given 50 mL of fertilizer and cones were given 15 mL.

For analysis of the back-crossed *lyk10* mutants, plants were inoculated and grown as in Bravo et al. 2016. Briefly, plants were grown in cones similarly to experiments with *G. gigantea* (above), but with a 1:1 mixture of gravel and sand in place of turface, and 100 *G. versiforme* spores were pipetted onto the sand layer and covered with the gravel/sand mixture. Three 2-day-old seedlings were planted in each cone and treated as one biological sample together. Cones were fertilized after 5 days with modified Hoaglands containing 200 μM potassium phosphate, and twice weekly thereafter. At each harvest, only the roots from 2 cm above to 2 cm below the spore/sand layer were analyzed for colonization or gene expression.

Expression analyses

Approximately one-third of the root systems were randomly sampled and immediately frozen in liquid nitrogen. RNA was extracted using the Trizol method (Invitrogen) and 500 ng of each sample were used as template for cDNA synthesis using SuperScript III Reverse Transcriptase (Invitrogen), as previously reported in Gomez et al. 2009. Quantitative PCR was done on an ABI PRISM 7900 HT sequence detection system in 384-well plates with SYBR Green PCR Master Mix (Applied Biosystems, http://www.applied- biosystems.com) according to methods outlined in Breuillin-Sessoms et al. 2015.

Analysis of colonization by microscopy

Roots harvested for microscopy were dehydrated overnight in 50% ethanol, then transferred to 10% KOH and left at room temperature for 1 week. For quick test of colonization levels, roots were cleared in 2 hours by boiling in KOH. After KOH, roots were rinsed at least 5 times with tap water, then left overnight in ddH_2O. The next morning they

were transferred to PBS, which was replaced by a solution of WGA-Alexafluor488 (Molecular Probes) in PBS and kept in the dark. Colonization was analyzed using an Olympus SZX-12 stereo microscope. Length of colonization units was determined by imaging complete units from end to end at a consistent magnification and resolution. Using ImageJ, lines were drawn from the end of one end of the colonization unit to the other, from the tips of hyphae, then the lines were measured in pixels.

Protein alignment and phylogenetic analysis

All protein sequence alignments were done with MUSCLE using the Jalview alignment software (Waterhouse et al. 2009). Phylogenetic reconstruction of all LysM-RLKs was done with MrBayes 3.2.2 on XSEDE through the CIPRES Science Gateway (Ronquist et al., 2012; Towns et al., 2014; Miller et al., 2010) using the WAG substitution model. Other parameters included 2 runs with 4 chains, 1 million generations, sampling every 500, with a burn-in of 2500 samples (25%). Trees were formatted using FigTree version 1.4.0 (http://tree.bio.ed.ac.uk/software/figtree/).

Primers used in this study

G. versiforme α-tubulin	F: 5'-TCTCCAATGCGGCCAAATCT-3'
	R: 5'-TCTCCAATGCGGCCAAATCT-3'
G. gigantea α-tubulin	F: 5'-TCGTCGACTTGGAACCTACC-3'
	R: 5'-CCACCTCCAAAGGAGTGAAA-3'
Medtr6g021800 (EF1-α)	F: 5'-GAGACCCACAGACAAGCC-3'
	R: 5'-ACTGGCACAGTTCCAATACC-3'
Medtr1g028600 (Pt4)	F: 5'-GACACGAGGCGCTTTCATAGCAGC-3'
	R: 5'-GTCATCGCAGCTGGAACAGCACCG-3'
Medtr5g031030 (Lec5)	F: 5'-TCAAGTTGCTGAAACACATGAT-3'

	R: 5'-GAGCAGAACCATTGCAACAA-3'
Medtr8g078300 (Lyr1)	F: 5’-GGCAGTGAATTGCATAGAAG-3’
	R: 5’-CCATTTCAGCAACCTCTACA-3’
Medtr5g019040 (NFP)	F: 5’-CAACCAACCATCATCTGAACC-3’
	R: 5’-ATAAAGATGTAAGCAAAGTAGTACCA-3’
Medtr5g033490 (Lyk10)	F: 5’-AAGCTTACATGGAGCCTTATAAATG-3’
	R: 5’-AATTCTCACCATGCCATCAA-3’
Medtr4g058570 (Lyr8)	F: 5’-AGGAAAATTGGCAGATGTGG-3’
	R: 5’-CCACAGTTGGCCTATGCAAT-3’
Medtr3g080170 (Lyr7)	F: 5’-TGTTGTTGGCACTCATGGTT-3’
	R: 5’-TTGGACGCAAATTGTGGTAA-3’
Medtr5g042440 (Lyr2)	F: 5’-AGCCGATGGTATCGTGTCAACG-3’
	R: 5’-GCCACCAACCTTTCTGAACCAAACC-3’
Medtr8g078320 (LysM320)	F: 5’-TTCCCTTGTTCTGTAACTGTCC-3’
	R: 5’-ACAAGGGCGAGGTTGTCA-3’
Medtr8g078360 (LysM360)	F: 5’-TCCTACTTGCCACAAACCAA-3’
	R: 5’-CCAGCAAAGGTTGGTCTTCA-3’

REFERENCES

Arrighi, J.-F., Barre, A., Amor, B. Ben, Bersoult, A., Soriano, L. C., Mirabella, R., de Carvalho-Niebel, F., Journet, E.-P., Ghérardi, M., Huguet, T., Geurts, R., Dénarié, J., Rougé, P., and Gough, C. 2006. The Medicago truncatula Lysine Motif-Receptor-like Kinase Gene Family Includes NFP and New Nodule-Expressed Genes. Plant Physiol. 142:265

Aslam, S. N., Newman, M. A., Erbs, G., Morrissey, K. L., Chinchilla, D., Boller, T., Jensen, T. T., Castro, C. De, Ierano, T., Molinaro, A., Jackson, R. W., Knight, M. R., and Cooper, R. M. 2008. Bacterial Polysaccharides Suppress Induced Innate Immunity by Calcium Chelation. Curr. Biol. 18:1078–1083

Bateman, A., and Bycroft, M. 2000. The structure of a LysM domain from E. coli membrane-bound lytic murein transglycosylase D (MltD). J. Mol. Biol. 299:1113–9

Ben Amor, B., Shaw, S. L., Oldroyd, G. E. D. D., Maillet, F., Penmetsa, R. V., Cook, D., Long, S. R., Dénarié, J., and Gough, C. 2003. The NFP locus of Medicago truncatula controls an early step of Nod factor signal transduction upstream of a rapid calcium flux and root hair deformation. Plant J. 34:495–506

Ben, C., Toueni, M., Montanar, S., Tardin, M.-C., Fervel, M., Negahi, A., Saint-Pierre, L., Mathieu, G., Gras, M.-C., Noel, D., Prosperi, J.-M., Pilet-Nayel, M.-L., Barnger, A., Julier, B., Rickauer, M., and Gentzbittel, L. 2012. Natural diversity in the model legume Medicago truncatula allows identifying distinct genetic mechanisms conferring partial resistance to Verticillium wilt. J. Exp. Bot. 64:317–332

Bozsoki, Z., Cheng, J., Feng, F., Gysel, K., Vinther, M., Andersen, K. R., Oldroyd, G., Blaise, M., Radutoiu, S., and Stougaard, J. 2017. Receptor-mediated chitin perception in legume roots is functionally separable from Nod factor perception. PNAS. 114:E8118–E8127

Bravo, A., York, T., Pumplin, N., Mueller, L. A., and Harrison, M. J. 2016. Genes conserved for arbuscular mycorrhizal symbiosis identified through phylogenomics. Nat. Plants. 2:15208

Breuillin, F., Schramm, J., Hajirezaei, M., Ahkami, A., Favre, P., Druege, U., Hause, B., Bucher, M., Kretzschmar, T., Bossolini, E., Kuhlemeier, C., Martinoia, E., Franken, P., Scholz, U., and Reinhardt, D. 2010. Phosphate systemically inhibits development of arbuscular mycorrhiza in Petunia hybrida and represses genes involved in mycorrhizal functioning. Plant J. 64:1002–1017

Buendia, L., Wang, T., Girardin, A., and Lefebvre, B. 2016. The LysM receptor-like kinase SlLYK10 regulates the arbuscular mycorrhizal symbiosis in tomato. New Phytol. 210:184–195

Buist, G., Steen, A., Kok, J., and Kuipers, O. P. 2008. LysM, a widely distributed protein motif for binding to (peptido)glycans. Mol. Microbiol. 68:838–847

Cao, Y., Liang, Y., Tanaka, K., Nguyen, C. T., Jedrzejczak, R. P., Joachimiak, A., and Stacey, G. 2014. The kinase LYK5 is a major chitin receptor in *Arabidopsis* and forms a chitin-induced complex with related kinase CERK1. Elife. 3:e03766

Carotenuto, G., Chabaud, M., Miyata, K., Capozzi, M., Takeda, N., Kaku, H., Shibuya, N., Nakagawa, T., Barker, D. G., and Genre, A. 2017. The rice LysM receptor-like kinase OsCERK1 is required for the perception of short-chain chitin oligomers in arbuscular mycorrhizal signaling. New Phytol. 214:1440–1446

Catford, J.-G., Staehelin, C., Lerat, S., Piché, Y., and Vierheilig, H. 2003. Suppression of arbuscular mycorrhizal colonization and nodulation in split-root systems of alfalfa after pre-inoculation and treatment with Nod factors. J. Exp. Bot. 54:1481–1487

Czaja, L. F., Hogekamp, C., Lamm, P., Maillet, F., Martinez, E. A., Samain, E., Denarie, J., Kuster, H., and Hohnjec, N. 2012. Transcriptional Responses toward Diffusible Signals from Symbiotic Microbes Reveal MtNFP- and MtDMI3-Dependent Reprogramming of Host Gene Expression by Arbuscular Mycorrhizal Fungal Lipochitooligosaccharides. Plant Physiol. 159:1671–1685

De Mita, S., Streng, A., Bisseling, T., and Geurts, R. 2014. Evolution of a symbiotic receptor through gene duplications in the legume-rhizobium mutualism. New Phytol. 201:961–972

Desaki, Y., Miyata, K., Suzuki, M., Shibuya, N., and Kaku, H. 2017. Plant immunity and symbiosis signaling mediated by LysM receptors. Innate Immun. 24:92–100

Floss, D. S., Gomez, S. K., Park, H. J., MacLean, A. M., Müller, L. M., Bhattarai, K. K., Lévesque-Tremblay, V., Maldonado-Mendoza, I. E., and Harrison, M. J. 2017. A Transcriptional Program for Arbuscule Degeneration during AM Symbiosis Is Regulated by MYB1. Curr. Biol. 27:1206–1212

Genre, A., Chabaud, M., Balzergue, C., Puech-Pagès, V., Novero, M., Rey, T., Fournier, J., Rochange, S., Bécard, G., Bonfante, P., and Barker, D. G. 2013. Short-chain chitin oligomers from arbuscular mycorrhizal fungi trigger nuclear Ca2+ spiking in Medicago truncatula roots and their production is enhanced by strigolactone. New Phytol. 198:190–202

Gomez, S. K., Javot, H., Deewatthanawong, P., Torres-jerez, I., Tang, Y. H., Blancaflor, E. B., Udvardi, M. K., and Harrison, M. J. 2009. Medicago truncatula and Glomus intraradices gene expression in cortical cells harboring arbuscules in the arbuscular mycorrhizal symbiosis. BMC Plant Biol. 9:10–29

Harrison, M. J., and Dixon, R. a R. A. 1993. Isoflavonoid accumulation and expression of defense gene transcripts during the establishment of vesicular-arbuscular mycorrhizal associations in roots of Medicago truncatula. MPMI. 6:643–654

He, J., Benedito, V. a, Wang, M., Murray, J. D., Zhao, P. X., Tang, Y., and Udvardi, M. K. 2009. The Medicago truncatula gene expression atlas web server. BMC Bioinformatics. 10:441

Hohmann, U., Lau, K., and Hothorn, M. 2017. The Structural Basis of Ligand Perception and Signal Activation by Receptor Kinases. Annu. Rev. Plant Biol. 68:109–137

Indrasumunar, A., Kereszt, A., Searle, I., Miyagi, M., Li, D., Nguyen, C. D. T., Men, A., Carroll, B. J., and Gresshoff, P. M. 2010. Inactivation of duplicated Nod factor receptor 5 (NFR5) genes in recessive loss-of-function non-nodulation mutants of allotetraploid soybean (Glycine max L. Merr.). Plant Cell Physiol. 51:201–214

Indrasumunar, A., Searle, I., Lin, M.-H. H., Kereszt, A., Men, A., Carroll, B. J., and Gresshoff, P. M. 2010. Nodulation factor receptor kinase 1a controls nodule organ number in soybean (Glycine max L. Merr). Plant J. 65:39–50

Javot, H., Penmetsa, R. V., Terzaghi, N., Cook, D. R., and Harrison, M. J. 2007. A Medicago truncatula phosphate transporter indispensable for the arbuscular mycorrhizal symbiosis. PNAS. 104:1720–1725

Jones, J. D. G., and Dangl, J. L. 2006. The plant immune system. Nature. 444:323–329

Jones, K. M., and Walker, G. C. 2008. Responses of the model legume Medicago truncatula to the rhizobial exopolysaccharide succinoglycan. Plant Signal. Behav. 3:888–890

Kawaharada, Y., Kelly, S., Nielsen, M. W., Hjuler, C. T., Gysel, K., Muszyński, A., Carlson, R. W., Thygesen, M. B., Sandal, N., Asmussen, M. H., Vinther, M., Andersen, S. U., Krusell, L., Thirup, S., Jensen, K. J., Ronson, C. W., Blaise, M., Radutoiu, S., and Stougaard, J. 2015. Receptor-mediated exopolysaccharide perception controls bacterial infection. Nature. 523:308–312

Lambais, M. R., and Mehdy, M. C. 1995. Differential expression of defense-related genes in arbuscular mycorrhiza. Can. J. Bot. 73:S533–S540

Lefebvre, B., Klaus-Heisen, D., Pietraszewska-Bogiel, A., Hervé, C., Camut, S., Auriac, M.-C. C., Gasciolli, V., Nurisso, A., Gadella, T. W. J., and Cullimore, J. 2012. Role of N-glycosylation sites and CXC motifs in trafficking of Medicago truncatula Nod factor perception protein to plasma membrane. J. Biol. Chem. 287:10812–10823

Leppyanen, I. V., Shakhnazarova, V. Y., Shtark, O. Y., Vishnevskaya, N. A., Tikhonovich, I. A., and Dolgikh, E. A. 2018. Receptor-like kinase LYK9 in Pisum sativum L. Is the

CERK1-like receptor that controls both plant immunity and AM symbiosis development. Int. J. Mol. Sci. 19:E8

Liang, Y., Cao, Y., Tanaka, K., Thibivilliers, S., Wan, J., Choi, J., Kang, C. H., Qiu, J., and Stacey, G. 2013. Nonlegumes respond to rhizobial Nod factors by suppressing the innate immune response. Science. 341:1384–1387

Limpens, E., Franken, C., Smit, P., Willemse, J., Bisseling, T., and Geurts, R. 2003. LysM Domain Receptor Kinases Regulating Rhizobial Nod Factor-Induced Infection. Science. 302:630–633

Liu, J., Blaylock, L., Endre, G., Cho, J., Town, C. D., Vandenbosch, K. A., and Harrison, M. J. 2003. Transcript profiling coupled with spatial expression analyses reveals genes involved in disinct developmental stages of an arbuscular mycorrhizal symbiosis. Plant Cell. 15:2106–2123

Liu, B., Li, J.-F., Ao, Y., Qu, J., Li, Z., Su, J., Zhang, Y., Liu, J., Feng, D., Qi, K., He, Y., Wang, J., and Wang, H.-B. 2012a. Lysin Motif-Containing Proteins LYP4 and LYP6 Play Dual Roles in Peptidoglycan and Chitin Perception in Rice Innate Immunity. Plant Cell. 24:3406–3419

Liu, T., Liu, Z., Song, C., Hu, Y., Han, Z., She, J. J., Fan, F. F., Wang, J., Jin, C., Chang, J., Zhou, J.-M. J.-M., and Chai, J. 2012b. Chitin-induced dimerization activates a plant immune receptor. Science. 336:1160–1164

Lohmann, G. V., Shimoda, Y., Nielsen, M. W., Jørgensen, F. G., Grossmann, C., Sandal, N., Sørensen, K., Thirup, S., Madsen, L. H., Tabata, S., Sato, S., Stougaard, J., and Radutoiu, S. 2010. Evolution and regulation of the Lotus japonicus LysM receptor gene family. MPMI. 23:510–21

Madsen, E. B., Madsen, L. H., Radutoiu, S., Olbryt, M., Rakwalska, M., Szczyglowski, K., Sato, S., Kaneko, T., Tabata, S., Sandal, N., and Stougaard, J. 2003. A receptor kinase gene of the LysM type is involved in legume perception of rhizobial signals. Nature. 425:637–40

Maillet, F., Poinsot, V., André, O., Puech-Pagès, V., Haouy, A., Gueunier, M., Cromer, L., Giraudet, D., Formey, D., Niebel, A., Martinez, E. A., Driguez, H., Bécard, G., and Dénarié, J. 2011. Fungal lipochitooligosaccharide symbiotic signals in arbuscular mycorrhiza. Nature. 469:58–63

Mélida, H., Sopeña-Torres, S., Bacete, L., Garrido-Arandia, M., Jordá, L., López, G., Muñoz-Barrios, A., Pacios, L. F., and Molina, A. 2018. Non-branched β-1,3-glucan oligosaccharides trigger immune responses in Arabidopsis. Plant J. 93:34–49

Meneses, C. H. S. G., Rouws, L. F. M., Simoes-Araujo, J. L., Vidal, M. S., and Baldani, J. I. 2011. Exopolysaccharide production is required for biofilm formation and plant colonization by the nitrogen-fixing endophyte Gluconacetobacter diazotrophicus. MPMI. 24:1448–58

Miyata, K., Kozaki, T., Kouzai, Y., Ozawa, K., Ishii, K., Asamizu, E., Okabe, Y., Umehara, Y., Miyamoto, A., Kobae, Y., Akiyama, K., Kaku, H., Nishizawa, Y., Shibuya, N., and Nakagawa, T. 2014. The bifunctional plant receptor, OsCERK1, regulates both chitin-triggered immunity and arbuscular mycorrhizal symbiosis in rice. Plant Cell Physiol. 55:1864–1872

Nolen, B., Taylor, S., and Ghosh, G. 2004. Regulation of protein kinases: Controlling activity through activation segment conformation. Mol. Cell. 15:661–675

Op Den Camp, R., Streng, A., De Mita, S., Cao, Q., Polone, E., Liu, W., Ammiraju, J. S. S., Kudrna, D., Wing, R., Untergasser, A., Bisseling, T., and Geurts, R. 2011. LysM-type mycorrhizal receptor recruited for rhizobium symbiosis in nonlegume Parasponia. Science. 331:909–912

Petutschnig, E. K., Stolze, M., Lipka, U., Kopischke, M., Horlacher, J., Valerius, O., Rozhon, W., Gust, A. a, Kemmerling, B., Poppenberger, B., Braus, G. H., Nürnberger, T., and Lipka, V. 2014. A novel Arabidopsis CHITIN ELICITOR RECEPTOR KINASE 1 (CERK1) mutant with enhanced pathogen-induced cell death and altered receptor processing. New Phytol. 204:955–67

Pinto, M. C. De, Lavermicocca, P., Evidente, A., Corsaro, M. M., Lazzaroni, S., Gara, L. De, Vegetale, P., Orabona, V. E., Bari, I.-, De Pinto, M. C., Lavermicocca, P., Evidente, A., Corsaro, M. M., Lazzaroni, S., and De Gara, L. 2003. Exopolysaccharides produced by plant pathogenic bacteria affect ascorbate metabolism in Nicotiana tabacum. Plant Cell Physiol. 44:803–810

Pumplin, N., Mondo, S. J., Topp, S., Starker, C. G., Gantt, J. S., and Harrison, M. J. 2010. *Medicago truncatula* Vapyrin is a novel protein required for arbuscular mycorrhizal symbiosis. Plant J. 61:482–494

Radutoiu, S., Madsen, L. H., Madsen, E. B., Felle, H. H., Umehara, Y., Grønlund, M., Sato, S., Nakamura, Y., Tabata, S., Sandal, N., and Stougaard, J. 2003. Plant recognition of symbiotic bacteria requires two LysM receptor-like kinases. Nature. 425:585–92

Rasmussen, S. R., Füchtbauer, W., Novero, M., Volpe, V., Malkov, N., Genre, A., Bonfante, P., Stougaard, J., and Radutoiu, S. 2016. Intraradical colonization by arbuscular mycorrhizal fungi triggers induction of a lipochitooligosaccharide receptor. Sci. Rep. 6:29733

Rey, T., Nars, A., Bonhomme, M., Bottin, A., Huguet, S., Balzergue, S., Jardinaud, M.-F., Bono, J.-J., Cullimore, J., Dumas, B., Gough, C., and Jacquet, C. 2013. NFP, a LysM protein controlling Nod factor perception, also intervenes in *Medicago truncatula* resistance to pathogens. New Phytol. 198:875–886

Shimizu, T., Nakano, T., Takamizawa, D., Desaki, Y., Ishii-Minami, N., Nishizawa, Y., Minami, E., Okada, K., Yamane, H., Kaku, H., and Shibuya, N. 2010. Two LysM receptor molecules, CEBiP and OsCERK1, cooperatively regulate chitin elicitor signaling in rice. Plant J. 64:204–214

Skorupska, A., Janczarek, M., Marczak, M., Mazur, A., and Król, J. 2006. Rhizobial exopolysaccharides: Genetic control and symbiotic functions. Microb. Cell Fact. 5:1–19

Spanu, P., Boller, T., Ludwig, A., Wiemken, A., Faccio, A., and Bonfante-Fasolo, P. 1989. Chitinase in roots of mycorrhizal *Allium porrum*: regulation and localization. Planta. 177:447–455

Spanu, P., and Bonfante-Fasolo, P. 1988. Cell-wall-bound peroxidase activity in roots of mycorrhizal *Allium porrum*. New Phytol. 109:119–124

Streng, A., op den Camp, R., Bisseling, T., and Geurts, R. 2011. Evolutionary origin of rhizobium Nod factor signaling. Plant Signal. Behav. 6:1510–1504

Sun, J., Miller, J. B., Granqvist, E., Wiley-Kalil, A., Gobbato, E., Maillet, F., Cottaz, S., Samain, E., Venkateshwaran, M., Fort, S., Morris, R. J., Ané, J.-M., Dénarié, J., and Oldroyd, G. E. D. 2015. Activation of Symbiosis Signaling by Arbuscular Mycorrhizal Fungi in Legumes and Rice. Plant Cell. 27:823–838

Tadege, M., Wen, J., He, J., Tu, H., Kwak, Y., Eschstruth, A., Cayrel, A., Endre, G., Zhao, P. X., Chabaud, M., Ratet, P., and Mysore, K. S. 2008. Large-scale insertional mutagenesis using the Tnt1 retrotransposon in the model legume Medicago truncatula. Plant J. 54:335–347

Tang, H., Krishnakumar, V., Bidwell, S., Rosen, B., Chan, A., Zhou, S., Gentzbittel, L., Childs, K. L., Yandell, M., Gundlach, H., Mayer, K. F. X., Schwartz, D. C., and Town, C. D. 2014. An improved genome release (version Mt4.0) for the model legume Medicago truncatula. BMC Genomics. 15:312

van der Heijden, M. G. A. G., Bruin, S. De, Luckerhoff, L., van Logtestijn, R. S. P. S., and Schlaeppi, K. 2015. A widespread plant-fungal-bacterial symbiosis promotes plant biodiversity, plant nutrition and seedling recruitment. ISME J. 10:389–99

Vierheilig, H., Bennett, R., Kiddle, G., Kaldorf, M., and Ludwig-Müller, J. 2000. Differences in glucosinolate patterns and arbuscular mycorrhizal status of glucosinolate-containing plant species. New Phytol. 146:343–352

Willmann, R., Lajunen, H. M., Erbs, G., Newman, M., Kolb, D., Tsuda, K., Katagiri, F., Fliegmann, J., Bono, J. J., Cullimore, J. V., Jehle, A. K., Götz, F., Kulik, A., Molinaro, A., Lipka, V., Gust, A. A., and Nürnberger, T. 2011. *Arabidopsis* lysin-motif proteins LYM1 LYM3 CERK1 mediate bacterial peptidoglycan sensing and immunity to bacterial infection. PNAS. 108:19824–19829

Zamioudis, C., and Pieterse, C. M. J. 2012. Modulation of host immunity by beneficial microbes. Mol. Plant. Microbe. Interact. 25:139–150

Zhan, H., Lee, C. C., and Leigh, J. A. 1991. Induction of the second exopolysaccharide (EPSb) in Rhizobium meliloti SU47 by low phosphate concentrations. J. Bacteriol. 173:7391–7394

Zhang, X., Dong, W., Sun, J., Feng, F., Deng, Y., He, Z., Oldroyd, G. E. D., and Wang, E. 2015. The receptor kinase CERK1 has dual functions in symbiosis and immunity signalling. Plant J. 81:258–267

Zhang, X.-C., Cannon, S. B., and Stacey, G. 2009. Evolutionary genomics of LysM genes in land plants. BMC Evol. Biol. 9:183

Zipfel, C., and Oldroyd, G. E. D. 2017. Plant signalling in symbiosis and immunity. Nature. 543:328–336

CHAPTER 4

SMALL, CYSTEINE-RICH LYSM PROTEINS ARE INDUCED BY ARBUSCULAR MYCORRHIZAL SYMBIOSIS

Abstract

Arbuscular mycorrhiza (AM) occurs in over 80% of land plants, which accommodate the fungal symbiont through concerted, often specific, signaling. Many genes involved in AM symbiosis are found only in plants capable of entering into this symbiosis, and often the deletion of these genes will preclude normal symbiotic function. The LysM domain plays an important role in signaling for many plant-microbe interactions, including both symbioses and antagonistic plant-microbe interactions. We have identified three small, putatively-secreted proteins containing only a single LysM domain that are conserved for AM symbiosis, which we refer to as AM-SLMs. We show that expression of *AM-SLMs* is specific to plant cells accommodating arbuscules, and their proteins localize to the area surrounding arbuscule branches. Investigation of ligand-binding revealed that AM-SLMs do not bind to chitin, and simultaneous RNA silencing of all three *AM-SLMs* in *Medicago truncatula* had no effect on the ability of AM fungi to colonize roots. Conversely, ectopic expression of two *AM-SLMs* led to an increase in AM fungal growth, indicating two different roles for these genes in AM symbiosis. An alignment and phylogenetic reconstruction of SLM proteins from many species that can or cannot establish AM symbiosis reveals a clear divide into two clades, one of which contains SLMs from AM-compatible plants only. Proteins in the AM-relevant clade contain several cysteines, classifying this group as a new type of cysteine-rich protein. Modeling of protein structure reveals a putative disulfide bond at the site of ligand binding in similar proteins, hinting at a mechanism for regulation and post-translational activation of these proteins.

Introduction

For over 400 million years, certain land plants have harbored fungi from the subphylum Glomeromycotina in their roots where they live symbiotically in a relationship called arbuscular mycorrhiza (AM) (Remy et al. 1994). Land plants have evolved to possess a set of essential genes for accommodating AM fungi in their roots. While several of these symbiosis genes are also important for other mechanisms, and thus contain homologs in plants that do not harbor AM fungi, many are specific to AM symbiosis and absent in non-compatible plant species (Bravo et al. 2016).

Cellular accommodation by the plant begins upon sensing AM fungal signals in the rhizosphere. These signals include lipochitooligosaccharides (LCOs) (Maillet et al. 2011), which are similar to rhizobial nod factors, and short chain chitooligosaccharides CO4/5 (Genre et al. 2013), which are similar to the longer-chain CO7/8 that elicit a defense response (Shibuya et al. 1996; Liu et al. 2012). The receptors for AM fungal signals are yet unconfirmed, but perception of the signals leads to induction of specific sets of symbiosis-associated genes, as well as lateral root formation (Maillet et al. 2011; Delaux et al. 2013; Genre et al. 2013). Upon contact with a plant roots, AM fungi form a penetration structure, called the hyphopodium. The fungus enters the root by passing through an epidermal cell into the root cortex (Genre et al. 2005), but this process is facilitated in part by the plant's formation of a prepenetration apparatus, which includes invagination of the plasma membrane and reorganization of the cytoskeleton and endoplasmic reticulum (Genre et al. 2008). Within the cortex, the fungus grows intercellularly along the root and enters inner cortical cells to create intracellular arbuscules – tree-like hyphae surrounded by plant cell membrane. At every step of symbiosis development, the host plant accommodates the fungus through carefully-timed gene expression facilitated by AM-specific transcription factors (Choi, Summers and Paszkowski 2018).

A successful symbiosis is marked by nutrient transfer between fungus and plant, as the plant provides carbohydrates and lipids in return for inorganic phosphate and nitrogen (Smith and Read 2008; Fiorilli and Gutjar 2018). This exchange takes place in the arbuscules, which are fungal hyphae surrounded by a specialized plant membrane, the periarbuscular membrane (PAM), that is contiguous with the plasma membrane (Pumplin et al. 2009). The arbuscule contains two domains – the trunk and branches. Each relies on specific symbiosis genes for formation, and deletion of such genes interferes with arbuscule maturity and nutrient exchange. The *Medicago truncatula* protein, Vapyrin, a novel protein predicted to mediate protein-protein interactions, is essential for any arbuscule formation, as fungi colonizing roots in which *Vapyrin* is silenced are unable to penetrate cortical cells (Pumplin et al. 2010). MtPt4, the AM-specific phosphate transporter in *M. truncatula* localizes to the fine branches of the PAM (Pumplin et al. 2012). AM fungi colonizing *mtpt4* roots are able to form arbuscules, but they degenerate prematurely, before reaching maturity. Colonized roots of *mtpt4* mutants are enriched in degenerating arbuscules, and thus have been used to identify genes that may be involved in this process (Floss et al. 2017).

Both *MtPt4* and *vapyrin* are induced by AM fungal colonization, an indicator that a gene may be important for the symbiosis. Many genes essential for AM symbiosis are also necessary for other biological functions, such as rhizobial symbiosis (Genre and Russo 2016) and pathogen immunity (Zipfel and Oldroyd 2017). Homologs of these genes exist in non-host plant species, including *Lupinus angustifolus*, a legume that establishes symbiosis with rhizobia, but does not establish AM symbiosis, and therefore does not contain homologs of AM-specific genes (Bravo et al. 2016). The duality of genes participating in both AM symbiosis and defense varies greatly by the species. In rice and pea, the major chitin receptor LysM-RLK is also necessary for establishment of AM symbiosis (Miyata et al. 2014; Leppyanen et al. 2018), whereas in *Lotus japonicus*, LysM-RLK chitin receptors are dispensable for both rhizobial and AM symbiosis, while paralogous LysM-RLK proteins are

responsible for perception of rhizobial nod factors and establishment of rhizobial symbiosis (Bozsoki et al. 2017).

LysM (lysin motif) domains are found in proteins of organisms from all kingdoms of life and are able to interact with a diversity of glycans, including nod factors, myc-LCOs, peptidoglycan, chitosan and chitin, all of which are based on an N-acetyl-glucosamine backbone (Buist et al. 2008). For many fungal pathogens, LysM effectors are necessary to evade the plant's immune response for successful infection. These effector proteins contain one to many LysM domains, either alone or with other protein domains (de Jonge and Thomma 2009). In angiosperms, several types of LysM-containing proteins have been identified. The best-studied group are the LysM-RLKs mentioned above that signal in both symbiosis and defense (Desaki et al 2017). Another type involved in defense signaling are the LYM/LYPs, which are GPI-anchored extracellular LysM proteins, including the rice chitin receptor, OsCEBiP (Kaku et al. 2006) and peptidoglycan receptors AtLYM1/3 and OsLYP4/6 (Willmann et al. 2013; Liu et al. 2013). Other types of LysM proteins include extracellular F-box proteins, non-secretory single LysM proteins, and extracellular single LysM proteins (Zhang, Cannon and Stacey 2009). Only a few of the other types, specifically the extracellular LysM proteins, have been characterized. In cotton, silencing of the single-LysM secreted protein, LysMe3, leads to a reduction in defense responses and a higher susceptibility to the fungal pathogen, *Verticillium dahliae* (Xu et al. 2017). In rice, the single-LysM domain protein, OsEMSA1, is necessary for normal development of the embryo sac (Zhu et al. 2017).

Two other extracellular single LysM proteins in rice, *AM3* and *AM15*, are specifically expressed during AM symbiosis, and have been used as markers for early and late colonization, respectively, in rice (Güimil et al. 2005; Gutjahr et al 2008). Neither gene is expressed in mock-inoculated or pathogen-infected roots, nor is their expression influenced by phosphate homeostasis in rice (Gutjahr et al. 2008). Gutjahr et al. 2008 showed that *AM3* is expressed earlier than *PT11*, the rice AM phosphate transporter, and *AM15* was expressed

later with *PT11*. Although they detected *AM3* transcript in the uninoculated side of a split-root system through RT-PCR, they were only able to localize its transcript in cells containing arbuscules. Despite this expression specificity, *AM3* is induced by AM fungal germinating spore extracts, and this induction is dependent on the common symbiosis signaling components, *Castor* and *Pollux* (nucleoporins) and *DMI3* (CCaMK) (Mukherjee and Ané 2011), which, when deleted, do not allow AM fungal colonization beyond hyphopodium formation. *AM3* expression was still induced by germinating spore exudates in the *cyclops* mutant, which does allow arbuscule formation. Neither *AM3* nor *AM15* were induced by Myc-LCOs, known to induce expression of symbiosis genes (Camps et al. 2015).

Medicago truncatula is a model legume species capable of establishing both AM and rhizobial symbiosis. Previously, seven single-LysM proteins were predicted from the *M. truncatula* draft genome, five of which were predicted to be extracellular (Zhang, Cannon and Stacey 2009). Here we present our results of a new survey of *M. truncatula* for small, single-LysM proteins, which we refer to as SLMs. Our results reveal previously unidentified SLMs in the *M. truncatula* published genome, version 4.0 (Tang et al. 2014), including an ortholog of *AM3*. We have tested expression of all *M. truncatula SLMs* and further characterize the extracellular SLMs that are specifically expressed during AM symbiosis. A comparison of protein sequences reveals a clear distinction between those that are AM-specific and those that are not, offering a new theory for how LysM proteins may differentiate between symbiotic and defense signaling.

Table 4-1: The twelve predicted SLMs in the *M. truncatula* genome. Gene IDs correspond to the *M. truncatula* genome version 4.0. Previously published lists corresponding name in Zhang, Cannon and Stacey 2009. TM = transmembrane, ND = not detected

Gene ID	Name	# exons	AA length	SP?	M. truncatula Gene Atlas ID	Expression in roots	Previously published
Medtr4g091000	SLM1	2	81	Y	Mtr.35466.1.S1_at	AM-Specific	LysMe2
Medtr4g091010	SLM2	2	85	Y	Mtr.37028.1.S1_at	AM-Specific	LysMe3
Medtr4g091020	SLM3	2	87	Y	Mtr.4380.1.S1_at	AM-Specific	
Medtr6g048040	SLM4	2	72	Y	none	ND	
Medtr5g038200	SLM5	1	74	Y	none	ND	LysMe5
Medtr7g104250	SLM6	1	96	Y	Mtr.26304.1.S1_at	Constitutive	LysMe1
Medtr1g101680	SLM7	1	104	Y	Mtr.9195.1.S1_at	Constitutive	LysMn2
Medtr1g060430	SLM8	1	116	Y	none	Constitutive	
Medtr8g043660	SLM9	1	116	TM	none	ND	LysMe4
Medtr8g032890	SLM10	1	116	N	none	ND	
Medtr8g032940	SLM11	1	116	N	none	ND	
Medtr1g101750	SLM7-like	2	66	N	Mtr.9195.1.S1_at	ND	

Results

Three SLMs are specific to arbuscular mycorrhizal symbiosis

A BLAST search of the *M. truncatula* genome, version 4.0, using all previously identified SLMs revealed twelve sequences with a single LysM domain and no other functional domain (Table 4-1). Of the seven previously identified (Zhang, Cannon and Stacey 2009), two lacked signal peptides, one of which we found to contain an F-box domain, precluding its classification as an SLM. The second is lacking part of its 5' end in the updated *M. truncatula* genome, but the new 5' end encodes a signal peptide. All five previously identified extracellular SLMs are annotated in the updated genome; however, one of these is predicted to contain a transmembrane domain rather than a signal peptide. Eight of the twelve SLM are predicted to contain a signal peptide. The *M. truncatula* SLMs are summarized in Table 4-1.

To identify SLMs that may play a role in AM symbiosis, we tested their expression in mock and AM fungal-inoculated *M. truncatula* roots at 21 days post-inoculation (dpi). Transcripts from six *SLMs* were detected in roots, and all six are predicted to be extracellular (Table 4-1). Of those six, *SLM1*, *SLM2*, and *SLM3* were detected only in roots colonized by AM fungi. All three are highly expressed during colonization by both *Rhizophagus irregularis* and *Glomus versiforme* and not expressed in mock-inoculated roots (Figure 4-1). The other three *SLMs* detected in roots, *SLM6*, *SLM7*, and *SLM8*, were highly expressed in both mock and inoculated roots. Due to their specific expression, we refer to *SLM1*, *SLM2* and *SLM3* collectively as *AM-SLM*. None of the *AM-SLM* were detected in leaves of plants colonized by *G. versiforme*[8] (Appendix 4-1). The three *AM-SLM* genes occur in tandem on chromosome 4 (Appendix 4-2), while *SLM6*, *SLM7*, and *SLM8* are located on different chromosomes and separate from each other. *SLM2* and *SLM3* are 91% identical at the

[8] cDNA from leaves of colonized *Medicago* was provided by Xinchun Zhang.

nucleotide level, while *SLM1* and *SLM2*, and *SLM1* and *SLM3* are 71% and 70% identical, respectively (Appendix 4-3).

All three AM-SLMs are represented on the Affymetrix Medicago Gene Chip®, which has yielded a vast array of normalized expression data accessible through the *Medicago truncatula* Gene Expression Atlas (Benedito et al. 2008; He et al. 2009). Using these data, we found that *AM-SLMs* are expressed only in AM-fungal colonized roots. Looking specifically at expression in laser-capture microdissected root cells, we found that *AM-SLMs* are predominantly expressed in cells containing arbuscules, and at a lower level in adjacent cells (Appendix 4-4). None of the genes are expressed in response to germinating spore extracts, myc-LCOs, COs, or nod factors; however, their expression may be dependent on *DMI3*, as early contact by *Gigaspora gigantea* induces expression in wild type roots, but not in *dmi3*. None of the other represented microbe-interacting conditions, including colonization/challenge by rhizobia, *Ralstonia*, *Aphanomyces*, and *Macrophomina*, induced expression of any *AM-SLMs*.

AM-SLMs are expressed only in cells containing arbuscules

Considering that *AM3* is induced by germinating spore extracts (Mukherjee and Ané 2011), we predicted that one or more *AM-SLMs* may be induced by early contact between roots and AM fungi. To test this hypothesis, we analyzed expression of each *AM-SLM* in colonized roots[9] at 2, 4, 6, and 8 dpi using a double-cone system that allows root exudates to prime AM fungal spores, which subsequently colonize roots quickly upon contact (Lopez-Meyer and Harrison 2006). No transcript was detected for any AM-SLM at 2dpi, and all three were detected at 4 dpi. *MtLec5*, a lectin specific to cells containing arbuscules (Frenzel et al. 2006), was also detected at 4dpi, indicating arbuscules were already present at this time point (Appendix 4-5).

[9] cDNA from double-cone experiment was provided by Melina Lopez-Meyer.

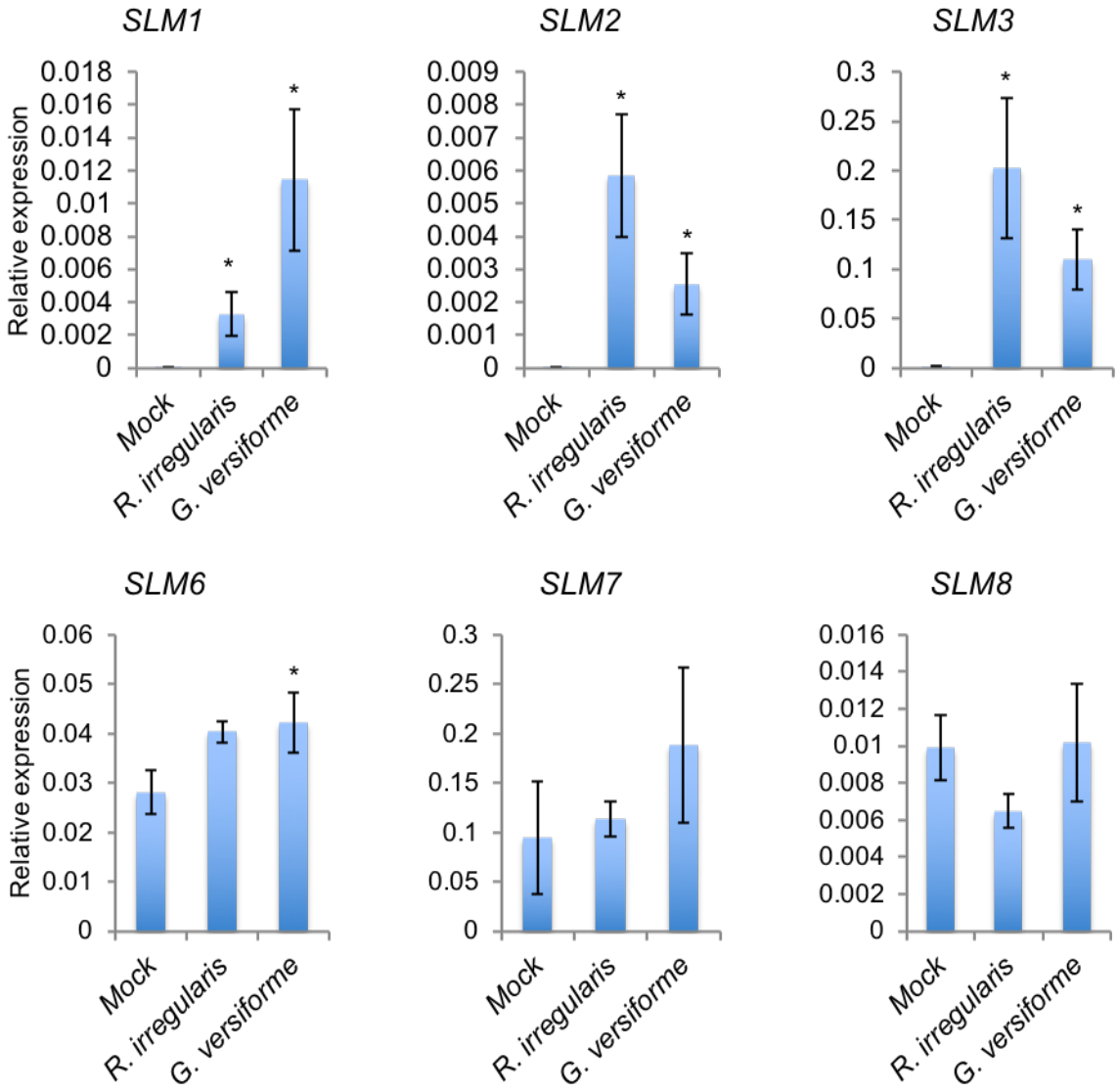

Figure 4-1: Six *M. truncatula SLMs* are expressed in roots. Quantitative PCR of cDNA from roots colonized by *Rhizophagus irregularis* or *Glomus versiforme*, or mock-inoculated roots. Expression is relative to *M. truncatula elongation factor* (*MtEF*). Bars represent standard deviation, n = 3. Stars denote significant difference relative to Mock, Student's t-test, $p < 0.05$.

Figure 4-2 (below): *AM-SLM* promoter-GUS activity in colonized roots. (a) Lateral root segments with fungal arbuscules (white arrowheads). Yellow arrowheads show arbuscules in cells lacking GUS-cleaved X-gluc. **(b)** Lateral sections of roots containing arbuscules (white arrowheads). Yellow arrowheads show GUS-cleaved X-gluc in cells adjacent to arbuscule-containing cells. White arrows show hyphopodium on cells lacking GUS-cleaved X-gluc. Bars = 100 μm

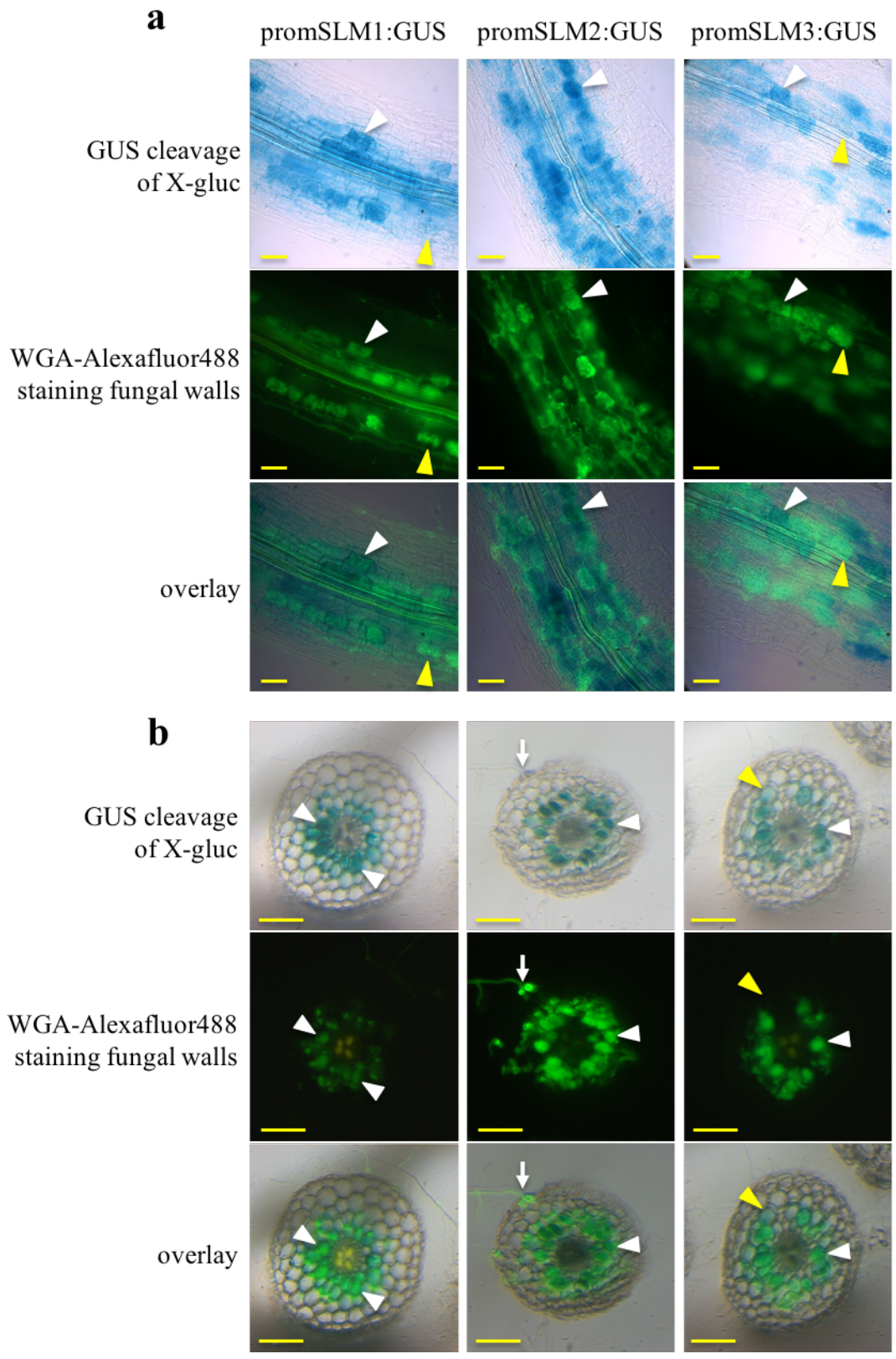
a
promSLM1:GUS
promSLM2:GUS
promSLM3:GUS
GUS cleavage of X-gluc
WGA-Alexafluor488 staining fungal walls
overlay
b
GUS cleavage of X-gluc
WGA-Alexafluor488 staining fungal walls
overlay

Gutjahr et al. 2008 found that *AM3* is expressed in the uninoculated side of a split-root rice plant, but using *in situ* hybridization could only detect transcripts *in vivo* in cells containing arbuscules, and very slightly in adjacent cells. Based on the expression data from the *M. truncatula* Gene Expression Atlas, we predicted *M. truncatula AM-SLMs* may be expressed specifically in cells containing arbuscules. To investigate this hypothesis, we fused 1 kb of the genomic region upstream of each *AM-SLM* to the *UidA* gene and transformed the resulting constructs into roots of *M. truncatula*, which we inoculated with *G. versiforme* spores. At 28 dpi, roots were harvested and stained for GUS activity. For all three *AM-SLMs* we were only able to clearly detect GUS-cleaved X-Gluc in cells containing arbuscules, visible as a blue precipitate, but not every cell containing an arbuscule demonstrated GUS activity (Figure 4-2). Closer observation of cells containing arbuscules that were stained versus unstained did not reveal any pattern of arbuscule maturity that might correlate with staining. Occasionally we observed very light GUS staining in cells adjacent to those with arbuscules (Figure 4-2b).

AM-SLM localize to the periarbuscular space (PAS)

To investigate sub-cellular localization of AM-SLMs, we fused the coding region of each gene to the mCherry fluorescent reporter under the same upstream promoter sequence used for the promoter-GUS analyses, transformed the resulting constructs separately into *M. truncatula* roots, and colonized with *G. versiforme*. After 21-28 dpi we visualized fluorescence with confocal microscopy. All three AM-SLMs fused to mCherry localized to the area surrounding the branches of arbuscules, but not around the arbuscule trunk or plasma membrane (Figure 4-3). In all roots we observed many cells with a "haze" that resembles vacuole localization, and in some roots we observed stationary dots on the arbuscule branches that resemble peroxisome localization (Ivanov and Harrison 2014). At no point did we observe fluorescence in cells lacking arbuscules, confirming our results from the *AM-SLM*

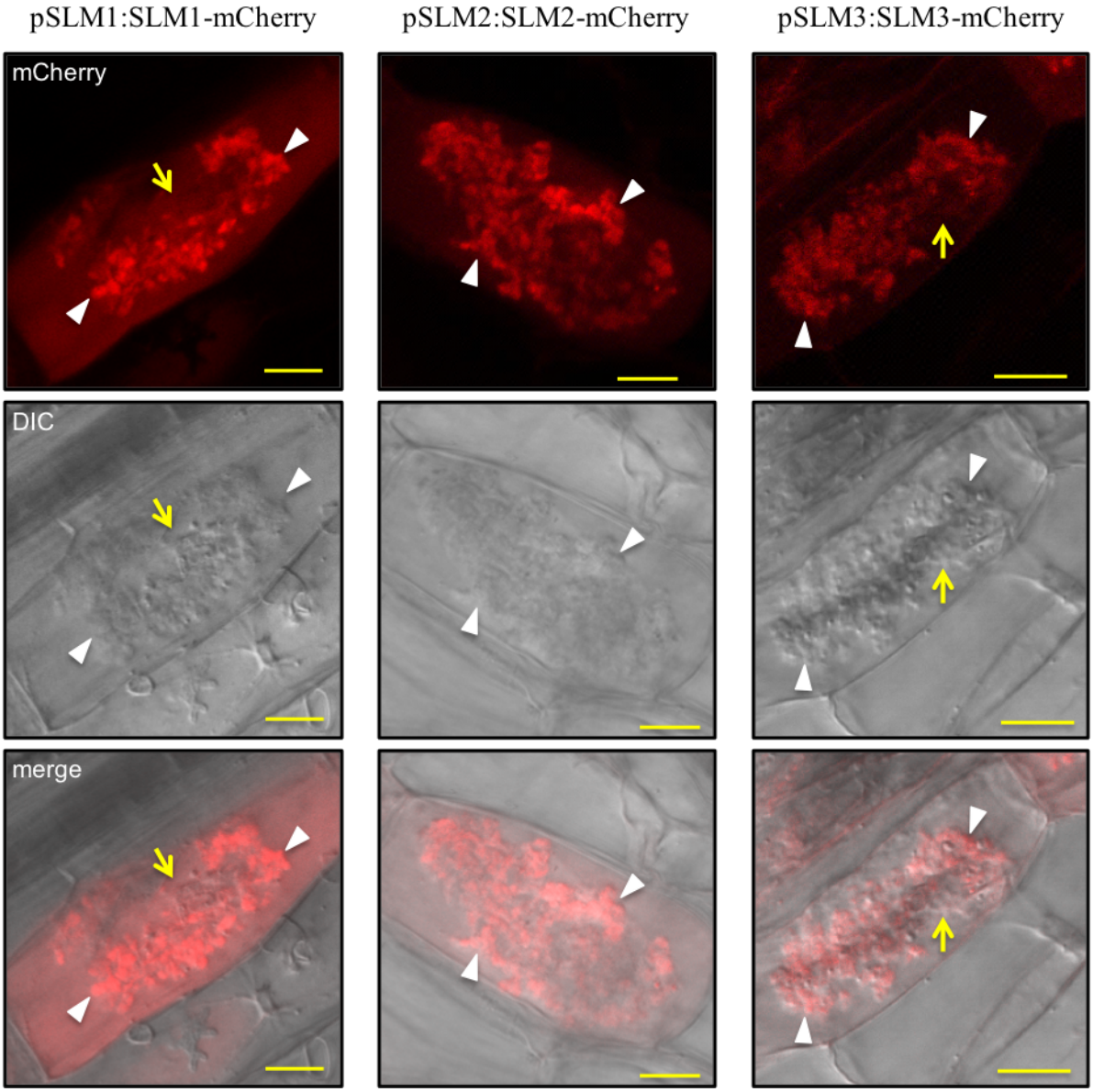

Figure 4-3: Subcellular localization of AM-SLMs in *M. truncatula* root cells with *G. versiforme* arbuscules. All three AM-SLMs localize to the arbuscule branches (white arrowheads), but not to the trunk (yellow arrows). Some vacuolar/cytoplasmic haze is visible, but none localize to the apoplast around the cell. Bar = 10 μm.

promotor:GUS expression analyses. The fluorescence pattern around the arbuscule did not clearly outline the branches, as previously observed for MtPt4, which localizes to the periarbuscular membrane (PAM) around fine branches (Pumplin et al. 2009). Rather, the fluorescence was much less resolved than the membrane-bound phosphate transporter and more similar to that of pMtPt4::BCP1sp-mCherry, which is secreted to the peri-arbuscular space (Ivanov and Harrison 2014).

To distinguish localization of AM-SLMs from that of MtPt4, we transformed the mCherry constructs into *M. truncatula* roots stably transformed with pMtPt4::MtPt4-GFP. Unfortunately, we were only able to find roots expressing both constructs for SLM1-mCherry. Although we found both SLM1 and MtPt4 within the same cells, they localized to different regions of the PAS and PAM respectively (Appendix 4-6a); SLM1-mCherry surrounded the lower order branches and did not localize to the finer arbuscule branches where MtPt4-GFP was located (Appendix 4-6b). Often, we found SLM1-mCherry localized to the PAS in cells lacking GFP, or vacuolar mCherry where MtPt4-GFP localized to the PAM; however, we did not observe SLM1-mCherry in the PAS with vacuolar GFP.

AM-SLMs are variably expressed in mutant roots affecting arbuscule formation

In *M. truncatula* roots lacking *Vapyrin*, AM fungi are unable to penetrate cortical cells to form arbuscules (Pumplin et al. 2010). In *M. truncatula* roots lacking *STR*, AM fungi can penetrate cortical cells, but form stunted arbuscules that never reach maturity (Zhang, Blaylock and Harrison 2010). In roots of *MtPt4*, arbuscules degenerate before they reach maturity, leading to a root system enriched in degenerating arbuscules and genes involved in the degenerating process (Floss et al. 2017). None of the *AM-SLMs* were detected by RT-PCR in *R. irregularis*-colonized roots of *vapyrin*. All three were detected in roots of *str* and *pt4* (Appendix 4-7).

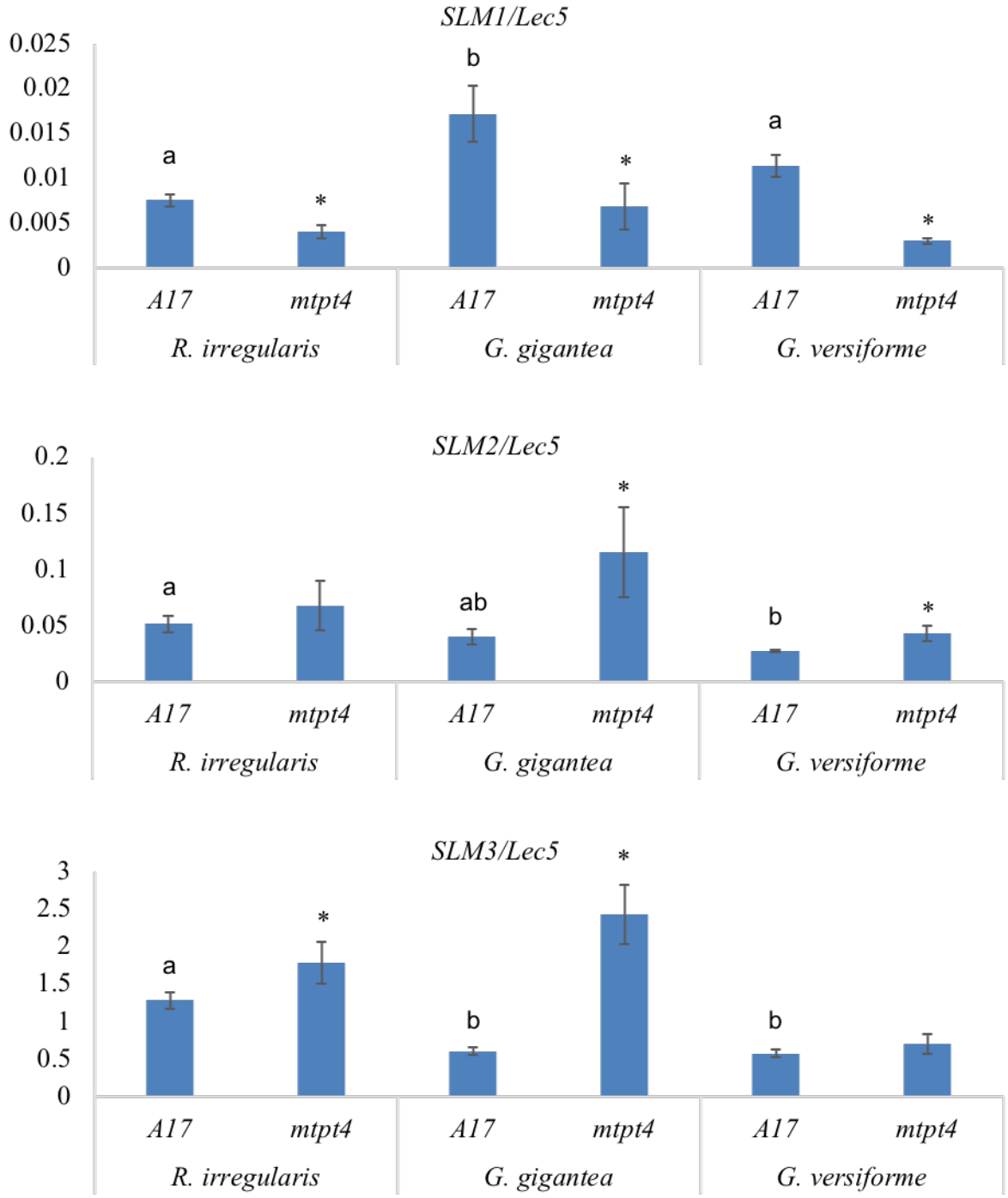

Figure 4-4: Expression of *AM-SLMs*, in wild type (A17) and *mtpt4* roots colonized by *Rhizophagus irregularis*, *Gigaspora gigantea*, or *Glomus versiforme*. Expression is normalized to the arbuscule marker *MtLec5* Bars represent standard deviation, n = 3. Stars denote significant difference in expression between *mtpt4* and A17, Student's t-test, $p < 0.05$. Letters denote significant differences between expression in A17 roots colonized by three different fungi, one-way ANOVA, $p < 0.05$

To determine if AM-SLMs may be important for arbuscule degeneration, we measured their expression in wild type (A17) *M. truncatula* and *mtpt4* mutants colonized with *R. irregularis, Gigaspora gigantea*, and *G. versiforme*. After normalizing expression to *MtLec5* to account for differences in numbers of arbuscules, we found that *SLM1* expression is decreased in the *mtpt4* mutant while *SLM2* and *SLM3* are both slightly higher (Figure 4-4). These results were similar for roots colonized by all three fungi.

AM-SLM do not bind chitin, but may inhibit the host's immune response to chitin

Many extracellular LysM proteins from fungi can bind chitin, resulting in inhibition of its perception by plant receptors that signal for an immune response, or protection of fungal hyphae from plant chitinases (Akcapinar et al. 2015). Considering a similar role for AM-SLMs in the protection of AM fungi, we tested their ability to bind to chitin. We used a small LysM protein from *R. irregularis*, RiSLM, previously shown to bind chitin, as a positive control, and binding was tested with chitin-coated magnetic beads and free, insoluble chitin from shrimp shells (data not shown), as used previously for RiSLM (Chapter 5, Submitted manuscript). All proteins were tagged with a single FLAG peptide and expressed in *Nicotiana benthamiana*. None of the AM-SLMs were able to bind chitin when expressed alone, or when all three were mixed together (Figure 4-5). We tested for binding to chitin beads with and without the reducing agent, dithiothreitol (DTT), and in high and low pH buffer (data not shown).

Despite not binding chitin, AM-SLMs may still interfere with the plant's defense responses through other interactions, such as direct binding of chitin receptors. To test for inhibition of chitin-elicited responses, we transiently expressed AM-SLM-FLAG and FLAG-GFP constructs in leaves of *N. benthamiana* and measured production of reactive oxygen species by transformed leaf discs exposed to CO8 or ddH_2O using HRP-catalyzed luminescence. We measured ROS production in response to flg22 peptide from flagellin as a

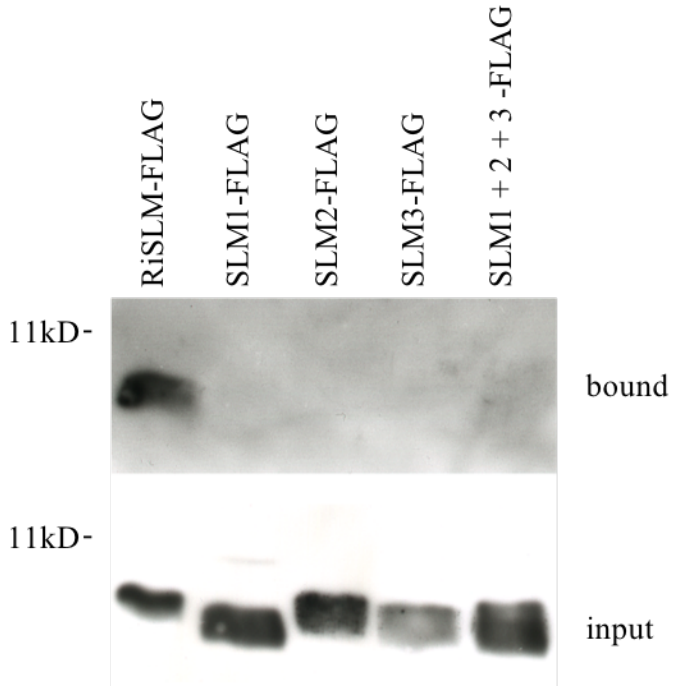

Figure 4-5: Western blots demonstrating chitin-binding properties of SLM from *M. truncatula* and *R. irregularis*. Bottom panel shows equal volumes of protein input to chitin beads. Top panel shows protein bound to chitin beads. Only RiSLM bound to the beads. A mixture of SLM1, SLM2, and SLM3 did not facilitate binding.

positive control (Chakravarthy et al. 2010). Initially the experiments were remarkably successful, and we found that SLM3-FLAG could repress ROS production in response to chitin (Appendix 4-8); however, we were never able to repeat this experiment due to a loss of any ROS production in response to the chitin elicitors, including a higher concentration of CO8, CO6, and chitin from shrimp shells. We then decided to look at gene expression in roots as a more sensitive assay, following a published method for chitin elicitors of specific gene expression in *M. truncatula* roots (Nars et al. 2013). We overexpressed each AM-SLM-FLAG in roots using the CaMV 35S promoter, exposed the transgenic roots to chitin, and checked for induction of pathogenesis-related genes previously shown to respond to chitin, including *PR10.2* and *Thaumatin* (Nars et al. 2013; Rey et al. 2013). Initially, we tested four genes via RT-PCR to verify their induction by chitin and chose two that clearly responded to four hours of chitin exposure in the roots (Appendix 4-9). We then used quantitative RT-PCR to measure differences in gene induction by chitin between roots overexpressing each *AM-SLM* and the control. Although *PR10.2* expression was lower in all three *AM-SLM* overexpressing roots, it was only significantly so in roots expressing *SLM3*. *Thaumatin* was not significantly lower in any samples (Figure 4-6).

Silencing AM-SLMs does not affect symbiosis, but ectopic expression promotes colonization

To test if the AM-SLMs are essential for AM symbiosis, we developed an RNAi construct to silence all three simultaneously. Although the construct succeeded in greatly reducing transcript of all three *AM-SLMs*, fungal colonization was unaffected in the RNAi plants, as demonstrated by a lack of difference in expression of fungal *α-tubulin* or AM-induced plant genes relative to the control plants (Figure 4-7). We observed no difference in ability of the fungus to form arbuscules, which we quantified by comparing levels of *MtLec5* and *MtPt4* in control and RNAi roots. Furthermore, we did not see any increase in *MtCp3* expression, which is a marker for arbuscule degeneration (Floss et al. 2017). The experiment

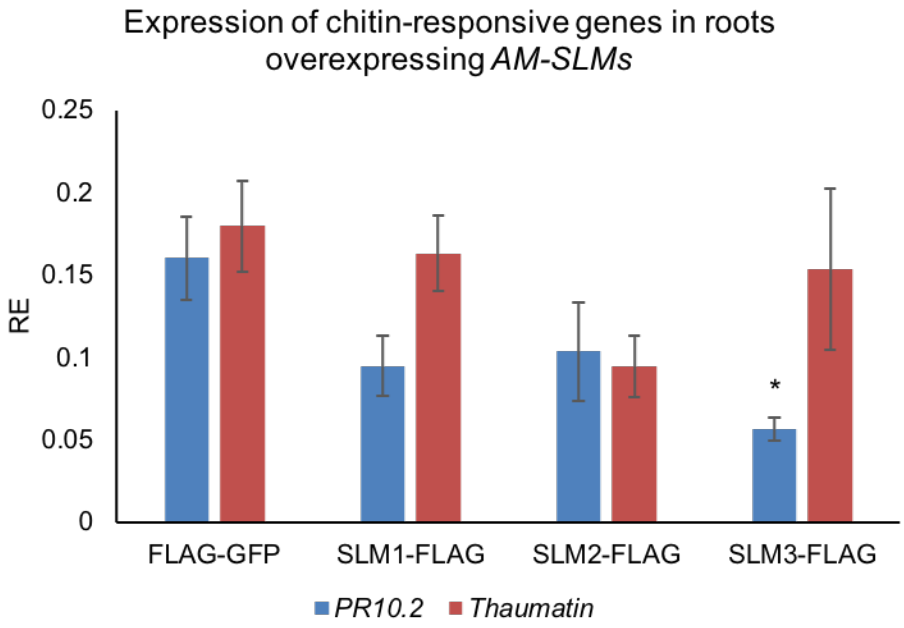

Figure 4-6: Expression, relative to *MtEF,* of two chitin-responsive genes, *PR10.2* and *Thaumin* in *M. truncatula* roots overexpressing *AM-SLM-FLAG* or *FLAG-GFP* and exposed to chitin for 4 hours. Bars represent standard error, n = 6. Star denotes significance vs. FLAG-GFP, Student's t-test, $p < 0.05$.

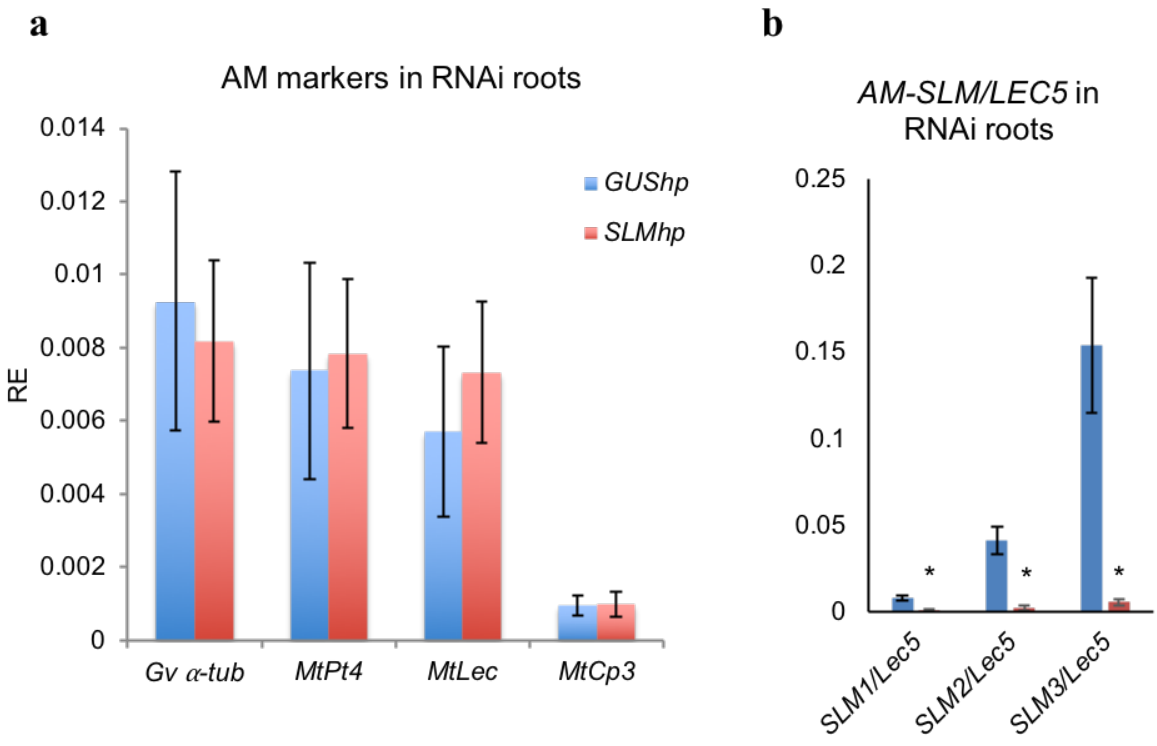

Figure 4-7: RNAi of all three *AM-SLMs* does not affect AM fungal colonization.
(a) Expression of *AM-SLMs* relative to *MtEF* with and without silencing all three *AM-SLMs*. **(b)** Expression of *AM-SLMs* relative to *MtLEC5* demonstrating silencing in the RNAi roots. Bars are standard deviation, n = 8. Stars denote significant difference between RNAi roots and control roots, Student's t-test, $p < 0.05$.

was done twice with *G. versiforme* and *R. irregularis*, with similar results. Since RNAi does not completely eliminate transcript, and thus protein production, we wanted to test a loss-of-function mutant for the AM-SLM. We obtained two *M. trunctula Tnt1* insertion lines, one with an insertion in the second exon of *SLM2*, and one with an insertion in the first exon of *SLM1*, both of which we determined to be null mutations. We identified homozygous mutants and wild type for each and colonized them with *G. versiforme*. None of the mutant plants showed a significant and consistent change in colonization relative to their segregating wild type (data not shown). Specifically, fungal colonization was significantly increased in one *slm2* mutant, and significantly decreased in the other.

Several small, secreted proteins from plants, such as defensins, nodule, and other cysteine-rich peptides, have anti-microbial properties, or control the growth and differentiation of microbial symbionts (Maróti, Downie and Kondorosi 2015). To test if AM-SLMs can regulate AM fungal colonization, we expressed each gene under the *MtBCP1* promoter, which is strongly induced in cells containing arbuscules, and those directly surrounding, or ahead of progressing fungal colonization (Pumplin et al. 2012). We did not use the CaMV 35S promoter for this experiment due to its down-regulation in colonized areas of the root (Pumplin et al. 2012). Exogenous expression was confirmed in each root system with RT-PTR using a forward primer directly upstream from the gene, and a reverse primer within the expressed gene (Appendix 4-10). The experiment was repeated twice with *G. versiforme*, and both times, expression of *SLM1* and *SLM3* under the BCP1 promoter yielded a small, but significant increase in length of individual colonization events, although percent root colonization was not significantly higher (Figure 4-8). Ectopic expression of *SLM2* did not have any significant effect on fungal colonization.

SLM1 may interact with the LysM-RLK, NFP

Some LysM effectors of fungi inhibit the host immune response through interactions

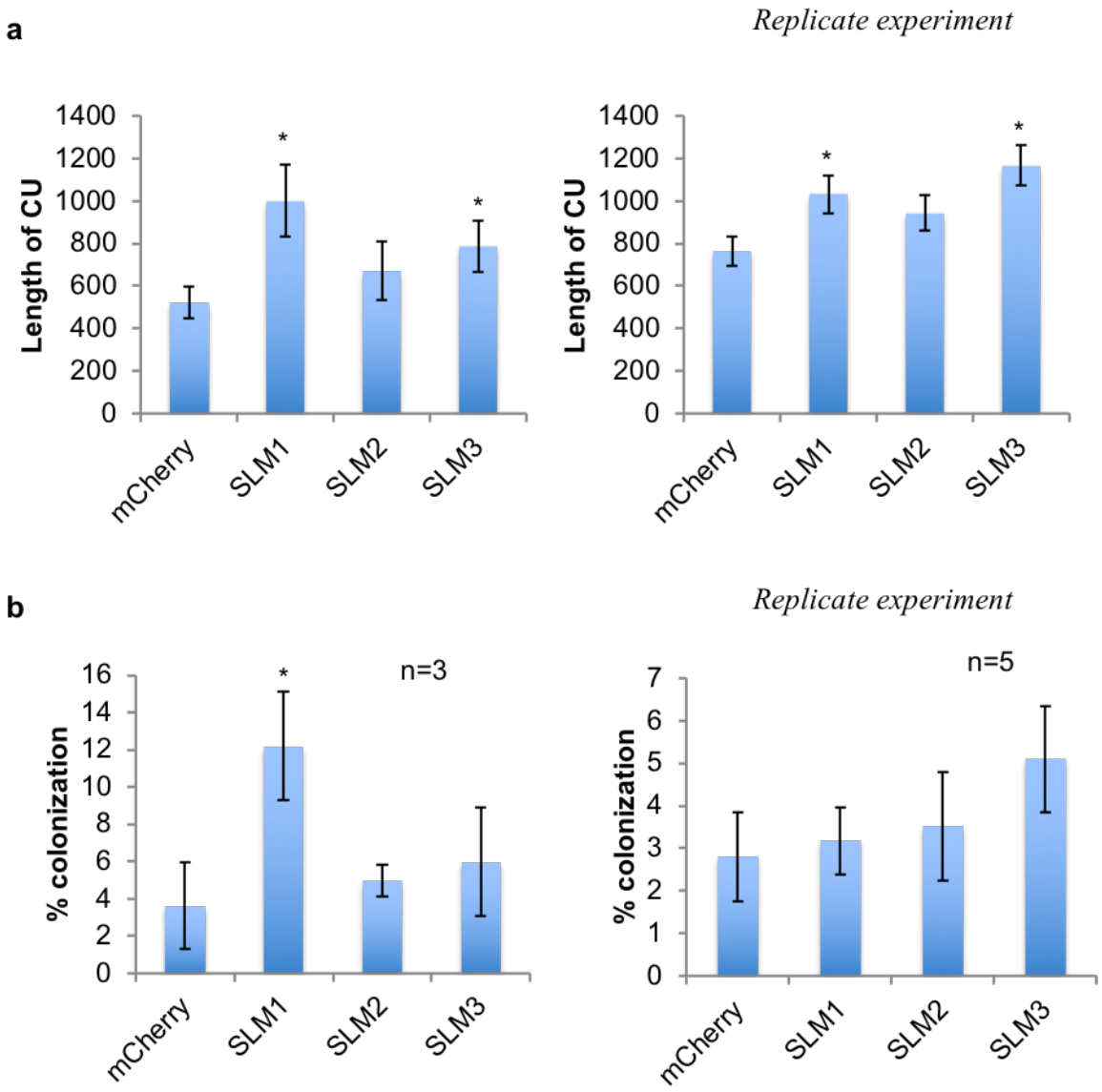

Figure 4-8: Ectopic expression of *AM-SLMs* enhances fungal growth. (a) Length of individual colonization units (CU) in pixels measured by ImageJ. All samples were taken with the same resolution at the same magnification. Bars are standard deviation, n = 30. **(b)** Percent colonization by the grid intersect method. Bars are standard deviation. Stars denote significance vs. control, Student's t-test, $p < 0.05$.

with plant receptors (Sánchez-Vallet, Mesters, and Thomma 2015). Considering the possibility that AM-SLMs might act as signaling molecules through LysM-RLKs, we tested for interactions using the yeast 2-hybrid assay. Our previous results showed that *MtLyk10* expression is slightly induced by AM, and that *mtlyk10* plants are slightly less colonized than wild type (Chapter 3), implicating this gene in symbiosis functioning. Deletion of another LysM-RLK, *NFP* leads to a partial loss of Myc-LCO induced lateral root formation and 95% loss of LCO-induced gene expression (Maillet et al. 2011; Czaja et al. 2012), and silencing its ortholog in *Parasponia andersonii* caused a severe reduction in arbuscule formation (Op den Camp et al. 2011). Furthermore, *nfp* mutants are more susceptible to fungal and oomycete pathogens (Rey et al. 2013), and in our hands they have shown a slight increase in AM fungal colonization (Chapter 3).

To test for interactions in a yeast two-hybrid assay, we used only the ectodomains of NFP and Lyk10, which contain three LysMs, to avoid instability due to the presence of a transmembrane domain. Furthermore, we removed the signal peptides to ensure that the proteins would be able to interact with and activate the reporter gene in the nucleus. We fused each of SLM1, SLM2, SLM3, NFPecto, and Lyk10ecto to the *GAL4* activation and binding domains, and tested for interactions restoring histidine auxotrophy in yeast. Unfortunately, we found that many of the proteins when fused to the *GAL4* binding domain were able to autoactivate transcription. However, we were able to detect activation above background in the interaction between SLM1 and NFP (Appendix 4-11). This work remains to be verified by co-immunoprecipitation.

AM-SLM are specific to plants capable of establishing AM symbiosis

An alignment of all SLM protein sequences from *M. truncatula* revealed a clear distinction between AM-SLMs and the other SLMs, notably in the number and location of cysteine residues. We then included the rice SLMs in the alignment and found that only the

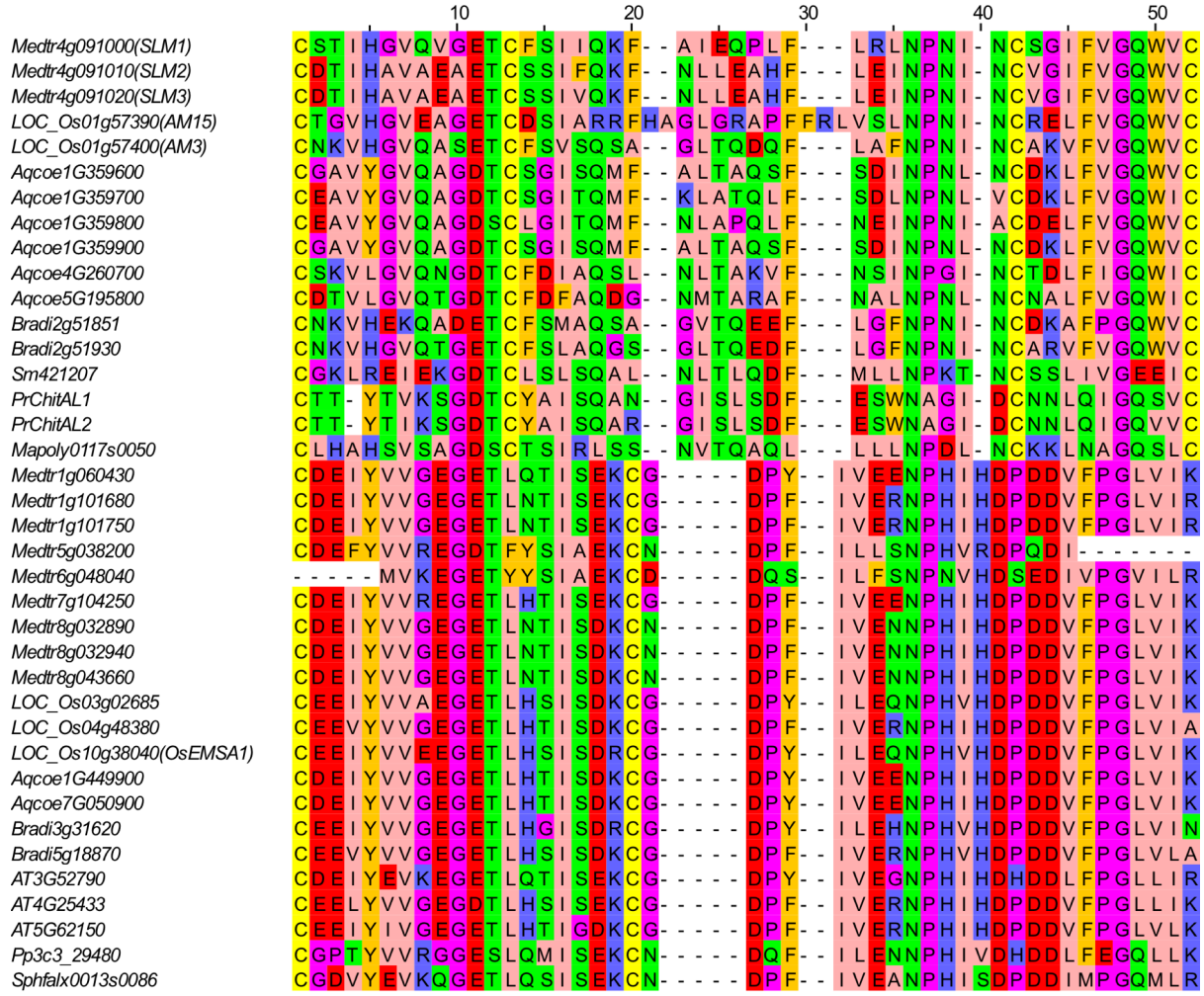

Figure 4-9: Alignment of SLM LysM domains from a subset of species: *Medicago truncatula, Oryza sativa, Aquilegia coerulea, Brachypodium distachyon, Arabidopsis thaliana, Physcomitrella patens,* and *Sphagnum fallax*. Sequences were aligned with Mafft using default settings in Jalview 2.10.4b1. Amino acids are colored according to the Zappo Color Scheme: blue = positive, red = negative, green = hydrophyllic, salmon = aliphatic/hydrophobic, orange = aromatic, pink = conformationally special, yellow = cysteine.

previously identified markers, AM3 and AM15, group with the AM-SLMs, while OsEMSA1 does not (Figure 4-9). To determine if the AM-SLM group is specific to plants that can establish AM symbiosis, we searched for SLM orthologs in all published plant genomes on Phytozome 12 (Goodstein et al. 2012), as well as draft genomes for known non-hosts of AM fungi (Bravo et al. 2016) using protein BLAST with SLM3 and SLM7 as separate queries. Our search retrieved all twelve *M. truncatula* SLMs, as well as all previously reported extracellular LysM proteins (Zhang, Cannon and Stacey 2009). Of the 73 plant genomes searched, 61 contained *SLM* orthologs, and 39 of those contained *AM-SLM* orthologs (Appendix 4-13).

To confirm the distinction between AM-SLMs and other SLMs, we used a smaller group of sequences (Appendix 4-13 – bold) for Bayesian phylogenetic reconstruction. The resulting phylogram revealed two distinct clades, one of which contained AM-SLMs from *M. truncatula* and *O. sativa*, and no sequences from non-hosts (Figure 4-10). Within their clade, AM-SLM paralogs from each species mostly grouped together. There were four angiosperms (*Amaranthus hypochondriacus*, *Cucumis sativus* Hyg14, *Lotus japonicus*, and *Musa acuminata*) that are AM hosts, but whose genomes lack annotated AM-SLMs. The average ratio of AM-SLMs to other SLMs among the plants with both types was 1.25, indicating that there are typically more AM-SLMs than other SLMs. One species, *Fragaria vesca* (strawberry) has 13 AM-SLMs and no other SLMs. *Lupinus angustifolius* is a legume capable of establishing rhizobial symbiosis, but cannot associate with AM fungi, and thus has lost the core set of genes necessary for AM symbiosis. We were not able to identify *AM-SLMs* orthologs in *L. angustifolius*.

Many plants from early diverging lineages, including lycophytes, ferns, liverworts, and gymnosperms, are able to establish AM symbiosis, and thus have retained orthologues of the core necessary genes (Wang and Qiu 2006; Bravo et al. 2016). The gymnosperm, *Picea abies* is capable of establishing ectomycorrhizal symbiosis, but not AM symbiosis (Wang and

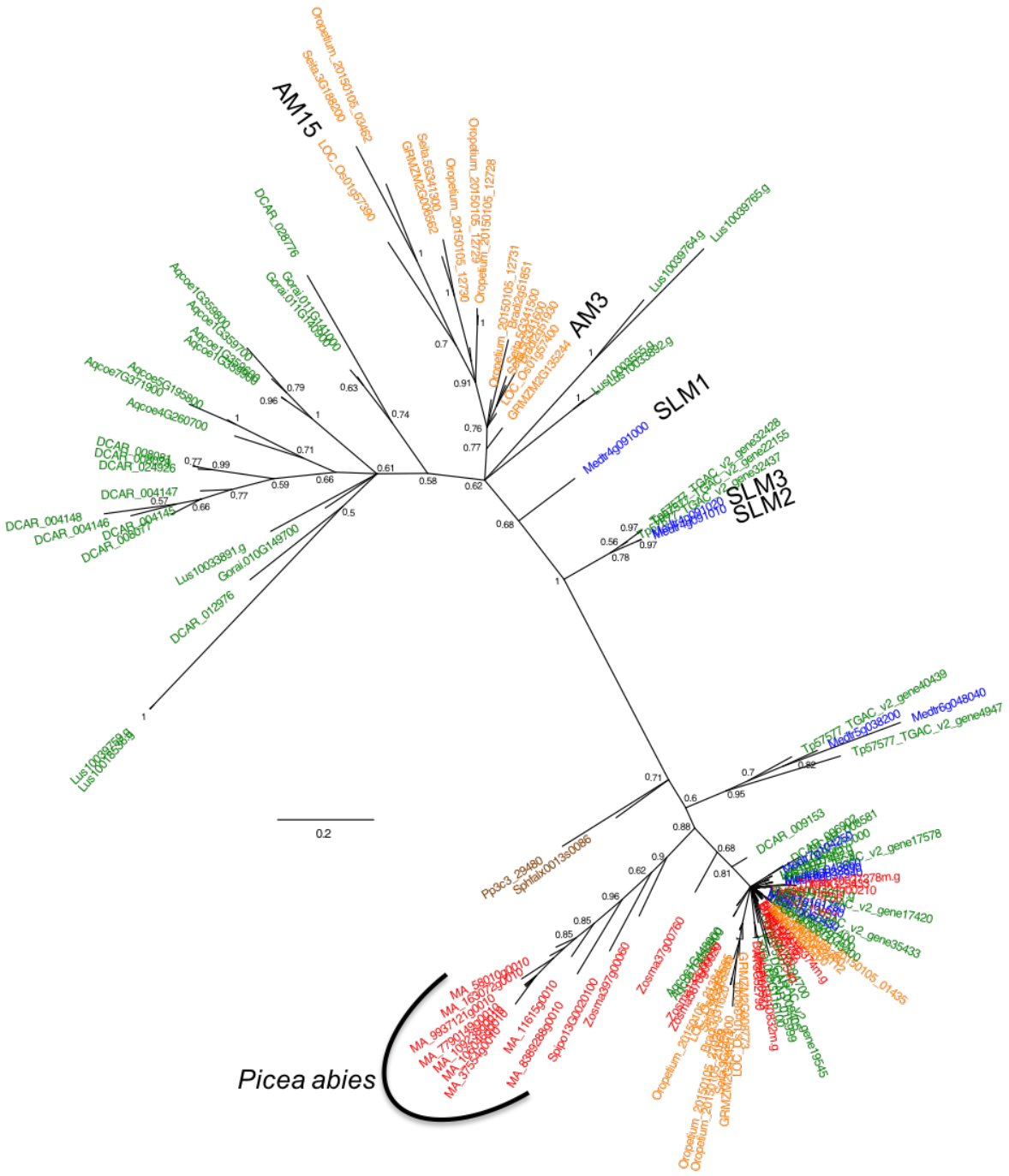

Figure 4-10: Phylogenetic reconstruction of SLM peptides from host and non-host plants. Red gene IDs are from non-AM plants. Dark blue are *Medicago*. Green are eudicots other than *Medicago*, orange are monocots, and brown are Embryophytes (also non-host). Sequences were aligned with Mafft, and phylogeny was reconstructed with MrBayes 3.2.2. Numbers represent node posterior probabilities. Scale represents amino acid substitutions.

Qiu 2006). A search of its genome identified 9 SLMs, but no AM-SLMs. The lycophyte *Selaginella moellendorffii* is capable of establishing AM symbiosis and contains the necessary core genes (Bravo et al. 2016). Although we were unable to identify any SLMs in its genome, we did discover a LysM-chitinase (glucoside hydrolase 18) whose LysM domain is similar to that of the AM-SLMs. We also identified a LysM-chitinase in the host liverwort, *Marchantia polymorpha*, and two host ferns, *Equisetum arvense*, and *Pteris ryukyuensis*. The LysM-chitinase from *P. ryukyuensis*, PrChi-A, contains two LysM domains and a chitinase, and can bind to and hydrolyze chitin (Onaga and Taira 2008). Considering that the LysM domains from all the LysM-chitinases are of the AM-SLM type, we investigated if the chitinase may also be AM-related. A pBLAST search of the *M. truncatula* genome revealed the closest ortholog is a chitinase (Medtr6g079630) induced by AM symbiosis that is more highly expressed in roots of *mtpt4* and regulated by the MYB1 transcription factor, a regulator of arbuscule degeneration (Floss et al. 2017). Using the *M. truncatula* Gene Atlas we found that the chitinase is expressed in cells containing arbuscules, but also in late-stage nodules, beginning at 10 days post inoculation (Appendix 4-12). Surprisingly, we also identified a LysM-chitinase ortholog in the water fern, *Azolla filliculoides* (Li et al. 2018), which is a non-host.

AM-SLMs are cysteine-rich with potential for intramolecular disulfide bonds

A major distinguishing feature between AM-SLMs and the other SLMs are two extra cysteines in the LysM domain (Figure 4-9). The mature SLM1, SLM2 and SLM3 proteins are 53, 60, and 62 amino acids long, respectively, and all contain four cysteine residues, classifying them as cysteine-rich peptides (Marshall, Costa and Gutierrez-Marcos 2011). Their isoelectric points are 7.9, 4.8, and 4.5 for SLM1, SLM2, and SLM3, respectively. The fungal protein, RiSLM, is also a cysteine-rich LysM protein, with an isoelectric point of 9.4, and is able to bind chitin and chitosan (submitted manuscript). We aligned the AM-SLM

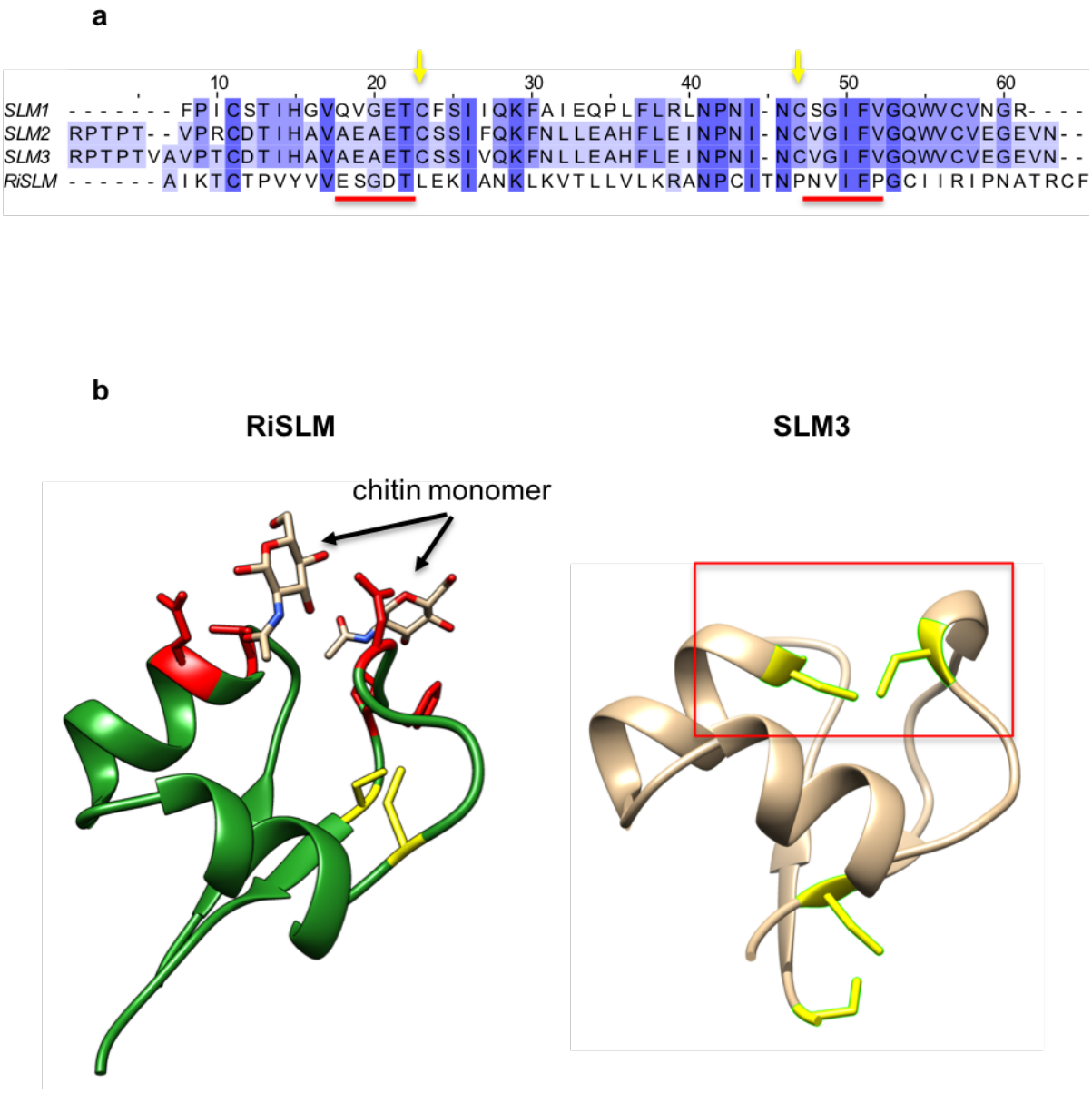

Figure 4-11: Comparison of putative ligand binding sites for RiSLM with corresponding location on AM-SLMs. (a) Mafft alignment of all AM-SLMs and RiSLM. Red lines mark amino acids in RiSLM predicted to participate in chitin binding. Yellow arrows show AM-SLMs' central cysteines. **(b)** Predicted three-dimensional structure for RiSLM and SLM3. RiSLM chitin monomers dock to the equivalent area of the protein where AM-SLMs' cysteines align and possibly form disulfide bonds (red box).

protein sequences with that of RiSLM to compare where their cysteine residues are located. Only the first cysteine residue from all SLMs, both plant and fungal, align (Figure 4-11a). Interestingly, the two inner cysteines of the AM-SLMs are located directly adjacent to the putative chitin-binding regions of RiSLM. To determine the potential for the cysteines of AM-SLMs to form disulfide bonds, we modelled the three-dimensional protein structure of SLM3 to compare to that of RiSLM. The cysteines in the AM-SLMs align in a direction that may allow for disulfide bond formation (Figure 4-11b). Furthermore, they do so in the same location where RiSLM is predicted to interact with its chitin ligand.

Discussion

The majority of land plants are capable of establishing AM symbiosis, and thus maintain a conserved set of genes specialized for accommodating the fungal partner (Bravo et al. 2016). In this study, we present a new group of genes specific to the AM symbiosis that was not previously identified as AMS-conserved. Mature AM-SLM proteins are small and consist solely of a single LysM domain. All *M. truncatula AM-SLM* genes are located in tandem in the genome, as is the case for the *O. sativa AM-SLMs*, indicating they arose through recent duplication events, which is supported by the grouping of paralogs from the same species in the phylogenetic reconstruction. Previous studies in rice have demonstrated symbiosis-specific expression of both its *AM-SLMs*, *AM3* and *AM15* (Güimil et al. 2005; Gutjahr et al 2008). Our results confirm an AM-specific expression for the *AM-SLMs* in *M. truncatula* roots colonized by three different AM fungi, demonstrating that these genes may be generally important for AM formation.

AM-SLMs likely function in arbuscules

Through GUS expression analyses we observed that *AM-SLM* promoters are active in

cells containing arbuscules. Although we saw a faint hint of GUS activity in cells directly adjacent to those with arbuscules, this may have been contamination from the adjacent cut cell with an arbuscule. Gutjahr et al. 2008 observed the same result for transcripts of *AM3* in rice; however, in our protein localization studies, we never observed fluorescence in any cells without arbuscules, confirming specificity to cells containing arbuscules.

Within cells containing arbuscules, we found that all three AM-SLM proteins localize to the space surrounding the fungal arbuscule, and not to the plasma membrane or apoplast surrounding the rest of the plant cell. Additionally, we did not observe any localization to the area surrounding the arbuscule trunk. Such a distinction between arbuscule branches and trunk localization has been observed previously, hinting at a physical barrier between PAS and the apoplast (Kobae and Hata 2010; Ivanov and Harrison 2014). The lack of a clear outline of the PAM, in contrast to MtPt4 localization (Pumplin et al. 2009), and the resemblance of localization pattern seen previously for pMtPt4::BCP1sp-mCherry, which secretes mCherry to the PAS (Ivanov and Harrison 2014), indicates that AM-SLMs are most likely secreted to the PAS. Further supporting the secretion of AM-SLMs to the PAS, our first attempts at sub-cellular localization used GFP constructs, but we were only able to see occasional, very weak fluorescence around arbuscules, which may have been due to the low pH of the PAS, and the higher sensitivity of GFP than mCherry to acidic pH (Ivanov and Harrison 2014).

Previous studies have clearly demonstrated that localization of proteins in the PAM and PAS is dependent on a reorientation of secretion to the PAM coincident with gene expression (Pumplin et al. 2012). Secreted proteins expressed prior to reorientation will localize to the plasma membrane and trunk, whereas those expressed after the switch to polar secretion will go to the PAM/PAS (Pumplin et al. 2012; Ivanov and Harrison 2014). Based on the specific localization of AM-SLM to the PAS, and exclusion from the trunk and remaining apoplast, we can infer that AM-SLM are expressed after the arbuscule begins to form. In

petunia, all three *AM-SLM* are highly induced in wild type roots, but not in the *ram1* mutant, in which arbuscules do not grow beyond trunk formation (Park et al. 2015; Rich et al. 2015). These results combined indicate that AM-SLM are not important for arbuscule initiation and trunk formation.

The lack of co-localization of SLM1-mCherry with MtPt4-GFP indicates that these two proteins may not function at the same arbuscule stage. We clearly observed SLM1-mCherry alone in cells with small, presumably immature arbuscules, with no MtPt4-GFP (Pumplin et al. 2012). In cells with mature arbuscules clearly outlined by MtPt4-GFP, SLM1-mCherry was mostly observed in the vacuole, indicating the protein may not have been trafficked correctly. At the point when arbuscule degeneration has begun, MtPt4 disappears from the PAM, and GFP is visible in the vacuole (Pumplin and Harrison 2009). Although we observed cells with vacuolar GFP fluorescence, none of these cells contained mCherry, indicating that SLM1 was no longer expressed during degeneration. In the few cells that did contain both MtPt4 and SLM1 at the arbuscule, the lack of colocalization with MtPt4 indicates SLM1 localizes to the lower order branches.

Differential roles for AM-SLM

While our colocalization results suggest that SLM1 is not involved in the degeneration process, we cannot extrapolate the same for SLM2 and SLM3, since we are lacking these data. Expression of *SLM1* is reduced in colonized roots of *mtpt4*, further indicating that *SLM1* is not involved in arbuscule degeneration. This result was also observed in an RNAseq analysis of colonized *mtpt4* roots (Floss et al. 2017). Conversely, we observed an increase in expression of *SLM2* and *SLM3* in *mtpt4*, indicating that these two genes may be important for the degeneration process. Further efforts to compare localization of these latter two proteins with that of MtPt4 will be necessary to resolve this question. *SLM2* and *SLM3* were not

among the genes determined to be upregulated in *mtpt4* roots by RNAseq analysis (Floss et al. 2017).

The differences in expression of *AM-SLMs* in *mtpt4* roots indicates that these genes may not all function at the same time or for the same purpose. Considering the predicted protein sequences, the diverging results between SLM1 and SLM2/3 are not surprising. SLM2 and SLM3 share a much higher identity, even at the nucleotide level, than either does with SLM1. Furthermore, the isoelectric points of SLM2 and SLM3 are below 5, while that of SLM1 is nearly 8, indicating that this protein would be positively charged in the acidic PAS (Guttenberger 2000).

In the case that *SLM2* and *SLM3* are important for arbuscule degeneration, we might not observe any difference in fungal colonization when these genes are silenced, as previously observed for *myb1* (Floss et al. 2017). In the case of MYB1, the authors were able to demonstrate its role in degeneration by crossing *myb1* with *mtpt4* and demonstrating a loss of programmed degeneration. To determine if *SLM2* and *SLM3* are necessary for arbuscule degeneration, a logical next step will be to silence the genes in the *mtpt4* background and investigate if programmed degeneration can still proceed. However, this possibility does not explain why silencing *SLM1* had no effect on colonization. Furthermore, ectopic expression of both *SLM1* and *SLM3* promoted fungal growth, hinting at a developmental role. The lack of a similar result for *SLM2* further differentiates the three AM-SLMs into three different but overlapping sets of functions.

While it may be possible that *AM-SLMs* are non-essential for symbiosis, our RNAi experimental conditions may not have provided an environmental context in which *AM-SLMs* are relevant. For example, the *mtpt4* mutant phenotype is lost when roots are starved for nitrogen (Javot et al. 2011). Alternatively, although the RNAi experiment succeeded in greatly reducing transcript of all three *AM-SLMs*, it did not eliminate production, and very low levels of protein may be sufficient to allow for normal progression of symbiosis in our

experimental conditions. With methods for mutation using CRISPR/Cas9 in *M. truncatula* now available, a triple mutant could be made to truly test if *AM-SLM* are dispensable for symbiosis. Additionally, our qPCR of *SLM6, SLM7,* and *SLM8* demonstrated these genes are also expressed in mycorrhizal roots, and while they may not be specific to the symbiosis, they might be able to compensate for the loss of the AM-specific SLMs.

AM-SLMs as possible redox switches

Overall, our results indicate two potential roles for AM-SLMs – one in fungal development, and another in arbuscule degeneration. This is especially apparent for SLM3, which both promotes fungal growth but may also be upregulated for degeneration. This duality of function in AM symbiosis is not without precedent, as two transcription factors, DELLA and NSP1, contribute to both development and degeneration of arbuscules, depending on which interacting partners are available (Floss et al. 2013a; Primprikar et al. 2016; Floss et al. 2017). For the cysteine-rich AM-SLMs, such a switch in roles could be facilitated by a change in redox state of their cysteine residues. Reactive oxygen species, which are produced in low levels in response to AM fungi (Puppo et al. 2013), would oxidize AM-SLMs, catalyzing formation of disulfide bonds, while the induction of reducing factors, such as the glutathione-S-reducatase upregulated by MYB1 for arbuscule degeneration (Floss et al. 2017), would reduce disulfide bonds and likely alter protein function, as seen for other classes of small, cysteine-rich proteins (Marshall, Costa and Gutierrez-Marcos 2011; Werner Ribeiro et al. 2017).

Recently, several studies have pointed to the importance of redox status for different functions of nodule-specific cysteine-rich (NCR) in rhizobial symbiosis, such as bacterial translation and inhibition of cell division (Haag et al. 2012; Shabab et al. 2016; Pan and Wang 2017). Interestingly, NCR peptides, which are secreted to the symbiotic bacteroid, are a similar length as AM-SLMs, and often contain a pattern of two pairs of cysteine residues

similar to that of AM-SLMs. Based on this striking parallel, we can speculate that AM-SLMs may contribute similar functions during arbuscule formation, possibly even regulating fungal differentiation, such as arbuscule branching, then acting antagonistically once reduced. One way to investigate this hypothesis would be to expose germinating spores to purified AM-SLMs and check for hyphal branching. Alternatively, reducing the proteins first may limit fungal growth.

Possible ligand targets for AM-SLMs

The LysM domain can interact with a variety of ligands containing an *N*-acetyl-glucosamine backbone, most commonly chitin, peptidoglycan, and LCOs, which are the basis of both rhizobial and AM fungal signaling molecules (Buist et al. 2008; Maillet et al. 2011). Since AM fungal cell walls are rich in chitin, many possibilities exist throughout the different stages of symbiosis where binding chitin may be important, however, we were unable to demonstrate any chitin binding for any AM-SLMs. Another major component of AM fungal walls is β-1,3-glucan, which can elicit a CERK-dependent immune response in *Arabidopsis thaliana* (Mélida et al. 2018). Interestingly, this is the third reported ligand for CERK1 LysM domains, which can also interact with chitin and peptidoglycan, each requiring a different interacting partner (Willmann et al. 2011; Wan et al. 2012). Considering the high pI of SLM1, we would expect it to be positively charged in the acidic PAS and likely to interact with a negatively charged ligand, such as pectin components in the primary cell wall (Alberts et al. 2002; Balestrini and Bonfante 2014).

Based on reports in the literature that the LysM domain from *Pteris ryukyuensis* Chitinase-A interacts with chitin (Onaga and Taira 2008), we were surprised that AM-SLMs do not bind chitin. The proximity of the two cysteine residues to the putative binding region of the protein raises the possibility that binding affinity could also be dependent on the redox state of the AM-SLM cysteines. Protein stability studies and crystal structure determination of

the second LysM domain from PrChit-A revealed two disulfide bonds between the four cysteines are important for protein stability (Ohnuma et al. 2008; Ohnuma et al. 2017). They further demonstrated that the two inner cysteines that form a disulfide bond near the ligand-binding region directly participate in chitin binding (Ohnuma et al. 2017). Although we performed chitin binding assays with and without the addition of a reducing agent (DTT) to the protein extraction buffer, we did not measure the presence of free thiols before or after reduction. A lack of disulfide formation in the AM-SLM could have interfered with chitin binding or destabilized the proteins, although the latter is unlikely since we were able to detect strong bands of recombinant protein in our soluble protein extracts.

Other possible ligands are the AM fungal signals, CO4/5 and LCOs, both of which are structurally similar to chitin. Although CO4/5 are essentially smaller forms of chitin oligomers, the longer chains in chitin may cause a steric hindrance to AM-SLM binding. Both CO4/5 and LCOs are able to attenuate chitin-elicited responses in *Arabidopsis thaliana*, and do so via the LysM-RLK AtLyk3. LCO signaling in both rhizobial and AM symbiosis is dependent on NFP, although the gene itself is not required for AM symbiosis (Ben Amor et al. 2003; Maillet et al. 2011; Czaja et al. 2012). The increased susceptibility of *mtnfp* to a fungal pathogen implies at an additional role for *NFP* in defense signaling (Rey et al. 2013). A dual role in defense and symbiosis has been described for multiple LysM-RLK proteins. Our results hint at an interaction between SLM1 and NFP, as well as AM-SLM inhibition of a chitin-elicited immune response. Both of these results may have been strengthened by the presence of a target ligand. Future work should further investigate interactions with LysM-RLKs, and inhibition of chitin-induced defenses as facilitated by AM fungal signals.

Conclusion

Our BLAST search and phylogenetic reconstruction revealed that AM-SLMs make up an AMS-conserved group of genes. Furthermore, our expression analysis and data from the

Medicago truncatula Gene Expression Atlas have shown that *AM-SLMs* are AM-specific, making them the only type of LysM-containing protein exclusively expressed during AM symbiosis. For constitutively-expressed LysM proteins that function in both defense and symbiosis signaling pathways, such as NFP and OsCERK1, AM-SLMs may be AM-associated receptors that divert signaling towards symbiosis. Alternatively, such specificity would be expected for proteins that act specifically on the fungal partner, like plant "effectors", possibly regulating fungal differentiation, such as arbuscule branching. In either case, at the end of the arbuscule lifespan, reduction of disulfide bonds could deactivate or switch function of AM-SLMs, resulting in protein degeneration, in the case of SLM1, or a secondary function in arbuscule degeneration, in the case of SLM2 and SLM3, and possibly in concert with the ancestral chitinase. Much work remains to investigate these theories, but our results provide the first step towards resolving the bigger picture.

Materials and Methods

Gene and protein predictions

M. truncatula SLM were identified through a protein BLAST search of the *Medicago* genome version 4.0 (Tang et al. 2014) using each previously identified extracellular LysM protein as a query (Zhang, Cannon and Stacey 2009). Protein predictions and exon numbers were retrieved through MedicMine, the Medicago genome database (Krishnakumar et al. 2014). Signal peptides were predicted using both SignalP 4.1 Server (http://www.cbs.dtu.dk/services/SignalP/, Petersen et al. 2011) and PrediSi (http://www.predisi.de/, Hiller et al. 2004).

Plant growth and fungal inoculation

Except where stated otherwise, all *M. truncatula* plants (Jemalong A17, R108, mutants, and composite plants with transformed roots) were grown as previously reported (Floss et al. 2017). Spores of *R. irregularis* (DAOM197198) were harvested from *Daucus carotus-R. irregularis* cultures (Becárd and Fortin, 1988). Spores of *G. versiforme* and *G. gigantea* were cultured on leek and bahia grass, respectively, harvested, and surface sterilized as previously described (Liu et al. 2007). Briefly, *M. truncatula* were planted into cone-tainers containing a layer of sand 7 cm below the top of the cone and inoculated with either 200 spores of *G. versiforme*, 500 spores of *R. irregularis*, or 10 spores of *G. gigantea*. Composite plants with transformed roots were inoculated directly and covered with a gravel/sand mixture. Non-transformed 2-day-old seedlings, including *M. truncatula* symbiosis mutants, were planted into the gravel/sand mixture covering the spores. After 5 days, plants were fertilized twice per week with modified half-strength Hoagland's solution containing 20 μM potassium phosphate. For experiments measuring expression of all *SLM*, only 150 spores of *G. versiforme* were used, directly inoculated onto 1-wk-old seedlings grown in turface, and

plants were harvested at 28dpi. For RNAi experiments, plants were inoculated with 100 spores of *G. versiforme*, fertilized with half-strength Hoagland's solution with 200 μM potassium phosphate, and harvested at 29 days-post-planting.

For analysis of AM colonization in null mutants of *SLM1* and *SLM2*, *M. truncatula* R108 *Tnt1* insertion lines were obtained from the Noble Research Institute. The line NF18380 was identified with an insertion in the first exon of *SLM1*. The line NF10349 was identified with an insertion in the second exon of *SLM2*. Both mutants were selfed and genotyped for the identification of multiple homozygous mutants and segregating wild type plants for use in phenotyping experiments. Plants were grown and inoculated with *G. versiforme* as described above.

RNA extraction, cDNA synthesis, and quantitative RT-PCR

Immediately upon harvesting, any root material used for RNA analysis was frozen in liquid nitrogen and stored at -80°C. RNA extraction, cDNA synthesis, and quantitative RT-PCR were all done as previously described (Javot et al. 2011). All primers used for qRT-PCR are listed in Appendix 4-14.

Cloning and transformation of M. truncatula roots

All constructs were made and transformed into *M. truncatula* roots using Gateway cloning technology (Hartley, Temple and Brasch 2000; Vemanna et al. 2013). Primers used for cloning are listed in Appendix 4-14. For creation of GUS expression plasmids, 1 kb regions upstream from each *AM-SLM* gene was amplified with the addition of attB sites and recombined with pDONR207 by BP reaction. The resulting entry clones were recombined with pMDC162 via LR reaction to insert each promoter upstream from the *UidA* gene. For creation of mCherry fusion plasmids, 1kb of the upstream region with the gene sequence, lacking a stop codon, were amplified together from genomic DNA for *SLM2* and *SLM3*. For

SLM1, which contains a large intron, the CDS, lacking a stop codon, was amplified from cDNA including a portion of the 5' untranslated region to facilitate overlapping PCR to fuse promoter region to CDS. All resulting promoter-gene/CDS constructs were re-amplified to add attB sites and recombined with pDONR207 by BP reaction. The resulting pENTR2 clones, pENTR3-mCherry (Ivanov and Harrison 2014), and pENTR1-MCS, which was created as a placeholder for the attB4-attB1 site, were recombined with the plant transformation vector pK7m34GW via LR reaction.

For RNAi experiments, portions of CDS for *SLM1* and *SLM2*, where it is nearly identical to *SLM3*, were amplified from cDNA and fused together with overlapping PCR. The amplicon was re-amplified to add attB sites, and recombined with pDONR221 via BP reaction. The resulting pENTR2 clone was recombined with pHellsgate8 containing dsRed for the selection of transformed roots. A 400-bp fragment of the *UidA* gene was similarly cloned into pHellsgate8 for the control. For ectopic/over-expression of *AM-SLMs*, each CDS was amplified with its stop codon from cDNA, adding attB sites. The resulting amplicons were recombined with pDONR221 via BP reaction. The resulting pENTR2 clones, pENTR1-pBCP1 (Ivanov and Harrison 2014), and pENTR3-term35S (Ivanov and Harrison 2014) were recombined with the plant expression vector pKm43GW via LR reaction. Plants were transformed according to Floss et al. 2013b.

For investigation of chitin binding, each *AM-SLM* CDS was amplified with a reverse primer adding a portion of *FLAG*, which was extended by an additional round of PCR that also added attB sites. The amplicons were recombined with pDONR221 via BP reaction, and the resulting clones, along with pENTR1-promD35S and pENTR3-term35S, were recombined with pKm43GW via LR reaction. For yeast two-hybrid, *AM-SLM* CDS were amplified without their signal peptides and to add attB sites, and recombined with pDONR221 via BP reaction. The resulting clones were recombined with pDEST32 or pDEST22, containing the *GAL4* DNA binding and activation domains, respectively, via LR reaction.

Staining and determination of fungal colonization

Colonized roots ectopically expressing *AM-SLM* were harvested 17 dpi (experiment 1) and 25 dpi (experiment 2 – later based on low colonization in experiment 1). A portion of roots were kept for RNA extraction. The remainder were cleared and stained with WGA-Alexafluor488 (Molecular Probes) as previously described (Javot et al. 2007) and analyzed using an Olympus SZX-12 stereo microscope. Percent colonization was determined by the gridline-intersect method (McGonigle et al. 1990). Length of colonization units was determined by imaging complete units from end to end at a consistent magnification and resolution. Using ImageJ, lines were drawn from the end of one end of the colonization unit to the other, from the tips of hyphae, then the lines were measured in pixels.

GUS expression analysis

Expression of *pAM-SLM:UidA* was observed in transformed roots either mock-inoculated, or at 21 and 28 dpi with *G. versiforme*. Roots were evaluated for histochemical staining of β-glucoronidase activity as described previously (Liu et al. 2003).

Confocal microscopy

Colonized transgenic roots were removed from substrate between 4 – 5 weeks post inoculation. Roots containing units of infection were visualized using an Olympus SZX-12 stereo microscope, and 3-5 mm length segments were sliced longitudinally, placed flat side up on a microscope slide containing a drop of water, and covered with a cover slip. Fluorescence was observed with a Leica TCS-SP5 confocal microscope, and images were taken with either a 20X or 63X water-immersion objective. mCherry was excited with a Diode-Pumped Solid State laser at 561 nm and emitted fluorescence was collected from 605 to 630 nm. GFP was

excited with an argon ion laser (488 nm) and emitted fluorescence was collected from 505 to 545 nm. Images were processed in Leica LAS-AS 2.6.0.

Agrobacterium infiltration of Nicotiana benthamiana and protein extraction

Constructs were transformed into *Agrobacterium tumefaciens* strain GV3101, and then infiltrated into 3-4 week old *Nicotiana benthamiana*, grown at 25°C 16h/8h light/dark. The infiltrations were all done at a final OD_{600} of 0.1 in induction buffer (10mM MES, 10mM $MgCl_2$, 100μM acetosyringone, pH 5.6), and each vector was coinfiltrated with the p19 silencing suppression plasmid (Voinnet et al. 2003), at a final OD_{600} of 0.8. For chitin-binding experiments, each construct was infiltrated into three leaves which were harvested approximately 48 hours post-infiltration and frozen at -80°C. Leaf material was ground with a mortar and pestle. Whole protein was extracted from ground leaf material with extraction buffer (150 mM Tris-HCl, pH 7.5, 150 mM NaCl, 10% glycerol, 10 mM EDTA, 0.5% (wt/v) polyvinylpolypyrrolidone, 0.1% Triton-X, protease cocktail inhibitor (Sigma Chemical), with or without 10 mM DTT) at a ratio of 2.5 mL per gram of tissue, centrifuged at 16,000g in the cold for 2X 15 minutes.

Chitin-binding assays

Chitin binding was determined by adding 100 μL whole leaf protein extract to 20 μL magnetic chitin bead slurry (New England Biolabs) prewashed 5 times with 1 mL cold binding buffer (500 mM NaCl, 20 mM Tris-HCl, 1 mM EDTA, 0.05% Triton X-100, pH 8.0). Beads and extract mixed for 30 minutes at 4°C, and unbound supernatant was collected. Beads were then washed 5 times with cold binding buffer. Bound protein was eluted with 50 μL 2X SDS-PAGE loading buffer (100 mM Tris-Cl pH 6.8, 4% (w/v) SDS, 0.2% (w/v) bromophenol blue, 20% (v/v) glycerol, 200 mM β-mercaptoethanol). Displacement assays were done with 200 μL binding buffer alone, or 10 mg/mL free shrimp shell chitin (Sigma),

free chitosan (Sigma-Aldrich), or peptidoglycan from *E. coli* (Invivogen) in binding buffer, and allowed to mix bound extract and beads for 30 minutes at 4°C before removed for analysis. Pre-mixing of extract was done by mixing 100 µL protein extract with 200 µL binding buffer alone, 10 mg/mL free chitin, or 10 mg/mL free chitosan and mixing for 30 minutes at 4°C. All samples were separated by 12% SDS-PAGE gels, and transferred to PVDF membrane. Blotted membranes were blocked with 5% milk powder and 0.1% Tween-20 in PBS for 30 minutes, incubated in the same solution plus rabbit anti-FLAG primary antibody for at least 4 hours, rinsed 3 x with 0.1% Tween-20 in PBS, and incubated with anti-rabbit secondary antibody conjugated to horseradish peroxidase for 1 hr. FLAG-tagged protein was detected with the addition of HRP substrate (EMD Millipore) for 5 minutes, and film exposure.

ROS burst assay in N. benthamiana leaf discs

To investigate AM-SLM inhibition of chitin-elicted ROS production, leaf discs were punched from infiltrated leaves of *N. benthamiana* and placed adaxial side up in 100 µL ddH_2O overnight. Approximately 12 hours later, water was removed and replaced with elicitor solution: 10µM CO8 (IsoSep) or 100nM flg22 (GenScript). Production of ROS was detected as HRP (type VI-A; Sigma-Aldrich)-catalyzed luminescence of luminol (Sigma-Aldrich) with a GENios Pro plate reader (Tecan, San Jose, CA, U.S.A.), as previously described (Chakravarthy et al. 2010).

Defense assay in M. truncatula hairy roots

Seedlings of *M. truncatula* transiently transformed with FLAG-GFP, SLM1-FLAG, SLM2-FLAG, or SLM3-FLAG under the double CaMV35S promoter were hardened and transferred to turface in pots to develop longer root systems. After one week, transformed plants were removed, rinsed, and left overnight in 1 mL of ddH_2O in the light. Approximately 14 hours

later, the water was removed and replaced with 1 mL of fresh ddH_2O, or 1 mL of 250 μg/mL shrimp shell chitin (Sigma), ground with a small pestle in a 1 mL Eppendorf tube. Plants were left in the elicitor solution for 4 hours, then roots were removed and immediately frozen for RNA extraction.

Yeast two-hybrid

Yeast two-hybrid analyses were done using the ProQuest™ Two-Hybrid System. Coding sequences were cloned into both pDEST32 and pDEST22, containing the *GAL4* promoter binding and activation domains, and conferring LEU and TRP auxotrophy, respectively. Construct pairs were then transformed together into Mav203 yeast lacking *HIS3* auxotrophy. Transformed yeast were recovered on SC -Leu -Trp, and then individual transformants were picked, subcultured, and used for binding analysis. For the binding assay, 10 μL of yeast at OD600 = 0.05 were pipetted onto SD – Leu -Trp -His with 10, 20, or 50 mM of 3-aminotriazole added. Growth was observed at 48 through 72 days post plating.

APPENDICES

Appendix 4-1: *AM-SLMS* are not expressed in leaves of *M. truncatula* colonized by *G. versiforme*.

Appendix 4-2: *AM-SLMs* in chromosome 4 of the *M. truncatula* genome. Rectangles and arrows represent exons. Gray lines represent introns.

```
           1                                                                                                  100
MtSLM1     ATGACCAAGT CTAGTAGTAG CAGTTTTGCT CTGGTTTTAT CATTTCTTCT CATTACGATG TTTAGTACAG CA------CC AACCGC---- --TGGATTTC
MtSLM2     ATGGCCAAGT TTACTAAAAT CAGCTTTGCT CTAATTTTTG CACTCATTCT CATTATGATG TTTATCGCTG AAAGTCGACC AACACC---- --TACAGTCC
MtSLM3     ATGGCTAAGT CAACTAACAT CTACTTTGCT CTAATTTTTT CACTTATTCT CGTTATGATG TTTATTGTTG AAAGTCGACC AACACCAACA GTTGCAGTCC
Consensus  ATGgCcAAGT ctAcTAa.At CagcTTTGCT CTaaTTTTtt CAcTtaTTCT CaTTAtGATG TTTAttgctG aAagtcgaCC AACacC.... ..TgcAgTcC

           101                                                                                                200
MtSLM1     CAATATGCAG CACAATTCAT GGTGTGCAAG TAGGGGAAAC TTGTTTTAGC ATTATTCAAA AGTTTGCAAT AGAACAGCCT CTGTTCTTGA GGTTAAATCC
MtSLM2     CAAGATGTGA CACAATTCAT GCTGTGGCAG AAGCTGAAAC TTGCTCCAGC ATCTTTCAGA AGTTCAACCT ACTTGAAGCA CACTTCCTTG AGATCAATCC
MtSLM3     CAACATGTGA CACAATTCAT GCTGTGGCAG AAGCTGAAAC TTGCTCCAGC ATCGTTCAAA AGTTCAACCT ACTTGAAGCA CACTTCCTTG AGATCAATCC
Consensus  CAA.ATGtga CACAATTCAT GcTGTGgcAG aAGctGAAAC TTGcTccAGC ATc.TTCAaA AGTTcaaccT ActtgAagCa CacTTCcTtg aGaTcAATCC

           201                                                 264
MtSLM1     CAATATCAAC TGTTCCGGCA TCTTTGTGGG TCAATGGGTG TGTGTGAATG GC-AGGTAA
MtSLM2     TAACATTAAC TGCGTTGGCA TATTTGTGGG CCAATGGGTG TGTGTTGAGG GTGAAGTGAA TTGA
MtSLM3     TAACATTAAC TGCGTTGGCA TCTTTGTGGG CCAATGGGTA TGTGTTGAAG GTGAAGTGAA TTGA
Consensus  tAAcATtAAC TGcgttGGCA TcTTTGTGGG cCAATGGGTg TGTGTtgA.G GtgAaGTgAa ttga
```

Appendix 4-3: Mafft alignment of the three AM-SLM CDS using default settings in Jalview 2.10.4b1.

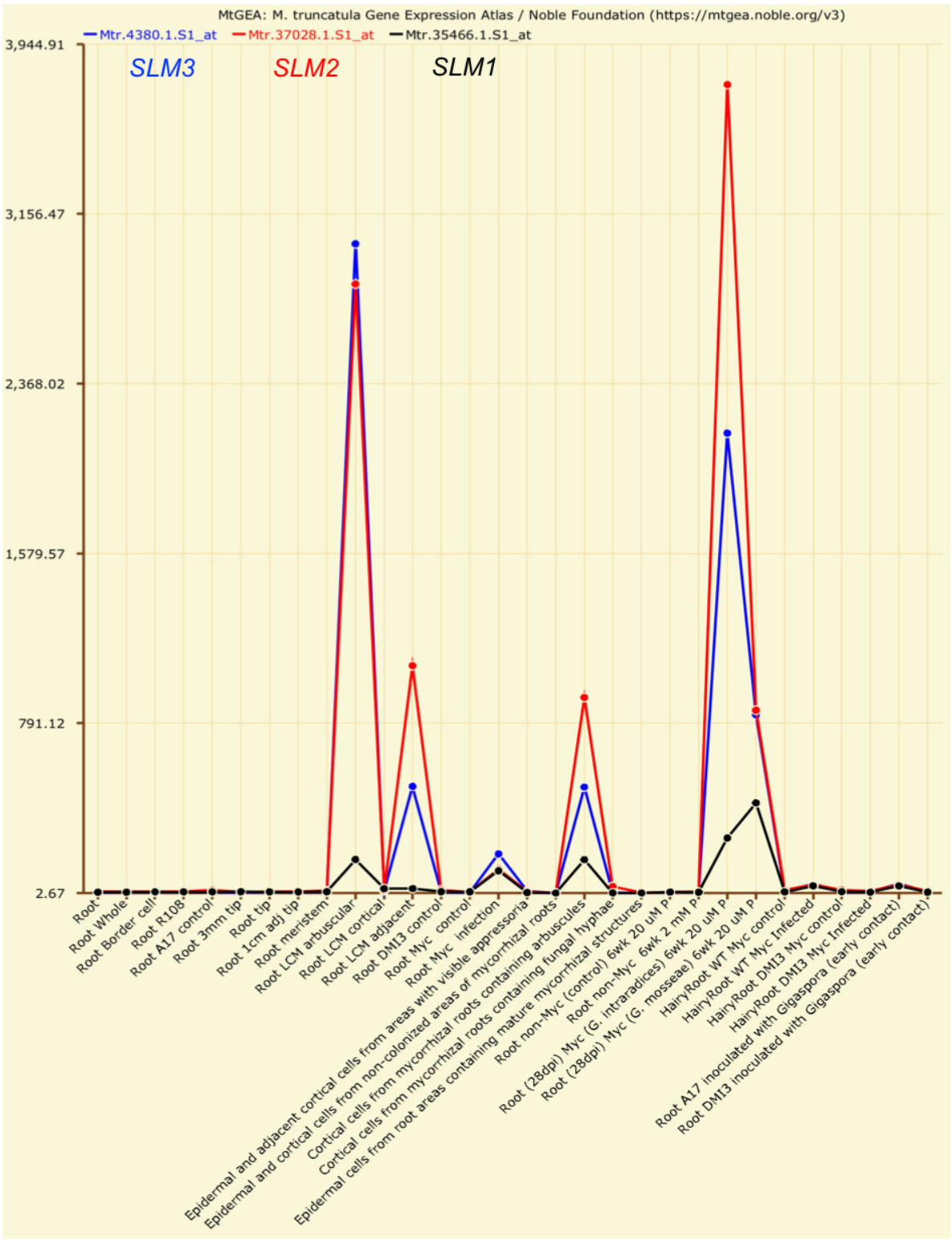

Appendix 4-4: *AM-SLM* transcript levels in the *Medicago truncatula* Gene Expression Atlas. Vertical axis is normalized transcript levels.

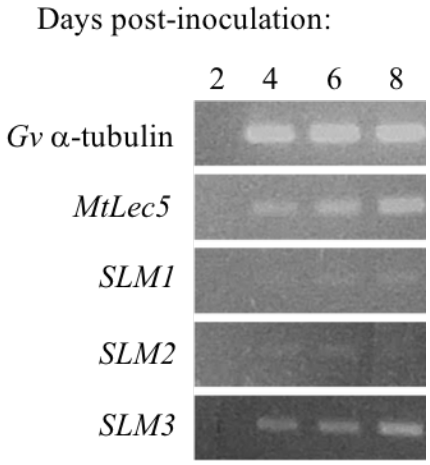

Appendix 4- 5: RT-PCR of *AM-SLM* expression in *G. versiforme*-inoculated roots using the double-cone system, at 2 – 8 dpi. Transcripts from all three *AM-SLM* and the arbuscule marker, *MtLec5* were detected at 4 dpi.

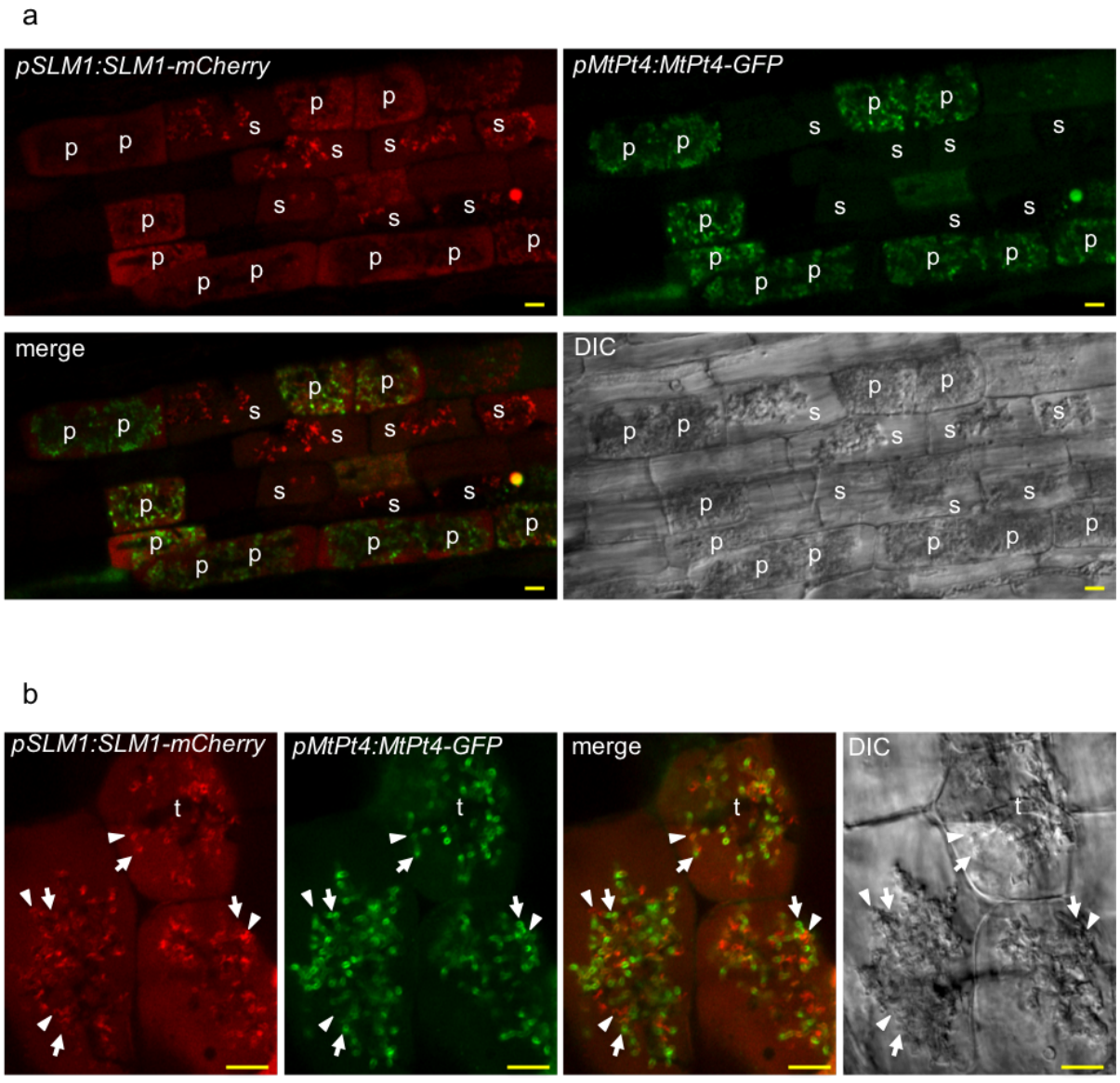

Appendix 4- 6: SLM1-mCherry does not co-localize with MtPt4-GFP. Stable transgenic line *M. truncatula* pMtPt4:MtPt4-GFP transformed with pSLM1:SLM1-mCherry. **(a)** Longitudinal cross-section cut along vascular tissue shows colonization throughout the inner cortex. Cells with SLM1-mCherry atthe arbuscule marked with s, and cells with MtPt4 at the arbuscule marked with p. **(b)** Closer view of arbuscules with both proteins localized to the branches. SLM1-mCherry localizes to the lower branches (arrowheads) while MtPt4-GFP localizes to the fine arbuscule branches (arrows). t = trunk, bar = 10 µm

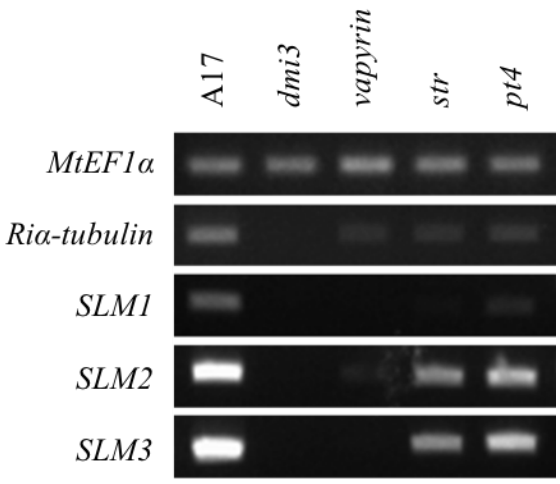

Appendix 4-7: RT-PCR of *AM-SLM* expression in *Rhizophagus intraradices*-colonized wild type (A17) and mutant *M. truncatula* roots. All three *AM-SLM* were detected in *pt4*.

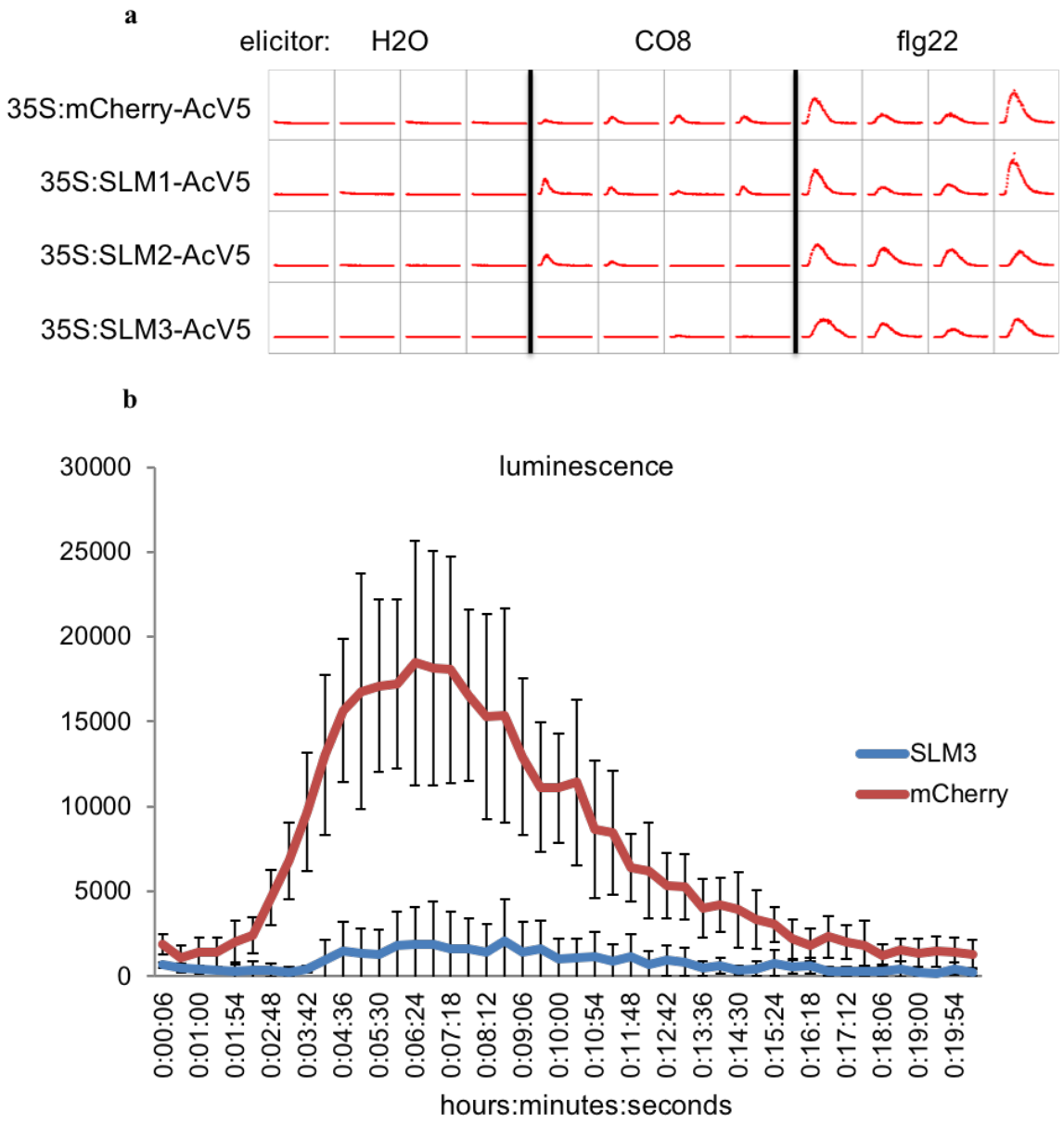

Appendix 4-8: ROS production of *Nicotiana benthamiana* leaf discs overexpressing AM-SLM or mCherry tagged with AcV5. **(a)** Luminescence spectra for all leaf discs exposed to water, CO8 or flg22. **(b)** Average luminescence readings at each time-point for leaf discs overexpressing SLM3-AcV5 (blue) or mCherry-AcV5 (red), exposed to CO8. Bars are standard deviation, n= 4.

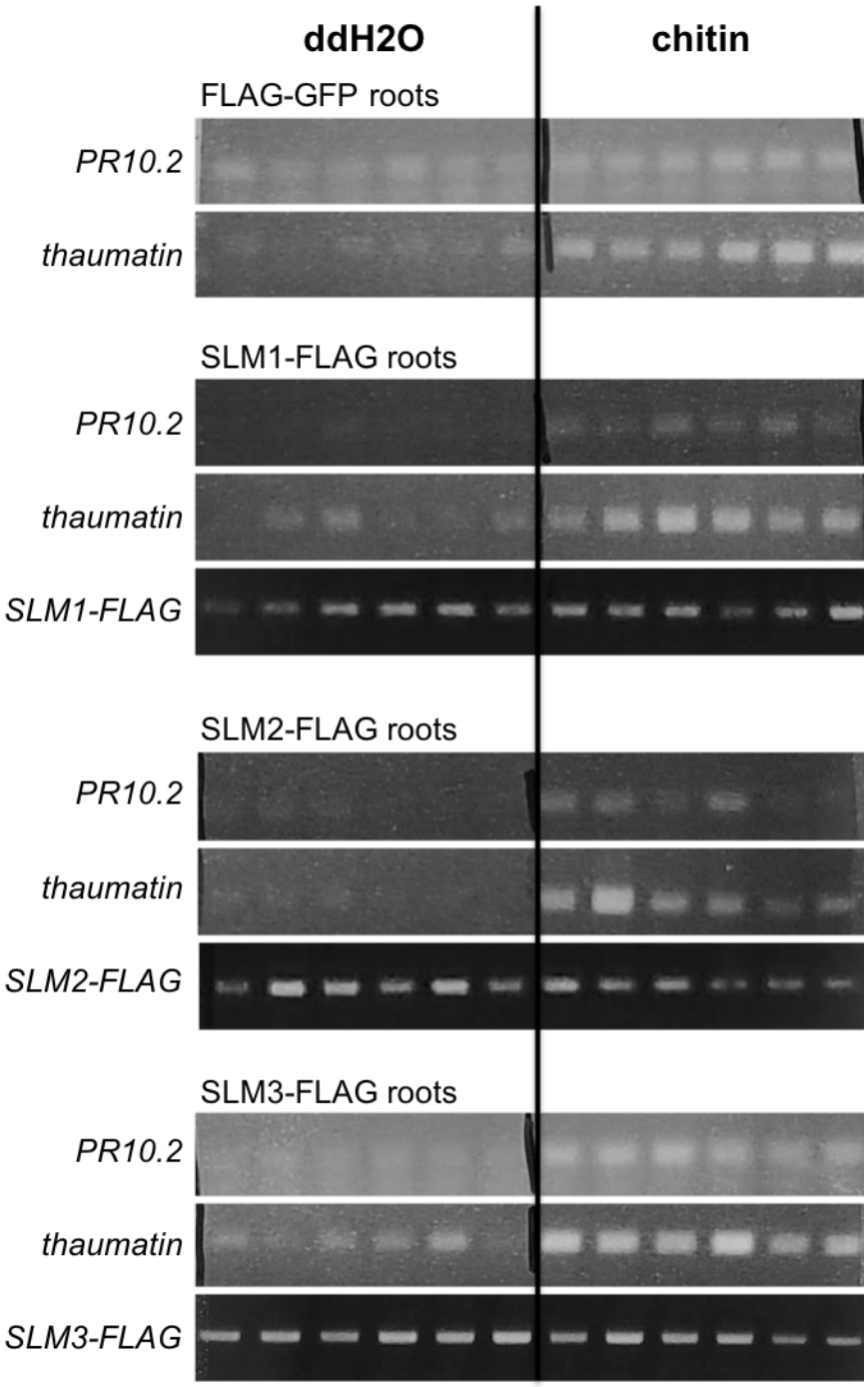

Appendix 4-9: RT-PCR showing induction of defense genes *PR10.2* and *thaumatin* in roots exposed to chitin for 4 hours.

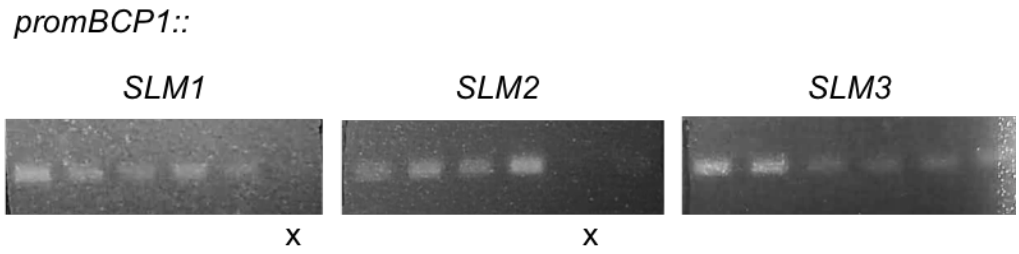

Appendix 4-10: RT-PCR of *AM-SLM* exogenous expression in *Glomus versiforme*-inoculated *M. truncatula* roots ectopically expressing either *SLM1*, *SLM2*, or *SLM3*. Expression was measured using forward primer pBCP1exo and the corresponding *AM-SLM* reverse primer (Appendix 4-13). X marks samples that were removed from analysis due to possible lack of exogenous expression.

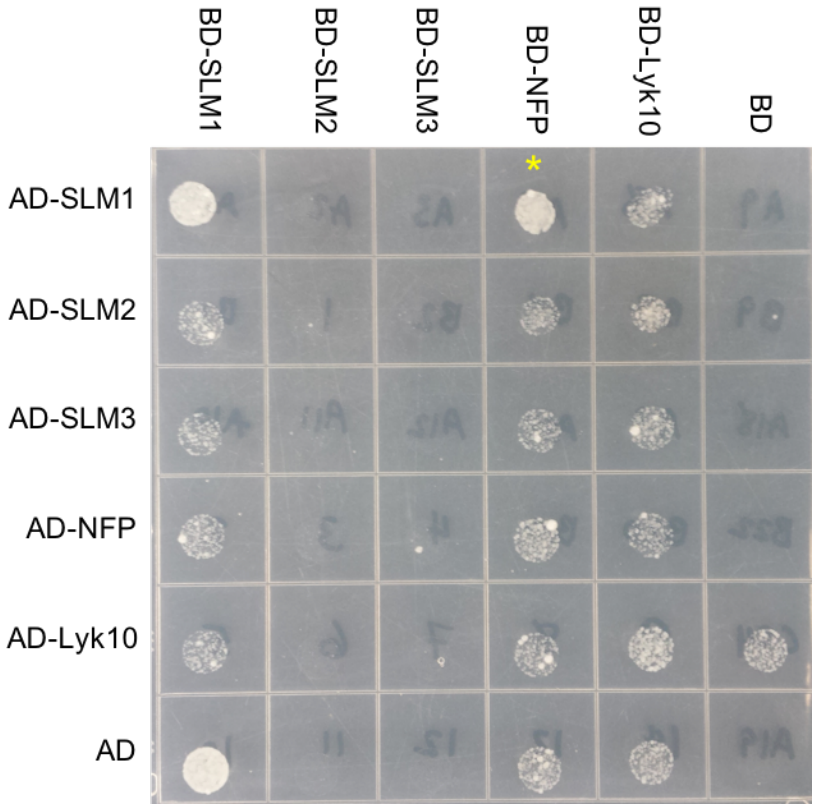

Appendix 4-11: Yeast two-hybrid demonstrating potential interaction between SLM1 and the ectodomain of NFP (yellow asterix). Media shown contains 20 mM 3AT. Yeast were plated at OD600 = 0.05 and imaged on the third day.

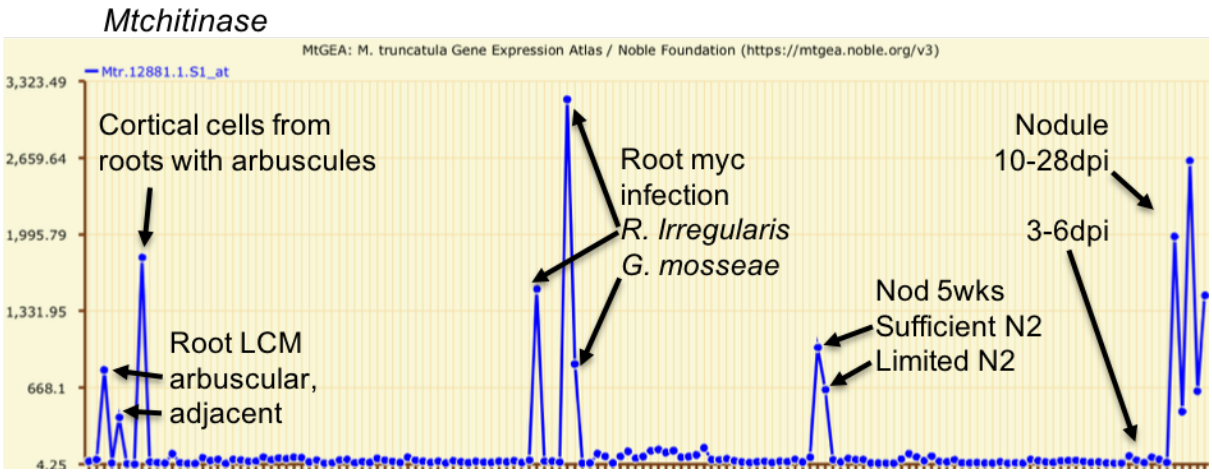

Appendix 4-12: The MYB1-induced chitinase transcript levels in the *Medicago truncatula* Gene Expression Atlas. Vertical axis is normalized transcript levels. Transcript present only samples with arbuscular mycorrhizal fungi, or late-stage nodules.

Group	Common Name	Genus	species	AMS status	Total	AM-SLM	Others
Basal angiosperm	Amborella	*Amborella*	*trichopoda*	host	3	1	2
Monocot	Pineapple	*Ananus*	*comosus*	host[1]	4	1	3
Eudicot	**Colombine**	***Aquilegia***	***coerulea***	**host**	**10**	**8**	**2**
Monocot	**Purple false brome**	***Brachypodium***	***distachyon***	**host**	**4**	**2**	**2**
Monocot		*Brachypodium*	*stacei*	unknown	4	2	2
Eudicot	Papaya	*Carica*	*papaya*	host	3	1	2
Eudicot	Clementine	*Citrus*	*clementina*	host	7	4	3
Eudicot	Sweet orange	*Citrus*	*sinensis*	host	4	1	3
Eudicot	Cucumber	*Cucumis*	*sativus Hyg14*	host	2	0	2
Eudicot	**Carrot**	***Daucus***	***carota***	**host**	**15**	**10**	**5**
Fern	Field horsetail	Equisetum	*arvense*	host	0	0	0
Eudicot	Eucalyptus	*Eucalyptus*	*grandis*	host	6	2	4
Eudicot	Strawberry	*Fragaria*	*vesca*	host	13	13	0
Eudicot	Soybean	*Glycine*	*max*	host	17	3	14
Eudicot	**Cotton**	***Gossypium***	***raimondii***	**host**	**9**	**3**	**6**
Eudicot	diploid Kalanchoe	*Kalanchoe*	*fedtschenkoi*	unknown	7	5	2
Eudicot	Milky widow's thrill	*Kalanchoe*	*laxiflora*	unknown	18	13	5
Eudicot	**Flax**	***Linum***	***usitatissimum***	**host**	**10**	**7**	**3**
Eudicot	Birdsfoot trefoil	*Lotus*	*japonicus*	host	4	0	4
Eudicot	Apple	*Malus*	*domestica*	host	11	7	4
Eudicot	Cassava	*Manihot*	*esculenta*	host	6	2	4
Embryophyte	Common liverwort	*Marchantia*	*polymorpha*	host	0	0	0
Eudicot	**Barrel medic**	***Medicago***	***truncatula***	**host**	**12**	**3**	**9**
Eudicot	Monkey flower	*Mimulus*	*guttatus*	host	8	4	4
Monocot	Banana	*Musa*	*acuminata*	host	4	0	4
Monocot		***Oropetium***	***thomaeum***	**unknown**	**9**	**5**	**4**
Monocot	**Rice**	***Oryza***	***sativa***	**host**	**5**	**2**	**3**
Monocot	Hall's panicgrass	*Panicum*	*hallii*	host	8	5	3
Monocot	Switchgrass	*Panicum*	*virgatum*	host	23	17	6
Eudicot	Petunia	*Petunia*	*axillaris*	host	7	3	4
Eudicot	Common bean	*Phaseolus*	*vulgaris*	host	6	1	5
Eudicot	Poplar	*Populus*	*trichocarpa*	host	10	4	6
Eudicot	Peach	*Prunus*	*persica*	host	10	7	3
Fern		Pteris	ryukyuensis	host[2]	0	0	0
Eudicot	Castor bean	*Ricinus*	*communis*	host	7	5	2
Eudicot	Purple osier willow	*Salix*	*purpurea*	host	10	2	8
Lycophyte	Spikemoss	*Selaginella*	*mellindorfii*	host	0	0	0
Monocot	**Foxtail millet**	***Setaria***	***italica***	**host**	**7**	**4**	**3**
Monocot	Green foxtail	*Setaria*	*viridis*	host	6	4	2
Eudicot	Tomato	*Solanum*	*lycopersicum*	host	5	2	3
Eudicot	Potato	*Solanum*	*tuberosum*	host	4	2	2
Monocot	Cereal grass	*Sorghum*	*bicolor*	host	14	11	3
Eudicot	Cacao	*Theobroma*	*cacao*	host	3	1	2
Eudicot	**Clover**	***Trifolium***	***pratense***	**host**	**9**	**3**	**6**
Monocot	**Maize**	***Zea***	***mays***	**host**	**5**	**2**	**3**
Monocot	Maize	*Zea*	*mays PH207*	host	5	2	3

Group	Common Name	Genus	species	AMS status	Total	AM-SLM	Others
Eudicot		*Arabidopsis*	*halleri*	non-host	2	0	2
Eudicot	Lyre-leaved rock cress	*Arabidopsis*	*lyrata*	non-host	3	0	3
Eudicot	**Thale Cress**	***Arabidopsis***	***thaliana***	**non-host**	**3**	**0**	**3**
Eudicot	Prince's feather	*Amaranthus*	*hypochondriacus*	unclear[3]	3	0	3
Fern	Water fern	*Azolla*	*filliculoides*	non-host	0	0	0
Eudicot	Sugar beet	*Beta*	*vulgaris*	non-host	2	0	2
Eudicot	Drummond's rock cress	*Boechera*	*stricta*	non-host	3	0	3
Eudicot	Savoy cabbage	*Brassica*	*oleracea capitata*	non-host	2	0	2
Eudicot	**Turnip mustad**	***Brassica***	***rapa FPsc***	**non-host**	**4**	**0**	**4**
Eudicot		*Capsella*	*grandiflora*	non-host	3	0	3
Eudicot	Pink shepherd's purse	*Capsella*	*rubella*	non-host	3	0	3
Chlorophyta		*Chlamydomonas*	*reinhardtii*	non-host	0	0	0
Chlorophyta		*Coccomyxa*	*subellipsoidea C-169*	non-host	0	0	0
Eudicot	Carnation	*Dianthus*	*caryophyllus*	non-host	0	0	0
Chlorophyta		*Dunaliella*	*salina*	non-host	0	0	0
Eudicot	**Salt Cress**	***Eutrema***	***salsugineum***	**non-host**	**3**	**0**	**3**
Eudicot	**Lupine**	***Lupinus***	***angustifolius***	**non-host**	**2**	**0**	**2**
Chlorophyta		*Micromonas*	*pusilla CCMP1545*	non-host	0	0	0
Chlorophyta		*Micromonas*	*sp. RCC299*	non-host	0	0	0
Eudicot	Sacred lotus	*Nelumbo*	*nucifera*	non-host	1	0	1
Chlorophyta		*Ostreococcus*	*tauri*	non-host	0	0	0
Chlorophyta		*Ostreococcus*	*lucimarinus*	non-host	0	0	0
Bryophyte	**Moss**	***Physcomitrella***	***patens***	**non-host**	**1**	**0**	**1**
Gymnosperms	**Norway spruce**	***Picea***	***abies***	**non-host**	**9**	**0**	**9**
Bryophyte	**Bog moss**	***Sphagnum***	***fallax***	**non-host[4]**	**1**	**0**	**1**
Monocot	**Greater duckweed**	***Spirodela***	***polyrhiza***	**non-host**	**1**	**0**	**1**
Eudicot	Spider flower	*Tarenaya*	*hassleriana*	non-host	4	0	4
Eudicot	**Floating bladderwort**	*Utricularia*	*gibba*	non-host	0	0	0
Chlorophyta	Volvox	*Volvox*	*carteri*	non-host	0	0	0
Monocot	**Common Eelgrass**	***Zostera***	***marina***	**non-host[5]**	**5**	**0**	**5**

Appendix 4-13: List of plant species whose genomes were searched for *SLM* genes in this study. First part lists known AM hosts, and second part lists known non-hosts. Light gray shading indicates lineages ancestral to angiosperms. Bold rows are species whose SLM were used for phylogenetic reconstruction. Unless otherwise annotated, AM host status was based on Wang and Qiu 2006, Bravo et al. 2016, or Cosme et al. 2018 except where noted: [1]Jaizme-Vega and Azcón 1995, [2]Onaga and Taira 2008, [3]Moreno-Espíndola et al. 2007, [4]Read et al. 2000, [5]Nielsen, Thingstrup and Wigand 1999.

Appendix 4-14: List of primers used for this study

RT-PCR/qPCR Primers

SLM1	F: 5'-ACCGCTGGATTTCCAATATG-3'
	R: 5'-TTGTTGGCACATCTCACAAA-3'
SLM2	F: 5'-CCAACACCTACAGTCCCAAG-3'
	R: 5'-TGGAGTACGTAATTTCATTCACA-3'
SLM3	F: 5'-CAACAGTTGCAGTCCCAACA-3'
	R: 5'-ACAGAGCGGCGTAATCTCAT-3'
SLM4	F: 5'-TGGGGGAGCATCAGTTTTAC-3'
	R: 5'-GGACTTGAGAACAAGAAACTCCA-3'
SLM5	F: 5'-ACAAGGGCTTGTAGGGGAGT-3'
	R: 5'-ACAACACAAGCAAAGCAAGC-3'
SLM6	F: 5'-TGACGGTTGAGATGAAGCAG-3'
	R: 5'-CCTTCAACAAGACCCCAAAA-3'
SLM7	F: 5'-AGAGGTGATTCAGCATCATGG-3'
	R: 5'-CCAGGGAAAACATCATCTGG-3'
SLM8	F: 5'-TGTTGGTTTTGAGCTTCTGCG-3'
	R: 5'-GTCTCTCCCTCGCCAACAAC-3'
SLM9	F: 5'-AACCATGCGACGAAATCTATG-3'
	R: 5'-AAAGTAAAAGTTTGTTGATCAAATTCC-3'
SLM10	F: 5'-TGATCTTGATCATCATGGTTCCT-3'
	R: 5'-TTTCGTCGCATGGTTTGGAC-3'
SLM11	F: 5'-TCAACTCAAGAAAGGGAGCAGTT-3'
	R: 5'-GTCGCATGGTTTGGACAACA-3'
SLM7-like	F: 5'-GGCTAAAACAATTCACAAAGCATGT-3'
	R: 5'-TGCTCTCTATCTAGGTCTTCAACA-3'

MtEF1α	F: 5'-GAGACCCACAGACAAGCC-3'
	R: 5'-ACTGGCACAGTTCCAATACC-3'
MtLec5	F: 5'-TCAAGTTGCTGAAACACATGAT-3'
	R: 5'-GAGCAGAACCATTGCAACAA-3'
MtPt4	F: 5'-GACACGAGGCGCTTTCATAGCAGC-3'
	R: 5'-GTCATCGCAGCTGGAACAGCACCG-3'
MtCP3	F: 5'-AACAATGATGCCAATAACAAGC-3'
	R: 5'-GGAGCACATATGACCCTTGA-3'
Ri α-tubulin	F: 5'-TGTCCAACCGGTTTTAAAGT-3'
	R: 5'-AAAGCACGTTTGGCGTACAT-3'
Gv α-tubulin	F: 5'-TCTCCAATGCGGCCAAATCT-3'
	R: 5'-TCTCCAATGCGGCCAAATCT-3'
thaumatin	F: 5'-GGCGCAATCCCACCAGCAAC-3'
	R: 5'-ACCACTCCCACCTTGTGGCG-3'
PR10.2	F: 5'-AGCGAAATTGGTTGAAGGCT-3'
	R: 5'-ATCTCCTTTGGTTTGGTATTTAACT-3'

Cloning Primers

SLM1 promoter F: 5'-TTGTTGAAAATGACTCCGTTATTAT-3'

SLM1 promoter R: 5'-TCTTCCTCTTCCAACTTCCTTT-3'

SLM2 promoter F: 5'-CATCTTTATATTTTGGGAAATGGG-3'

SLM2 promoter R: 5'-TCTTCTCAATTCTTCCAAACCC-3'

SLM3 promoter F: 5'-CACTTATTGAACTTGTTTTAATTTTGT-3'

SLM3 promoter R: 5'-TCTTCTTGTTCCAAACCTTTTTAAC-3'

SLM1 promoter attB1 F:

5'-GGGGACAAGTTTGTACAAAAAAGCAGGCTTCTTGTTGAAAATGACTCCGTT-3'

SLM1 promoter attB2 R:

5'-GGGGACCACTTTGTACAAGAAAGCTGGGTGTCTTCCTCTTCCAACTTCCT-3'

SLM1no stop attB2 R:

5'-GGGGACCACTTTGTACAAGAAAGCTGGGTGCCTGCCATTCACACACAC-3'

SLM1 5' UTR F: 5'-AAAGGAAGTTGGAAGAGGAAGA-3'

SLM2 promoter attB1 F:

5'-GGGGACAAGTTTGTACAAAAAAGCAGGCTTCCATCTTTATATTTTGGGAAA-3'

SLM2 promoter attB2 R:

5'-GGGGACCACTTTGTACAAGAAAGCTGGGTGTCTTCTCAATTCTTCCAAAC-3'

SLM2 no stop attB2 R:

5'-GGGGACCACTTTGTACAAGAAAGCTGGGTGATTCACTTCACCCTCAACAC-3'

SLM3 promoter attB1 F:

5'-GGGGACAAGTTTGTACAAAAAAGCAGGCTTCCACTTATTGAACTTGTTTTA-3'

SLM3 promoter attB2 R:

5'-GGGGACCACTTTGTACAAGAAAGCTGGGTGTCTTCTTGTTCCAAACCTTT-3'

SLM3 no stop attB2 R:

5'-GGGGACCACTTTGTACAAGAAAGCTGGGTGATTCACTTCACCTTCAACACAT-3'

SLM1 fragment F: 5'-ATGACCAAGTCTAGTAGTAGCAGTTTT-3'

SLM1 fragment R: 5'-TGCACACCATGAATTGTG-3'

SLM2/3 fragment F: 5'-CACAATTCATGCTGTGGCAG-3'

SLM2/3 fragment R: 5'-TCAATTCACTTCACCCTCAAC-3'

SLM1/2/3 RNAi attB1 F:

5'-GGGGACAAGTTTGTACAAAAAAGCAGGCTATGACCAAGTCTAGTAGTAGCAG-3'

SLM1/2/3 RNAi attB2 R:

5'-GGGGACCACTTTGTACAAGAAAGCTGGGTTCAATTCACTTCACCCTCAAC-3'

UidA RNAi attB1 F:

5'-GGGGACAAGTTTGTACAAAAAAGCAGGCTCCCTTACGCTGAAGAGATGC-3'

UidA RNAi attB2 R:

5'-GGGGACCACTTTGTACAAGAAAGCTGGGTGGCACAGCACATCAAAGAGA-3'

SLM1 ATG attB1 F:

5'-GGGGACAAGTTTGTACAAAAAAGCAGGCTTCACCATGACCAAGTCTAGTAGTAGCA-3'

SLM2 ATG attB1 F:

5'-GGGGACAAGTTTGTACAAAAAAGCAGGCTTCACCATGGCCAAGTTTACTAAAATC-3'

SLM3 ATG attB1 F:

5'-GGGGACAAGTTTGTACAAAAAAGCAGGCTTCACCATGGCTAAGTCAACTAACATCT-3'

SLM1 stop attB2 R:

5'-GGGGACCACTTTGTACAAGAAAGCTGGGTTTTACCTGCCATTCACACACAC-3'

SLM2 stop attB2 R:

5'-GGGGACCACTTTGTACAAGAAAGCTGGGTTTTAATTCACTTCACCCTCAACAC-3'

SLM3 stop attB2 R:

5'-GGGGACCACTTTGTACAAGAAAGCTGGGTTTTAATTCACTTCACCTTCAACACAT-3'

SLM3 2FLAG R:

5'-TCGTCGTCCTTGTAGTCTTTGTCATCGTCGTCCTTGTAGTCATTCACTTCACCTTCAACA-3'

SLM1 FLAG R: 5'-GTCGTCCTTGTAGTCCCTGCCATTCACACA-3'

SLM2 FLAG R: 5'-GTCGTCCTTGTAGTCATTCACTTCACCCTC-3'

FLAG stop attB2 R:

5'-GGGGACCACTTTGTACAAGAAAGCTGGGTTCATTTGTCATCGTCGTCCTTGTAGTC-3'

SLM1 no SP attB1 F:

5'-GGGGACAAGTTTGTACAAAAAAGCAGGCTTCTTTCCAATATGCAGCACAAT-3'

SLM2 no SP attB1 F:

5'-GGGGACAAGTTTGTACAAAAAAGCAGGCTTCCGACCAACACCTACAGTCC-3'

SLM3 no SP attB1 F:

5'-GGGGACAAGTTTGTACAAAAAAGCAGGCTTCAGTCGACCAACACCAACA-3'

REFERENCES

Akcapinar, G. B., Kappel, L., Sezerman, O. U., and Seidl-Seiboth, V. 2015. Molecular diversity of LysM carbohydrate-binding motifs in fungi. Curr. Genet. 61:102–113

Alberts B, Johnson A, Lewis J, et al. 2002 Molecular Biology of the Cell. 4th Edition. New York: Garland Science; 2002.

Amor, B. Ben, Shaw, S. L., Oldroyd, G. E. D. D., Maillet, F., Penmetsa, R. V., Cook, D., Long, S. R., Dénarié, J., and Gough, C. 2003. The NFP locus of Medicago truncatula controls an early step of Nod factor signal transduction upstream of a rapid calcium flux and root hair deformation. Plant J. 34:495–506

Balestrini, R., and Bonfante, P. 2014. Cell wall remodeling in mycorrhizal symbiosis: a way towards biotrophism. Front. Plant Sci. 5:237

BÉCARD, G., and FORTIN, J. A. 1988. Early events of vesicular–arbuscular mycorrhiza formation on Ri T-DNA transformed roots. New Phytol. 108:211–218

Benedito, V. a, Torres-Jerez, I., Murray, J. D., Andriankaja, A., Allen, S., Kakar, K., Wandrey, M., Verdier, J., Zuber, H., Ott, T., Moreau, S., Niebel, A., Frickey, T., Weiller, G., He, J., Dai, X., Zhao, P. X., Tang, Y., and Udvardi, M. K. 2008. A gene expression atlas of the model legume Medicago truncatula. Plant J. 55:504–13

Bozsoki, Z., Cheng, J., Feng, F., Gysel, K., Vinther, M., Andersen, K. R., Oldroyd, G., Blaise, M., Radutoiu, S., and Stougaard, J. 2017. Receptor-mediated chitin perception in legume roots is functionally separable from Nod factor perception. PNAS. 114:E8118–E8127

Bravo, A., York, T., Pumplin, N., Mueller, L. A., and Harrison, M. J. 2016. Genes conserved for arbuscular mycorrhizal symbiosis identified through phylogenomics. Nat. Plants. 2:15208

Buist, G., Steen, A., Kok, J., and Kuipers, O. P. 2008. LysM, a widely distributed protein motif for binding to (peptido)glycans. Mol. Microbiol. 68:838–847

Camps, C., Jardinaud, M.-F., Rengel, D., Carrère, S., Hervé, C., Debellé, F., Gamas, P., Bensmihen, S., and Gough, C. 2015. Combined genetic and transcriptomic analysis reveals three major signalling pathways activated by Myc-LCOs in Medicago truncatula. New Phytoogist. 208:224–240

Chakravarthy, S., Velásquez, A. C., Ekengren, S. K., Collmer, A., and Martin, G. B. 2010. Identification of Nicotiana benthamiana genes involved in pathogen-associated molecular pattern-triggered immunity. Mol. Plant. Microbe. Interact. 23:715–726

Choi, J., Summers, W., and Paszkowski, U. 2018. Mechanisms Underlying Establishment of Arbuscular Mycorrhizal Symbioses. Annu Rev Phytopathol. 56:7.1-7.26

Czaja, L. F., Hogekamp, C., Lamm, P., Maillet, F., Martinez, E. A., Samain, E., Denarie, J., Kuster, H., and Hohnjec, N. 2012. Transcriptional Responses toward Diffusible Signals from Symbiotic Microbes Reveal MtNFP- and MtDMI3-Dependent Reprogramming of Host Gene Expression by Arbuscular Mycorrhizal Fungal Lipochitooligosaccharides. Plant Physiol. 159:1671–1685

de Jonge, R., and Thomma, B. P. H. J. 2009. Fungal LysM effectors: extinguishers of host immunity? Trends Microbiol. 17:151–157

Delaux, P. M., Séjalon-Delmas, N., Bécard, G., and Ané, J. M. 2013. Evolution of the plant-microbe symbiotic "toolkit." Trends Plant Sci. 18:298–304

Desaki, Y., Miyata, K., Suzuki, M., Shibuya, N., and Kaku, H. 2017. Plant immunity and symbiosis signaling mediated by LysM receptors. Innate Immun. 24:92–100

Fiorilli, V., and Gutjahr, C. 2018. Partner communication and role of nutrients in the arbuscular mycorrhizal symbiosis. New Phytol. [Epub ahea

Floss, D. S., Levy, J. G., Levesque-Tremblay, V., Pumplin, N., and Harrison, M. J. 2013a. DELLA proteins regulate arbuscule formation in arbuscular mycorrhizal symbiosis. PNAS. 110:5025–5034

Floss, D. S., Schmitz, A. M., Starker, C. G., Gantt, J. S., and Harrison, M. J. 2013b. Gene Silencing in Medicago truncatula Roots Using RNAi. Pages 163–177 in: Legume Genomics: Methods and Protocols.

Floss, D. S., Gomez, S. K., Park, H. J., MacLean, A. M., Müller, L. M., Bhattarai, K. K., Lévesque-Tremblay, V., Maldonado-Mendoza, I. E., and Harrison, M. J. 2017. A Transcriptional Program for Arbuscule Degeneration during AM Symbiosis Is Regulated by MYB1. Curr. Biol. 27:1206–1212

Frenzel, A., Tiller, N., Hause, B., and Krajinski, F. 2006. The conserved arbuscular mycorrhiza-specific transcription of the secretory lectin MtLec5 is mediated by a short upstream sequence containing specific protein binding sites. Planta. 224:792–800

Genre, A., Chabaud, M., Balzergue, C., Puech-Pagès, V., Novero, M., Rey, T., Fournier, J., Rochange, S., Bécard, G., Bonfante, P., and Barker, D. G. 2013. Short-chain chitin oligomers from arbuscular mycorrhizal fungi trigger nuclear Ca2+ spiking in Medicago truncatula roots and their production is enhanced by strigolactone. New Phytol. 198:190–202

Genre, A., Chabaud, M., Faccio, A., Barker, D. G., and Bonfante, P. 2008. Prepenetration apparatus assembly precedes and predicts the colonization patterns of arbuscular

mycorrhizal fungi within the root cortex of both Medicago truncatula and Daucus carota. Plant Cell. 20:1407–1420

Genre, A., Chabaud, M., Timmers, T., Bonfante, P., and Barker, D. G. 2005. Arbuscular Mycorrhizal Fungi Elicit a Novel Intracellular Apparatus in Medicago truncatula Root Epidermal Cells before Infection. Plant Cell. 17:3489–3499

Genre, A., and Russo, G. 2016. Does a Common Pathway Transduce Symbiotic Signals in Plant–Microbe Interactions? Front. Plant Sci. 7:1–8

Goodstein, D. M., Shu, S., Howson, R., Neupane, R., Hayes, R. D., Fazo, J., Mitros, T., Dirks, W., Hellsten, U., Putnam, N., and Rokhsar, D. S. 2012. Phytozome: A comparative platform for green plant genomics. Nucleic Acids Res. 40:1178–1186

Güimil, S., Chang, H., Zhu, T., Sesma, A., Osbourn, A., Roux, C., Ioannidis, V., Oakeley, E. J., Docquier, M., Descombes, P., Briggs, S. P., Paszkowski, U., Gu, S., Oakeley, E. J., Descombes, P., Briggs, S. P., and Paszkowski, U. 2005. Comparative transcriptomics of rice reveals an ancient pattern of response to microbial colonization. PNAS. 102:8066–70

Gutjahr, C., Banba, M., Croset, V., An, K., Miyao, A., An, G., Hirochika, H., Imaizumi-Anraku, H., and Paszkowski, U. 2008. Arbuscular Mycorrhiza-Specific Signaling in Rice Transcends the Common Symbiosis Signaling Pathway. Plant Cell Online. 20:2989–3005

Guttenberger, M. 2000. Arbuscules of vesicular-arbuscular mycorrhizal fungi inhabit an acidic compartment within plant roots. Planta. 211:299–304

Haag, A. F., Kerscher, B., Dall'Angelo, S., Sani, M., Longhi, R., Baloban, M., Wilson, H. M., Mergaert, P., Zanda, M., and Ferguson, G. P. 2012. Role of cysteine residues and disulfide bonds in the activity of a legume root nodule-specific, cysteine-rich peptide. J. Biol. Chem. 287:10791–10798

Hartley, J. L., Temple, G. F., and Brasch, M. A. 2000. DNA cloning using in vitro site-specific recombination. Genome Res. 10:1788–1795

Hiller, K., Grote, A., Scheer, M., Münch, R., and Jahn, D. 2004. PrediSi: Prediction of signal peptides and their cleavage positions. Nucleic Acids Res. 32:375–379

Ivanov, S., and Harrison, M. J. 2014. A set of fluorescent protein-based markers expressed from constitutive and arbuscular mycorrhiza-inducible promoters to label organelles, membranes and cytoskeletal elements in Medicago truncatula. Plant J. 80:1151–1163

Javot, H., Penmetsa, R. V., Breuillin, F., Bhattarai, K. K., Noar, R. D., Gomez, S. K., Zhang, Q., Cook, D. R., and Harrison, M. J. 2011. Medicago truncatula mtpt4 mutants reveal a role for nitrogen in the regulation of arbuscule degeneration in arbuscular mycorrhizal symbiosis. Plant J. 68:954–65

Kaku, H., Nishizawa, Y., Ishii-Minami, N., Akimoto-Tomiyama, C., Dohmae, N., Takio, K., Minami, E., and Shibuya, N. 2006. Plant cells recognize chitin fragments for defense signaling through a plasma membrane receptor. PNAS. 103:11086–11091

Kobae, Y., and Hata, S. 2010. Dynamics of periarbuscular membranes visualized with a fluorescent phosphate transporter in arbuscular mycorrhizal roots of rice. Plant Cell Physiol. 51:341–353

Krishnakumar, V., Kim, M., Rosen, B. D., Karamycheva, S., Bidwell, S. L., Tang, H., and Town, C. D. 2015. MTGD: The medicago truncatula genome database. Plant Cell Physiol. 56:e1

Leppyanen, I. V., Shakhnazarova, V. Y., Shtark, O. Y., Vishnevskaya, N. A., Tikhonovich, I. A., and Dolgikh, E. A. 2018. Receptor-like kinase LYK9 in Pisum sativum L. Is the CERK1-like receptor that controls both plant immunity and AM symbiosis development. Int. J. Mol. Sci. 19

Li, F., Brouwer, P., Carretero-paulet, L., Cheng, S., Vries, J. De, Eily, A., Koppers, N., Kuo, L., Li, Z., Simenc, M., Small, I., Angarita, S., Barker, M. S., Braeutigam, A., Hosmani, P. S., Huang, Y., Huettel, B., Kato, Y., Liu, X., Mcdowell, R., Mueller, L. A., Nierop, K. G. J., Rensing, S. A., Robison, T., Rothfels, C. J., Sigel, E. M., Song, Y., Timilsina, P. R., Peer, Y. Van De, Wang, H., Wilhelmsson, P. K. I., Wolf, P. G., Xu, X., Der, J. P., Schluepmann, H., Pryer, K. M., Section, P. B., Zone, I., District, Y., Toulouse, D., Tolosan, C., Heine, H., Biology, E., Genome, M. P., Cologne, C., and Services, A. 2018. Fern genomes elucidate land plant evolution and cyanobacterial symbioses. Nat. Plants.

Liu, B., Li, J. F., Ao, Y., Li, Z., Liu, J., Feng, D., Qi, K., He, Y., Zeng, L., Wang, J., and Wang, H. B. 2013. OsLYP4 and OsLYP6 play critical roles in rice defense signal transduction. Plant Signal Behav. 8:e22980

Liu, J., Blaylock, L., Endre, G., Cho, J., Town, C. D., Vandenbosch, K. A., and Harrison, M. J. 2003. Transcript profiling coupled with spatial expression analyses reveals genes involved in disinct developmental stages of an arbuscular mycorrhizal symbiosis. Plant Cell. 15:2106–2123

Liu, J., Maldonado-Mendoza, I., Lopez-Meyer, M., Cheung, F., Town, C. D., and Harrison, M. J. 2007. Arbuscular mycorrhizal symbiosis is accompanied by local and systemic alterations in gene expression and an increase in disease resistance in the shoots. Plant J. 50:529–544

Liu, T., Liu, Z., Song, C., Hu, Y., Han, Z., She, J. J., Fan, F., Wang, J., Jin, C., Chang, J., Zhou, J.-M. J.-M., and Chai, J. 2012. Chitin-induced dimerization activates a plant immune receptor. Science. 336:1160–1164

Lopez-Meyer M, Harrison MJ (2006) An experimental system to synchronize the early events of development of the arbuscular mycorrhizal symbiosis. Biology of Molec- ular Plant-

Microbe Interactions, eds Sánchez F, Quinto C, López-Lara IM, Geiger O (International Society for Molecular Plant-Microbe Interactions, St. Paul), Vol 5, pp 546–551.

Maillet, F., Poinsot, V., André, O., Puech-Pagès, V., Haouy, A., Gueunier, M., Cromer, L., Giraudet, D., Formey, D., Niebel, A., Martinez, E. A., Driguez, H., Bécard, G., and Dénarié, J. 2011. Fungal lipochitooligosaccharide symbiotic signals in arbuscular mycorrhiza. Nature. 469:58–63

Marshall, E., Costa, L. M., and Gutierrez-Marcos, J. 2011. Cysteine-Rich Peptides (CRPs) mediate diverse aspects of cell – cell communication in plant reproduction and development. J. Exp. Bot. 62:1677–1686

McGonigle, T. P., Miller, M. H., Evans, D. G., Fairchild, G. L., and Swan, J. A. 1990. A New Method which Gives an Objective Measure of Colonization of Roots by Vesicular-Arbuscular Mycorrhizal Fungi. New Phytol. 115:495–501

Mélida, H., Sopeña-Torres, S., Bacete, L., Garrido-Arandia, M., Jordá, L., López, G., Muñoz-Barrios, A., Pacios, L. F., and Molina, A. 2018. Non-branched β-1,3-glucan oligosaccharides trigger immune responses in Arabidopsis. Plant J. 93:34–49

Miyata, K., Kozaki, T., Kouzai, Y., Ozawa, K., Ishii, K., Asamizu, E., Okabe, Y., Umehara, Y., Miyamoto, A., Kobae, Y., Akiyama, K., Kaku, H., Nishizawa, Y., Shibuya, N., and Nakagawa, T. 2014. The bifunctional plant receptor, OsCERK1, regulates both chitin-triggered immunity and arbuscular mycorrhizal symbiosis in rice. Plant Cell Physiol. 55:1864–1872

Mukherjee, A., and Ané, J.-M. 2011. Germinating Spore Exudates from Arbuscular Mycorrhizal Fungi: Molecular and Developmental Responses in Plants and Their Regulation by Ethylene. Mol. Plant-Microbe Interact. 24:260–270

Nars, A., Rey, T., Lafitte, C., Vergnes, S., Amatya, S., Jacquet, C., Dumas, B., Thibaudeau, C., Heux, L., Bottin, A., and Fliegmann, J. 2013. An experimental system to study responses of *Medicago truncatula* roots to chitin oligomers of high degree of polymerization and other microbial elicitors. Plant Cell Rep. 32:489–502

Ohnuma, T., Onaga, S., Murata, K., Taira, T., and Katoh, E. 2008. LysM domains from Pteris ryukyuensis chitinase-A: A stability study and characterization of the chitin-binding site. J. Biol. Chem. 283:5178–5187

Ohnuma, T., Taira, T., Umemoto, N., Kitaoku, Y., Sørlie, M., Numata, T., and Fukamizo, T. 2017. Crystal structure and thermodynamic dissection of chitin oligosaccharide binding to the LysM module of chitinase-A from Pteris ryukyuensis. Biochem. Biophys. Res. Commun. 494:736–741

Onaga, S., and Taira, T. 2008. A new type of plant chitinase containing LysM domains from a fern (Pteris ryukyuensis): roles of LysM domains in chitin binding and antifungal activity. Glycobiology. 18:414–23

Op Den Camp, R., Streng, A., De Mita, S., Cao, Q., Polone, E., Liu, W., Ammiraju, J. S. S., Kudrna, D., Wing, R., Untergasser, A., Bisseling, T., and Geurts, R. 2011. LysM-type mycorrhizal receptor recruited for rhizobium symbiosis in nonlegume Parasponia. Science (80-.). 331:909–912

Pan, H., and Wang, D. 2017. Nodule cysteine-rich peptides maintain a working balance during nitrogen-fixing symbiosis. Nat. Plants. 3:17048

Park, H., Floss, D. S., Levesque-Tremblay, V., Bravo, A., and Harrison, M. J. 2015. Hyphal branching during arbuscule development requires RAM1. Plant Physiol. 169:2774–2788

Petersen, T. N., Brunak, S., von Heijne, G., and Nielsen, H. 2011. SignalP 4.0: Discriminating signal peptides from transmembrane regions. Nat. Methods. 8:785–786

Pimprikar, P., Carbonnel, S., Paries, M., Katzer, K., Klingl, V., Bohmer, M. J., Karl, L., Floss, D. S., Harrison, M. J., Parniske, M., and Gutjahr, C. 2016. A CCaMK-CYCLOPS-DELLA complex activates transcription of RAM1 to regulate arbuscule branching. Curr. Biol. 26:987–998

Pumplin, N., and Harrison, M. J. 2009. Live-cell imaging reveals periarbuscular membrane domains and organelle location in *Medicago truncatula* roots during arbuscular mycorrhizal symbiosis. Plant Physiol. 151:809–819

Pumplin, N., Mondo, S. J., Topp, S., Starker, C. G., Gantt, J. S., and Harrison, M. J. 2010. *Medicago truncatula* Vapyrin is a novel protein required for arbuscular mycorrhizal symbiosis. Plant J. 61:482–494

Pumplin, N., Zhang, X., Noar, R. D., and Harrison, M. J. 2012. Polar localization of a symbiosis-speci fi c phosphate transporter is mediated by a transient reorientation of secretion. PNAS. 109:E665–E672

Puppo, A., Pauly, N., Boscari, A., Mandon, K., and Brouquisse, R. 2013. Hydrogen peroxide and nitric oxide: key regulators of the Legume-Rhizobium and mycorrhizal symbioses. Antioxid. Redox Signal. 18:2202–19

Remy, W., Taylor, T. N., Hass, H., and Kerp, H. 1994. Four hundred-million-year-old vesicular arbuscular mycorrhizae. PNAS. 91:11841–11843

Ribeiro, C. W., Baldacci-Cresp, F., Pierre, O., Larousse, M., Benyamina, S., Lambert, A., Hopkins, J., Castella, C., Cazareth, J., Alloing, G., Boncompagni, E., Couturier, J., Mergaert, P., Gamas, P., Rouhier, N., Montrichard, F., and Frendo, P. 2017. Regulation of Differentiation of Nitrogen-Fixing Bacteria by Microsymbiont Targeting of Plant Thioredoxin s1. Curr. Biol. 27:250–256

Rich, M. K., Schorderet, M., Bapaume, L., Falquet, L., Morel, P., Vandenbussche, M., and Reinhardt, D. 2015. The Petunia GRAS Transcription Factor ATA/RAM1 Regulates

Symbiotic Gene Expression and Fungal Morphogenesis in Arbuscular Mycorrhiza. Plant Physiol. 168:788–797

Sánchez-Vallet, A., Mesters, J. R., and Thomma, B. P. H. J. 2015. The battle for chitin recognition in plant-microbe interactions. FEMS Microbiol. Rev. 39:171–183

Shabab, M., Arnold, M. F. F., Penterman, J., Wommack, A. J., Bocker, H. T., Price, P. A., Griffitts, J. S., Nolan, E. M., and Walker, G. C. 2016. Disulfide cross-linking influences symbiotic activities of nodule peptide NCR247. Proc. Natl. Acad. Sci. 113:10157–10162

Shibuya, N., Ebisu, N., Kamada, Y., Kaku, H., Conn, J., and Ito, Y. 1996. Localization and binding characteristics of a high-affinity binding site for *N*-acetylchitooligosaccharide elicitor in the plasma membrane from suspension-cultured rice cells suggest a role as a receptor for the elicitor signal at the cell surface. Plant Cell Physiol. 37:894–898

Smith, S., and Read, D. 2008. *Mycorrhizal Symbiosis*.

Tang, H., Krishnakumar, V., Bidwell, S., Rosen, B., Chan, A., Zhou, S., Gentzbittel, L., Childs, K. L., Yandell, M., Gundlach, H., Mayer, K. F. X., Schwartz, D. C., and Town, C. D. 2014. An improved genome release (version Mt4.0) for the model legume Medicago truncatula. BMC Genomics. 15:1–14

Vemanna, R. S., Chandrashekar, B. K., Hanumantha Rao, H. M., Sathyanarayanagupta, S. K., Sarangi, K. S., Nataraja, K. N., and Udayakumar, M. 2013. A modified multisite gateway cloning strategy for consolidation of genes in plants. Mol. Biotechnol. 53:129–138

Voinnet, O., Rivas, S., Mestre, P., and Baulcombe, D. 2003. An enhanced transient expression system in plants based on suppression of gene silencing by the p19 protein of tomato bushy stunt virus. Plant J. 33:949–956

Wan, J., Tanaka, K., Zhang, X.-C., Son, G. H., Brechenmacher, L., Nguyen, T. H. N., and Stacey, G. 2012. LYK4, a Lysin Motif Receptor-Like Kinase, Is Important for Chitin Signaling and Plant Innate Immunity in Arabidopsis. PLANT Physiol. 160:396–406

Wang, B., and Qiu, Y.-L. 2006. Phylogenetic distribution and evolution of mycorrhizas in land plants. Mycorrhiza. 16:299–363

Willmann, R., Lajunen, H. M., Erbs, G., Newman, M., Kolb, D., Tsuda, K., Katagiri, F., Fliegmann, J., Bono, J. J., Cullimore, J. V., Jehle, A. K., Götz, F., Kulik, A., Molinaro, A., Lipka, V., Gust, A. A., and Nürnberger, T. 2011. *Arabidopsis* lysin-motif proteins LYM1 LYM3 CERK1 mediate bacterial peptidoglycan sensing and immunity to bacterial infection. PNAS. 108:19824–19829

Xu, J., Wang, G., Wang, J., Li, Y., Tian, L., Wang, X., and Guo, W. 2017. The lysin motif-containing proteins, Lyp1, Lyk7 and LysMe3, play important roles in chitin perception and defense against Verticillium dahliae in cotton. BMC Plant Biol. 17:1–18

Zhang, Q., Blaylock, L. a, and Harrison, M. J. 2010. Two Medicago truncatula half-ABC transporters are essential for arbuscule development in arbuscular mycorrhizal symbiosis. Plant Cell. 22:1483–97

Zhang, X.-C., Cannon, S. B., and Stacey, G. 2009. Evolutionary genomics of LysM genes in land plants. BMC Evol. Biol. 9:183

Zhu, Q., Zhang, X.-L., Nadir, S., DongChen, W.-H., Guo, X.-Q., Zhang, H.-X., Li, C.-Y., Chen, L.-J., and Lee, D.-S. 2017. A LysM Domain-Containing Gene OsEMSA1 Involved in Embryo sac Development in Rice (Oryza sativa L.). Front. Plant Sci. 8:1–13

Zipfel, C., and Oldroyd, G. E. D. 2017. Plant signalling in symbiosis and immunity. Nature. 543:328–336

CHAPTER 5

A SHORT CHITIN-BINDING PROTEIN WITH HIGH MOLECULAR DIVERSITY FROM AN ARBUSCULAR MYCORRHIZAL FUNGUS, *RHIZOPHAGUS IRREGULARIS*[10]

Abstract

Arbuscular mycorrhizal (AM) fungi form an intimate symbiosis with roots of more than 80% of land plants without eliciting a significant defense response, and how they do so is yet to be determined. Typically, plants mount a defense response upon sensing chitin in fungal walls, and to counteract this response, plant-pathogenic fungi secrete small effector proteins with chitin-binding LysM domains. In the AM fungus, *Rhizophagus irregularis*, a small, putatively-secreted LysM protein, which we refer to as RiSLM, is among the most highly expressed effector-like proteins during symbiosis. Here, we show that *RiSLM* expression is reduced during non-functional symbiosis with *Medicago* mutants, *mtpt4-2* and *vapyrin*. We demonstrate that RiSLM can bind to both chitin and chitosan, and we model the protein-ligand interaction to identify possible binding sites. Finally, we have identified *RiSLM* homologs in five published *R. irregularis* isolate genomes and demonstrate that the gene is subject to a high rate of evolution and is experiencing positive selection, while still conserving putative function. Our results present important clues for elucidating a role for a LysM effector, RiSLM, in AM symbiosis.

[10] This chapter has been conditionally accepted by the journal, Mycoscience as Schmitz, AM, Pawlowska, TE, and Harrison, MJ. A short chitin-binding protein with high molecular diversity from an arbuscular mycorrhizal fungus, *Rhizophagus irregularis*.

Introduction

Plants have evolved mechanisms to recognize potential pathogens via perception of pathogen-associated molecular patterns (Jones and Dangl, 2006). During plant-fungal interactions, chitin fragments are released from the fungal wall and interact with receptors in the plant cell membrane. This interaction triggers an antagonistic response in the plant cell, preventing ingress of the fungal pathogen (Boller and Felix, 2009), which can be overcome in certain cases when the fungus is able to inhibit or evade recognition.

Arbuscular mycorrhizal (AM) fungi (subphylum Glomeromycotina) associate with the roots of over 80% of land plants in mutually-beneficial symbioses. Despite the presence of chitin in their cell walls, these fungi are able to maintain close proximity with plant cell membranes throughout their life cycle. Only a small and quickly attenuated defense-like response has been observed when AM fungi first come into contact with a host plant root (Harrison and Dixon, 1993; Kapulnik et al., 1996; Liu et al., 2003; Giovannetti et al., 2015). During symbiosis, the fungus develops branched hyphae, called arbuscules, that may fill root cortical cells when mature. Arbuscules are surrounded by plant cell membrane and interfacial wall-like matrix; the latter is thin around hyphae of a mature arbuscule, exposing chitin and other fungal molecular patterns prevalent at the interface (Balestrini and Bonfante, 2014; Bonfante-Fasolo et al., 1990). The arbuscule life span is shorter than that of the root cell, and after several days the arbuscule degenerates, leaving the root cell intact (Bonfante-Fasolo, 1984; Pumplin and Harrison, 2009). How it is that AM fungal chitin can come into such close contact with the plant membrane during arbuscule formation, maintenance and degradation and not trigger a defense response is yet unknown.

The major chitin-receptors in plants interact with chitin fragments via an extracellular region with three lysin-motif (LysM) domains (Shinya et al., 2012). Upon ligand binding, the receptors dimerize or interact with co-receptors to relay the signal via an internal kinase (Willmann and Nürnberger, 2012). Many plant-pathogenic fungi inhibit this interaction

through secretion of effector proteins that contain one or multiple LysM domains, which facilitate chitin binding (Sánchez-Vallet et al., 2014). Slp1 from *Magnaporthe oryzae* and ECP6 from *Cladisporium fulvum* can both bind chitin in a manner that outcompetes plant chitin-receptors and inhibits host defenses (Mentlak et al., 2012; de Jonge et al., 2010). Structural analyses of ECP6 revealed two chitin-binding sites, one of which may facilitate inter-chain dimerization, or perhaps interaction with plant chitin-receptors, preventing the necessary dimerization for signal transduction (Sánchez-Vallet et al., 2013).

Several LysM effectors from pathogenic fungi have been characterized, revealing diversity in function and number of LysM domains (Akcapinar et al., 2015). Mg3LysM and Mg1LysM from *Zymoseptoria tritici* are strongly upregulated during infection of wheat, but only Mg3LysM is able to subvert host defenses, and Mg1LysM, with only one LysM, is dispensable for virulence (Marshall et al., 2011; Lee et al., 2014). LysM domains from both effectors show evidence of positive selection, indicating they may be under evolutionary pressure from the plant (Marshall et al., 2011). Two-LysM proteins ChELP1 and ChELP2 from the hemibiotroph *Colletotrichum higginsianum* are highly upregulated during the biotrophic phase of infection, bind strongly and specifically to chitin in fungal walls and are necessary for anthracnose on *Arabidopsis thaliana* (Takahara et al., 2016). ChELP1 and ChELP2 can inhibit the plant's chitin response; however, they also play a developmental role in the fungus' lifecycle, as *chelp1/2* RNAi mutant spores displayed morphological abnormalities during germination, and appressoria did not penetrate cellophane membrane (Takahara et al., 2016).

A role in fungal development has also been identified for the seven-LysM effector TAL6 from the plant-beneficial fungus, *Trichoderma atroviride,* which inhibits germination of spores from *Trichoderma* spp. but not of other fungi (Seidl-Seiboth et al., 2013). Furthermore, TAL6 can bind to chitosan in addition to chitin, which has not been shown for other LysM effectors, and indicates diversity in ligand targets for this type of fungal protein.

TAL6 was the first LysM effector characterized from a fungus that is not a plant pathogen, but many putative effectors have been identified for other plant-biotrophic fungi through genome sequencing (de Jonge and Thomma 2009). The endophytic mutualistic root symbiont, *Piriformospora indica*, expresses eleven proteins comprised only of LysM domains, many of which are predicted to be secreted, although none has yet been characterized (Zuccaro et al., 2011). The AM fungus, *Rhizophagus irregularis*, expresses a small (81 amino acids) putatively-secreted LysM protein (Protein ID 348911), which we refer to here as RiSLM. Many studies have demonstrated high expression of *RiSLM* in mycorrhizal roots, including in both arbuscules and intraradical mycelium, and low expression in spores (Tisserant et al., 2013; Tsuzuki et al., 2016; Sugimura and Saito, 2017; Zeng et al., 2018). Tsusuki et al., (2016) reported high expression of *RiSLM* at four and six weeks post-inoculation relative to non-symbiotic germinating spores, but showed the gene is upregulated in spores in response to treatment with strigolactones, plant hormones that induce branching of AM fungal hyphae and upregulate fungal metabolism and growth (Akiyama et al., 2005; Besserer et al., 2008). In mycorrhizal roots of *Lotus japonicus*, *RiSLM* expression is strongly downregulated by high levels of inorganic phosphate, which has been well demonstrated to inhibit formation of AM (Kobae et al., 2016; Sugimura and Saito, 2017).

Considering the high expression of *RiSLM* in mycorrhizal roots, and upregulation of the gene under conditions that promote symbiosis, we predict an important role for RiSLM during symbiosis. In this report, we investigate such a potential role by quantifying *RiSLM* expression in non-functional symbiosis mutants of *Medicago truncatula* and testing RiSLM ligand-binding capabilities. Genomes of five additional *R. irregularis* isolates, A1, A4, A5, B3, and C2, have been published (Chen et al., 2018), allowing us to investigate the evolutionary history of *RiSLM* by comparing nucleotide and protein sequences of homologs in the fungal isolates. Our results present important clues for elucidating the role of this candidate LysM effector in AM symbiosis.

Materials and Methods

Expression analysis of AM-colonized Medicago truncatula

M. truncatula A17 and symbiosis mutants were grown and inoculated as previously reported (Floss et al., 2017), with approximately 500 spores of *R. irregularis* (DAOM197198) harvested from *Daucus carotus-R. irregularis* cultures (Becárd and Fortin, 1988). For *M. truncatula* non-functional symbiosis mutants we used *mtpt4-2* and *vapyrin*, which are enriched in degenerating arbuscules and completely lack arbuscules, respectively (Javot et al., 2007; Pumplin et al., 2010). Roots were harvested at 5 wk post-planting (about 4 wk post-inoculation), based on previous reports demonstrating high *RiSLM* expression at this timepoint (Tsusuki et al., 2016). RNA isolation and quantitative PCR were carried out as previously described (Javot et al., 2011). Primers used for RT-PCR and cloning are listed in Appendix 5-1.

Chitin-binding assay

Constructs for the expression of RiSLM-FLAG, AtCERKecto-FLAG and MtLysM-FLAG under the double CaMV35S promoter were made using Multisite Gateway technology (Thermo Fisher Scientific), involving three fragment LR recombination with the destination vector pKm43GW (Karimi et al., 2005). The double CaMV35S was amplified from an available construct and cloned into pDONR4-1 via BP recombination. *RiSLM* was amplified from *R. irregularis* genomic DNA, and *AtCERKecto* and *MtLysM* were amplified from plasmids. FLAG was added to all sequences via PCR, and the resulting constructs were cloned into pDONR221 via BP recombination. The CaMV35S terminator was amplified from a plasmid and cloned into pDONR2-3 via BP recombination. All three resulting pENTR constructs, including only one pENTR221 at a time, were then used to create the final plant expression vectors.

Each vector was transformed into *Agrobacterium tumefaciens* strain GV3101, and then infiltrated into 3–4 week old *Nicotiana benthamiana*, grown at 25 °C 16 h/8 h light/dark. The infiltrations were all done at a final OD_{600} of 0.1 in induction buffer (10 mM MES, 10 mM $MgCl_2$, 100 μM acetosyringone, pH 5.6), and each vector was coinfiltrated with the p19 silencing suppression plasmid at a final OD_{600} of 0.8. Each construct was infiltrated into three leaves which were harvested approximately 48 h post-infiltration and frozen at -80 °C. Whole protein was extracted from ground leaf material with extraction buffer (150 mM Tris-HCl, pH 7.5, 150 mM NaCl, 10% glycerol, 10 mM EDTA, 10 mM DTT, 0.5% (wt/v) polyvinylpolypyrrolidone, 0.1% Triton-X, protease cocktail inhibitor (Sigma-Aldrich)) at a ratio of 2.5 mL per gram of tissue, centrifuged at 16,000g in the cold for 2× 15 min.

Except when otherwise stated, chitin binding was determined by adding 100 μL whole protein extract to 20 μL magnetic chitin bead slurry (New England Biolabs) prewashed 5 times with 1 mL cold binding buffer (500 mM NaCl, 20 mM Tris-HCl, 1 mM EDTA, 0.05% Triton X-100, pH 8.0). Beads and extract were allowed to mix for 30 min at 4 °C, and unbound supernatant was collected for analysis. Beads were then washed 5 times with cold binding buffer. Bound protein was eluted with 50 μL 2X SDS-PAGE loading buffer (100 mM Tris-Cl pH 6.8, 4% (w/v) SDS, 0.2% (w/v) bromophenol blue, 20% (v/v) glycerol, 200 mM β-mercaptoethanol).

Ligand precipitation assays were done by adding 250 μL of binding buffer with 5 mg/mL shrimp shell chitin or chitosan (Sigma-Aldrich) to 300 μL of protein extract and mixing at 4°C for 3 h. Unbound supernatant was removed for analysis, and ligand precipitate was rinsed five times with binding buffer. Samples were centrifuged at 16,000 g for 5 min at 4 °C before removing each supernatant. Ligand competition with chitin beads was done by mixing 100 μL protein extract with 200 μL binding buffer alone, 10 mg/mL free chitin, or 10 mg/mL free chitosan and mixing for 30 min at 4 °C prior to adding to beads. Elution assays were done by mixing 200 μL binding buffer alone, or 10 mg/mL free shrimp shell chitin or

free chitosan in binding buffer with washed beads, allowed to mix for 30 min at 4 °C before collecting eluted supernatant.

All samples were separated by 12% SDS-PAGE gels and transferred to PVDF membrane. Blotted membranes were blocked with 5% milk powder and 0.1% Tween-20 in PBS for 30 min, incubated in the same solution plus rabbit anti-FLAG primary antibody for at least 4 h, rinsed 3× with 0.1% Tween-20 in PBS, and incubated with anti-rabbit secondary antibody conjugated to horseradish peroxidase for 1 h. FLAG-tagged protein was detected with the addition of HRP substrate (EMD Millipore) for 5 min, and film exposure. All binding assays were done at least three times with similar results.

Protein modelling

Signal peptides were predicted with both SignalP and PrediSi online programs (http://www.cbs.dtu.dk/services/SignalP/, Petersen et al., 2011; http://www.predisi.de/, Hiller et al., 2004). Identification of LysM domains was done with the ScanProsite web server (https://prosite.expasy.org/scanprosite/, de Castro et al., 2006). Protein structure and binding was predicted through the COACH program for protein-ligand binding site prediction (Yang, Roy and Zhang, 2013a, b). The amino acid sequence of RiSLM, without the signal peptide, was entered into their online interface at https://zhanglab.ccmb.med.umich.edu/COACH/. COACH uses I-TASSER (Yang et al., 2014) to first predict protein structure, which is then submitted for ligand-binding predictions. Molecular graphics and analyses were performed with the UCSF Chimera package. Chimera is developed by the Resource for Biocomputing, Visualization, and Informatics at the University of California, San Francisco (supported by NIGMS P41-GM103311) (Pettersen et al., 2004; https://www.cgl.ucsf.edu/chimera/).

Sequence alignments and phylogenetic reconstruction

Protein sequences were aligned in Jalview with the MUSCLE alignment web service

using default parameters (Katoh et al., 2002; Edgar, 2004; Waterhouse et al., 2009). Bacterial and non-AM fungal groups of sequences were each aligned to the RiSLM sequences separately, and then the two alignments were merged through manual alignment. Phylogenetic reconstruction was done with MrBayes 3.2.2 on XSEDE through the CIPRES Science Gateway (Ronquist et al., 2012; Towns et al., 2014; Miller et al., 2010) using the WAG substitution model. Other parameters included 2 runs with 4 chains, 2 million generations, sampling every 250, with a burn-in of 5000 samples (25%). Trees were formatted using FigTree version 1.4.0 (http://tree.bio.ed.ac.uk/software/figtree/).

Evolutionary Analyses

A codon-based alignment was done for all *RiSLM* using MEGA7 (Kumar, Stecher, and Tamura, 2016). Nucleotide diversity (π) was calculated using the DNA polymorphism calculation in DnaSP version 5.10.01 (Librado and Rozas, 2009). GARD (Genetic Algorithm for Recombination Detection; Kosakovsky Pond et al., 2006) and BUSTED (Branch-site Unrestricted Statistical Test for Episodic Diversification; Murrell et al., 2015) were both run on the DataMonkey online server (http://datamonkey.org/). GARD was run using the beta-gamma site-to-site rate variation and 2 rate classes. For BUSTED, all branches were selected for analysis.

Results

RiSLM expression is reduced during non-functional symbiosis

To investigate the effect of non-functional symbiosis condition on the expression of *RiSLM*, we measured its transcript levels in wild type *M. truncatula* A17 and two AM-related mutants, *mtpt4-2* and *vapyrin* colonized by *R. irregularis* DAOM197198. *MtPT4* encodes a symbiosis-specific phosphate transporter, and in *mtpt4* mutants, arbuscules degenerate prematurely, leading to an over-representation of degenerating arbuscules and host transcripts associated with degeneration (Harrison et al., 2002; Javot et al., 2007; Floss et al., 2017). *Vapyrin* encodes an AM-specific cytoplasmic protein predicted to play a role in cellular remodeling. In *vapyrin* roots, AM fungi are unable to form arbuscules, and infections show proliferating lattice-like runner hyphae (Pumplin et al., 2010). Genes specific to arbuscule function are not expressed in AMF-colonized *vapyrin* roots.

Mycorrhizal roots of both *mtpt4-2* and *vapyrin* had much lower *R. irregularis* colonization than A17, as evidenced by their lower levels of *R. irregularis* alpha tubulin transcripts, a common marker for fungal colonization (Figure 5-1A). As expected, *MtPT4* transcripts were not detected in mycorrhizal *vapyrin* roots (data not shown), demonstrating a lack of arbuscules. When normalized to *R. irregularis α-tubulin* transcripts, which accounts for differences in *R. irregularis* colonization between the genotypes (Isayenkov, Fester and Hause, 2004), *RiSLM* transcripts were significantly lower in both mutants relative to wild type *Medicago* (Figure 5-1B). To control for the possibility of a general effect on symbiosis-related fungal genes, we quantified *RiMST2* transcripts, which were not decreased relative to *R. irregularis α-tubulin*, and in fact slightly higher (Figure 5-1C).

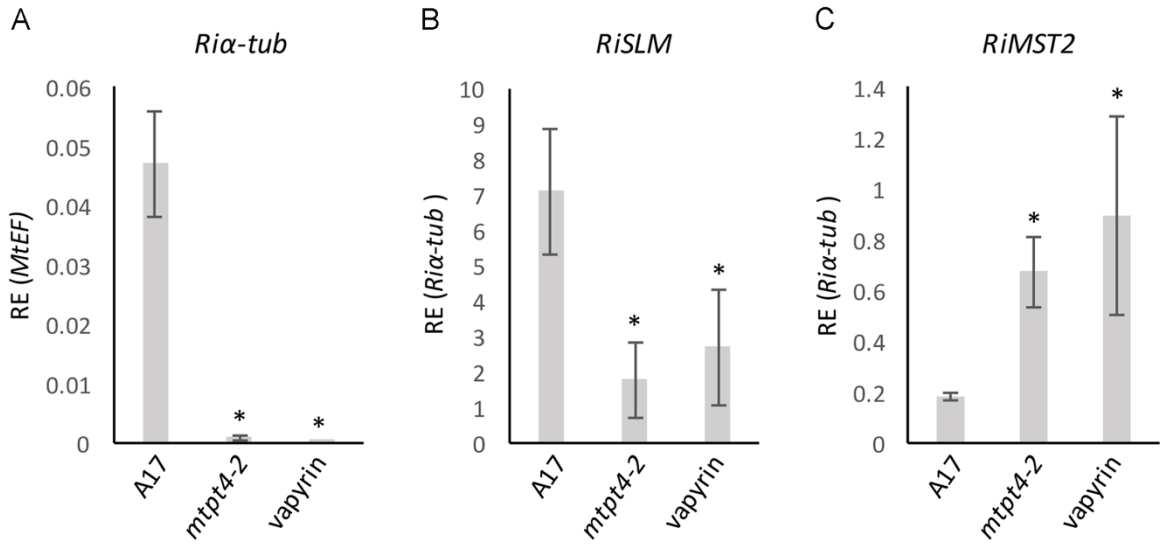

Figure 5-1: Quantitative RT PCR showing relative transcript levels in *Medicago truncatula* wild type (A17), *mtpt4-2*, and *vapyrin* roots colonized with *Rhizophagus irregularis*. (A) *R. irregularis α-tubulin* (*Riα-tub*) transcripts relative to *M. truncatula elongation factor* (*MtEF*). **(B)** *RiSLM* transcripts relative to *Riα-tub*. C: *RiMST2* transcripts relative to *Riα-tub*. * = $p < 0.05$, Student's t-test compared to A17

RiSLM is a cysteine-rich putatively secreted protein that can bind chitin and chitosan.

RiSLM encodes a protein of 81 amino acids with a signal peptide of 22 amino acids. We identified a single LysM domain spanning 46 of the remaining 59 amino acids in the putatively-secreted portion. The predicted mature sequence contains 4 cysteine residues, 6.8% of amino acids, making it a cysteine-rich protein (Marshall, Costa, and Gutierrez-Marcos, 2011). Prediction of RiSLM's three-dimensional structure revealed a potential disulfide interaction based on the alignment of the middle two cysteines and confirmed the canonical βααβ secondary structure of the LysM domain (Appendix 5-2).

To test the hypothesis that RiSLM binds chitin, we produced FLAG-tagged RiSLM in *Nicotiana benthamiana* leaves and evaluated binding of the RiSLM to magnetic chitin beads. We used a FLAG-tagged ectodomain of AtCERK1, which contains three LysM domains and has been demonstrated to bind chitin (Liu et al., 2012), as a positive control for binding. Additionally, we included a FLAG-tagged *M. truncatula* LysM domain-containing protein in the assay, as preliminary studies suggested that it did not bind chitin and therefore served as a useful negative control. Both the CERK ectodomain and RiSLM bound to the chitin beads (Figure 5-2A). To determine if RiSLM binds chitosan, we mixed the protein with free chitosan, which is insoluble in aqueous solution and can be precipitated through centrifugation. A similar assay with free chitin was used as a positive control. With both ligands, RiSLM remained completely bound to the precipitated chitin or chitosan, leaving no free protein in the supernatant. In contrast the *Medicago* LysM protein was not precipitated with either ligand (Figure 5-2B). In the chitin-bead pull-down, RiSLM was not detected in the unbound fraction (Figure 5-2C). Mixing the input protein with chitosan or chitin resulted in detection of RiSLM retained in unbound supernatant, but to a much greater extent after premixing with free chitin than chitosan (Fig 5-2C). We further tested the ability of both chitin and chitosan to elute bound RiSLM from chitin beads, but only free chitin was able to remove a detectable amount (Figure 5-2D).

Figure 5-2 (below): Chitin and chitosan-binding by RiSLM and protein alignment. Western blots showing **(A)** binding of AtCERK1 ectodomain (AtCERKecto) and RiSLM to chitin beads. Left panel shows input protein for FLAG(fl)-conjugated AtCERKecto, RiSLM, and a small LysM from *Medicago truncatula* (MtLM) as a negative control for binding. Right panel shows proteins bound to chitin beads. **(B)** Ligand precipitation assays showing RiSLM binds to free chitin (left) and chitosan (right). RiSLM-fl is only detected in the bound (B) fractions, while MtLM-fl is only detected in the unbound (UB) fractions. **(C)** Competition assay with buffer, free chitosan and free chitin vs. chitin beads. Premixing RiSLM with chitin, and to a lesser degree chitosan, leads to retention of the protein in the unbound fraction. **(D)** Elution of bound RiSLM from chitin beads with buffer, chitin or chitosan. Only chitin can displace the protein from the chitin beads. R = RiSLM-fl, LC = loading control. All Western blots were probed with anti-FLAG antibodies. Loading controls are endogenous proteins from *Nicotiana benthamiana* protein extract that interact with FLAG antibodies. **(E)** Alignment of RiSLM amino acid sequences from *R. irregularis* isolates. Sites with 100% identity are shaded dark gray. Sites with at least 50% identity are shaded light gray. Lines above indicate putative chitin binding sites. Secondary structure: arrows = beta sheet; helix = alpha helix.

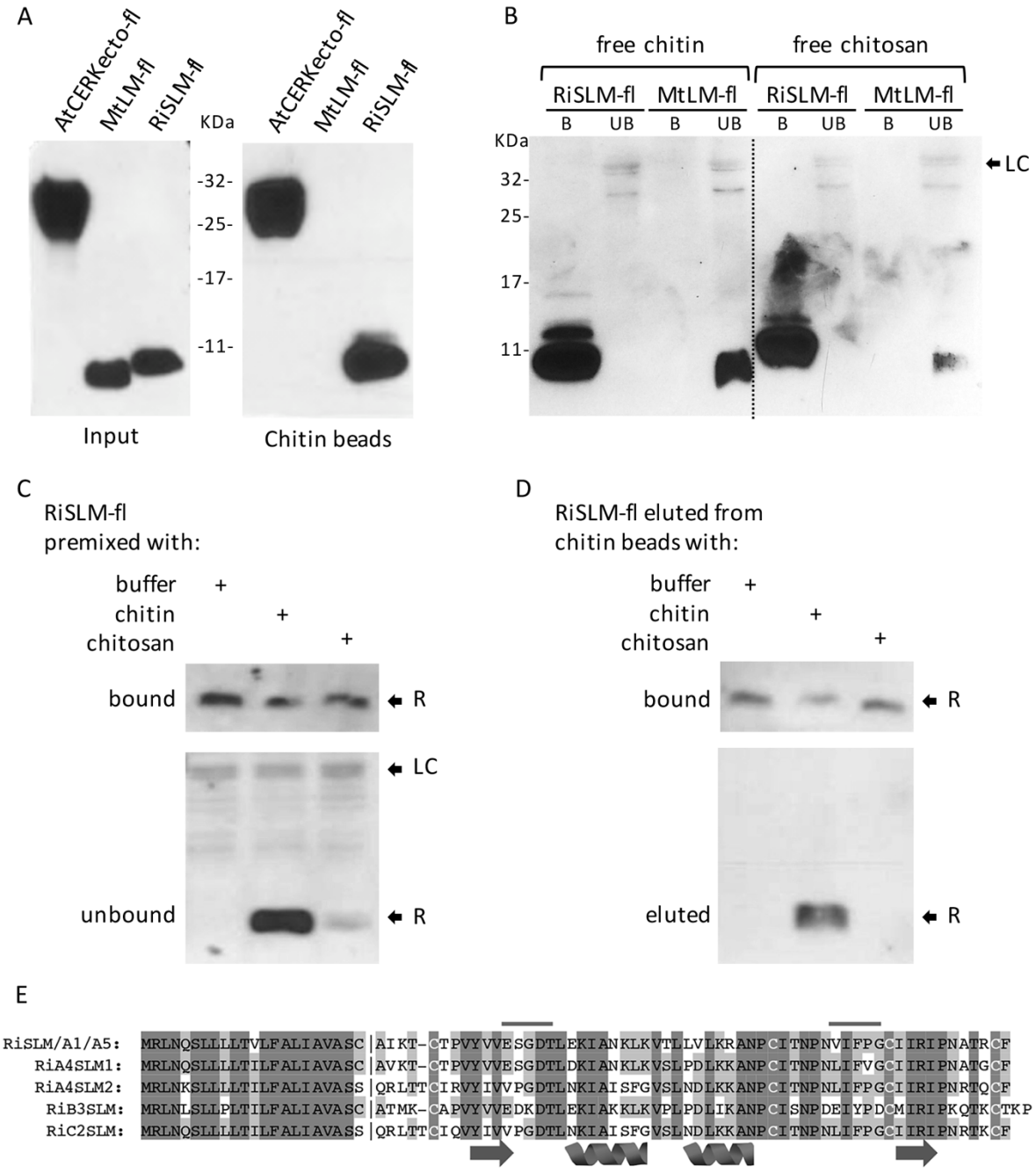
A
AtCERKecto-fl
MtLM-fl
RiSLM-fl
KDa
-32-
-25-
-17-
-11-
Input
Chitin beads
B
free chitin
free chitosan
RiSLM-fl
MtLM-fl
RiSLM-fl
MtLM-fl
B
UB
B
UB
B
UB
B
UB
KDa
32-
25-
17-
11-
LC
C
RiSLM-fl
premixed with:
buffer
chitin
chitosan
+
bound
unbound
R
LC
D
RiSLM-fl eluted from
chitin beads with:
buffer
chitin
chitosan
+
bound
eluted
R
E
RiSLM/A1/A5:
RiA4SLM1:
RiA4SLM2:
RiB3SLM:
RiC2SLM:

Having demonstrated that RiSLM binds chitin we used the COACH ligand prediction server to identify putative chitin-binding sites in the protein (Yang, Roy and Zhang, 2013a, b). The program predicted four potential N-acetyl-glucosamine (the monomer of chitin) interactions. The three most confident interactions align along a hydrophobic groove formed by the two β-α/α-β linker regions, while the fourth interaction is predicted to occur on the opposite side immediately below the aligned cysteines (Appendix 5-2B). COACH further provides the probability that each amino acid participates in ligand binding, which revealed two regions of amino acids likely involved in the interactions (Figure 5-2E; Appendix 5-2C).

RiSLM is present in all sequenced Rhizophagus genomes and is under diversifying selection.

A BLASTP search of the NCBI non-redundant protein database revealed homologs in all five sequenced *R. irregularis* isolates, A1, A4, A5, B3, and C2 (Chen et al., 2018), as well as in *Rhizophagus clarus* (Sędzielewska Toro and Brachmann, 2016). The genome of *R. irregularis* isolate A4 contains two paralogs of *RiSLM*, in tandem and separated by 3.8 kb. No homologs were reported in the published transcriptome of *Gigaspora rosea* (Tang et al., 2016) or *Gigaspora margarita* (Salvioli et al., 2015). Additionally, there are no homologs in the *Glomus versiforme* genome (Sun, Harrison, Fei unpublished data). A BLASTP search excluding Glomeromycotina (NCBI txid:214504) revealed that RiSLM has highest similarity to bacterial proteins, with an average of 47% identity at 75% query coverage, and most of the returned hits were from firmicutes (Appendix 5-3). Considering RiSLM's similarity to bacterial proteins, we hypothesized that the gene was horizontally acquired from a bacterial genome. To test this possibility, we reconstructed a phylogeny with *RiSLM* homologs, the top 20 BLASTP hits from bacteria (NCBI txid:2), the top 20 BLASTP hits from fungi (NCBI txid:4751), and a small LysM from *M. truncatula* as an outgroup. While the *R. irregularis* sequences separated from the *R. clarus* sequence with a posterior probability of 0.91, the placement of the *Rhizophagus* clade as a whole remained unresolved relative to both bacterial

and non-AM fungal sequences (Appendix 5-4). We also considered G+C content as a means for inferring horizontal gene transfer (Ravenhall et al., 2015). The G+C content for RiSLM is 38.7%, which is within the reported normal range for *R. irregularis* (Tisserant et al., 2013).

The aligned RiSLM protein sequences from the *R. irregularis* isolates revealed an average pairwise identity of only 78% (Fig. 2e; Appendix 5-5), which is much lower than previous reports for protein sequences from these isolates (Corradi et al., 2009). The aligned nucleotide sequences have an average pairwise identity of 89% (Appendix 5-5). To test if *RiSLM* is evolving at a faster rate than other genes in the *R. irregularis* genome, we calculated nucleotide diversity (π) for the *RiSLM* sequences, three housekeeping genes (ATPase, EF1-a, and beta tubulin) and three symbiosis genes (PT, MST2, and SOD1) (Nei and Li, 1979). Considering all *RiSLM* sequences, $\pi = 0.1163 \pm 0.027$, which is an order of magnitude higher than all the other genes we measured, for which π ranged from 0.0013 ± 0.0005 (EF1-a) to 0.0106 ± 0.0059 (SOD1) (Appendix 5-6). To test if this elevated rate of nucleotide substitution is a response to diversifying selection, we subjected the *RiSLM* sequences to the Branch-site Unrestricted Statistical Test for Episodic Diversification (BUSTED; Murrell et al., 2015) after ruling out with the Genetic Algorithm for Recombination Detection (GARD; Kosakovsky-Pond et al., 2006) that recombination could confound our results. We found significant gene-wide evidence for episodic diversifying selection ($p<0.000$) acting on *RiSLM*. Despite a high nucleotide substitution rate and diversifying selection, none of the *RiSLM* sequences have any early stop codons, and all were predicted to bind chitin, as modeled by the COACH server.

Discussion

In plant-pathogen interactions, LysM effector genes are highly expressed during fungal infection of the host plant, often during a biotrophic growth phase (El Hadrami et al., 2012; Akcapinar et al., 2015). During symbiosis between the AM fungus *R. irregularis* and several different plants, *RiSLM* is one of the most highly-expressed secreted proteins and is predominantly expressed in intraradical mycelium and arbuscules (Zeng et al., 2018). We have demonstrated that RiSLM can bind to chitin and chitosan, which can both elicit a defense response in plants (Hadwiger, 2013). Chitin is one of the major components of AM fungal walls, and chitosan is likely also a component, as it is present in the walls of AM fungal spores (Bonfante-Fasolo and Gripiollo, 1984), and abundant in the hyphal walls of closely-related Mucoromycota (Bartnicki-Garcia, 1968). By sequestering chitin at the fungal-plant interface, an abundance of RiSLM may provide a mechanism for avoiding recognition of fungal wall fragments by chitin receptors as the hyphal tips grow. This would be similar to several fungal LysM effectors that protect fungal walls from plant chitinases, including TAL6 from *Trichoderma*, which is also the only other LysM effector reported to bind chitosan (Marshall et al., 2011; Seidl-Seiboth et al., 2013). Plant chitinases do not localize to intra- or intercellular AM fungal hyphae (Spanu et al., 1989), possibly due to masking by other cell wall constituents, or fungal proteins like RiSLM. While RiSLM can bind to chitin and chitosan, it may also bind to related molecules, such as short-chain chitin oligomers or lipochitooligosaccharides shown to function in symbiotic signaling (Maillet et al., 2011; Genre et al., 2013). RiSLM binding to these ligands should be tested directly, as well as its interaction with potential ligand receptors (Fliegmann et al., 2013; Malkov et al., 2016), as such interactions would indicate a role for RiSLM in symbiotic signaling.

To reach the inner cortex of wild-type plant roots, such as *Medicago*, a hypha emerging from a hyphopodium will typically penetrate and grow intracellularly through the

epidermis, and possibly through outer cortical cells (Genre, 2008). Once in the inner cortex, while hyphae elongate intercellularly, they enter inner cortical cells to form arbuscules. Intracellular growth exposes the chitin in fungal walls, especially where hyphae penetrate host cells and particularly at the arbuscule interface (Bonfante-Fasolo et al., 1990). In *Medicago* mutants *mtpt4-2* and *vapyrin*, an AM fungus will still grow to and throughout the inner cortex. Colonized roots of *mtpt4-2* are enriched in degenerating arbuscules and transcript of genes associated with the degeneration process, including plant chitinases and other hydrolytic enzymes (Floss et al., 2017). Plant chitinases localize to the degenerated arbuscule clump, where they presumably break down chitin (Spanu et al., 1989; Bonfante-Fasolo et al., 1990). An abundance of RiSLM may provide a mechanism for sequestering free chitin during arbuscule degeneration. However, through qPCR of *mtpt4-2* roots colonized with *R. irregularis*, we found that *RiSLM* transcript levels are lower in these roots relative to those of wild type *Medicago*, indicating that the gene is not upregulated by the fungus during arbuscule degeneration. Arbuscules, including degenerating arbuscules, are overall infrequent in colonized *mtpt4* roots (Javot et al., 2007), and completely absent in colonized *vapyrin* roots (Pumplin et al., 2010). In both mutants we observed a significantly lower level of *RiSLM* transcript, which can be explained by the loss of arbuscule-associated transcription (Zeng et al., 2018). The presence of transcript in the *vapyrin* roots, in which the fungus does not even penetrate cortical cells (Pumplin et al., 2010), indicates that the gene is expressed during the non-arbuscule stages of symbiosis, such as hyphopodium penetration and hyphal elongation.

Recently published genome sequences for several *R. irregularis* isolates have allowed us to investigate the evolutionary history of *RiSLM* (Chen et al., 2018). A comparison of gene sequences from the different isolates revealed that the gene is evolving relatively quickly and experiences diversifying selection. Such positive selection has been observed for other LysM effectors of fungi (Marshall et al., 2011), as well as LysM domains in plant receptors (Lohmann et al., 2010; Sulima et al., 2017), and is characteristic of proteins involved in host-

microbe interactions that may undergo diversification through co-evolution (Raffaele and Kamoun, 2012; Tang et al., 2017). Conservation of function despite a high rate of non-synonymous substitution indicates that a functional RiSLM is necessary for fungal survival. Combined with its very high expression *in planta*, these data point to an important role for the gene during symbiosis; however published transcriptomes from other AM fungal genera do not contain transcripts homologous to *RiSLM* (Salvioli et al., 2015; Tang et al., 2016). Either the gene is not present in their genomes, or it is not expressed highly or at all by the fungi during AM symbiosis. A lack of *RiSLM* homologs in other AM genera would support the hypothesis that the gene was horizontally transferred to a *Rhizophagus* ancestor, which we could neither support nor disprove through phylogenetic reconstruction. Furthermore, although the G+C content of *RiSLM* is within the normal range for *R. irregularis*, many of the similar bacterial sequences are from firmicutes (Appendix 5-3), which typically have low G+C content similar to that of *R. irregularis* (Galperin, 2013; Tisserant et al., 2013), precluding this method for inferring horizontal gene transfer as well.

An important next step for this research will be to survey a variety of AM fungi for *RiSLM* homologs, which will shed light on the question of its origin and specificity. While all AM fungi confer a benefit to their host plant, these benefits vary depending on the fungal species (Verbruggen and Kiers, 2010). If *RiSLM* is specific to the *Rhizophagus* genus, it may be important for *Rhizophagus*-specific benefits, such as better host protection against pathogens (Maherali and Klironimos, 2007; Powell et al., 2009). A comparison of more *RiSLM* sequences would allow for identification of conserved sites, and sites under selection, which will provide clues to the relevant target ligand for this protein. Elucidating the role of RiSLM in AM symbiosis, and comparing this role to that of fungal plant-pathogens will reveal important insights into the ecology and evolution of AM fungi.

APPENDICES

Primer	Sequence	Purpose
qPCR-299	TGTCCAACCGGTTTTAAAGT	qPCR: *R. irregularis α-tubulin* Forward
qPCR-300	AAAGCACGTTTGGCGTACAT	qPCR: *R. irregularis α-tubulin* Reverse
B5394	AAATCGCGAATAAACTTAAGG	qPCR: *RiSLM* Forward
B5395	GGCTATTATTAATTAAAAGCACAGT	qPCR: *RiSLM* Reverse
B1887	GGGATGAAGAAGCAATAACAG	qPCR: *RiMST2* Forward
B1888	AACTCCCAACAACACTCTTC	qPCR: *RiMST2* Reverse
qPCR-820	TGACAGGCGATCTGGTAAGG	qPCR: *M. truncatula elongation factor* Forward
qPCR-821	TCAGCGAAGGTCTCAACCAC	qPCR: *M. truncatula elongation factor* Reverse
B3880	GGGGACAACTTTGTATAGAAAAGTTGTCCCAT ATGGTCGACTAGAGC	Add attB4 to 5' end of double CaMV35S promotor
B3881	GGGGACTGCTTTTTTGTACAAACTTGCGCGGC CGCCTGC	Add attB1 to 3' end of double CaMV35S promotor
B3869	ATGAGACTCAATCAATCTTTGCT	Amplify *RiSLM* (5' forward)
B3868	AAAACATCTAGTAGCATTAGGTATCCG	Amplify *RiSLM* (3' reverse)
B5065	TTTGTCATCGTCGTCCTTGTAGTCAAAACATCT AGTAGCATT	Add FLAG tag to *RiSLM 3'*
B3910	GGGGACAAGTTTGTACAAAAAAGCAGGCTTC ATGAGACTCAATCAATCTTTGC	Add attB1 to 5' end of *RiSLM*
B4352	GGGGACAAGTTTGTACAAAAAAGCAGGCTTC ATGAAGCTAAAGATTTCTCT	Amplify and add attB1 to 5' end of *AtCERK1ecto*
B4952	GTCGTCCTTGTAGTCACCATCTTGTTTACTTGA	Amplify and add FLAG tag to 3' end of *AtCERK1ecto*
B4119	GGGGACAAGTTTGTACAAAAAAGCAGGCTTC ACCATGGCTAAGTCAACTAACATCT	Amplify and add attB1 to 5' end of *MtLysM*
B4764	TCGTCGTCCTTGTAGTCTTTGTCATCGTCGTCC TTGTAGTCATTCACTTCACCTTCAACA	Amplify and add FLAG tag to 3' end of *MtLysM*
B4893	GGGGACCACTTTGTACAAGAAAGCTGGGTTC ATTTGTCATCGTCGTCCTTGTAGTC	Add stop codon and attB2 to 3' of FLAG tag
B3088	GGGGACAGCTTTCTTGTACAAAGTGGAAGCG GCCATGCTAGAGTCC	Add attB2 to 5'end of CaMV35S terminator
B3089	GGGGACAACTTTGTATAATAAAGTTGCGTCAC TGGATTTTGGTTTTAGGA	Add attB3 to 3' end of CaMV35S terminator

Appendix 5-1: Primers used in this study

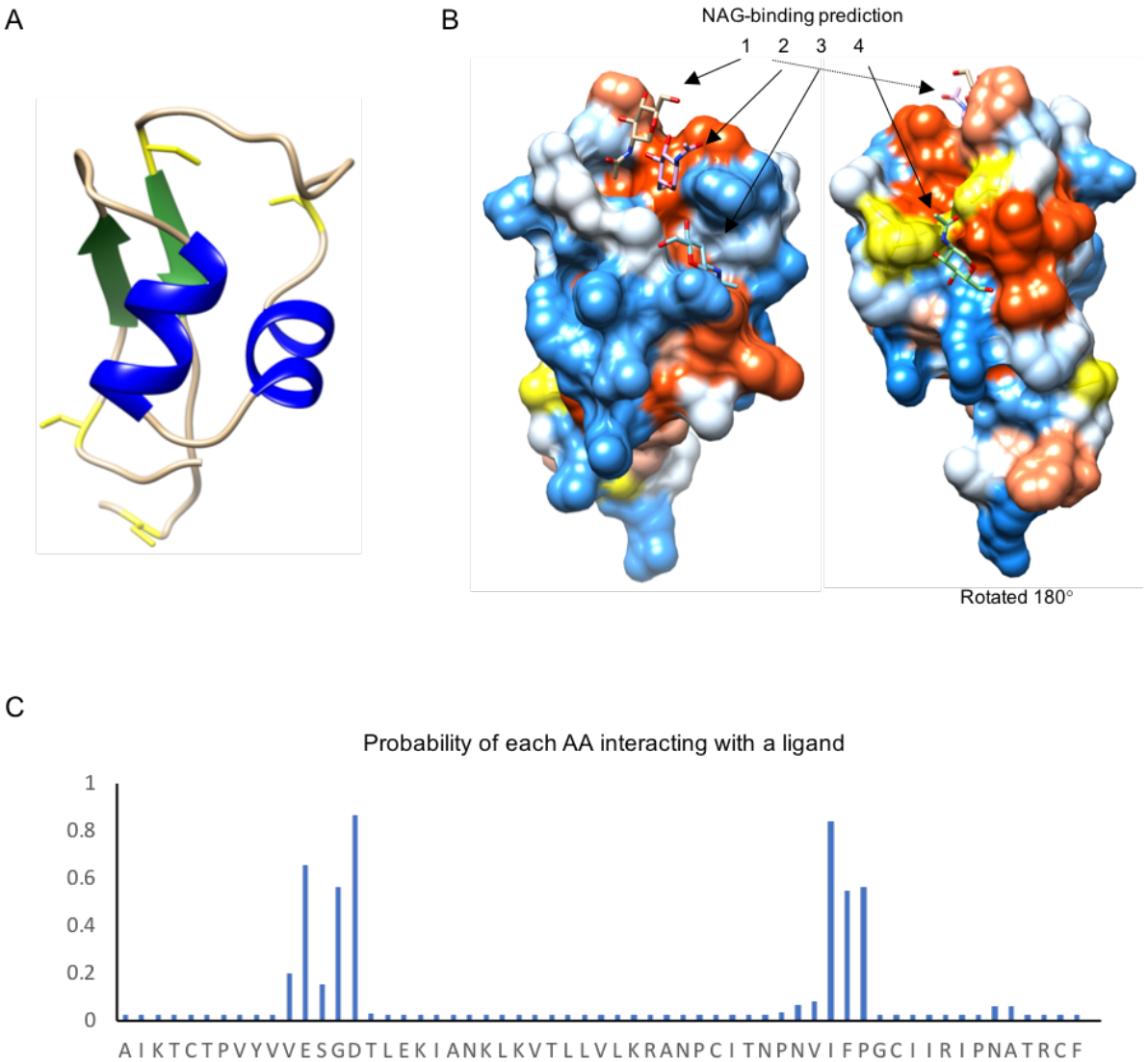

Appendix 5-2: COACH-predicted structure and chitin-binding of RiSLM. A: 3-D model of RiSLM showing secondary structure and cysteine alignment. Blue = alpha helix, green = beta sheet, yellow = cysteine residue B: COACH-predicted 3D structure demonstrating four N-acetyl glucosamine (NAG) ligand interactions. Residue surface color: orange = hydrophobic, white = neutral, blue = hydrophilic, yellow = cysteine residue. C: Graph of ligand-binding probability for each residue in the protein.

Description	Max score	Total score	Query cover	E value	Ident	Accession
LysM domain-containing protein [*Mycobacterium* sp. 1245111.1]	61.6	118	74%	2.00E-10	51%	WP_067331309.1
hypothetical protein BC6307_13240 [*Bacillus cohnii*]	61.6	61.6	77%	1.00E-09	44%	AST92179.1
LysM peptidoglycan-binding domain-containing protein [*Bacillus cohnii*]	61.6	61.6	77%	1.00E-09	44%	WP_084380604.1
LysM peptidoglycan-binding domain-containing protein [*Mycobacterium aquaticum*]	62	223	60%	2.00E-09	57%	WP_083161008.1
LysM peptidoglycan-binding domain-containing protein [*Mycobacterium dioxanotrophicus*]	59.7	220	60%	1.00E-08	60%	WP_087077690.1
LysM peptidoglycan-binding domain-containing protein [*Bacillus* sp. Marseille-P3661]	58.5	58.5	77%	2.00E-08	44%	WP_102347058.1
LysM peptidoglycan-binding domain-containing protein [*Bacillus indicus*]	58.2	58.2	88%	2.00E-08	39%	WP_081414245.1
LysM peptidoglycan-binding domain-containing protein [*Bacillus indicus*]	58.2	58.2	88%	2.00E-08	39%	WP_081870249.1
PREDICTED: uncharacterized protein LOC109043394 [*Bemisia tabaci*]	57.8	57.8	92%	3.00E-08	44%	XP_018916131.1
extracellular protein 6 [*Aureobasidium pullulans* EXF-150]	58.2	93.2	56%	3.00E-08	58%	KEQ84930.1
LysM peptidoglycan-binding domain-containing protein [*Bacillus kochii*]	57.8	57.8	92%	4.00E-08	39%	WP_095373145.1
LysM peptidoglycan-binding domain-containing protein [[*Clostridium*] *clariflavum*]	57.4	57.4	82%	4.00E-08	42%	WP_027621927.1
LysM peptidoglycan-binding domain-containing protein [*Thermoanaerobacter cellulolyticus*]	57.4	57.4	92%	4.00E-08	39%	WP_045166263.1
Uncharacterized protein AUREO_061790 [*Aureobasidium pullulans*]	57.8	57.8	55%	4.00E-08	58%	OBW63755.1
putative uncharacterized protein [*Oscillibacter* sp. CAG:155]	57	57	75%	5.00E-08	49%	CDC73265.1
spore coat assembly protein SafA/uncharacterized protein, YkwD family [*Clostridium caminithermale* DSM 15212]	57.4	57.4	92%	5.00E-08	37%	SHK18116.1
LysM peptidoglycan-binding domain-containing protein [*Bacillus* sp. HMSC76G11]	57	57	88%	6.00E-08	39%	WP_083328334.1
LysM peptidoglycan-binding domain-containing protein [*Dyella marensis*]	58.2	153	59%	6.00E-08	53%	WP_090423576.1
Phage-related lysozyme (muramidase), GH24 family [*Dyella marensis*]	58.2	202	72%	6.00E-08	53%	SFE92576.1
LysM peptidoglycan-binding domain-containing protein [*Pontibacillus chungwhensis*]	57	57	83%	6.00E-08	38%	WP_036786056.1

Appendix 5-3: Top 20 PBLAST hits recovered from the NCBI non-redundant database with the full RiLysM sequence as the query, excluding Glomeromycotina [txid:214504].

Appendix 5-4 (below): Reconstruction of a phylogeny including RiSLM homologs and the 20 most similar proteins from fungi (NCBI txid:4751) and bacteria (NCBI txid:2), as identified by BLASTP. Bacterial sequences are purple, fungal (non-AM) sequences are brown, and the outgroup, *M. truncatula* small LysM is green. Numbers represent posterior probabilities above 0.80.

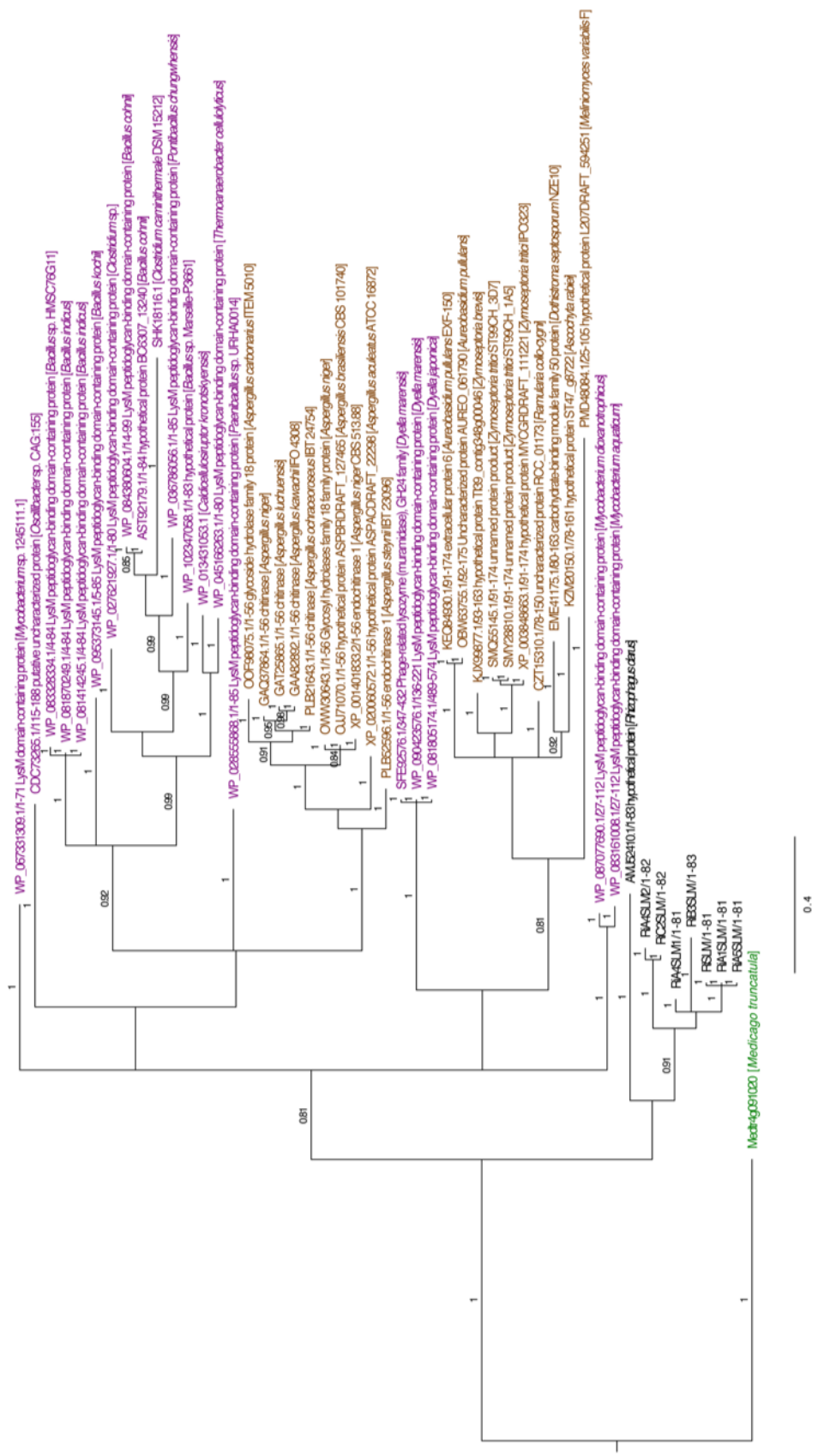
WP_057331309.1/1-71 LysM domain-containing protein [Mycobacterium sp. 1245111.1]
CDC73265.1/115-188 putative uncharacterized protein [Oscillibacter sp. CAG:155]
WP_083283334.1/4-84 LysM peptidoglycan-binding domain-containing protein [Bacillus sp. HMSC76G11]
WP_061870249.1/4-84 LysM peptidoglycan-binding domain-containing protein [Bacillus indicus]
WP_061414245.1/4-84 LysM peptidoglycan-binding domain-containing protein [Bacillus indicus]
WP_095373145.1/5-85 LysM peptidoglycan-binding domain-containing protein [Bacillus koohii]
WP_027821927.1/4-80 LysM peptidoglycan-binding domain-containing protein [Oscillibacter sp.]
WP_084380604.1/14-99 LysM peptidoglycan-binding domain-containing protein [Bacillus cohnii]
AST92179.1/1-84 hypothetical protein BO3317_13240 [Bacillus cohnii]
SHK18116.1 [Oscillibacter camirthermalis DSM 15212]
WP_095786056.1/1-85 LysM peptidoglycan-binding domain-containing protein [Pontibacillus chungwhensis]
WP_102347058.1/1-83 hypothetical protein [Bacillus sp. Marseille-P3661]
WP_013431053.1 [Caldicellulosiruptor kronotskyensis]
WP_045166283.1/1-80 LysM peptidoglycan-binding domain-containing protein [Thermoanaerobacter cellulolyticus]
WP_028553868.1/1-85 LysM peptidoglycan-binding domain-containing protein [Paenibacillus sp. URHA0014]
OOF98075.1/1-56 glycoside hydrolase family 18 protein [Aspergillus carbonarius ITEM 5010]
GAQ37864.1/1-56 chitinase [Aspergillus niger]
GAT25865.1/1-56 chitinase [Aspergillus luchuensis]
GAA92892.1/1-56 chitinase [Aspergillus kawachii IFO 4308]
PLB21643.1/1-56 chitinase [Aspergillus ochraceoroseus IBT 24754]
OWW30643.1/1-56 Glycosyl hydrolases family 18 family protein [Aspergillus niger]
CUJ71070.1/1-56 hypothetical protein ASPBRDRAFT_127465 [Aspergillus brasiliensis CBS 101740]
XP_001401833.2/1-56 endochitinase 1 [Aspergillus niger CBS 513.88]
XP_020060572.1/1-56 hypothetical protein ASPACDRAFT_22256 [Aspergillus aculeatus ATCC 16872]
PLB52566.1/1-56 endochitinase 1 [Aspergillus sitophila IBT 23096]
SFE25276.1/347-432 Phage-related lysozyme (muramidase), GH24 family [Dyella marensis]
WP_090423576.1/136-221 LysM peptidoglycan-binding domain-containing protein [Dyella marensis]
WP_061805174.1/489-574 LysM peptidoglycan-binding domain-containing protein [Dyella japonica]
KEQ84930.1/91-174 extracellular protein 6 [Aureobasidium pullulans EXF-150]
OBW63755.1/92-175 Uncharacterized protein AUREO_061790 [Aureobasidium pullulans]
KJX98977.1/83-163 hypothetical protein TI39_contig348g00046 [Zymoseptoria brevis]
SMQ55145.1/91-174 unnamed protein product [Zymoseptoria tritici ST99CH_3D7]
SMY28810.1/91-174 unnamed protein product [Zymoseptoria tritici ST99CH_1A5]
XP_003849863.1/91-174 hypothetical protein MYCGRDRAFT_111221 [Zymoseptoria tritici IPO323]
CZT15310.1/78-150 uncharacterized protein RCC_01173 [Ramularia collo-cygni]
EME41175.1/80-163 carbohydrate-binding module family 50 protein [Dothistroma septosporum NZE10]
KDN20150.1/78-161 hypothetical protein ST47_g8722 [Aspergillus ruber]
PMD48084.1/25-105 hypothetical protein L207DRAFT_594251 [Melanomyces variabilis F]
WP_087077690.1/27-112 LysM peptidoglycan-binding domain-containing protein [Mycobacterium chlorophenolicum]
WP_083161008.1/27-112 LysM peptidoglycan-binding domain-containing protein [Mycobacterium aquaticum]
AMB24101.1/1-83 hypothetical protein [Phytophthora sojae]
RAASLM2/1-82
RC2SLM1/1-82
RAASLM1/1-81
RBSLM1/1-83
RBSLM1/1-81
RA1SLM1/1-81
RASSLM1/1-81
Medtr4g091020 [Medicago truncatula]
0.4

AA pairwise identities (gray)

	Ri/A1/A5	A4-1	A4-2	B3	C2
Ri/A1/A5SLM	-	70.73	87.65	69.14	71.95
RiA4SLM1	95.53	-	75.61	71.60	76.83
RiA4SLM2	85.43	86.96	-	60.98	96.34
RiB3SLM	84.06	81.82	77.73	-	62.20
RiC2SLM	85.77	86.96	98.39	77.82	-

nucleotide pairwise identities (white)

Appendix 5-5: Pairwise identities of gene (no shading) and protein (gray shading) sequences of RiSLM from all *R. irregularis* isolates.

	Gene	π	st dev
housekeeping	*ATPase*	0.00235	0.00103
	Elongation factor 1-a	0.00127	0.00054
	β-tubulin	0.00142	0.00072
symbiosis	*Phosphate transporter (PT)*	0.00503	0.00168
	Monosaccharide transporter 2 (MST2)	0.00341	0.00116
	Superoxide dismutase 1 (SOD1)	0.01062	0.00585
	RiSLM	0.12278	0.02908

Appendix 5-6: Nucleotide diversity (π) and standard deviation (st dev) for *RiSLM* and various housekeeping- and symbiosis-related genes from all *R. irregularis* isolates.

REFERENCES

Akcapinar, G.B., Kappel, L., Sezerman, O.U., and Seidl-Seiboth, V. (2015). Molecular diversity of LysM carbohydrate-binding motifs in fungi. *Current Genetics*, *61*,102–113. https://dx.doi.org/10.1007%2Fs00294-014-0471-9

Akiyama, K., Matsuzaki, K., and Hayashi, H. (2005). Plant sesquiterpenes induce hyphal branching in arbuscular mycorrhizal fungi. *Nature*, *435*,824–827. https://doi.org/10.1038/nature03608

Balestrini, R., and Bonfante, P. (2014). Cell wall remodeling in mycorrhizal symbiosis: a way towards biotrophism. *Frontiers in Plant Science*, *5*, 237. https://dx.doi.org/10.3389%2Ffpls.2014.00237

Bartnicki-Garcia, S. (1968). Cell wall chemistry, morphogenesis, and taxonomy of fungi. *Annual Review of Microbiology*, *22*, 87–108. https://doi.org/10.1146/annurev.mi.22.100168.000511

Bécard, G., and Fortin, J.A. (1988). Early events of vesicular–arbuscular mycorrhiza formation on Ri T-DNA transformed roots. *New Phytologist*, *108*, 211–218. https://doi.org/10.1111/j.1469-8137.1988.tb03698.x

Besserer, A., Becard, G., Jauneau, A., et al., (2008). GR24, a synthetic analog of strigolactones, stimulates the mitosis and growth of the arbuscular mycorrhizal fungus *Gigaspora rosea* by boosting its energy metabolism. *Plant Physioogyl*, *148*, 402–413. https://doi.org/10.1104/pp.108.121400

Boller, T., and Felix, G. (2009). A Renaissance of Elicitors: Perception of Microbe-Associated Molecular Patterns and Danger Signals by Pattern-Recognition Receptors. *Annual Reviews in Plant Biology*, *60*, 379–406. https://doi.org/10.1146/annurev.arplant.57.032905.105346

Bonfante-Fasolo, P. (1984). Anatomy and morphology of VA mycorrhizae. In *VA Mycorrhizas*. Edited by Powell, C.L. and Bagyaraj, D.J. pp 5–33. CRC Press, Boca Raton, FL, USA.

Bonfante-Fasolo, P. and Grippiolo, R. (1984). Cytochemical and biochemical observations on the cell wall of the spore of *Glomus epigaeum*. *Protoplasma*, *123*, 140–151. https://doi.org/10.1007%2FBF01283584

Bonfante-Fasolo, P., Faccio, A., Perotto, S., and Schubert, A. (1990). Correlation between chitin distribution and cell wall morphology in the mycorrhizal fungus *Glomus versiforme*. *Mycological Research*, *94*, 157–165. https://doi.org/10.1016/S0953-7562(09)80607-2

Chen, E.C.H., Morin, E., Beaudet, D., et al. (2018). High intraspecific genome diversity in the model arbuscular mycorrhizal symbiont *Rhizophagus irregularis*. *New Phytologist* https://doi.org/10.1111/nph.14989 [Epub ahead of print]

Corradi, N., Ruffner, B., Croll, D., Colard, A., Horák, A., and Sanders, I.R. (2009). High-level molecular diversity of copper-zinc superoxide dismutase genes among and within species of arbuscular mycorrhizal fungi. *Applied Environmental Microbiology*, *75*, 1970–1978. https://doi.org/10.1128/AEM.01974-08

de Castro, E., Sigrist, C.J.A., Gattiker, A., et al. (2006). ScanProsite: Detection of PROSITE signature matches and ProRule-associated functional and structural residues in proteins. *Nucleic Acids Research*, *34*, W362–W365. https://doi.org/10.1093/nar/gkl124

de Jonge, R., and Thomma, B.P.H.J. (2009). Fungal LysM effectors: extinguishers of host immunity? *Trends in Microbiology*, *17*, 151–157. https://doi.org/10.1016/j.tim.2009.01.002

de Jonge, R., Van Esse, H.P., Kombrink, A. et al. (2010). Conserved Fungal LysM Effector Ecp6 Prevents Chitin-Triggered Immunity in Plants. *Science*, *329*, 953–955. https://doi.org/10.1126/science.1190859

Edgar, R.C. (2004). MUSCLE: Multiple sequence alignment with high accuracy and high throughput. *Nucleic Acids Research*, *32*, 1792–1797. https://doi.org/10.1093/nar/gkh340

El Hadrami, A., El-Bebany, A.F., Yao, Z., Adam, L.R., El Hadrami, I., and Daayf, F. (2012). Plants versus fungi and oomycetes: Pathogenesis, defense and counter-defense in the proteomics era. *International Journal of Molecular Science*, *13*,7237–7259. https://doi.org/10.3390/ijms13067237

Fliegmann, J., Canova, S., Lachaud, C., et al. (2013). Lipo-chitooligosaccharidic symbiotic signals are recognized by LysM receptor-like kinase LYR3 in the legume *Medicago truncatula*. *ACS Chemical Biology*, *8*, 1900–1906. https://doi.org/10.1021/cb400369u

Floss, D.S., Gomez, S.K., Park, H.J., et al. (2017). A transcriptional program for arbuscule degeneration during AM symbiosis is regulated by MYB1. *Current Biology*, *27*,1206–1212. https://doi.org/10.1016/j.cub.2017.03.003

Galperin, M.Y. (2013). Genome diversity of spore-forming firmicutes. *Microbiology Spectrum*, *1*. https://doi.org/10.1128/microbiolspectrum.TBS-0015-2012

Genre, A., Chabaud, M., Balzergue, C., et al. (2013). Short-chain chitin oligomers from arbuscular mycorrhizal fungi trigger nuclear Ca^{2+} spiking in *Medicago truncatula* roots and their production is enhanced by strigolactone. *New Phytologist*, *198*, 190–202. https://doi.org/10.1111/nph.12146

Genre, A., Chabaud, M., Faccio, A., Barker, D.G., and Bonfante, P. (2008). Prepenetration apparatus assembly precedes and predicts the colonization patterns of arbuscular mycorrhizal fungi within the root cortex of both *Medicago truncatula* and *Daucus carota. The Plant Cell*, *20*, 1407–1420. https://doi.org/10.1105/tpc.108.059014

Giovannetti, M., Mari, A., Novero, M., and Bonfante, P. (2015). Early *Lotus japonicus* root transcriptomic responses to symbiotic and pathogenic fungal exudates. *Frontiers in Plant Science*, *6*, 480. https://doi.org/10.3389/fpls.2015.00480

Hadwiger, L.A. (2013). Multiple effects of chitosan on plant systems: solid science or hype. *Plant Science*, *208*, 42–49. https://doi.org/10.1016/j.plantsci.2013.03.007

Harrison, M.J., Dewbre, G.R., and Liu, J. (2002). A phosphate transporter from *Medicago truncatula* involved in the acquisition of phosphate released by arbuscular mycorrhizal fungi. *The Plant Cell*, *14*, 2413–2429. https://dx.doi.org/10.1105%2Ftpc.004861

Harrison, M.J., and Dixon, R. (1993). Isoflavonoid accumulation and expression of defense gene transcripts during the establishment of vesicular-arbuscular mycorrhizal associations in roots of *Medicago truncatula.* Molecular Plant-Microbe Interactions, 6, 643–654.

Hiller, K., Grote, A., Scheer, M., Münch, R., and Jahn, D. (2004). PrediSi: Prediction of signal peptides and their cleavage positions. *Nucleic Acids Research*, *32*, 375–379. https://doi.org/10.1093/nar/gkh378

Isayenkov, S., Fester, T., and Hause, B. (2004). Rapid determination of fungal colonization and arbuscule formation in roots of Medicago truncatula using real-time (RT) PCR. *Journal of Plant Physiology*, *161*, 1379–1383. https://doi.org/10.1016/j.jplph.2004.04.012

Javot, H., Penmetsa, R.V., Breuillin, F., et al. (2011). *Medicago truncatula mtpt4* mutants reveal a role for nitrogen in the regulation of arbuscule degeneration in arbuscular mycorrhizal symbiosis. *Plant Journal*, *68*, 954–65. https://doi.org/10.1111/j.1365-313X.2011.04746.x

Javot, H., Penmetsa, R.V., Terzaghi, N., Cook, D.R., and Harrison, M.J. (2007). A *Medicago truncatula* phosphate transporter indispensable for the arbuscular mycorrhizal symbiosis. *Proceedings of the National Academy of Sciences of the U.S.A.*, *104*, 1720–1725. https://doi.org/10.1073/pnas.0608136104

Jones, J.D.G., and Dangl, J.L. (2006). The plant immune system. *Nature*, *444*, 323–329. https://doi.org/10.1038/nature05286

Kapulnik, B.Y.Y., Volpin, H., Itzhakp, H., et al. (1996). Suppression of defence responses in mycorrhizal alfalfa and tobacco roots. *New Phytologist*, *133*, 59–64. https://doi.org/10.1111/j.1469-8137.1996.tb04341.x

Karimi, M., De Meyer, B., and Hilson, P. (2005). Modular cloning in plant cells. *Trends in Plant Science*, *10*, 103–105. https://doi.org/10.1016/j.tplants.2005.01.008

Katoh, K., Misawa, K., Kuma, K., and Miyata, T. (2002). MAFFT: a novel method for rapid multiple sequence alignment based on fast Fourier transform. *Nucleic Acids Research*, *30*, 3059–3066. https://doi.org/10.1093/nar/gkf436

Kobae, Y., Ohmori, Y., Saito, C., Yano, K., Ohtomo, R., and Fujiwara, T. (2016). Phosphate treatment strongly inhibits new arbuscule development but not the maintenance of arbuscule in mycorrhizal rice roots. *Plant Physiology*, *171*, 566–579. https://doi.org/10.1104/pp.16.00127

Kumar, S., Stecher, G., and Tamura, K. (2016). MEGA7: molecular evolutionary genetics analysis version 7.0 for bigger datasets. *Molecular Biology and Evolution*, *33*, 1870–1874. https://doi.org/10.1093/molbev/msw054

Lee, W., Rudd, J., Hammon-Kosack, K., and Kanyuka, K. (2014). *Mycosphaerella graminicola* LysM effector-mediated stealth pathogenesis subverts recognition through both CERK1 and CEBiP homologues in wheat. *Molecular Plant-Microbe Interactions*, *27*, 236–243. https://doi.org/10.1094/MPMI-07-13-0201-R

Librado, P., and Rozas, J. (2009). DnaSP v5: A software for comprehensive analysis of DNA polymorphism data. Bioinformatics, 25, 1451–1452. https://doi.org/10.1093/bioinformatics/btp187

Liu, J., Blaylock, L., Endre, G., Cho, J., Town, C.D., Vandenbosch, K.A., and Harrison, M.J. (2003). Transcript profiling coupled with spatial expression analyses reveals genes involved in disinct developmental stages of an arbuscular mycorrhizal symbiosis. *The Plant Cell*, *15*, 2106–2123. https://www.ncbi.nlm.nih.gov/pmc/articles/PMC181334/

Liu, T., Liu, Z., Song, C., et al. (2012). Chitin-induced dimerization activates a plant immune receptor. *Science*, 336, 1160–1164. https://doi.org/10.1126/science.1218867

Lohmann, G.V., Shimoda, Y., Nielsen, M.W., et al. (2010). Evolution and regulation of the *Lotus japonicus* LysM receptor gene family. *Molecular Plant-Microbe Interactions*, *23*, 510–521. https://doi.org/10.1094/MPMI-23-4-0510

Maherali, H., and Klironomos, J.N. (2007). Influence of phylogeny on fungal community assembly and ecosystem functioning. *Science*. *316*, 1746–1748. https://doi.org/10.1126/science.1143082

Maillet, F., Poinsot, V., André, O., et al. (2011). Fungal lipochitooligosaccharide symbiotic signals in arbuscular mycorrhiza. *Nature*, *469*, 58–64. https://doi.org/10.1038/nature09622

Malkov, N., Fliegmann, J., Rosenberg, C., et al. (2016). Molecular basis of lipo-chitooligosaccharide recognition by the lysin motif receptor-like kinase LYR3 in legumes. *Biochemical Journal*, *473*, 1369–1378. https://doi.org/10.1042/BCJ20160073

Marshall, E., Costa, L.M., and Gutierrez-Marcos, J. (2011). Cysteine-Rich Peptides (CRPs) mediate diverse aspects of cell–cell communication in plant reproduction and development. *Journal of Experimental Botany*, *62*, 1677–1686. https://doi.org/10.1093/jxb/err002

Marshall, R., Kombrink, A., Motteram, J., et al. (2011). Analysis of two in planta expressed LysM effector homologs from the fungus *Mycosphaerella graminicola* reveals novel functional properties and varying contributions to virulence on wheat. *Plant Physiology*, *156*, 756–769. https://doi.org/10.1104/pp.111.176347

Mentlak, T., Kombrink, A, Shinya, T., et al. (2012). Effector-mediated suppression of chitin-triggered immunity by *Magnaporthe oryzae* is necessary for rice blast disease. *The Plant Cell*, *24*, 322–335. https://doi.org/10.1105/tpc.111.092957

Miller, M.A., Pfeiffer, W., and Schwartz, T. "Creating the CIPRES Science Gateway for inference of large phylogenetic trees" in *Proceedings of the Gateway Computing Environments Workshop (GCE)*, 14 Nov. 2010, New Orleans, LA pp 1-8. https://doi.org/10.1109/GCE.2010.5676129

Murrell, B., Weaver, S., Smith, M.D., et al. (2015). Gene-wide identification of episodic selection. *Molecular Biology and Evolution*, *32*, 1365–1371. https://doi.org/10.1093/molbev/msv035

Nei, M., and Li, W.-H. (1979). Mathematical model for studying genetic variation in terms of restriction endonucleases. *Proceedings of the National Academy of Sciences of the U.S.A.*, *76*, 5269–5273. https://www.ncbi.nlm.nih.gov/pmc/articles/PMC413122/

Petersen, T.N., Brunak, S., von Heijne, G., and Nielsen, H. (2011). SignalP 4.0: Discriminating signal peptides from transmembrane regions. *Nature Method*, *8*, 785–786. https://doi.org/10.1038/nmeth.1701

Pettersen, E.F., Goddard, T.D., Huang, C.C., et al. (2004). UCSF Chimera—a visualization system for exploratory research and analysis. *Journal of Computational Chemistry*, *25*, 1605–12. https://doi.org/10.1002/jcc.20084

Pond, S.L.K., Posada, D., Gravenor, M.B., Woelk, C.H., and Frost, S.D.W. (2006). Automated phylogenetic detection of recombination using a genetic algorithm.

Molecular Biology and Evolution, *23*, 1891–1901. https://doi.org/10.1093/molbev/msl051

Powell, J.R., Parrent, J.L., Hart, M.M., Klironomos, J.N, Rillig, M.C., and Maherali, H. (2009). Phylogenetic trait conservatism and the evolution of functional trade-offs in arbuscular mycorrhizal fungi. *Proceedings of the Royal Society B Biological Sciences*, *276*, 4237–4245. https://doi.org/10.1098/rspb.2009.1015

Pumplin, N., and Harrison, M.J. (2009). Live-cell imaging reveals periarbuscular membrane domains and organelle location in *Medicago truncatula* roots during arbuscular mycorrhizal symbiosis. *Plant Physiology*, *151*, 809–819. https://doi.org/10.1104/pp.109.141879

Pumplin, N., Mondo, S.J., Topp, S., Starker, C.G., Gantt, J.S., and Harrison, M.J. (2010). *Medicago truncatula* Vapyrin is a novel protein required for arbuscular mycorrhizal symbiosis. *The Plant Journal*, *61*, 482–494. https://doi.org/10.1111/j.1365-313X.2009.04072.x

Raffaele, S., and Kamoun, S. (2012). Genome evolution in filamentous plant pathogens: why bigger can be better. *Nature Reviews Microbiology*, *10*, 417–430. https://doi.org/10.1038/nrmicro2790

Ravenhall M, Nives Š, Lassalle F, Dessimoz C (2015) Inferring horizontal gene transfer. PLOS Comput Biol 11:e1004095. https://doi.org/10.1371/journal.pcbi.1004095

Ronquist, F., Teslenko, M., Van Der Mark, P., et al. (2012). MrBayes 3.2: Efficient bayesian phylogenetic inference and model choice across a large model space. *Systematic Biology*, *61*, 539–542. https://doi.org/10.1093/sysbio/sys029

Salvioli, A., Ghignone, S., Novero, M., Navazio, L., Venice, F., Bagnaresi, P., and Bonfante, P. (2015). Symbiosis with an endobacterium increases the fitness of a mycorrhizal fungus, raising its bioenergetic potential. *The ISME Journal*, *10*, 130–144. https://doi.org/10.1038/ismej.2015.91

Sánchez-Vallet, A., Mesters, J.R., and Thomma, B.P.H.J. (2014). The battle for chitin recognition in plant-microbe interactions. *FEMS Microbiology Reviews*, *39*, 171–183. https://doi.org/10.1093/femsre/fuu003

Sánchez-Vallet, A., Saleem-Batcha, R., Kombrink, A., Hansen, G., Valkenburg, D.-J., Thomma, B.P.H.J., and Mesters, J.R. (2013). Fungal effector Ecp6 outcompetes host immune receptor for chitin binding through intrachain LysM dimerization. *Elife*, *2*, e00790. https://doi.org/10.7554/eLife.00790

Sędzielewska Toro, K., and Brachmann, A. (2016). The effector candidate repertoire of the arbuscular mycorrhizal fungus *Rhizophagus clarus*. *BMC Genomics*, *17*, 101. https://doi.org/10.1186/s12864-016-2422-y

Seidl-Seiboth, V., Zach, S., Frischmann, A., et al. (2013). Spore germination of *Trichoderma atroviride* is inhibited by its LysM protein TAL6. *FEBS Journal*, *280*, 1226–1236. https://doi.org/10.1111/febs.12113

Shinya, T., Motoyama, N., Ikeda, A., et al. (2012). Functional characterization of CEBiP and CERK1 homologs in arabidopsis and rice reveals the presence of different chitin receptor systems in plants. *Plant Cell Physiology*, *53*, 1696–1706. https://doi.org/10.1093/pcp/pcs113

Spanu, P., Boller, T., Ludwig, A., Wiemken, A., Faccio, A., and Bonfante-Fasolo, P. (1989). Chitinase in roots of mycorrhizal *Allium porrum*: regulation and localization. *Planta*, *177*, 447–455. https://doi.org/10.1007/BF00392612

Sugimura, Y., and Saito, K. (2017). Transcriptional profiling of arbuscular mycorrhizal roots exposed to high levels of phosphate reveals the repression of cell cycle-related genes and secreted protein genes in *Rhizophagus irregularis*. *Mycorrhiza*, *27*, 139–146. https://doi.org/10.1007/s00572-016-0735-y

Sulima, A.S., Zhukov, V.A., Afonin, A.A., et al. (2017). Selection signatures in the first exon of paralogous receptor kinase genes from the *Sym2* region of the *Pisum sativum* L. genome. *Frontiers in Plant Science*, *8*, 1957. https://doi.org/10.3389/fpls.2017.01957

Takahara, H., Kombrink, A., Hughes, H.B., et al. (2016). *Colletotrichum higginsianum* extracellular LysM proteins play dual roles in appressorial function and suppression of chitin-triggered plant immunity. *New Phytologist*, *211*, 1323–1337. https://doi.org/10.1111/nph.13994

Tang, D., Wang, G., and Zhou, J.-M. (2017). Receptor kinases in plant-pathogen interactions: more than pattern recognition. *The Plant Cell*, *29*, 618–637. https://doi.org/10.1105/tpc.16.00891

Tang, N., Clemente, H.S., Roy, S., Bécard, G., Zhao, B., and Roux, C. (2016). A survey of the gene repertoire of *Gigaspora rosea* unravels conserved features among Glomeromycota for obligate biotrophy. *Frontiers in Microbiology*, *7*, 233. https://doi.org/10.3389/fmicb.2016.00233

Tisserant, E., Malbreil, M., Kuo, A., et al. (2013). Genome of an arbuscular mycorrhizal fungus provides insight into the oldest plant symbiosis. *Proceedings of the National Academy of Sciences of the U.S.A.*, *110*, 20117–20122. https://doi.org/10.1073/pnas.1313452110

Towns, J., Cockerill, T., Dahan, M., et al. (2014). XSEDE: Accelerating scientific discovery. *Computing in Science & Engineering*, *16*, 62–74. https://doi.org/10.1109/MCSE.2014.80

Tsuzuki, S., Handa, Y., Takeda, N., and Kawaguchi, M. (2016). Strigolactone-induced putative secreted protein 1 is required for the establishment of symbiosis by the arbuscular mycorrhizal fungus *Rhizophagus irregularis.* Molecular Plant-Microbe Interactions, 29, 277–286. https://doi.org/10.1094/MPMI-10-15-0234-R

Verbruggen, E. and Toby Kiers, E. (2010). Evolutionary ecology of mycorrhizal functional diversity in agricultural systems. *Evolutionary Applications*, *3*, 547–560. https://doi.org/10.1111/j.1752-4571.2010.00145.x

Waterhouse, A.M., Procter, J.B., Martin, D.M.A., Clamp, M., and Barton, G.J. (2009). Jalview Version 2 – A multiple sequence alignment editor and analysis workbench. *Bioinformatics*, *25*, 1189–1191. https://doi.org/10.1093/bioinformatics/btp033

Willmann, R., and Nürnberger, T. (2012). How plant lysin motif receptors get activated: lessons learned from structural biology. *Science Signaling*, *5*, pe28. https://doi.org/10.1126/scisignal.2003274

Yang, J., Roy, A., and Zhang, Y. (2013a). BioLiP: A semi-manually curated database for biologically relevant ligand-protein interactions. *Nucleic Acids Research*, *41*, D1096–D1103. https://doi.org/10.1093/nar/gks966

Yang, J., Roy, A., and Zhang, Y. (2013b). Protein-ligand binding site recognition using complementary binding-specific substructure comparison and sequence profile alignment. *Bioinformatics*, *29*, 2588–2595. https://doi.org/10.1093/bioinformatics/btt447

Yang, J., Yan, R., Roy, A., Xu, D., Poisson, J., and Zhang, Y. (2014). The I-TASSER suite: Protein structure and function prediction. *Nature Methods*, *12*, 7–8. https://doi.org/10.1038/nmeth.3213

Zeng, T., Holmer, R., Hontelez, J., et al. (2018). Host- and stage-dependent secretome of the arbuscular mycorrhizal fungus *Rhizophagus irregularis. The Plant Journal* https://doi.org/10.1111/tpj.13908 [Epub ahead of print]

Zuccaro, A., Lahrmann, U., Güldener, U., et al. (2011). Endophytic life strategies decoded by genome and transcriptome analyses of the mutualistic root symbiont *Piriformospora indica*. *PLOS Pathogens*, *7*, e1002290. https://doi.org/10.1371/journal.ppat.1002290

CHAPTER 6

CONCLUSION

For at least 400 million years, plants have harbored arbuscular mycorrhizal fungi in their roots. Fungus and plant have evolved complex mechanisms to facilitate the interaction – a symbiosis conferring such a benefit to the fungus that it has lost the ability to complete its lifecycle without the host. In return for photosynthates, the fungus delivers inorganic phosphates, among many measurable benefits (Smith and Read 2008). The underlying inspiration for the research conducted in this dissertation has been to better understand how the plant and fungus maintain mutualism, with the hopes to improve upon those benefits conferred, not only to the plant, but also to the environment. Could we enhance nutrient transfer to the plant in such a way that application of AM fungi would eliminate a need for chemical fertilizers in agriculture? Could we improve the transfer of photosynthates from trees to fungi, increasing the potential for forests to act as a sink for CO_2 by storing it in living underground networks?

These big-picture questions trigger a chain of smaller and smaller questions, eventually leading to investigations of the subcellular processes that make the symbiosis tick. All of the work done in this thesis is at the level of basic science, but the eventual applications of such discoveries are only a few steps away. Visions of these applications, and their potentially global impact drive us to push onward with basic investigations, even despite the many failures we inevitably endure as scientists; and as obligate, yet genetically intractable organisms, arbuscular mycorrhiza fungi offer many challenges, and often many failures. Yet many promising discoveries have been made in the past decade, especially with the influx of genomic data and new techniques.

Genomic and transcriptomic data have revealed many interesting candidates for forward genetics aimed at the identification of genes involved in AM symbiosis. While null mutations in many such genes have led to the discovery of important players in symbiosis, this approach is often not so simple. In Chapter 3 we identified a LysM-RLK, *Lyr1*, strongly induced by AM fungal colonization as compared to roots lacking AM fungi. We had optimistic expectations that this gene would be like Nod factor receptors, which alone are necessary for establishment of root-nodule symbiosis, and that we would find a dramatic interruption in AM fungal colonization of the null mutant; however, we quickly realized the expansive LysM-RLK family may preclude easy identification of genes contributing to symbiosis. Our experiments, and others that have been published since (Zhang et al. 2015; Rasmussen et al. 2016), emphasize the importance of carefully fine-tuning certain experimental variables, such as spore load or nutrient concentrations, in order to uncover partial contributions of redundant genes.

In Chapter 4, we again faced redundancy with our identification of three SLMs that are conserved for AM symbiosis, and specifically induced by AM fungal colonization. Despite strong indicators that these genes are important for the symbiosis, a nearly-complete loss of transcript had no effect on the interaction. Other SLMs present in the root may still function redundantly in the RNAi mutant, and even if they do so less efficiently, any subtle phenotype may have been lost without the right experimental variables. Instead of attempting to silence all six root-expressed SLMs simultaneously, we took a simpler approach by ectopically expressing the AM-SLMs. The small, but consistent enhancement of AM fungal growth suggests these proteins may be important for fungal development. Our results, combined with parallels between AM-SLMs and nodule-specific cysteine-rich peptides, should guide future studies towards investigating direct effects of the proteins on AM fungi, or mutational studies that investigate the importance of the cysteine residues.

A similar ectopic expression may help investigate what role, if any, *Lyr1*, *NFP* or *Lyk10* play in AM symbiosis, rather than continuing to silence or delete more genes simultaneously in the hopes of finding the right combination among the 21 possibilities. In the case of *Lyk10*, in Chapter 3 we speculate that this LysM-RLK may be important for the contribution of other microorganisms to AM symbiosis. Considering that AM symbiosis has evolved in soils flush with diverse microorganisms competing for many of the same resources, many important mechanisms are likely to be missed by eliminating all other possible interactions. Certainly, isolating plant and fungus is a necessary starting point; however, no conclusion can be drawn from a negative phenotype as to a gene's contribution to AM symbiosis without considering all possible environmental conditions that may have shaped the evolution of the interaction – indeed, an impossible feat. A simple experiment to test this theory as it pertains to *Lyk10* would involve AM fungal colonization of the mutant and wild type roots with and without the application of rhizobial exopolysaccharides. If Lyk10 perception of EPS enhances AM fungal colonization, we would expect to see an even greater decrease in the mutant relative to its segregating wild type.

An important precautionary tale comes with our analysis of a second *Lyk10* mutant that did not exhibit the same decrease in colonization relative to its segregating wild type. While this does not falsify the phenotype seen with the first mutant, as there may have been a separate mechanism decreasing colonization in the second wild type, it does emphasize the need for considering multiple mutants when using imprecise mutagenesis techniques. In Chapter 3 we saw an excellent example of this problem when we tested two null mutants of *slm2* which each had a significant effect on fungal colonization, but in opposite directions. The null mutants analyzed in Chapter 3 and Chapter 4 were identified from random mutagenesis populations, and each mutant line may contain one or more unrelated mutations that could affect the development of AM symbiosis just enough to miss a subtle phenotype. Since the time these experiments were done, greatly improved technologies for generating

null mutants, such as CRISPR/Cas9 (Doudna and Chapentier 2014), have become widely available. Such technologies should be a default for investigations of potentially redundant genes in the future.

These new technologies also hold promise for increasing tractability of AM fungi. At this time, we still do not have methods for genetically manipulating AM fungi. Although two reports of host-induced gene silencing in AM fungi indicate this method may work (Helber et al. 2011; Tsuzuki et al. 2016), in our hands we have had little success. In Chapter 5, we identify a putative LysM effector from *Rhizophagus irregularis* that is able to bind to chitin and chitosan. Without a transformation system for the fungus, we were unable to feasibly investigate where the *RiSLM* gene is expressed or where the protein localizes. Considering its similarity to the AM-SLMs identified in Chapter 4, we can speculate that RiSLM may add yet another level of functional redundancy to certain roles these proteins may plan in AM symbiosis. Interestingly, we were unable to identify an ortholog of *RiSLM* in available sequences from other genera of AM fungi. The next steps for this research should focus on the evolutionary biology of the gene by screening several different fungi for orthologs using degenerate primers. The existence of a LysM effector in some but not all AM fungi would suggest a difference among AM fungi in how they interact with their host – something also hinted at by the opposite colonization phenotypes of the *nfp* mutant when colonized by *G. versiforme* or *G. gigantea*. Not all AM fungi may be triggering the same exact mechanisms in the plant to facilitate colonization.

While much of the work in this thesis did not reveal the exciting phenotypes we had hoped for, the negative results will hopefully contribute to the literature by allowing others to avoid testing these mutants under the same conditions. Furthermore, the characterization of small LysM proteins in Chapter 4 and Chapter 5 lay the foundation for many more questions and hypotheses to be tested. In particular, the identification of a LysM effector-like protein in an AM fungus suggests parallels between strategies employed by pathogenic and symbiotic

fungi. How it is that AM fungi do not trigger host defenses has been a long-time question. Demonstration that RiSLM is able to bind chitin presents a potential mechanism for defense inhibition during AM symbiosis. Furthermore, in Chapter 3, the *lyk10* mutant exhibited a decrease in colonization and, combined with the importance of its paralog in suppressing defense responses, we can hypothesize that this gene may also contribute to such a mechanism for AM symbiosis.

Two major discoveries greatly inspired the hypotheses tested in this thesis: the identification of fungal signaling molecules and their similarity to Nod factors and chitin, and the release of the *Rhizophagus irregularis* genome sequence, which was a first for Glomeromycotina (Tisserant et al. 2013). The results of our work have both contributed to the literature and generated many more important hypotheses to test. As more sequence data becomes available, and better methods are developed for genetic manipulation of plant and fungus, many of these hypotheses will become easier to test. A recent report demonstrated the use of a plasmid-free CRISPR/Cas9 system to genetically modify the fungus *Mucor circinelloides*, a Mucoralean fungus closely related to Glomeromycotina (Nagy et al. 2017). The development of such a system for AM fungi would revolutionize the field and allow for many of the hypotheses generated from data in this thesis to be easily tested.

In light of the earth's changing climate and steadily growing population, innovative solutions for food security are necessary now more than ever. AM symbiosis holds potential for application in many areas related to agriculture and climate change, and the basic science we pursue is necessary for making such advances. The results presented in this thesis are just small pieces that we hope will contribute to resolving the bigger pictures revealing ways in which AM fungi may someday be used to solve important problems at a global scale.

REFERENCES

Doudna, J. A., and Charpentier, E. 2014. The new frontier of genome engineering with CRISPR-Cas9. Science. 346

Helber, N., Wippel, K., Sauer, N., Schaarschmidt, S., Hause, B., and Requena, N. 2011. A versatile monosaccharide transporter that operates in the arbuscular mycorrhizal fungus *Glomus* sp is crucial for the symbiotic relationship with plants. Plant Cell. 23:3812–3823

Nagy, G., Szebenyi, C., Csernetics, Á., Vaz, A. G., Tóth, E. J., Vágvölgyi, C., and Papp, T. 2017. Development of a plasmid free CRISPR-Cas9 system for the genetic modification of Mucor circinelloides. Sci. Rep. 7:1–10

Rasmussen, S. R., Füchtbauer, W., Novero, M., Volpe, V., Malkov, N., Genre, A., Bonfante, P., Stougaard, J., and Radutoiu, S. 2016. Intraradical colonization by arbuscular mycorrhizal fungi triggers induction of a lipochitooligosaccharide receptor. Sci. Rep. 6:29733

Tisserant, E., Malbreil, M., Kuo, A., Kohler, A., Symeonidi, A., Balestrini, R., Charron, P., Duensing, N., Frei dit Frey, N., Gianinazzi-Pearson, V., Gilbert, L. B., Handa, Y., Herr, J. R., Hijri, M., Koul, R., Kawaguchi, M., Krajinski, F., Lammers, P. J., Masclaux, F. G., Murat, C., Morin, E., Ndikumana, S., Pagni, M., Petitpierre, D., Requena, N., Rosikiewicz, P., Riley, R., Saito, K., San Clemente, H., Shapiro, H., van Tuinen, D., Becard, G., Bonfante, P., Paszkowski, U., Shachar-Hill, Y. Y., Tuskan, G. a., Young, P. W., Sanders, I. R., Henrissat, B., Rensing, S. a., Grigoriev, I. V., Corradi, N., Roux, C., and Martin, F. 2013. Genome of an arbuscular mycorrhizal fungus provides insight into the oldest plant symbiosis. PNAS. 110:20117–20122

Tsuzuki, S., Handa, Y., Takeda, N., and Kawaguchi, M. 2016. Strigolactone-induced putative secreted protein 1 is required for the establishment of symbiosis by the arbuscular mycorrhizal fungus Rhizophagus irregularis. MPMI. 29:277–286

Zhang, X., Dong, W., Sun, J., Feng, F., Deng, Y., He, Z., Oldroyd, G. E. D., and Wang, E. 2015. The receptor kinase CERK1 has dual functions in symbiosis and immunity signalling. Plant J. 81:258–267